Newfoundland & Labrador

Energy and Mines

Mines

THE SOUTHERN BUCHANS–ROBERTS ARM BELT, CENTRAL NEWFOUNDLAND – VOLCANOGENIC MASSIVE SULPHIDE MINERALIZATION AND RELATED ALTERATION

G.W. Sparkes

Report 26-2

St. John’s, Newfoundland
2026

Newfoundland & Labrador

Energy and Mines

Mines

THE SOUTHERN BUCHANS–ROBERTS ARM BELT, CENTRAL NEWFOUNDLAND – VOLCANOGENIC MASSIVE SULPHIDE MINERALIZATION AND RELATED ALTERATION

G.W. Sparkes

Report 26-2

St. John's, NL
2026

Recommended citation:
Sparkes, G.W.
2026: The southern Buchans–Roberts Arm Belt, central Newfoundland – volcanogenic massive sulphide mineralization and related alteration. Government of Newfoundland and Labrador, Department of Energy and Mines, Geological Survey, St. John's, Report 26-2, 128 pages.

Author Address

G.W. Sparkes
Mineral Deposits Section
Department of Energy and Mines
P.O. Box 8700
St. John's, NL
A1B 4J6
Email: gregsparkes@gov.nl.ca

CONTENTS

Page

Page

Page

FIGURES

Page

Page

Page

Page

Page

PLATES

Page

Page

TABLES

ABSTRACT

The southern Buchans–Roberts Arm Belt (BRAB) has been the focus of considerable mineral exploration activities over the last one hundred years related to the original discovery and mining of world-class volcanogenic massive sulphide (VMS) deposits at Buchans. This intermittent exploration has resulted in the discovery of numerous zones of "sericite" alteration, largely through diamond drilling, in areas located to the east of the Buchans deposits. These alteration zones are hosted by felsic, intermediate and mafic volcanic and related volcaniclastic rocks of the Buchans, Mary March Brook and Red Indian Lake groups. The alteration is commonly associated with base- and precious-metal enrichment inferred to be related to the development of VMS-style mineralization. However, few detailed comparative studies exist that characterize the alteration and related geochemical signature of these prospects. This report primarily focuses on the area extending from the Buchans camp eastward to Mary March Brook, with only limited investigations of the Lucky Strike and Rothermere deposits in the immediate Buchans area for comparison purposes.

The application of short wavelength infrared (SWIR) spectrometry through the collection of systematic downhole measurements from drillcore allows for the detailed evaluation of the individual zones of hydrothermal alteration. Using this spectral data, the historical "sericite" alteration zones can be further subdivided into defined white mica minerals (paragonite, muscovite, phengite) that can be used to highlight areas associated with more acidic hydrothermal fluids and provide vectors toward vent-proximal environments. The downhole spectral data is used to calculate scalar variables, such as the Al-OH wavelength feature, which, when plotted against known mineralized intersections, demonstrate a notable shift to shorter spectral wavelengths with decreasing distance from mineralization at several of these prospects. Scalar variables allow for the quantitative characterization of the alteration, as opposed to previous methods that involved visual estimates that vary between geologists and exploration programs. Results from the SWIR analyses have identified two areas of advanced argillic alteration in the region, potentially related to the development of hybrid bimodal–felsic-style VMS mineralization. These zones of advanced argillic alteration are associated with $\delta^{34}S$ values ranging from 4.7 to -11.1 per mil, indicating a potential magmatic component of the fluids associated with these hydrothermal systems. The SWIR data suggests the zones of sericite alteration that were examined can be subdivided into five groups: 1) advanced argillic (Tower and Mary March prospects), 2) argillic (Powerhouse prospect), 3) phyllic–muscovite-dominated (Buchans area (Lucky Strike/Rothermere deposits), Airport, Woodman's Brook, Seal Pond, and Beaver Pond prospects), 4) phyllic–chlorite-dominated (Little Sandy prospect), and 5) sub-propylitic (Sandfill/Middle Branch, Middle Branch East, Mary March Brook and Connell prospects).

Select samples from the various styles of alteration identified using SWIR were also submitted for geochemical analysis. The combination of these two unique datasets allows for an in-depth comparison between the individual alteration zones. The spectral data correlates well with geochemical alteration indices such as the advanced argillic alteration, Ishikawa alteration, and the Duck Pond indices. Associations observed between the development of paragonite–paragonitic illite–muscovite–muscovitic illite ± montmorillonite alteration coupled with increased Hg/Na_2O and Ba/Sr ratios may aid future exploration efforts in the region, assisting in the recognition of prospective thrust panels for hosting VMS mineralization, both in archive and future drillholes. These features are important in identifying drillholes that represent potential near misses, highlighting those that are relatively unmineralized but contain anomalous alteration and associated geochemical enrichment of select elements, and thus worthy of additional follow-up. The recognition of such features may highlight areas that have been previously overlooked, despite the prolonged history of exploration of the region.

INTRODUCTION

OBJECTIVES

The Buchans–Roberts Arm Belt (BRAB) of central Newfoundland is host to numerous examples of volcanogenic massive sulphide (VMS) mineralization, which includes several notable deposits, namely the Buchans deposits (Lucky Strike, Rothermere, MacLean, Oriental 1 and 2), Lake Bond, Gullbridge and Pilley's Island (Swinden, 1991). Despite having more than one hundred years of mineral exploration history, the Newfoundland and Labrador Geological Survey has conducted limited systematic documentation of VMS-related occurrences within the central and southern parts of this belt.

To better document VMS-related occurrences and associated hydrothermal alteration within these regions, a deposit-level metallogenic study initiated in 2017, had the overall goal of collecting representative geochemical and shortwave infrared (SWIR) spectral data, largely from drillcore, related to VMS mineralization. Field work, related to this project, commenced in the vicinity of the Gullbridge deposit in 2017 and continued southward, culminating in 2022, at the southern end of the belt proximal to the Buchans deposits. Results from the study have been presented in a series of reports (Sparkes, 2018, 2019, 2020, 2022; Sparkes *et al.*, 2021; Sparkes and Hinchey, 2023; Allen *et al.*, 2024; Sparkes and Hamilton, 2024).

This report provides a detailed synthesis of the data collected within the southern part of the BRAB, focusing on alteration zones and related VMS mineralization developed in the area east of the main Buchans camp. These data provide new meaningful insights into the style and setting of the mineralization in the region. During the study, a significant amount of historical data was compiled from mineral assessment files. These data are included in the following appendices: 1) Appendix A: Sampling Framework, 2) Appendix B: New Analytical Data, 3) Appendix C: Historical Data and 4) Appendix D: Metadata.

Significant outcomes of the study include:

1) The documentation of VMS-related occurrences within the area through the collection of systematic, down-hole spectral data and representative geochemical samples allowing for the better characterization of hydrothermal alteration associated with VMS mineralization.

2) Geochronological data allowing for temporal constraints on VMS mineralization within the BRAB.

3) The proposed new deposit model for select occurrences.

4) A drillhole database compiled from industry-assessment files containing GIS-based reference data for drillhole collar locations and select compilation of associated geochemical data.

PREVIOUS WORK

A detailed summary of the more than one hundred years of exploration history within the BRAB is beyond the current scope of this review. Exploration work to the east of the main Buchans camp has identified several areas of alteration and anomalous mineralization, which were the focus of this study. These areas include the Airport, Sandfill, Middle Branch East, Powerhouse, Woodman's Brook, Tower, Little Sandy, Seal Pond, Beaver Pond, Connell, Mary March and Mary March Brook prospects (Figure 1). A summary of key results and most recent activities is provided for each of these areas (*see* below) and is summarized from Sparkes (2022). Much of this information has been reviewed in existing mineral assessment reports, with select references provided for areas that were investigated as part of this study. A detailed summary of existing mineral exploration reports, available within the Geofiles database, are in Appendix D.

METHODOLOGY

SWIR ALTERATION STUDIES

Short wavelength infrared (SWIR) spectrometry provides the ability to obtain mineralogical information on the crystallinity and/or compositional variations associated with certain mineral groups, such as white micas (*e.g.*, paragonite, muscovite and phengite). Illite variants of these white mica minerals are expressed by the spectral software (The Spectral Geologist) as either paragonitic-illite, muscovitic-illite, or phengitic-illite (*see* below). The variation in the Al-OH absorption feature (~2200 nm) is one example of a calculated scalar from the spectral data that can be utilized to gain insight regarding the compositional differences within various white mica minerals (*e.g.*, paragonite (2180–2195 nm), muscovite (2195–2215 nm) and phengite (2215–2225 nm); Pontual *et al.*, 1997; AusSpec, 2008). The position of the Al-OH feature can also be used as a hydrothermal pH indicator, with shorter wavelengths being representative of more acidic hydrothermal conditions (Halley *et al.*, 2015). Spectral measurements were collected using either a TerraSpec® Pro or TerraSpec® Halo spectrometer, and these spectra were subsequently processed using The Spectral Geologist (TSG™) software (version 8.0.7.4) to obtain mineral identifications. This software provides the two most abundant minerals present (Min 1 and Min 2) for each individual spectral analysis

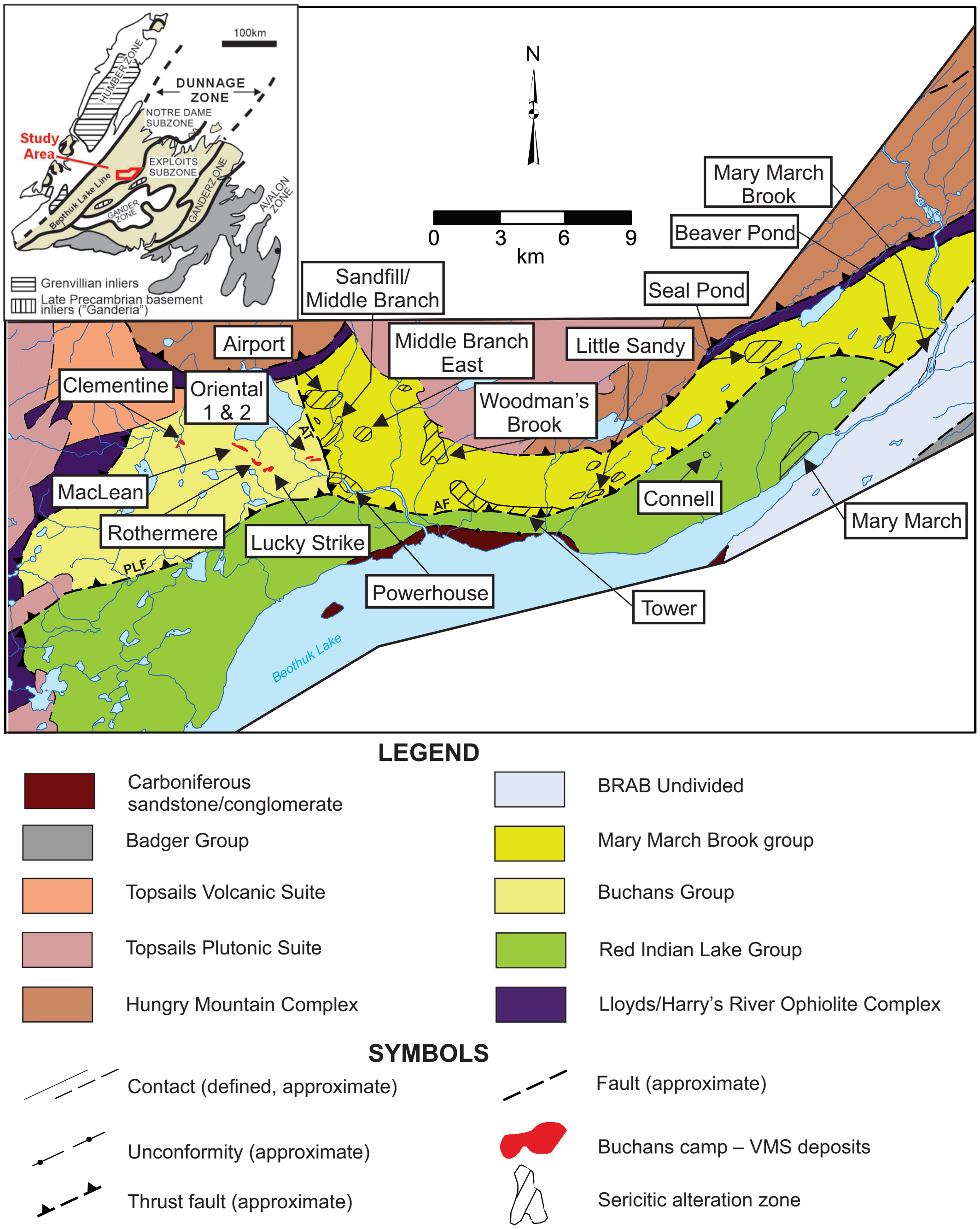

Figure 1. *Regional compilation map outlining the geology and location of select alteration zones relative to the Buchans VMS deposits; geology modified from Zagorevski* et al. *(2015). Note the alteration zones are drawn to encompass drillhole collar locations that are reported to have intersected "sericite" alteration at depth. BRAB–Buchans–Roberts Arm Belt; AT–Airport Thrust Fault; PLF–Powerline Fault; AF–Airport Fault.*

by comparing each spectra to a reference library of known minerals. When surveying drillholes, spectral data was collected at 1.5 m spacing unless otherwise noted. In addition, spectral data was obtained from representative samples that were submitted for geochemical analysis. Results from the spectral analyses are in Appendix B.

GEOCHEMISTRY

Geochemical sampling, mainly from drillcore, focused on alteration assemblages identified using SWIR, but also included representative samples of unaltered host rocks, where available. These samples were analyzed for major and trace elements using Inductively Coupled Plasma-Optical

Emission Spectrometry (ICP-OES) and Inductively Coupled Plasma-Mass Spectrometry (ICP-MS; Finch *et al.*, 2018). Select samples were also sent for external Instrumental Neutron Activation Analysis (INAA) at Bureau Veritas in Mississauga, Ontario, and Cold Vapour-Atomic Absorption Spectrometry (CV-AAS) at Actlabs in Ancaster, Ontario. The geochemical data are in Appendix B.

SULPHUR ISOTOPES

Select samples were submitted for Secondary Ion Mass Spectrometer (SIMS) analyses, which targeted pyrite intergrown with advanced argillic minerals or developed proximal to such alteration assemblages, as well as samples from the footwall zone of the Lucky Strike deposit. All samples were mounted and prepared at the Micro-analysis Facility of Memorial University and analyzed on the Cameca IMS 4f Secondary Ion Mass Spectrometer. In total, forty-nine δ^{34}S spot analyses were obtained from the six samples analyzed. In addition, nineteen δ^{34}S spot analyses of internal standards were also performed during the analysis. Based on these results, the overall reproducibility of individual measurements is typically better than 1 per mil. The analytical results from this work are in Appendix B.

REGIONAL GEOLOGY

The geology of the southern BRAB, primarily confined to the area north of Beothuk Lake (formerly known as Red Indian Lake), has most recently been discussed by Zagorevski and Rogers (2008, 2009) and Zagorevski *et al.* (2007, 2015, 2016). From this work, the geology of the area has been subdivided into five units, consisting of: the Lloyds/Harry's River Ophiolite and Hungry Mountain complexes, and the Mary March Brook, Buchans and the Red Indian Lake groups (Figure 1). The Mary March Brook group (MMBG; formerly the Seal Pond formation of Zagorevski *et al.* (2007)) includes rocks previously assigned to the Little Sandy Sequence of Thurlow and Swanson (1981) and includes rocks of the Lundberg Hill Formation of Thurlow and Swanson (1987). The Buchans Group was further subdivided by Thurlow and Swanson (1987) into the Lundberg Hill, Ski Hill, Buchans River and Sandy Lake formations. Only the Mary March Brook, Buchans and the Red Indian Lake groups are discussed in detail, as they host VMS mineralization and related alteration.

The MMBG (locally) structurally overlies rocks of the Buchans Group and is composed of bimodal tholeiitic and calc-alkalic volcanic rocks. Rocks of the MMBG are separated from those of the Buchans Group by the Airport Thrust Fault (Thurlow *et al.*, 1992). Rocks occurring immediately east of this structure are incorporated into the MMBG of Zagorevski *et al.* (2015) but were previously grouped within the Woodman's Brook volcanic rocks of Winter (2000) and Thurlow (2001); recent work by Allen and Schofield (2023) supports the inclusion of at least some of these rocks within the Lundberg Hill Formation of the Buchans Group of Thurlow and Swanson (1987). The formation of tholeiitic rhyolite cryptodomes and coeval island-arc tholeiitic basalts was accompanied by the deposition of rare polymictic debris flows and locally developed hydrothermal alteration and VMS mineralization (Zagorevski and Rogers, 2008, 2009). These rocks are conformably overlain by bimodal calc-alkalic volcanic rocks. The MMBG is interpreted to have formed within a back-arc or intra-arc rift setting and has been dated through Sensitive high-resolution ion microprobe (SHRIMP) analysis at 461.5 ± 4 Ma (Zagorevski *et al.*, 2015, 2016). This group hosts localized VMS mineralization and "sericitic" alteration zones, which include Middle Branch East, Woodman's Brook, Tower, Little Sandy, Seal Pond and Beaver Pond prospects (Figure 1).

The Buchans Group structurally underlies the MMBG within the footwall of the regionally extensive Airport Thrust Fault (Thurlow *et al.*, 1992). The Buchans Group is composed of calc-alkalic basaltic and rhyolitic rocks of continental-arc affinity, along with abundant granitoid-bearing conglomerate and debris flows (Thurlow and Swanson, 1987; Swinden *et al.*, 1997; Zagorevski *et al.*, 2015, 2016). SHRIMP geochronological data from volcanic rocks within lower stratigraphic levels of the group range from 465 ± 4 to 463 ± 4 Ma, while a felsic crystal tuff from stratigraphically higher in the sequence is dated at 462 ± 4 Ma (Zagorevski *et al.*, 2015). Thermal ionization mass spectrometry (TIMS) dating of granitoid clasts from within the debris flows of the Buchans mine area are dated at 464 ± 4 Ma (Whalen *et al.*, 2013). TIMS dating of a felsic volcanic rock located stratigraphically below one of the mineralized debris flows is dated at 471 ± 1.6 Ma (Sparkes *et al.*, 2021). Additional TIMS dating of various stratigraphic units within the Buchans Group now demonstrate that most formations within this group developed around *ca.* 470 Ma (Sparkes and Hamilton, 2024). The Buchans Group is well known for its VMS mineralization, which includes the past-producing Oriental, Lucky Strike, Rothermere and MacLean deposits. This VMS mineralization is inferred to have developed around *ca.* 470 Ma based on age constraints of key units within the Buchans Group stratigraphy (Sparkes and Hamilton, 2024).

The Red Indian Lake Group is composed of tholeiitic mafic, and overlying calc-alkalic bimodal, volcanic rocks, with the two sequences locally separated by polymictic conglomerate (Zagorevski *et al.*, 2006; Zagorevski and Rogers, 2008, 2009). Rocks at the base of this group are composed of island-arc tholeiites to back-arc basin basalts, along with minor felsic volcanic rocks, which are interpreted to have formed within a rifted-arc or back-arc type setting

(Zagorevski *et al.*, 2006). This group includes rocks previously assigned to the Footwall Arkose and Footwall Basalt of Thurlow and Swanson (1981), and the Sandy Lake Formation of Thurlow and Swanson (1987). Rocks included within the Red Indian Lake Group have produced SHRIMP ages ranging from 465 ± 4 to 462 +2/-9 Ma (Zagorevski *et al.*, 2015) and host several notable VMS occurrences including the Mary March and Connell prospects (Figure 1).

Rocks located in the eastern part of the southern BRAB remain poorly constrained, in part due to limited outcrop exposure (BRAB undivided; Figure 1). Much of the information about this area comes from drillcore, which contains structurally interleaved mafic and felsic volcanic rocks and related volcaniclastic units. Felsic volcanic rocks from the area have been dated using TIMS at 470.09 ± 0.39 Ma, demonstrating similar ages to units developed both to the southwest and to the northeast (Sparkes *et al.*, 2021; Sparkes and Hamilton, 2024). Regional mapping by Zagorevski *et al.* (2016) correlates these rocks with the Red Indian Lake Group, but immediately to the northeast, the same rocks are correlated with the Gullbridge structural tract by O'Brien (2009; *cf.* Sparkes *et al.*, 2021). Preliminary examination of airborne geophysical data suggests the presence of a significant northeast trending fault structure within the area of Mary March Brook (Figure 1), which locally displays a close spatial association with red sandstone and interbedded conglomerate of an inferred Carboniferous age, highlighting the presence of significant fault structures in the area.

ALTERATION AND VMS MINERALIZATION

This section summarizes results obtained from select drillholes that were examined using SWIR spectrometry to characterize the mineralogy of hydrothermal alteration zones that were historically described as "sericite". As much of this alteration is concealed by surficial cover, the distribution of these prospects is largely defined through diamond drilling, which has been conducted intermittently since the early 1920s. This discussion starts with the alteration zones developed immediately to the east of the main Buchans deposits and then continues along the belt as far east as the Mary March Brook prospect (Figure 1). The drillholes that were examined from each prospect, along with the total number of spectral measurements collected for each area, are summarized in Table 1.

BUCHANS AREA (LUCKY STRIKE/ ROTHERMERE DEPOSITS)

A limited study of the Buchans area (west of the Airport Thrust Fault) was initiated to examine the spectral signature of the hydrothermal alteration developed in the immediate footwall of *in-situ* massive sulphide mineralization at the Lucky Strike deposit (Figure 1). In addition, select drillholes from the Rothermere deposit were examined to compare the spectral signature of the alteration associated with transported ore proximal (<1 km) to *in-situ* mineralization (Lucky Strike deposit).

The use of SWIR spectroscopy has not been systematically applied in the area. The first use of this technique was by van Hees (2011), but this study only analyzed select samples and largely targeted the footwall zone to the Lucky Strike deposit (Lundberg deposit). The current study builds on this earlier spectral work and represents a more comprehensive collection of systematic downhole measurements from key areas. As part of this study, select intervals of three drillholes (H-08-3356, H-08-3407, Moore *et al.*, 2009; H-12-3447, Moore *et al.*, 2013b) were investigated to determine the nature of the "sericitic" alteration developed within the immediate footwall rocks of the Lucky Strike deposit. Investigation of the adjacent Rothermere deposit included the examination of select intervals from seven historical ASARCO drillholes (Plate 1; Table 1).

Previous Work

The Buchans area has an extensive history of mineral exploration, beginning in the early 1900s. For a detailed discussion of this exploration history the reader is referred to Winter (2000) and Moore and Butler (2019). More relevant work to the current investigation includes previous studies focused on the alteration associated with massive sulphide mineralization within the Buchans area, such as: Henley and Thornley (1981), Thurlow (1981), Winter (2000) and van Hees (2011). The first spectral studies of alteration in the area were conducted by van Hees (2011), which built on the early x-ray diffraction and microprobe work of Henley and Thornley (1981) and Winter (2000). These studies noted the phengitic affinity of white mica alteration within the upper stratigraphic levels of the Buchans Group, while white micas developed in footwall rocks to the mineralization contained characteristics indicative of more muscovitic compositions.

Local Geology

The Buchans area is divided into four main units by Thurlow and Swanson (1987), and in ascending stratigraphic order these are the Lundberg Hill, Ski Hill, Buchans River and Sandy Lake formations (Figure 2). However, the stratigraphy of the Buchans area has recently been modified by Allen and Schofield (2023), and now include the introduction of an upper (Buchans Camp member) and lower (Clementine, and Oriental–Sandfill members) Buchans River formation, in addition to re-introducing the Intermediate Footwall member within the Ski Hill Formation (Allen *et al.*, 2024 and references therein). Rocks of the Lundberg Hill Formation are

Table 1. Summary of the drillholes examined and the total number of spectra and geochemical samples collected from each alteration zone

Alteration Zone	Drillholes Examined	Spectra	Geochemical Analyses
*Lucky Strike	H-08-3356; H-08-3407; H-12-3447	202	18
*Rothermere	H-0813; H-0816; H-0817; H-0819; H-0823; H-0842; H-0843	478	0
Airport	H-0270	67	14
Sandfill	BR-2K-01-004; H-07-3349; H-09-3413; H-1683; H-1910	418	11
Powerhouse	BE-96-011; BE-97-019; BE-97-020; BR-99-04-001; H-3319; H-3320	452	31
Middle Branch East	BE-97-018	73	5
Woodman's Brook	BJ-046	118	28
Tower	BJ-011; BJ-012; BJ-023; BJ-034; BJ-035; BR-2K-08-005; BR-99-08-001; LS-2K-005	448	34
Little Sandy	BJ-013; BJ-016; BJ-021; BJ-022; BJ-055; BJ-056; BJ-058; BJ-049; LS-07-017; LS-94-001	265	14
Seal Pond	SP-95-001	66	12
Beaver Pond	BJ-083	38	8
Mary March Brook	BJ-03-015; BJ-92-005ext; BJ-97-007	234	20
Connell	CP-93-001; RI-001	155	8
Mary March	BJ-065; BJ-066; BJ-067; BJ-068; BJ-069; BJ-073; BJ-074; BJ-077; BJ-078; MM-04-002; MM-12-025; MM-14-033; MM-14-035; MM-19-036; MM-19-037	1163	67

* Select intervals only for some drillholes

Plate 1. *Aerial image of the Lucky Strike and Rothermere deposits outlining the geographical distribution of diamond-drill holes examined with SWIR as part of this study.*

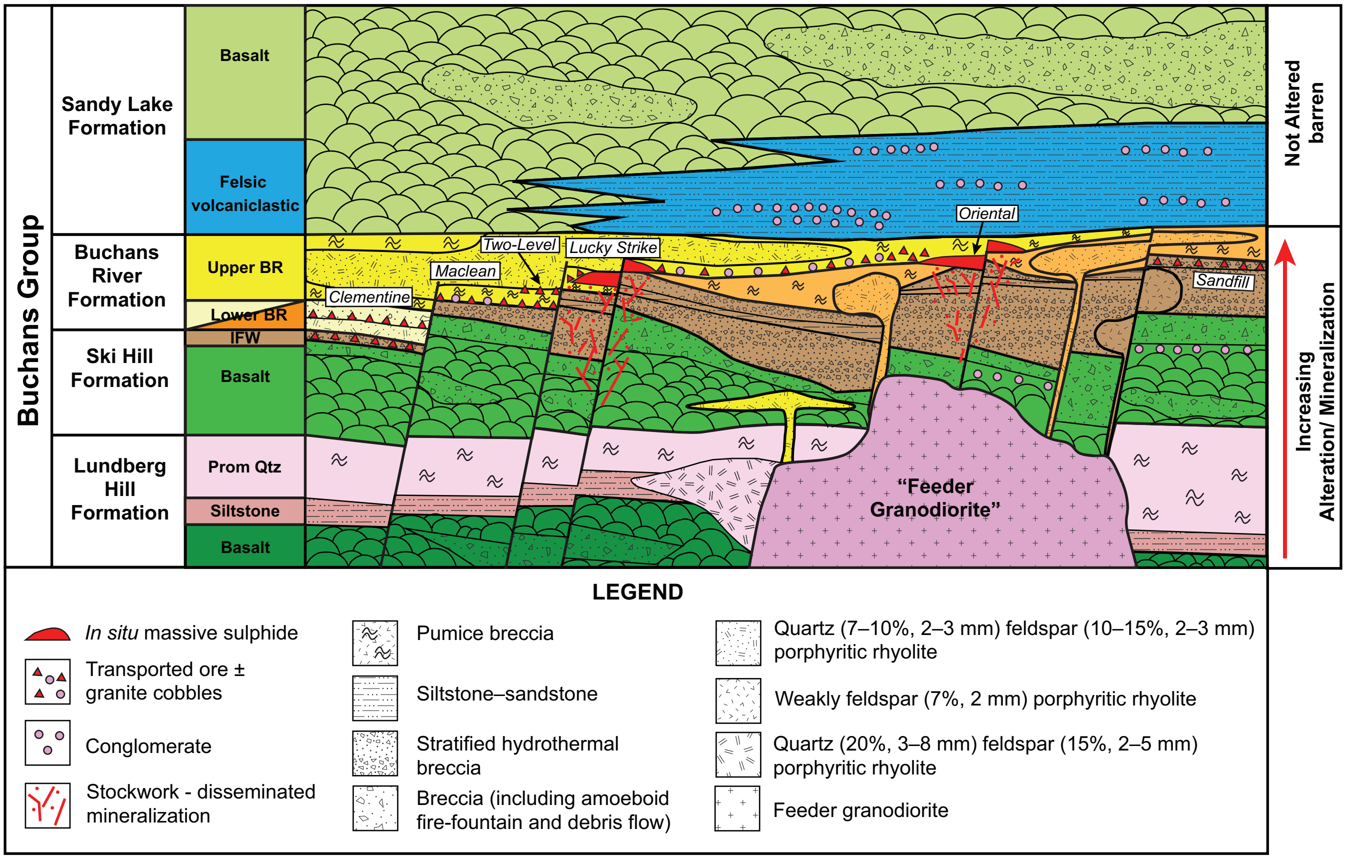

Figure 2. *Revised stratigraphic scheme for the Buchans area (Allen and Schofield, 2023; modified from Thurlow and Swanson, 1987). Abbreviations: Prom Qtz–Prominent quartz unit; IFW–Intermediate Footwall member of the Ski Hill Formation. The division of the lower Buchans River Formation illustrates the Clementine (light yellow) and Oriental-Sandfill (orange) members.*

composed of felsic dominated volcanic and volcaniclastic rocks and associated clastic sedimentary rocks along with lesser mafic volcanic rocks. This unit is, in turn, conformably overlain by mafic pillow lavas and associated hyaloclastite breccias of the Ski Hill Formation. These rocks display a gradational transition into overlying felsic volcanic rocks of the Buchans River Formation, the main host to VMS mineralization, along with lesser conglomeratic units hosting ore-clasts derived from *in situ* massive sulphide mineralization. The Buchans River Formation is locally conformably overlain by fine to coarse arkosic, felsic-dominated sedimentary rocks and pillow basalt of the Sandy Lake Formation. This unit postdates the development of mineralization and marks a change in the overall depositional environment. Numerous south-directed thrust faults transect the stratigraphy, locally resulting in the structural repetition of units (Thurlow and Swanson, 1987; Thurlow, 2010). These structures are interpreted to have reactivated earlier syn-volcanic normal faults, which were important controls on the local development of mineralization, with all major orebodies being bound on at least one side by a thrust fault (Thurlow, 2010).

Mineralization

The Buchans area has been the focus of numerous reports related to the development of its VMS mineralization (*e.g.*, Swanson *et al.*, 1981 and papers therein; Kirkham, 1987 and papers therein; Winter, 2000; Thurlow, 2010; van Hees, 2011; Harrington *et al.*, 2019); the following represents a summary from these sources.

Mineralization developed in the Buchans area generally conforms to three main styles of VMS mineralization, these include: *in-situ* (*e.g.*, Lucky Strike/Oriental), stringer or stockwork (*e.g.*, Lundberg), and transported ores (*e.g.*, Rothermere/MacLean; Thurlow, 2010). Recent work by Allen and Schofield (2023) have identified two camp-wide (at the top of the lower Buchans River Formation and at the top of the Intermediate Footwall member) and three additional, local, ore horizons in the Buchans area (Figure 2). Mineralogically, ore material consists of a complex intergrowth of fine-grained sphalerite, galena, barite and chalcopyrite; minor amounts of enargite, native silver, ruby silver, gold, argentite, tennantite–tetrahedrite and gold tellurides are also noted in association with the VMS mineralization (Thurlow *et al.*, 1975).

The stockwork zone locally contains veins of massive pyrite, massive quartz–carbonate containing disseminated sphalerite–galena–chalcopyrite, bladed barite, carbonate with disseminated sphalerite–galena–chalcopyrite and massive polymetallic sulphides (Plate 2; van Hees, 2011). The presence of bladed barite and calcite, which is noted to occur near the top of the stockwork zone, has been inferred to represent evidence of seawater infiltration and possibly boiling of the hydrothermal fluids (van Hees, 2011). Such features provide supporting evidence of a potential magmatic–hydrothermal fluid input, as suggested by Kowalik *et al.* (1981) and Sawkins and Kowalik (1981), and imply that VMS mineralization potentially formed within a transitional VMS to epithermal environment (van Hees, 2011).

Alteration

Within the footwall zone of the Lucky Strike deposit, spectral data demonstrates that the predominant alteration developed immediately beneath the massive sulphide mineralization consists of muscovitic illite, siderite, montmorillonite and lesser chlorite. In drillhole H-08-3356 (Plate 1), the upper part of the drillhole consists of massive sulphide mineralization crosscut by abundant carbonate veining. The SWIR spectral data from this mineralized zone is dominated by aspectral (no identifiable mineral signature) and siderite, along with lesser muscovite, muscovitic illite, chlorite and montmorillonite toward the base of the mineralization (Figure 3). Upon transitioning into the underlying siliciclastic and volcanic rocks, muscovitic illite and lesser chlorite become the dominate alteration minerals. Within these footwall rocks, there is a general trend from approximately 200 m depth toward the base of the massive sulphide mineralization (~50 m depth) which illustrates a shift in the Al-OH spectral feature (~2200 nm) to shorter spectral wavelengths (from ~2210 to 2202 nm) with decreasing distance from mineralization (Figure 3).

In drillhole H-08-3407 (Plate 1), the examined interval (130–165 m) consisted of footwall rocks hosting stockwork mineralization of the Lundberg deposit (Plate 3). Here, the "sericite" alteration, locally characteristically bright green, overprints basaltic rocks of the Ski Hill Formation (Figure 2) and is classified as a mixture of muscovitic illite and montmorillonite based on spectral data. The SWIR data collected

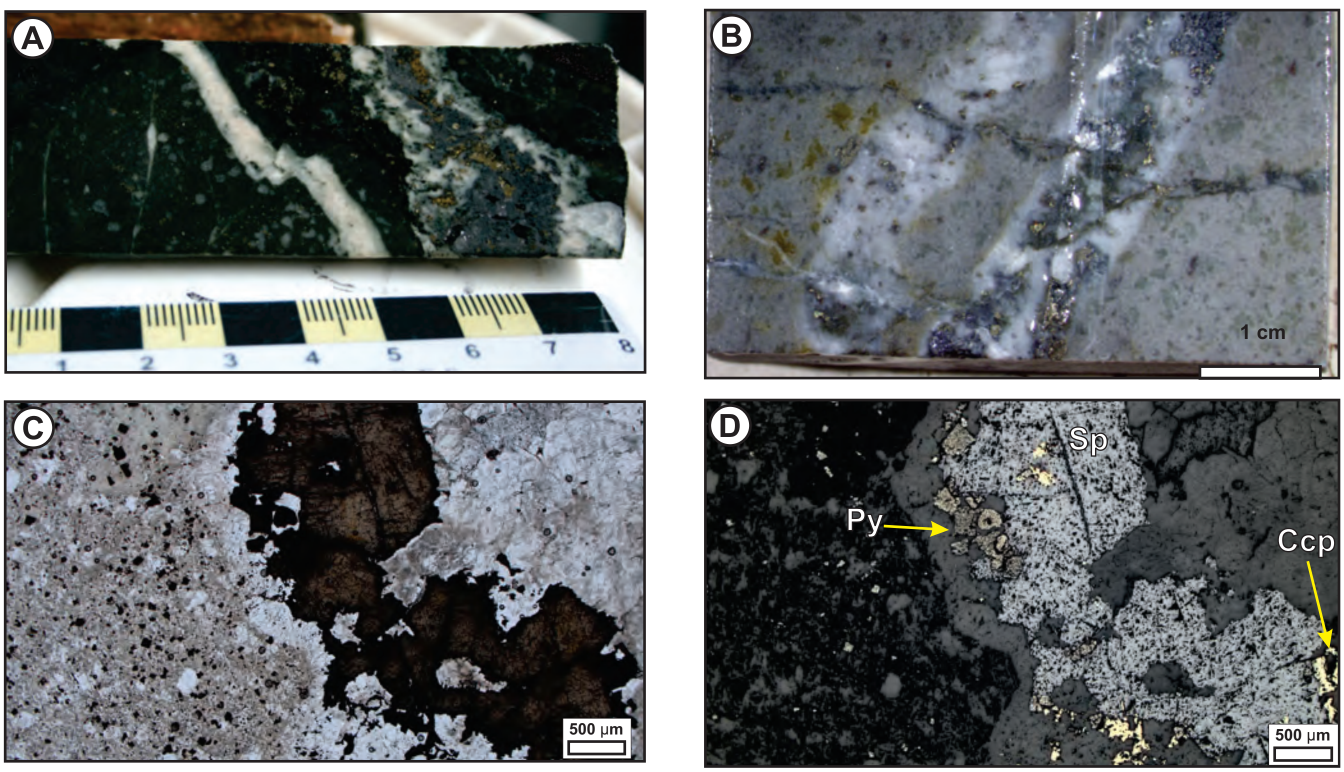

Plate 2. *A) Stockwork-style veining associated with strong Fe–Mg chlorite alteration, based on spectral data; DDH H-2871, 183.5 m depth; B) Stockwork veining hosted within a muscovitic illite–montmorillonite–pyrite altered mafic volcanic rock; DDH-0244, 140.5 m depth; C) Plane-polarized light photomicrograph of vein shown in (B), outlining the quartz–sphalerite–chalcopyrite–galena vein and marginal disseminated pyrite within the host rock; D) Reflected light image of (C) showing the distribution of sphalerite (Sp), chalcopyrite (Ccp), and pyrite (Py) within the stockwork veining.*

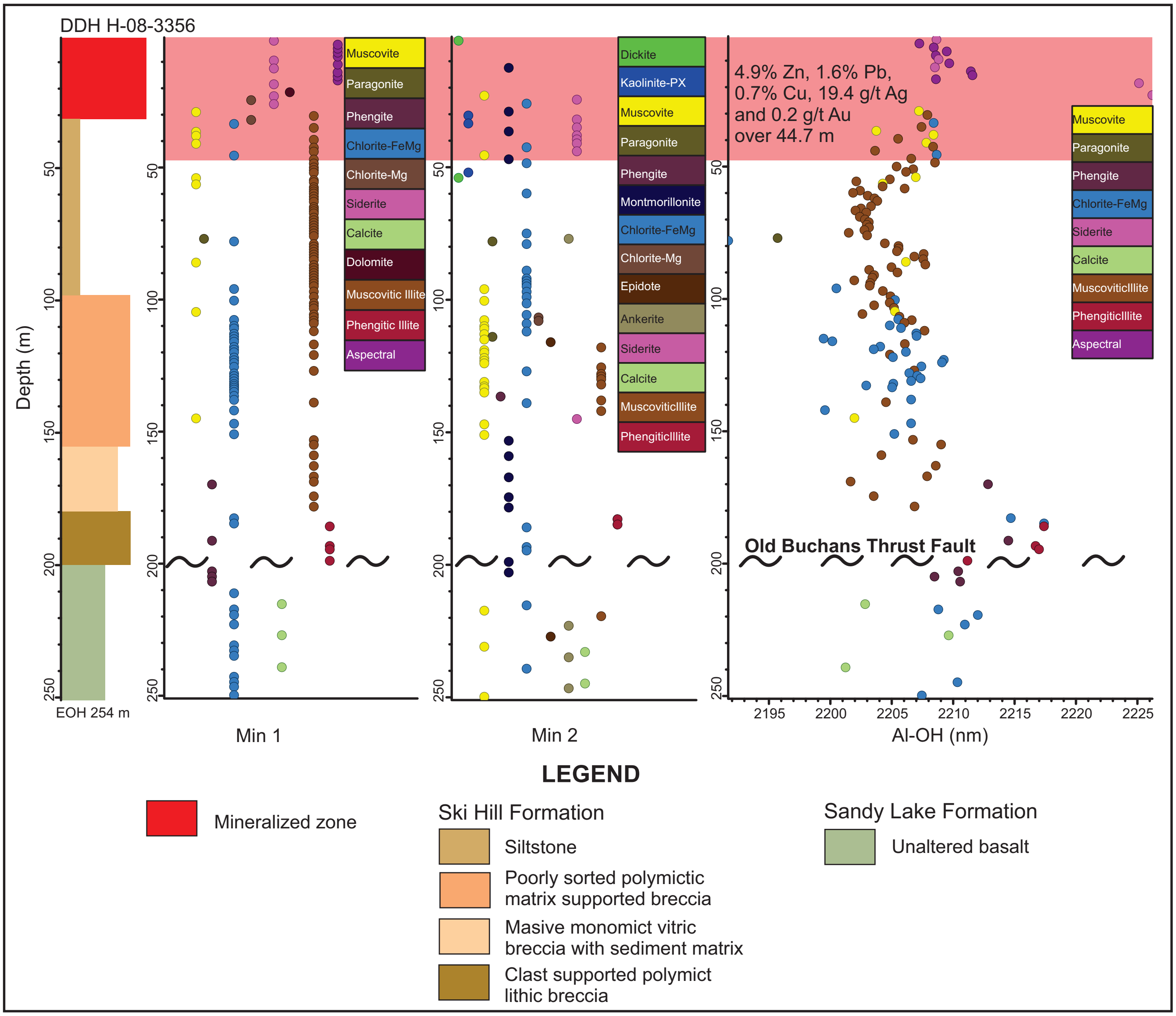

Figure 3. *Strip log for DDH H-08-3356, outlining the distribution of massive sulphide mineralization and underlying units, along with corresponding spectral data showing the distribution of mineral 1 (Min 1), mineral 2 (Min 2) and the related Al-OH absorption feature; Lucky Strike deposit. Assay values taken from Moore* et al. *(2009).*

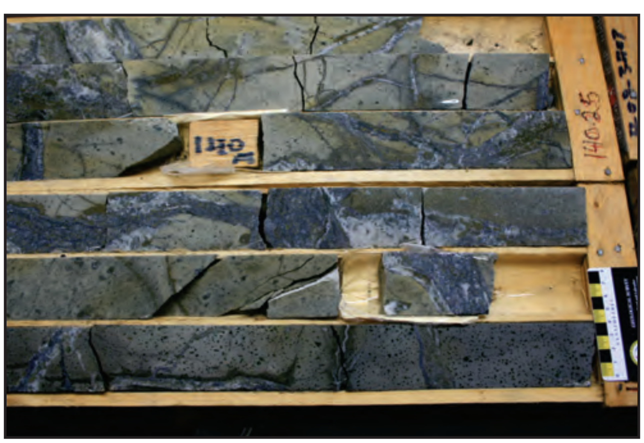

Plate 3. *Stockwork polymetallic sulphide and carbonate veining hosted within basaltic rocks of the Ski Hill Formation, displaying intense muscovitic illite white mica alteration; Lucky Strike deposit, DDH H-08-3407, 140 m depth.*

over this select interval displays consistent Al-OH values (~2207 nm) over its entire length (~35 m). These values are like those obtained from the rocks immediately underlying massive sulphide mineralization in drillhole H-08-3356, but given the narrow interval that was investigated, no systematic variation of the Al-OH feature was observed.

Within the area of the adjacent Rothermere deposit, select intervals were examined from both mineralized and barren drillholes (Table 1). In drillhole H-0817 (Plate 1), two intervals (100–260 m; 260–470 m) were examined which contain distinct structural panels hosting similar volcanic facies, but only one panel contains hydrothermal alteration and related mineralization (based on industry logging). The first structural panel (110–260 m) is characterized by phengite and phengitic illite white mica alteration of the rhyolite hyaloclastite unit, displaying Al-OH wavelengths between 2015–2025 nm (Figure 4). This unit displays weak to moderate white mica alteration of the feldspar phenocrysts and supporting matrix (Plates 4A and 5A, B).

Within the second structural panel, the upper portion of the quartz–feldspar-phyric rhyolite (320–430 m) overlying the mineralized zone displays similar alteration signatures to that of the overlying structural panel and is dominated by phengite and phengitic illite white mica alteration and have

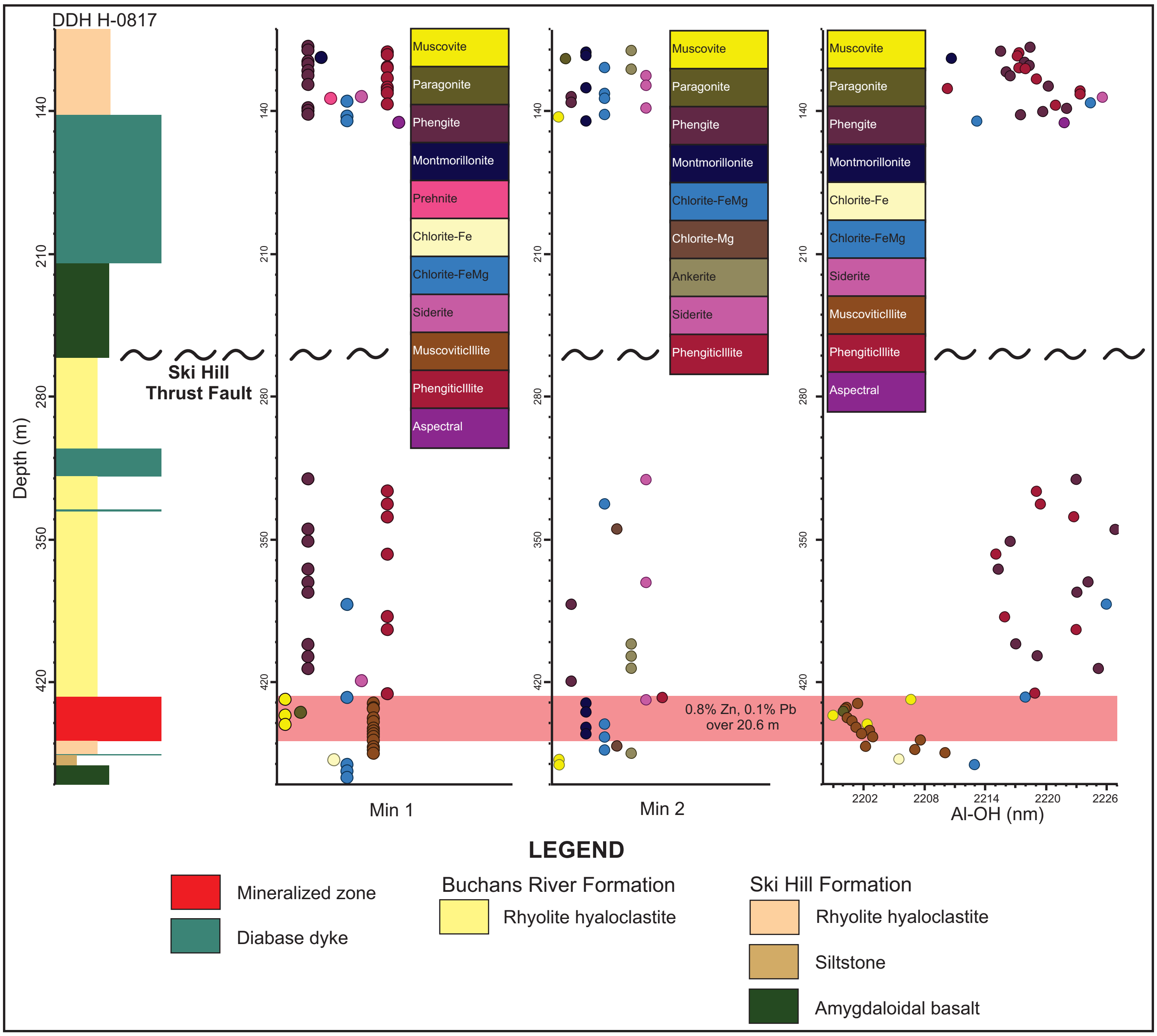

Figure 4. *Partial strip log for DDH H-0817, outlining the distribution of the mineralized horizon and significant fault structures within the drillhole. Also shown are the corresponding spectral data outlining the distribution of mineral 1 (Min 1), mineral 2 (Min 2) and the related Al-OH absorption feature; Rothermere deposit. Assay values taken from historical ASARCO drill logs.*

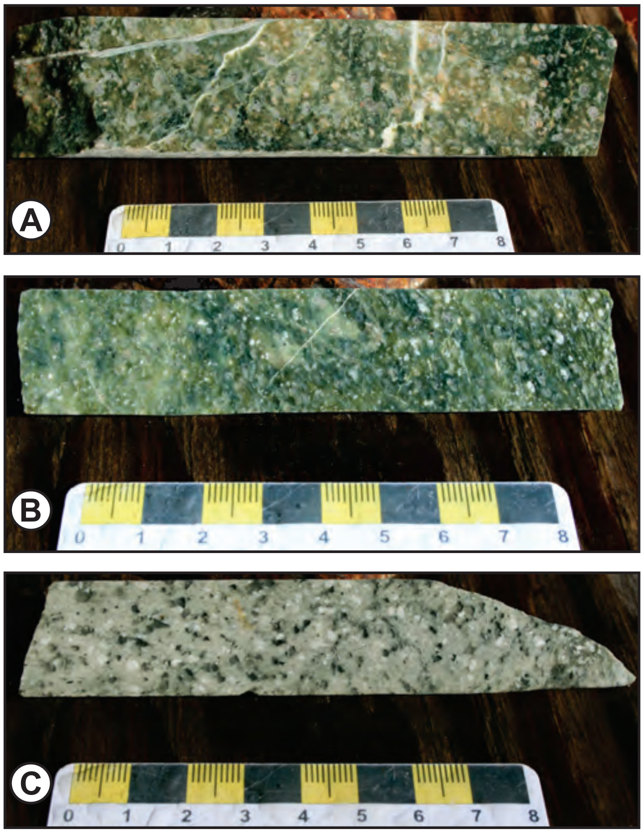

Plate 4. *Representative photographs of the Buchans area alteration. A) Quartz–feldspar-phyric rhyolite, containing phengite alteration, 130 m depth; Rothermere deposit, DDH H-813; B) Quartz–feldspar-phyric rhyolite, containing phengitic illite alteration, 220 m depth; Rothermere deposit, DDH H-813; C) Quartz–feldspar-phyric rhyolite, containing muscovite alteration, 380 m depth; Rothermere deposit, DDH H-813.*

Al-OH wavelengths between 2015–2025 nm (Plates 4B and 5C, D; Figure 4). However, around the mineralized zone there is a notable shift in the Al-OH values to shorter spectral wavelengths (~2200 nm) in association with the development of muscovitic illite and lesser muscovite and montmorillonite alteration (427–455 m; Plate 4C; Figure 4). In thin section, this alteration results in the complete destruction of primary feldspar, but the quartz phenocrysts displaying characteristic resorption textures like those observed in the less altered equivalents remain (Plate 5E, F). The sharp shift to phengite dominated alteration immediately above the mineralized zone may indicate a structurally modified contact, as spectral data from other drillholes in this area locally display a more gradational transition of the Al-OH wavelength values over an approximately 30 m interval (*see* below).

Drillhole H-0819 is located on the margin of the mineralized zone within the Rothermere deposit (Plate 1), intersecting weakly developed mineralization over approximately 3 m (Figure 5). Despite the lack of mineralization, this drillhole still displays the distinct shift of the Al-OH values to shorter spectral wavelengths (~2202 nm) in association with the mineralized horizon. In this drillhole, the hanging-wall rocks also display the effects of alteration related to the mineralized horizon, displaying a gradational transitioning up-section to background Al-OH values (~2225 nm), over approximately 30 m within the hanging-wall sequence (Figure 5).

AIRPORT

The Airport prospect represents the northernmost alteration zone examined and is located immediately east of the main Buchans camp and the Airport Thrust Fault (Figure 1). Although the Airport prospect is mapped as having a large aerial extent, the overall alteration and accompanying mineralization identified is relatively minor. A second zone of alteration, referred to as the Airport South prospect (Winter, 2000), located approximately 1 km south of the Airport prospect, is defined by only two drillholes. This area is associated with the local development of intense white mica alteration accompanied by anomalous zinc and gold enrichment, assaying up to 0.5% Zn and 128 ppb Au over 11.6 m (historical ASARCO drill log; DDH H-0395; Figure 6).

Previous Work

This prospect was originally drilled by ASARCO, first in the late 1930s, and again in the early 1970s. Subsequent investigations were conducted by Newfoundland Mining and Exploration Ltd., through geophysical surveying and diamond drilling in the late 1990s and early 2000s (Saunders and Scott, 1996; Saunders *et al.*, 2000a; Harris and Woods, 2001a). This work identified localized stockwork-style mineralization hosting anomalous zinc enrichment in association with quartz–sericite–chlorite–pyrite alteration. Local drillhole intersections assay up to 0.46% Zn, along with anomalous lead and gold over 4.0 m (Saunders *et al.*, 2000b).

Local Geology

The alteration and related mineralization is hosted within intermediate tuffs of the MMBG (Lundberg Hill Formation of Thurlow and Swanson, 1987; Winter 2000). These rocks structurally overlie arkosic sandstone, and basalt of the Sandy Lake Formation (Buchans Group; Thurlow and Swanson, 1987) and are separated by the Airport Thrust Fault (Thurlow *et al.*, 1992).

Mineralization

The Airport prospect is characterized by weak to moderate chlorite–quartz ± "sericite" ± carbonate alteration in association with stringer-stockwork style mineralization.

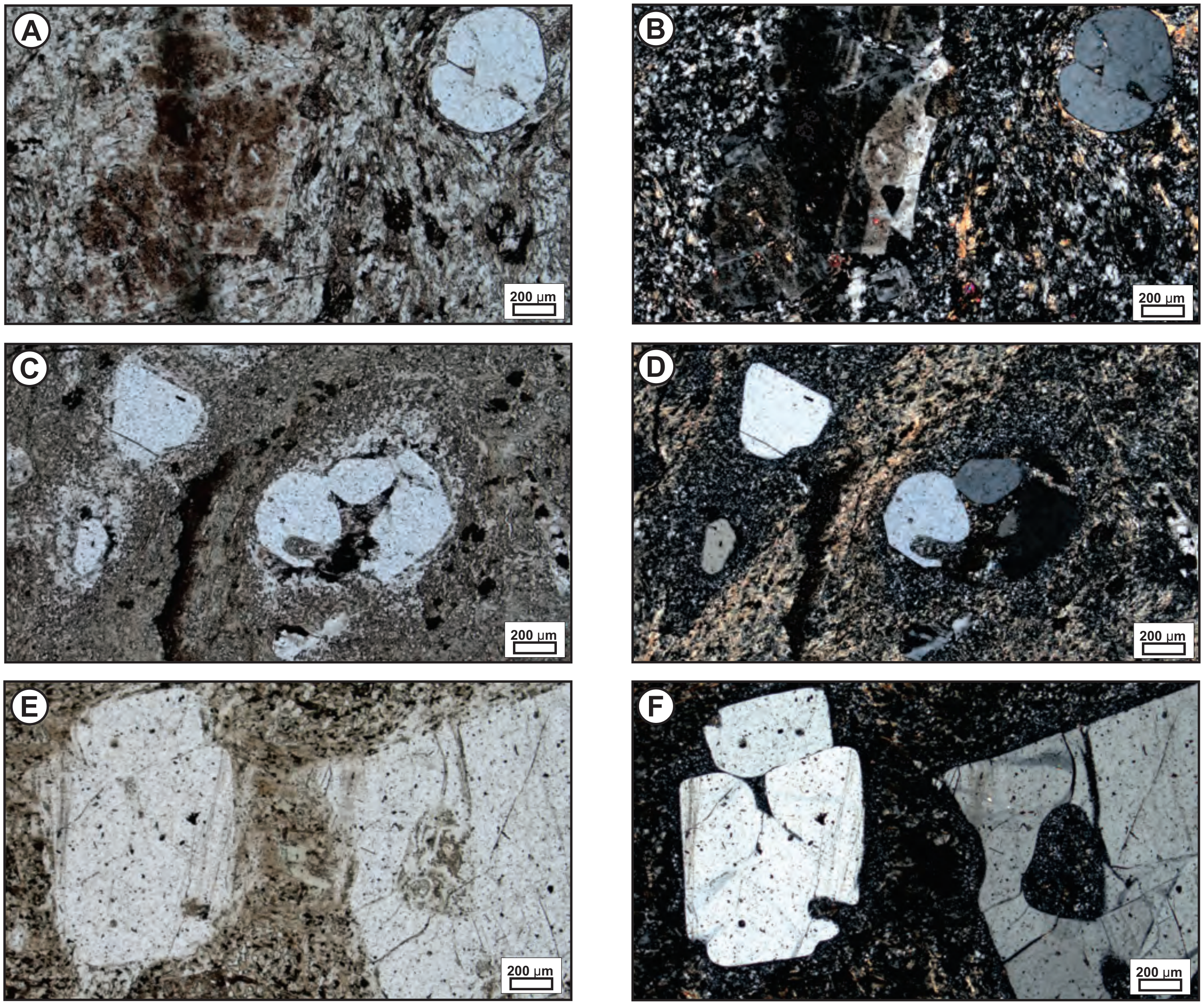

Plate 5. *Quartz–feldspar-phyric rhyolite, displaying distinct resorption textures of the quartz phenocrysts. A) Plane-polarized light image displaying primary feldspar and quartz phenocrysts in a fine-grained quartz-rich matrix displaying weakly developed white mica alteration; GS-21-189, 130 m depth; Rothermere deposit, DDH H-813; B) Cross-polarized image of (A); C) Plane-polarized light image displaying quartz phenocrysts in a fine-grained quartz-rich matrix displaying moderately developed white mica alteration; GS-21-190, 220 m depth; Rothermere deposit, DDH H-813; D) Cross-polarized image of (C); E) Plane-polarized light image displaying quartz phenocrysts in a fine-grained quartz-rich matrix displaying strongly developed white mica alteration; GS-21-191, 380 m depth; Rothermere deposit, DDH H-813; F) Cross-polarized image of (E).*

Sphalerite and chalcopyrite predominate, however anomalous gold and lead are also reported in some samples containing elevated zinc values (Saunders *et al.*, 2000b; Harris and Woods, 2001a).

Alteration

Limited spectral data from the area illustrates that Fe–Mg- and Mg-chlorite are predominant, along with discrete (10–40 m) zones of more intense white mica alteration characterized by paragonite–paragonitic illite and muscovitic illite and lesser montmorillonite (Figure 7; Plate 6). These zones of intense white mica alteration are generally devoid of any significant sulphides but are flanked by zones hosting weak to moderate disseminated pyrite, all of which is hosted within intermediate volcanic rocks of the Lundberg Hill Formation. Notably, the best assay from the drillhole shown in Figure 7 (0.7% Zn and 0.5% Pb over 1.5 m), is situated above a zone, up to 40 m thick, of muscovitic illite alteration. This altered zone is immediately underlain by rocks correlated with the

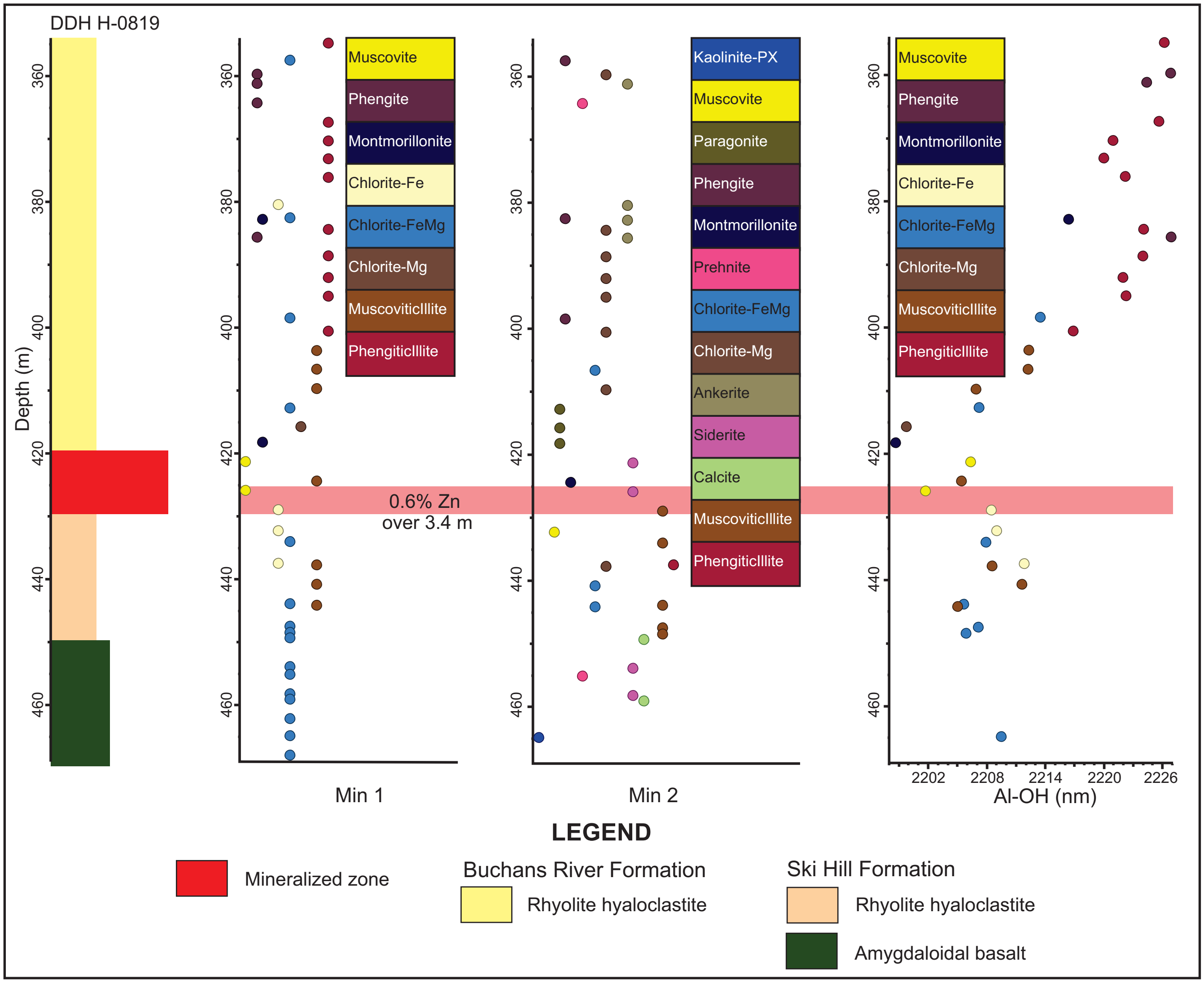

Figure 5. *Partial strip log for DDH H-0819, outlining the distribution of the mineralized horizon and the corresponding spectral data showing the distribution of mineral 1 (Min 1), mineral 2 (Min 2) and the related Al-OH absorption feature; Rothermere deposit. Assay values taken from historical ASARCO drill logs.*

Plate 6. *Fe–Mg chlorite–paragonitic illite altered intermediate volcanic rock, hosting local stringer pyrite, transitioning into bleached, paragonite–montmorillonite dominated alteration toward the bottom of the photograph, which is notably devoid of any significant disseminated pyrite. Airport prospect, DDH H-0270, 70–100 m depth.*

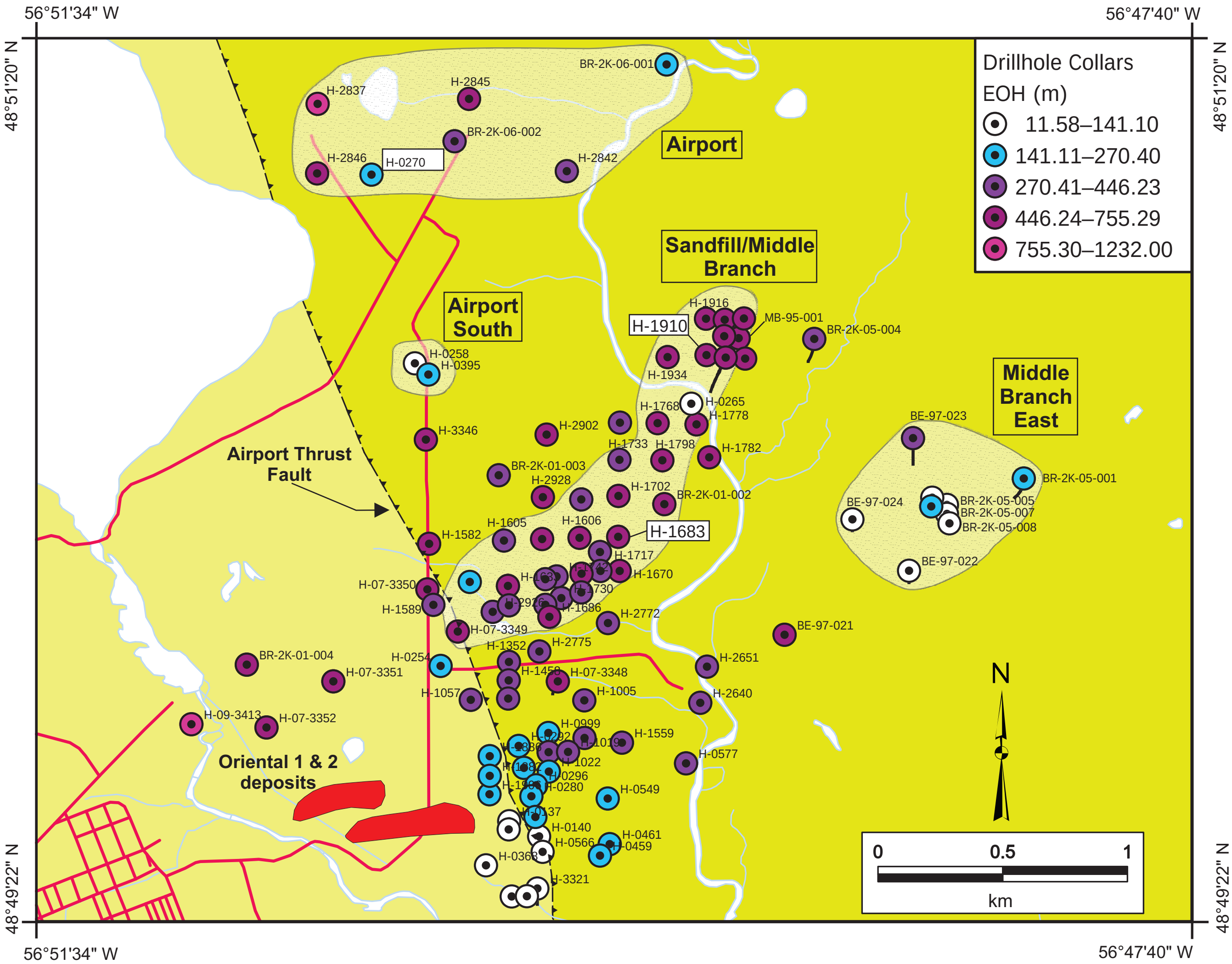

Figure 6. *Location map showing the distribution of diamond-drillholes and geology within the area of the Airport and Sandfill prospects. Refer to Figure 1 for legend. Note, only select drill holes are shown in the area west of the Airport Thrust Fault.*

Sandy Lake Formation, which is presumed to be separated from the overlying rocks by the Airport Thrust Fault. The immediate footwall rocks to the Airport Thrust Fault are dominated by phengitic illite spectral signatures and are unaltered but overlie altered volcanic rocks of an undetermined affinity, which host anomalous mineralization (Figure 7).

The Airport South prospect was only investigated through the limited evaluation of select grab samples of white mica alteration intersected in drillcore. However, these samples highlight the similar development of paragonite and paragonitic illite–montmorillonite alteration in association with base metal enrichment. The only difference being that this alteration is locally overprinted by an intense foliation developed within the strongly altered intermediate volcanic rocks, which is also accompanied by anomalous base- and precious-metal enrichment (*e.g.*, 0.6% Zn, 22 g/t Ag and 300 ppb Au over 1.5 m; historical ASARCO drill log; DDH H-0395, 40–43 m; Figure 6; Plate 7).

SANDFILL/MIDDLE BRANCH

Approximately 1.5 km south of the Airport prospect is the Sandfill prospect, which extends northeast into an area historically referred to as the Middle Branch prospect (Figure 1). The Sandfill and Middle Branch prospects were identified through diamond drilling and represent two areas noted to contain mineralized clasts hosted within a volcaniclastic debris flow/conglomerate unit, separated by approximately 1 km along a northeasterly trend (Figure 6). These two occurrences are similar in appearance to other examples of transported ore within the Buchans area and were originally interpreted to be hosted within the Buchans River Formation (Buchans Group; Thurlow and Swanson, 1987). However,

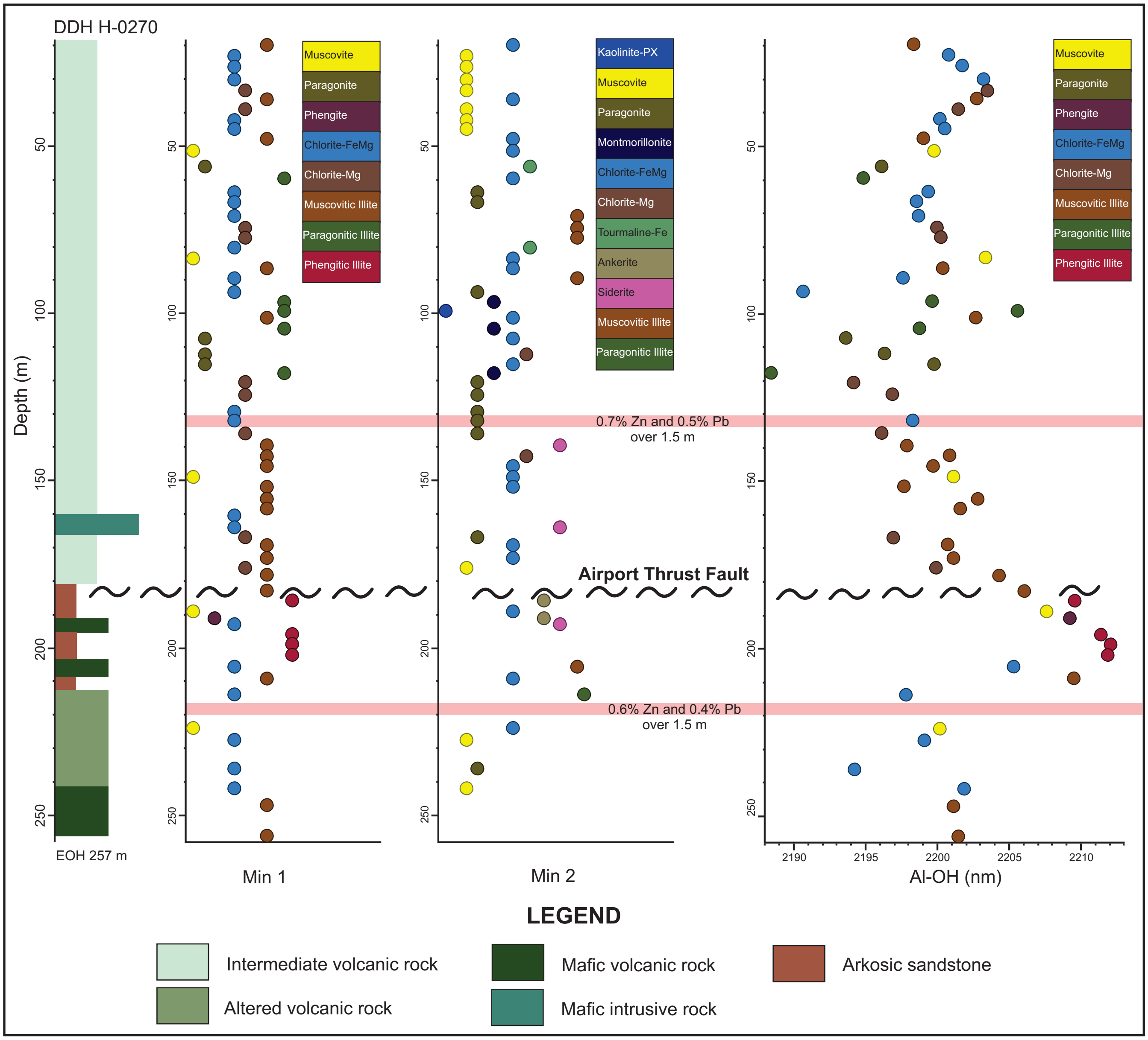

Figure 7. *Strip log for DDH H-0270, outlining the distribution of spectral data, mineral 1 (Min 1) and mineral 2 (Min 2), along with the related Al-OH absorption wavelength and location of select mineralization, Airport prospect. Assay values taken from historical ASARCO drill log.*

recent reinterpretations of the area by Allen and Schofield (2023) assign the unit hosting the transported ore to the Intermediate Footwall member of the Ski Hill Formation (Figure 2). This contrasts earlier interpretations of Thurlow and Swanson (1981) who inferred the source of the transported ore to be the Oriental deposit, which based on the work by Allen and Schofield (2023), is located stratigraphically above the transported ore of the Sandfill prospect.

In this area, diamond drilling has identified units of the Buchans River Formation within the structural footwall of the Airport Thrust Fault, extending for approximately 2 km along a northeasterly trend (Allen *et al.*, 2024 and references therein). However, in contrast to the Rothermere deposit, the Sandfill/Middle Branch prospect is not located proximal to any known *in situ* VMS mineralization and is therefore interpreted to represent an example of transported ore distal (>1 km) from a hydrothermal-vent environment.

Previous Work

This area has undergone considerable investigation due to the presence of transported ore clasts, like that observed in the main Buchans camp. The area was first drilled in the mid-

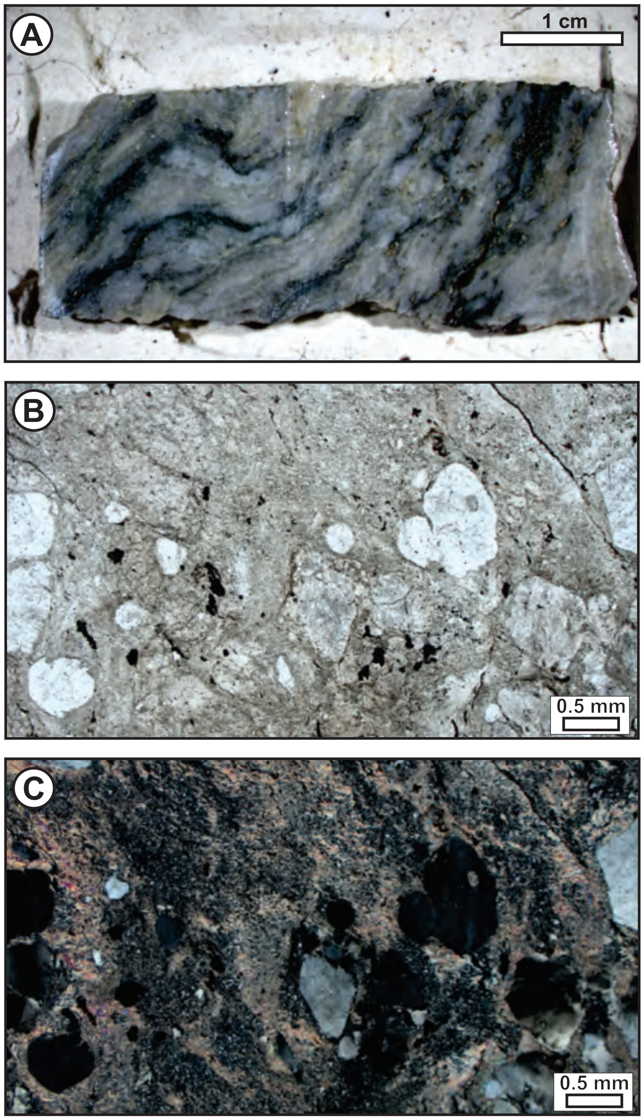

Plate 7. *A) Strongly foliated, paragonitic illite–montmorillonite–pyrite alteration from the Airport South prospect; DDH H-0258, 98.5 m depth; B) Plane-polarized light photomicrograph of the sample in (A), showing the distribution of disseminated pyrite within the white mica alteration, along with locally developed resorption textures within the quartz phenocrysts; C) Cross-polar photomicrograph of (B) highlighting the intense white mica alteration of the foliated volcanic protolith.*

1950s by ASARCO, and intermittent investigations continued up until the early 1970s. Through this work a historical estimated resource of 72 600 tonnes grading 9.2% Zn, 4.8% Pb, 1.4% Cu, 70.9 g/t Ag and 0.57 g/t Au was identified (Entwistle and Barnes, 1971). The area was subsequently investigated by BP Selco in the late 1980s (Thurlow *et al.*, 1987), Thunderwood Resources Ltd. in the mid-1990s (Tallman, 1995) and Buchans River Ltd. during the 2000s (Saunders *et al.*, 2000a; Moore *et al.*, 2008). Diamond drilling conducted during these exploration programs has continued to intersect anomalous zinc, lead and gold mineralization (*e.g.*, 0.71% Zn, 0.30% Pb and 0.81 g/t Au over 4.5 m; DDH H-07-3350; Moore *et al.*, 2008), along with more discrete zones of higher grade mineralization (*e.g.*, 1.2% Zn, 1.4% Pb and 0.03% Cu over 0.8 m; DDH BR-2K-01-002; Saunders *et al.*, 2000a). Most recently, the area has been investigated using airborne geophysical surveys and limited diamond drilling by Buchans Minerals during the late 2010s (Moore and Butler, 2019).

Local Geology

Rocks of the MMBG (Lundberg Hill Formation of Thurlow and Swanson, 1987; Winter, 2000) dominate the hanging wall of the Airport Thrust Fault and are predominantly composed of mafic to intermediate volcanic rocks along with lesser felsic tuffaceous and intrusive units. These rocks are locally host to zones of white mica alteration and associated, weakly developed, stringer-style mineralization. The rocks within the immediate footwall of the Airport Thrust Fault consist of either arkosic sandstone of the Sandy Lake Formation, or felsic volcanic rocks of the Buchans River Formation. The latter is host to the main mineralization developed in the area, which occurs as mineralized clasts within volcaniclastic debris flow/conglomerate.

Mineralization

Discrete zones of mineralization were noted within the hanging-wall rocks of the Airport Thrust Fault (*e.g.*, DDH H-1910, ~240 m), like those noted around the Airport prospect. Here, narrow, cm-scale stringer veinlets are host to anomalous zinc–lead–copper mineralization (Plate 8). Below the Airport Thrust Fault, rocks of the Buchans River Formation host mineralized clasts within conglomeratic units and lesser stringer stockwork-style mineralization hosted within felsic volcanic rocks (Winter, 2000; Plate 9). The mineralized clasts locally display precious-metal enrichment along with the base-metal mineralization, like that observed within the main Buchans camp (*e.g.*, 1.2% Zn, 0.4% Pb, 0.03% Cu and 2.3 g/t Au over 0.5 m; DDH H-07-3350; Moore *et al.*, 2008).

Alteration

Two drillholes, located approximately 1 km apart along the northeast–southwest trend of the Sandfill/Middle Branch prospect, were examined using SWIR. These two drillholes display many of the same characteristics regarding the overall alteration associated with mineralization in the area and highlight some key differences when compared with transported ore from a vent-proximal environment (*e.g.*, Rothermere deposit; *see* above).

For the southwestern-most drillhole examined, H-1683, the hanging-wall rocks of the Airport Thrust Fault are dominated by Fe- and Fe–Mg-chlorite, along with lesser muscovite, paragonite, muscovitic illite and paragonitic illite (Figure 8). Narrow zones of white mica-dominated alteration are commonly centred around the emplacement of felsic dykes (*e.g.*, ~120 m, Figure 8). Likewise, a distinct quartz-phyric rhyolite within the hanging-wall sequence is characterized by muscovitic illite, paragonitic illite and paragonite-dominated spectral signatures, which is interpreted as a syn-depositional alteration because it does not affect the surrounding units (Plate 10). This alteration is not inferred to be the result of hydrothermal alteration associated with VMS mineralization, as seen elsewhere in the region. Likewise, the general decrease in the Al-OH wavelength feature observed with increasing depth (80 to 250 m, Figure 8), is not related to hydrothermal alteration associated with the development of VMS mineralization but is, instead, related to the deposition of the distinct geological unit mentioned above (Plate 10). A sharp contrast in the Al-OH wavelength feature is observed across the Airport Thrust Fault, transitioning from shorter wavelength white micas in the hanging wall (<2200 nm) to longer wavelength (>2212 nm), phengite-dominated, white mica within the footwall. Of note is the predominant phengite- to phengitic-illite spectral signature associated

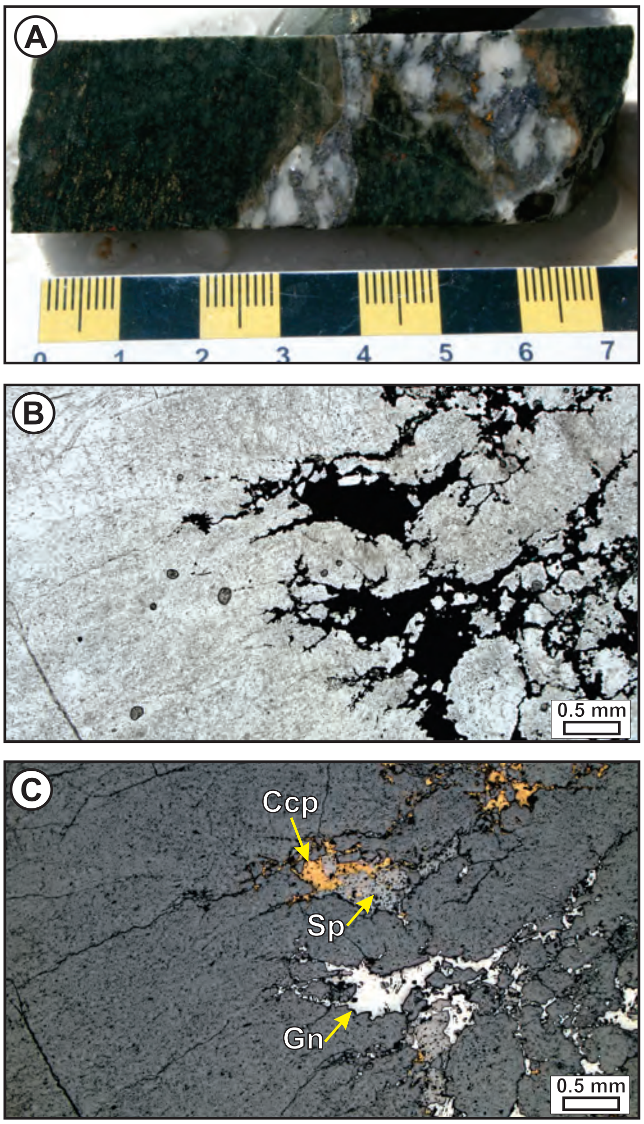

Plate 8. *A) Representative photo of rare sphalerite–galena–chalcopyrite-bearing stringer veinlets observed crosscutting the intermediate volcanic rocks within the hanging wall of the Airport Thrust Fault; Sandfill prospect, DDH H-1910, 56.5 m depth; B) Plane-polarized light photomicrograph of sample in (A), showing the brittle fracture-hosted distribution of the sulphides within the folded quartz vein; C) Reflected light image of (B) showing the distribution of sphalerite (Sp), galena (Gn), and chalcopyrite (Ccp).*

Plate 9. *Rare, sphalerite-rich, angular ore clast (yellow arrow) hosted within a conglomeratic unit of the Buchans River Formation; Sandfill prospect, DDH H-1683, 382 m depth.*

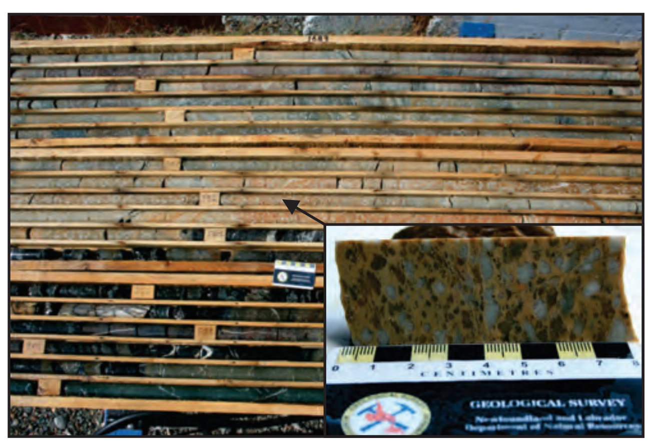

Plate 10. *Quartz-phyric rhyolite characterized by muscovitic illite and paragonitic illite spectral signatures, interbedded with relatively unaltered mafic volcanic rocks characterized by Fe–Mg-chlorite; Sandfill prospect, DDH H-1683, 156–180 m depth.*

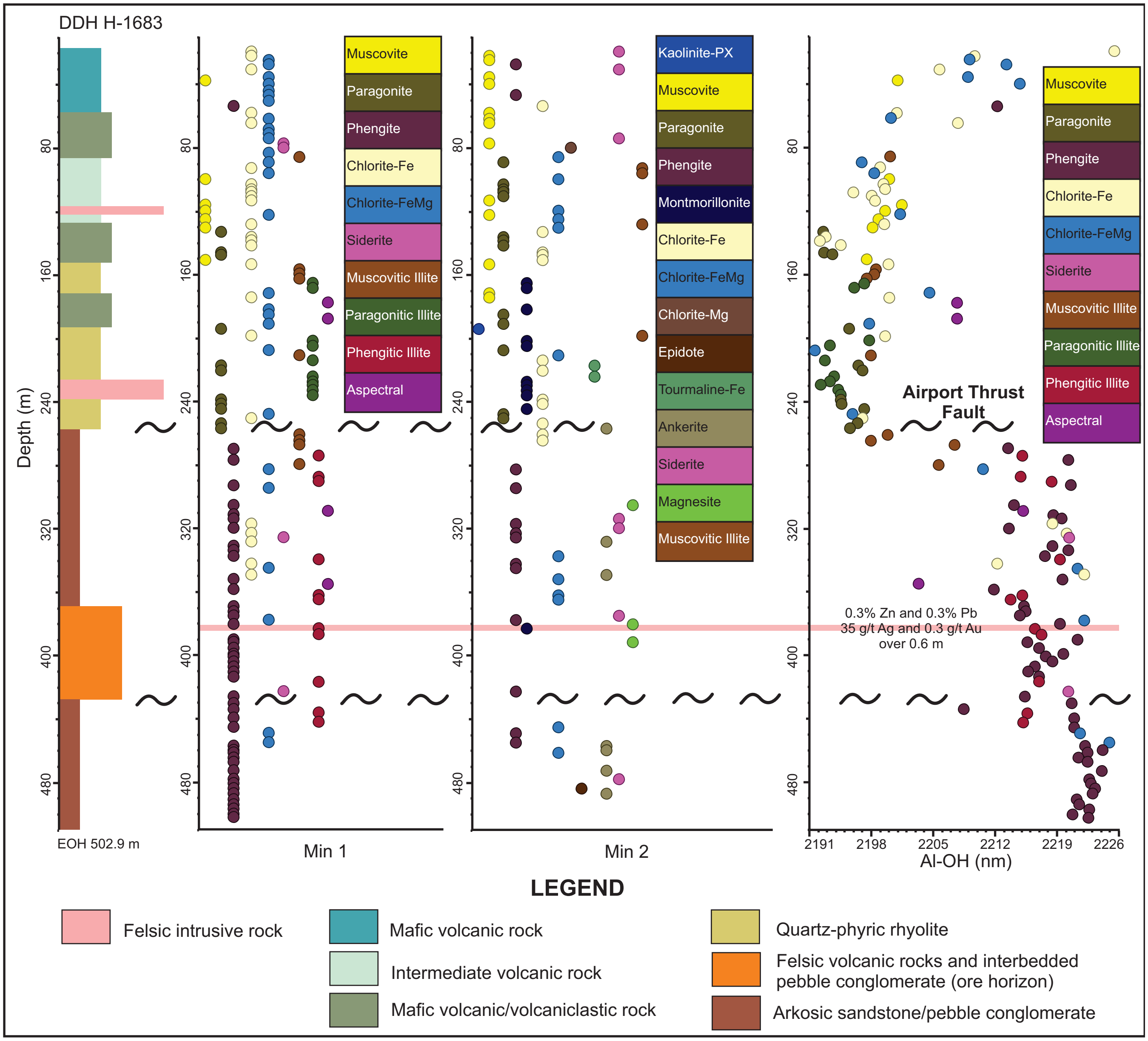

Figure 8. *Strip log for DDH H-1683, outlining the distribution of the spectral data, mineral 1 (Min 1) and mineral 2 (Min 2), along with the related Al-OH absorption feature and the location of select mineralization within the southwestern portion of the Sandfill/Middle Branch prospect. Assay values from Harris* et al. *(1997).*

with the ore horizon, which contrasts that of transported ore from a vent proximal environment (*e.g.*, Rothermere deposit).

In drillhole H-1910, located to the northeast, similar spectral results are observed. The hanging-wall sequence is dominated by Fe–Mg-chlorite along with lesser zones of white mica alteration (muscovite), commonly associated with the occurrence of weakly developed stringer mineralization (Figure 9). As observed in drillhole H-1683, the same quartz-phyric rhyolite unit, displaying a distinct muscovitic illite spectral signature, is developed towards the bottom of the hanging-wall structural panel (~450 m depth; Plate 11). The transition across the Airport Thrust Fault into the footwall zone is less apparent in the Al-OH values compared to that observed in drillhole H-1683 due to the similar spectral signatures of both the hanging wall and footwall rocks. Within the footwall zone, altered volcanic rocks of the Buchans River Formation immediately underlie the fault, displaying mixed spectral signatures ranging from muscovitic illite to phengitic illite. Like the drillhole to the southwest, the immediate area of the volcaniclastic debris flow/conglomerate ore horizon (~555 m), is characterized by a phengite dominated spectral signature.

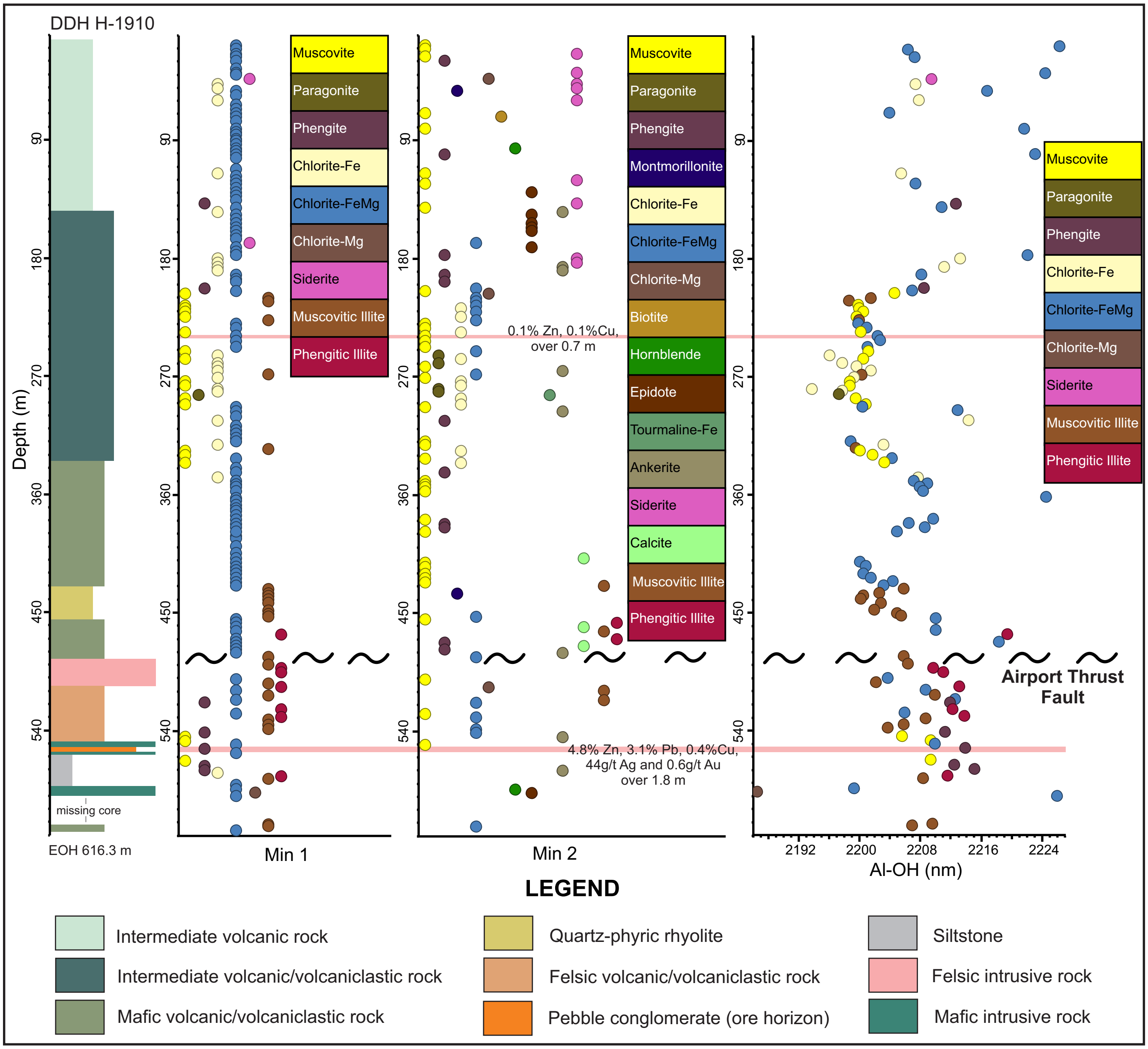

Figure 9. *Strip log for DDH H-1910, outlining the distribution of the spectral data, mineral 1 (Min 1) and mineral 2 (Min 2), along with the related Al-OH absorption wavelength and location of select mineralization within the northeastern portion of the Sandfill/Middle Branch Zone. Assay values from historical ASARCO drill log and this study.*

However, the overlying felsic volcanic rocks display Al-OH values indicative of hydrothermal alteration related to VMS mineralization as observed elsewhere in the region.

POWERHOUSE

The Powerhouse prospect is located approximately 2 km to the south of the Sandfill prospect and is proximal to the Oriental deposit, which is located 1 km to the northwest. The area of the Powerhouse alteration zone is covered by a thick blanket of quaternary material ranging from 10 to 20 m in thickness, thus most of the geological information on the area is obtained through diamond drilling. Exploration in the area has intersected anomalous zones of base and precious metal enrichment in association with significant thicknesses (up to 350 m) of altered felsic volcanic rocks inferred to be correlative with the Buchans River Formation (Saunders *et al.*, 1996, 1998; Harris *et al.*, 1999; Saunders *et al.*, 2000d). The alteration zone has been traced for upwards of 1.8 km along strike, has an apparent thickness of up to 350 m, and remains open both along strike and down dip (Saunders *et al.*, 2000a). This zone is situated proximal to the convergence of the

Plate 11. *Quartz-phyric rhyolite characterized by muscovitic illite spectral signature overlying relatively unaltered mafic volcanic rocks characterized by Fe–Mg-chlorite (bottom of photo); Sandfill prospect, DDH H-1910, 450 m depth.*

regionally extensive Powerline and Airport Thrust faults (Thurlow *et al.*, 1992), which bound the rocks assigned to the Buchans River Formation, and define its southeastern extent (Figure 10). However, given the structural complexity, combined with the extensive surficial cover, the exact distribution of the Buchans River Formation in this area is poorly constrained.

Previous Work

This area was first identified by regional drilling conducted by ASARCO and BP Selco in the mid-1980s and was later followed-up in the late 1990s and early 2000s, first by Newfoundland Mining and Exploration Ltd. and later by Buchans River Ltd. (Thurlow and Barbour, 1986; Saunders *et al.*, 1996, 1998, 2000a). Drilling at the Powerhouse prospect has outlined a zone of extensive alteration hosted within felsic volcanic rocks correlated with the Buchans River

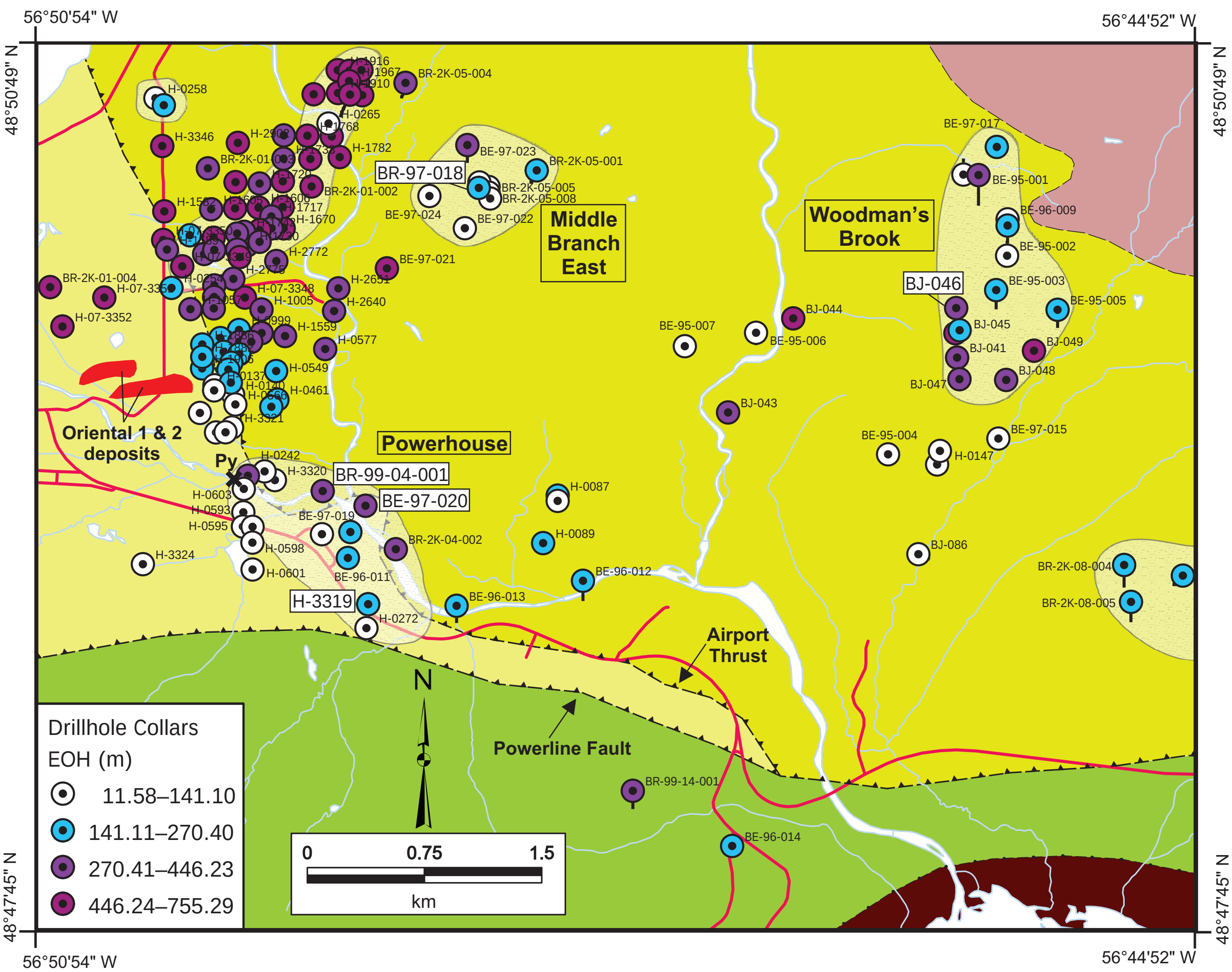

Figure 10. *Location map showing the distribution of diamond-drill holes and geology within the area of the Powerhouse, Middle Branch East and Woodman's Brook prospects. Refer to Figure 1 for legend.*

Formation (Saunders *et al.*, 1998). This alteration zone locally hosts disseminated zinc, lead and copper mineralization, assaying up to 3.90% Zn over 0.5 m (Saunders *et al.*, 2000a) as well as anomalous zones of precious-metal enrichment (*e.g.*, 0.2g/t Au and 9.6g/t Ag over 3.8 m; Saunders *et al.*, 1996).

Local Geology

Like that observed farther to the north, the hanging-wall rocks of the Airport Thrust Fault in the area of the Powerhouse prospect are dominated by mafic to intermediate volcanic rocks, which, locally, host weakly developed stringer mineralization (*e.g.*, DDH H-3320; >1.0% Zn, 0.1% Cu, 2.6 g/t Ag and 0.1 g/t Au over 0.7 m). These rocks are included within the MMBG (Lundberg Hill Formation of Thurlow and Swanson, 1987; Winter 2000; Saunders *et al.*, 1998; Allen *et al.*, 2024 and references therein). Most of the drillholes in the area collar directly into altered felsic volcanic rocks that are inferred to be correlative with the Buchans River Formation (Plate 12; Saunders *et al.*, 2000a). These rocks consist of variably altered felsic volcanic rocks along with lesser, quartz- and feldspar-phyric, syn-volcanic felsic intrusive units. The altered volcanic rocks are structurally truncated by both the overlying Airport Thrust Fault, and at depth by the Buchans River–Old Buchans Thrust Fault. The latter forms a moderate north–northeasterly dipping structure, below which unaltered arkosic sandstone, conglomerate and mafic volcanic rocks of the Sandy Lake Formation predominate.

Mineralization

As noted above, weakly developed stringer mineralization is locally observed within the hanging-wall rocks of the Airport Thrust Fault. However, most mineralization is hosted within the footwall rocks to this structure within strongly altered rocks of the Buchans River Formation. Mineralization is both disseminated and vein-hosted, occurring in association with white mica alteration and disseminated pyrite, which is subsequently overprinted by base-metal bearing quartz veining, potentially representing remobilized sulphides (Plate 13). The primary zinc-dominated mineralization is also locally accompanied by anomalous gold (<200 ppb). Rare zones of hydrothermal brecciation are observed within the altered felsic volcanic rocks, which are locally accompanied by minor base- and precious-metal enrichment (Plate 14).

Plate 12. *Paragonitic illite–montmorillonite altered felsic volcanic of the Powerhouse prospect; DDH BE-97-020, 30 m.*

Alteration

The hanging-wall rocks of the Airport Thrust Fault are predominantly composed of Fe- and Fe–Mg-chlorite, along with lesser muscovite, paragonite, and paragonitic illite (Figure 11). Below the thrust fault, footwall rocks contain variable white mica alteration along with localized base- and precious-metal enrichment. Spectral data from the Powerhouse prospect supports an overall north–northeastward increase in the intensity of white mica alteration, up to the current limits of diamond drilling. This altered sequence is subsequently truncated at depth by the Buchans River–Old Buchans Thrust Fault, below which there is a marked shift to phengite and Fe–Mg-chlorite-dominated spectral signatures associated with sandstone and interbedded conglomerate and mafic volcanic rocks of the Sandy Lake Formation, respectively (Figure 11).

The southernmost drillhole examined (DDH H-3319) consists of intermixed white mica (muscovite, paragonite, muscovitic illite and paragonitic illite) and Fe–Mg chlorite alteration hosted within a felsic-dominated volcanic sequence (Figure 12). The contact between the chlorite- and white-mica-dominated assemblages is sharp and is not associated with a change in lithology (Plate 15). Observations from drillcore support the chlorite alteration as being early and is subsequently overprinted by the white mica-dominated assemblages. Given the presence of both chlorite and white mica, this drillhole is inferred to represent the margins of the white mica alteration zone, which becomes more prevalent towards the north. Within the altered volcanic sequence, the local emplacement of syn-volcanic intrusive units also displays similar styles of white mica alteration and are locally host to base- and precious-metal enrichment (*e.g.*, 80–90 m; DDH H-3319; Figure 12). Toward the end of the drillhole, in the vicinity of the Buchans River–Old Buchans Thrust Fault, there is a marked shift from shorter wavelength Al-OH values associated with the hanging-wall rocks to longer wavelength Al-OH values associated with the footwall rocks, as seen elsewhere in area (Figure 12).

The northeasternmost drillhole examined from this zone displays the strongest alteration observed within the area. This drillhole, DDH BE-97-020, collars directly into altered felsic

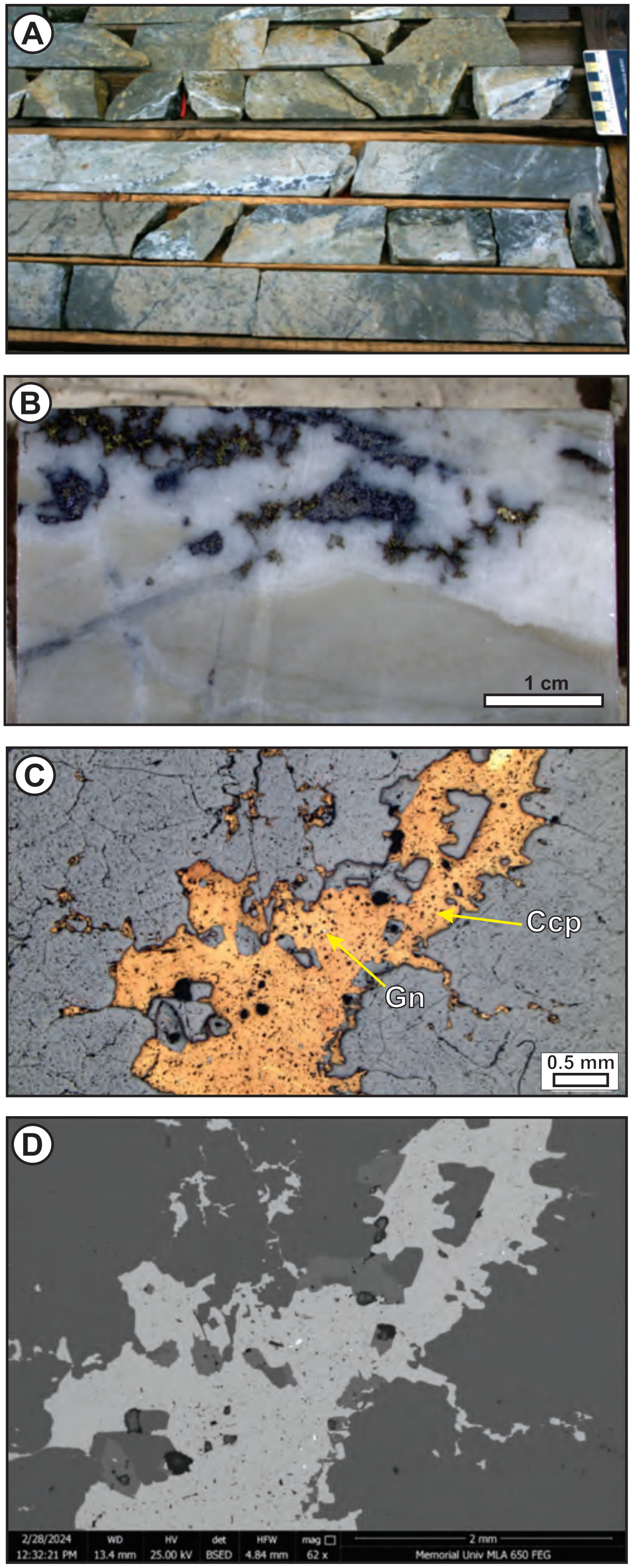

Plate 13. *A) Muscovite–muscovitic illite (dark grey) altered felsic volcanic rock, overprinted by quartz–sphalerite–chalcopyrite-bearing veins associated with paragonite alteration (bleached areas); Powerhouse prospect, DDH BE-97-019, 180 m. Assays from this interval returned up to 0.6% Zn, 0.3% Cu, 0.1% Pb and 10.6g/t Ag over 2 m; Saunders* et al.*, 1998; B) Quartz dominated vein hosting sphalerite–chalcopyrite–pyrite mineralization, crosscutting paragonite–montmorillonite alteration; DDH BE-97-019, 179.2 m depth; C) Reflected light image of sample in (B) showing chalcopyrite (Ccp) with very fine inclusions of galena (Gn) hosted within the quartz vein; D) SEM image of (C) highlighting the fine-grained galena (bright colour) contained within the chalcopyrite.*

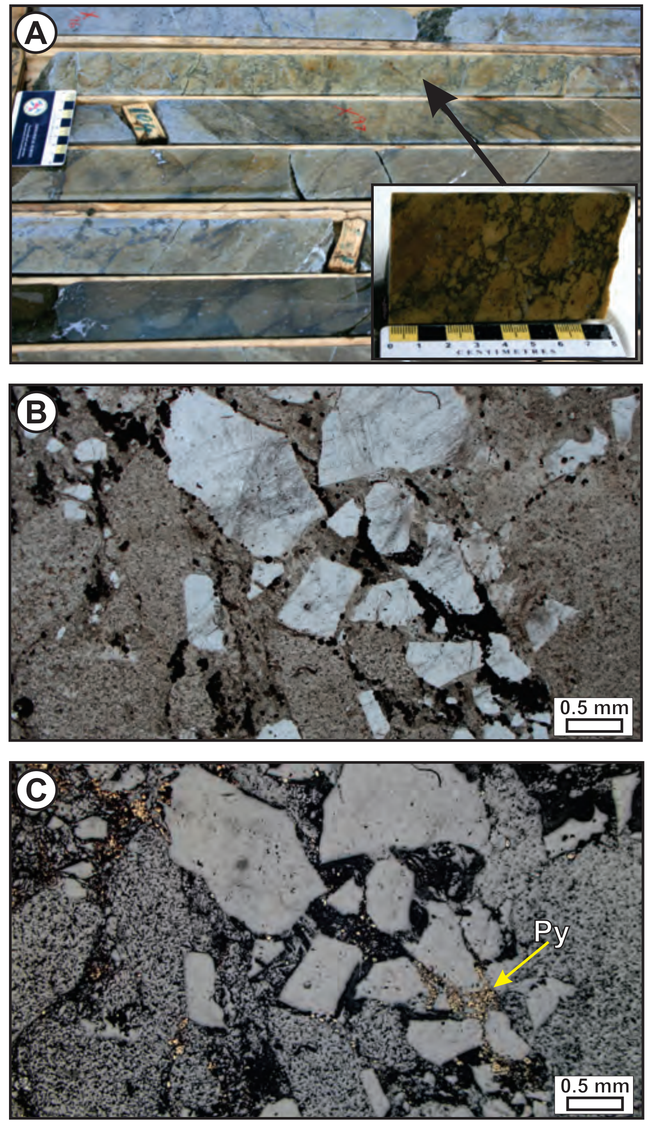

Plate 14. *A) Paragonite–montmorillonite altered hydrothermal breccia hosting angular to subrounded fragments within a pyrite-rich matrix; Powerhouse prospect, DDH BE-97-020, 102 m; B) Plane-polarized light photomicrograph of hydrothermal breccia shown in (A) highlighting the angular quartz-rich fragments and the pyrite-rich matrix; C) Reflected light image of (B) showing the distribution of pyrite (Py) within the matrix of the hydrothermal breccia.*

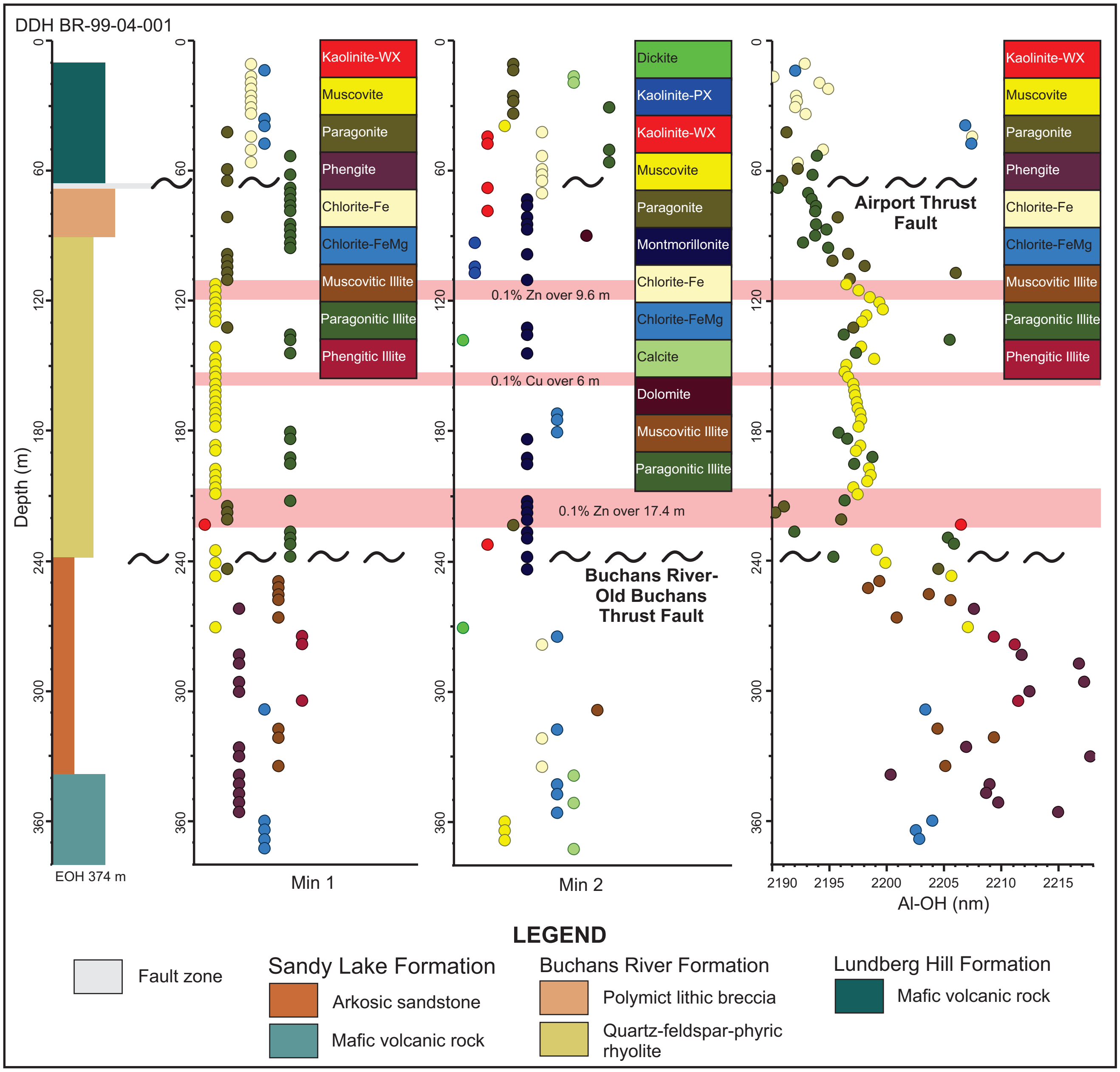

Figure 11. *Strip log for DDH BR-99-04-001, outlining the distribution of the spectral data, mineral 1 (Min 1) and mineral 2 (Min 2), along with the related Al-OH absorption feature and location of select mineralization within the western portion of the Powerhouse prospect. Assay values from Harris* et al. *(1999).*

volcanic rocks of the Buchans River Formation, with the first 180-m of core consisting of paragonitic illite–montmorillonite alteration (Figure 13), which also contains localized zones of base- and precious-metal enrichment. For example, paragonitic illite–montmorillonite-dominated alteration associated with a pyritic stringer zone assays 0.1 g/t Au and 3.1 g/t Ag over 4.4 m (Plates 16A and 17; Saunders *et al.*, 1998; 2000d), and the same alteration is also locally host to disseminated sulphide mineralization assaying 0.7% Zn and 0.2% Pb over 8.5 m (Plate 16B; Saunders *et al.*, 1998). Below the paragonitic illite–montmorillonite-dominated alteration, Al-OH values display a moderate increase to ~2199 nm, consisting of muscovite–muscovitic illite. The altered felsic volcanic sequence is also intruded by syn-volcanic felsic dykes that display similar spectral signatures as the surrounding altered volcanic rocks. Both the dykes and the altered volcanic rocks are locally crosscut by high-grade, sphalerite-rich veins assaying up to 2.3% Zn, 0.5% Pb and 1.6 g/t Ag over 1.0 m (Plate 18; Saunders *et al.*, 1998). The white mica alteration persists up to the Buchans River–Old Buchans Thrust Fault (~350 m),

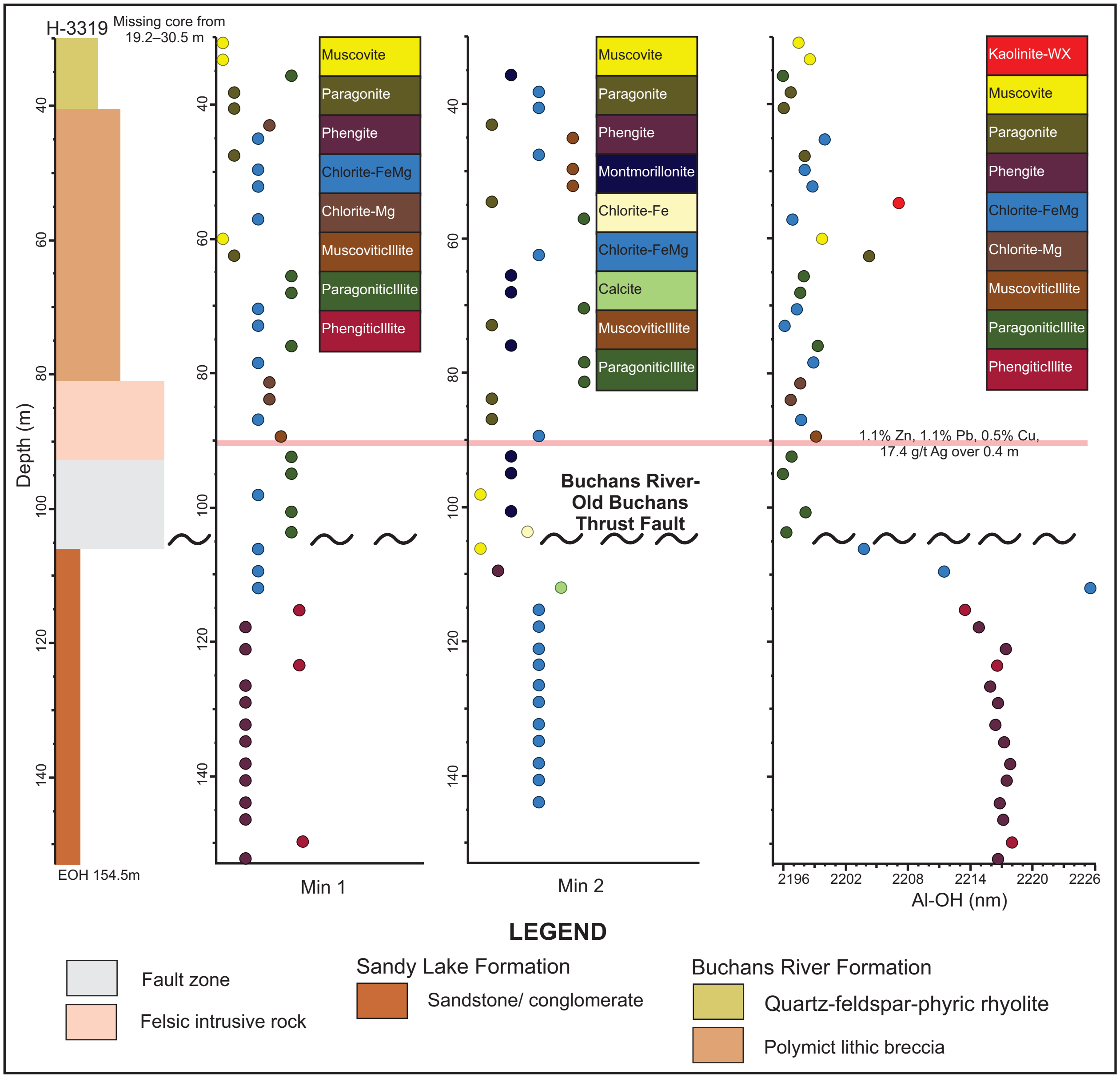

Figure 12. *Strip log for DDH H-3319, outlining the distribution of the spectral data, mineral 1 (Min 1) and mineral 2 (Min 2), along with the related Al-OH absorption feature and location of select mineralization within the southern portion of the Powerhouse prospect. Assay values from Thurlow and Barbour (1986).*

where it is structurally truncated (Figure 13). Below the thrust fault, there is a prominent shift in the overall Al-OH values to longer wavelengths, characteristic of the phengitic spectral signature associated with the siliciclastic rocks of the Sandy Lake Formation.

MIDDLE BRANCH EAST

The Middle Branch East prospect, located approximately 1 km east of the Sandfill prospect, is covered by 3–8 m of Quaternary cover, thus most of the geological information about the area is obtained from drillcore (Figure 10). In the late 1990s, Buchans River Limited discovered the Middle Branch East prospect using geophysical and geochemical surveys, followed by diamond drilling. This work identified a fragmental volcanic unit, inferred to be correlative with the Buchans River Formation, hosting mineralized clasts that resemble other occurrences of transported ore in the area (Saunders *et al.*, 1998). In addition to the base-metal mineralization, a zone of anomalous gold enrichment was also identified by Buchans River Limited within a strongly foliated, white mica altered, felsic volcaniclastic unit, forming a strat-

Plate 15. *Sharp transition, from Fe–Mg-chlorite–muscovitic illite dominated alteration to intermixed paragonite–paragonitic illite–montmorillonite and Fe–Mg-chlorite–paragonitic illite assemblages. Powerhouse prospect, DDH H-3319, 40 to 64 m. Note that one row of drillcore is approximately 1.5 m in length.*

iform zone dipping to the north-northeast. However, the exact nature of this mineralization has yet to be determined.

Previous Work

Diamond drilling targeting a basal-till zinc anomaly intersected mineralized clasts within a fragmental volcanic unit assaying up to 0.8% Zn, 0.1% Pb, 0.2% Ba, 9.7 g/t Ag and 0.3 g/t Au over 5 m (Saunders *et al.*, 1998). Subsequent investigations further extended this prospect up to 400-m along strike, with local intersections of up to 3.5% Zn and 1.3 g/t Au over 1.2 m (Saunders *et al.*, 2000a). In addition to the identified base-metal mineralization, a stratiform zone of anomalous gold enrichment was also intersected in drillcore, assaying 0.9 g/t Au over 22 m, which includes a higher grade interval of up to 7.4 g/t Au over 0.2 m (DDH BE-97-023; Saunders *et al.*, 1998, 2000d).

Local Geology

Drillholes targeting a basal-till zinc anomaly collared in a fragmental volcanic unit containing cm-scale fragments of massive sulphide mineralization (Saunders *et al.*, 1998; 2000a). As the Buchans River Formation and the underlying Intermediate Footwall member of the Ski Hill Formation (Figure 2) are the only units noted to host such fragments (Allen *et al.*, 2024 and references therein), this area is interpreted to represent a structural panel not identified on geology maps of the area, and is currently the only noted occurrence of such mineralization within the hanging-wall sequence of the Airport Thrust Fault. These rocks are associated with a prominent IP chargeability anomaly (Saunders *et al.*, 2000a), and air-

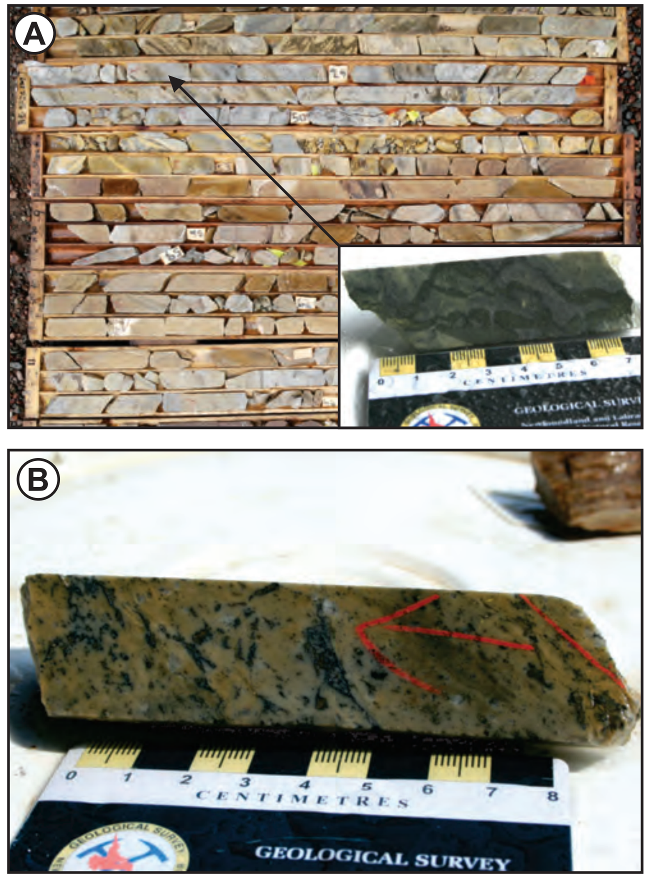

Plate 16. *A) Paragonitic illite–montmorillonite alteration crosscut by pyrite-rich stringer mineralization hosting anomalous Au, Ag, As, Hg and Zn; Powerhouse prospect, DDH BE-97-020, 47 m; B) Quartz-phyric felsic volcanic rock, displaying paragonitic illite–montmorillonite alteration and hosting disseminated sulphide mineralization. Sample contains 1.4% Zn, 0.15% Pb and 2.3 ppm Hg over 0.7 m; Powerhouse prospect, DDH BE-97-020, 81 m.*

borne geophysical surveys display a transition to more strongly magnetic rocks immediately to the northeast (Moore and Butler, 2019). These data suggest that the area is more structurally complex than shown on the published geology maps (*cf.* Saunders *et al.*, 1998). Altered felsic volcanic rocks associated with the mineralized zone, locally up to 150-m thick, dip gently to the north-northeast (Saunders *et al.*, 2000a).

A strongly foliated zone of white mica alteration is developed within a felsic volcaniclastic rock immediately underling the fragmental volcanic unit hosting the mineralized clasts. This zone dips moderately to the north-northeast, separates the overlying rocks from underlying intermediate volcanic rocks of the MMBG, and contains anomalous gold enrichment (Lundberg Hill Formation of Thurlow and Swanson, 1987; Saunders *et al.*, 1998; Winter, 2000).

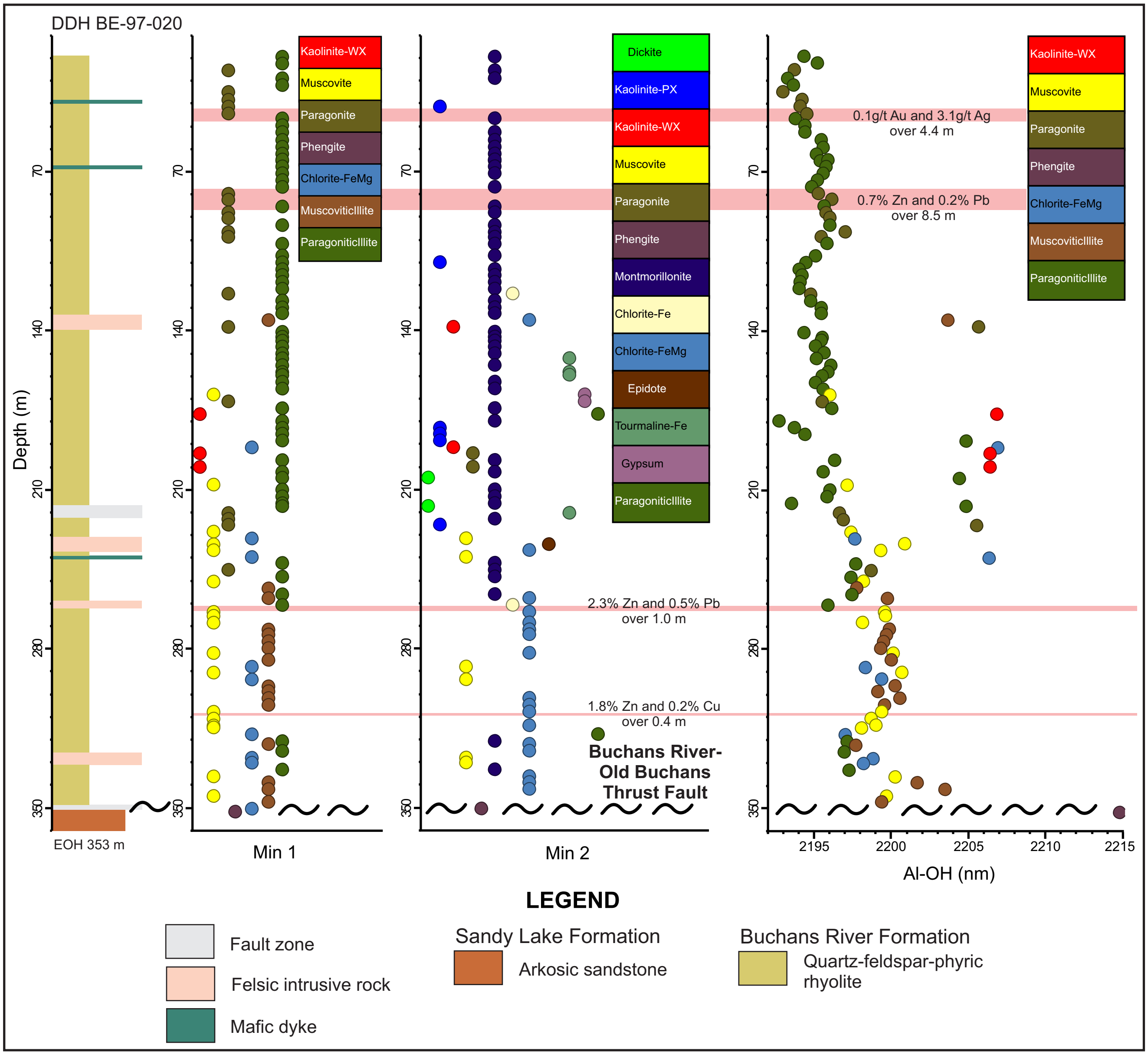

Figure 13. *Strip log for DDH BE-97-020, outlining the distribution of the spectral data, mineral 1 (Min 1) and mineral 2 (Min 2), along with the related Al-OH absorption wavelength feature and location of select mineralization within the northern portion of the Powerhouse prospect. Assay values from Saunders* et al. *(1998, 2000d).*

Mineralization

The mineralization identified at the Middle Branch East prospect consists of cm-scale, massive sulphide clasts, which are inferred to represent transported ore as observed elsewhere in the Buchans area. The mineralized fragmental unit has produced assay values of up to 3.5% Zn, 0.8% Pb, 0.1% Cu, 113 g/t Ag, 1.3 g/t Au and 0.6% Ba over 1.2 m (Saunders *et al.*, 2000a; Plates 19 and 20).

In addition to the base-metal mineralization, a separate zone of anomalous gold enrichment has also been identified in association with phengite dominated white mica alteration hosted within a strongly foliated felsic volcaniclastic protolith (Plates 21 and 22). This zone is associated with Au–Ag enrichment, assaying up to 0.4 g/t Au, 19 g/t Ag over 26 m (Figure 14), along with anomalous Ba (up to 0.6% over 0.7 m), zinc (< 0.2%), lead (<0.1%) and copper (<0.1%; Saunders *et al.*, 1998, 2000d).

Alteration

Spectral data was collected from a single drillhole, DDH BE-97-018, which collared in a chloritic intermediate vol-

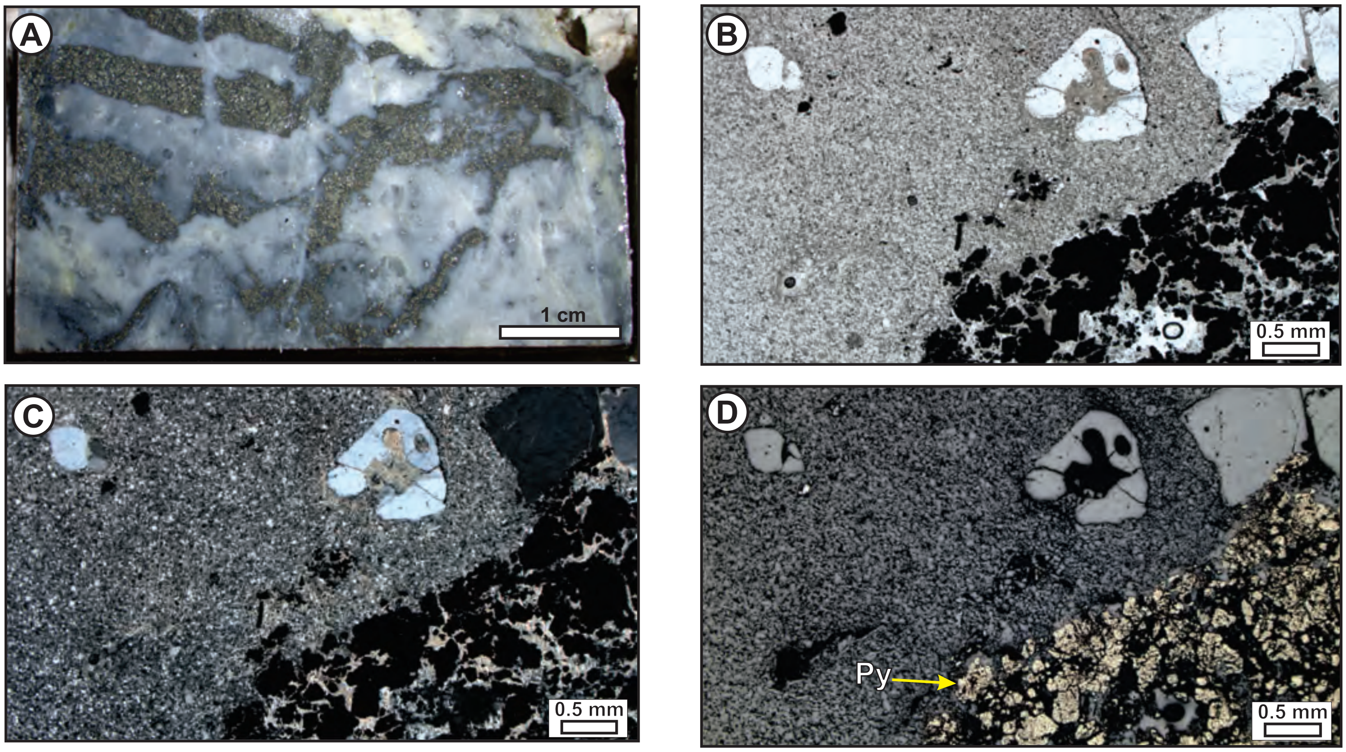

Plate 17. *A) Paragonite-dominated white mica alteration crosscut by pyrite-rich sulphide veining. Note the veins are hosted by a strongly altered, quartz-phyric, felsic volcanic rock; B) Plane-polarized light photomicrograph of sample shown in (A). Note the locally developed resorption texture in the quartz phenocrysts of the host rock; C) Cross-polar photomicrograph of (B) highlighting the intense white mica alteration of the host rock; D) Reflected light image of (C) showing the pyrite (Py)-dominated sulphide vein. Note that the pyrite is host to fine-grained inclusions of galena based on SEM imaging.*

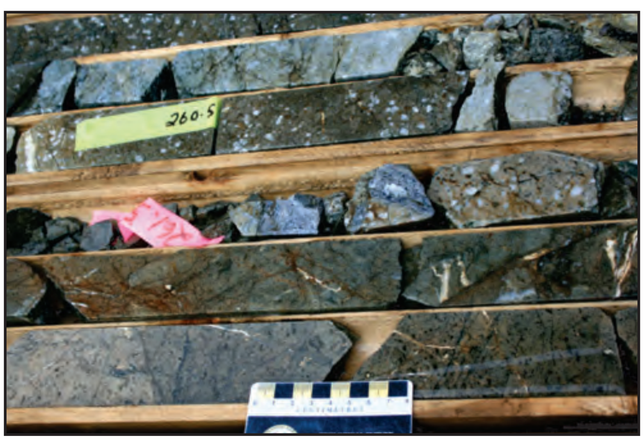

Plate 18. *High-grade, sphalerite-rich vein (centre of photo) crosscutting muscovite altered, quartz-phyric, felsic dyke; Powerhouse prospect, DDH BE-97-020, 261 m.*

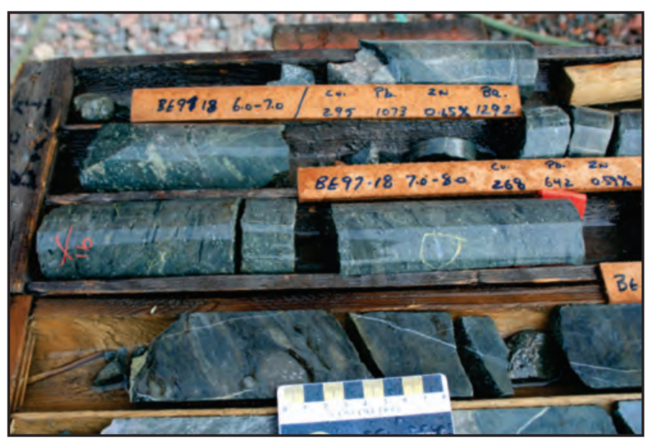

Plate 19. *Chloritic fragmental volcanic unit hosting rare, cm-scale, massive sulphide clasts associated with anomalous Zn–Pb–Cu mineralization; Middle Branch East prospect, DDH BE-97-018, 9 m.*

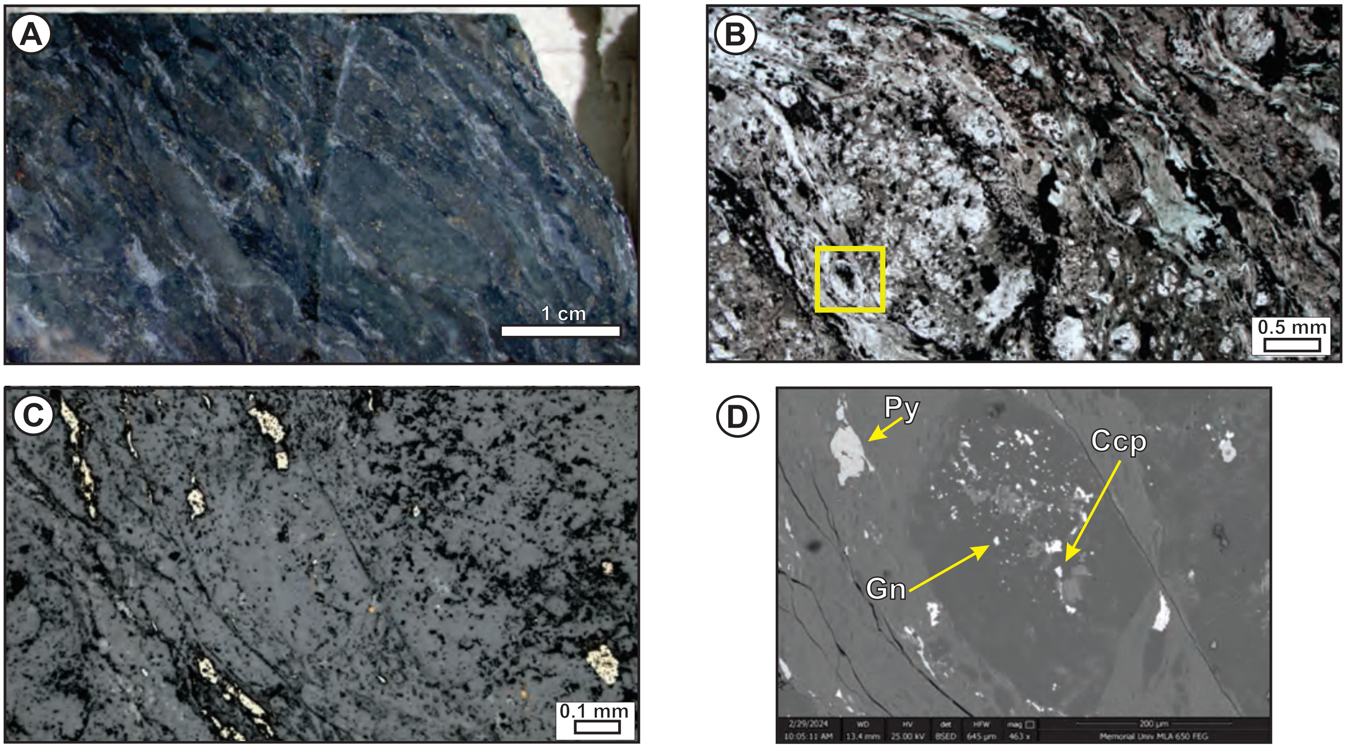

Plate 20. *A) Fe–Mg-chlorite–muscovite altered fragmental volcanic containing 1.1% Zn, 0.1% Pb, 0.05% Cu, 0.2% Ba, 7.5 g/t Ag, 0.5 g/t Au and 678 ppb Hg over 0.8 m; Middle Branch East prospect, DDH BE-97-018, 8.8-9.6 m; sample GS-22-141; B) Plane-polarized light photomicrograph of (A), highlighting the fragmental nature of the mineralized unit; note yellow inset box shows the location of (C); C) Reflected light image of (B) showing predominantly pyrite (Py) within the white mica altered matrix of the fragmental unit. Note the rare quartz-rich clast containing minor disseminated chalcopyrite and galena at the centre of the photograph; D) SEM image of the quartz-rich fragment shown in (C), highlighting the disseminated galena (Gn) and chalcopyrite (Ccp) within the subrounded quartz-rich clast, indicating potential transported mineralization.*

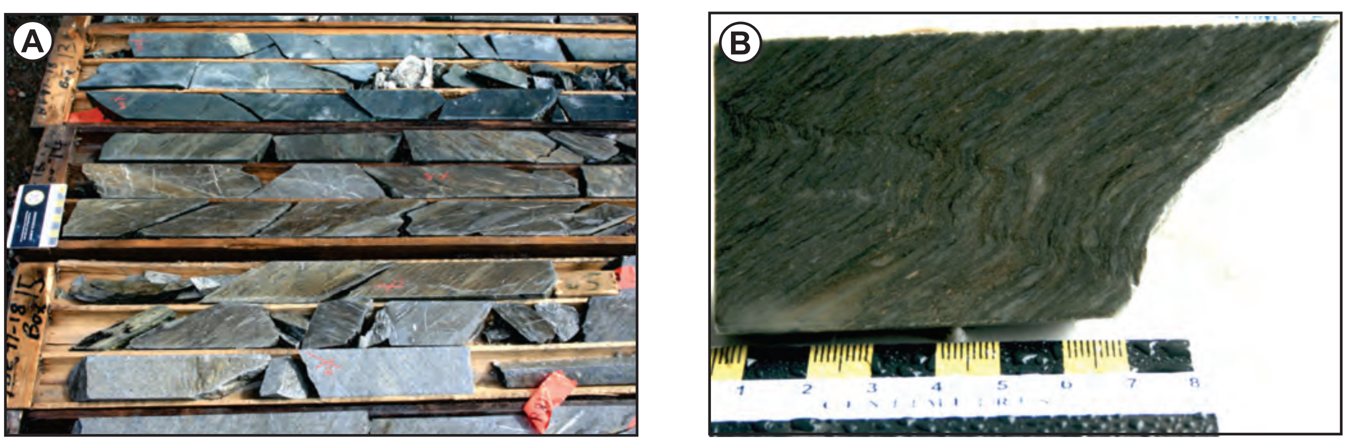

Plate 21. *A) Transition from chloritic fragmental volcanic unit into strongly foliated, phengite altered, felsic volcaniclastic unit hosting anomalous gold–silver mineralization; Middle Branch East prospect, DDH BE-97-018, 60 m; B) Sample of the strongly foliated, phengite altered, felsic volcanic rock, which assayed 0.3 g/t Au, 2.7 g/t Ag and 0.3% Ba over 0.7 m; sample GS-22-143.*

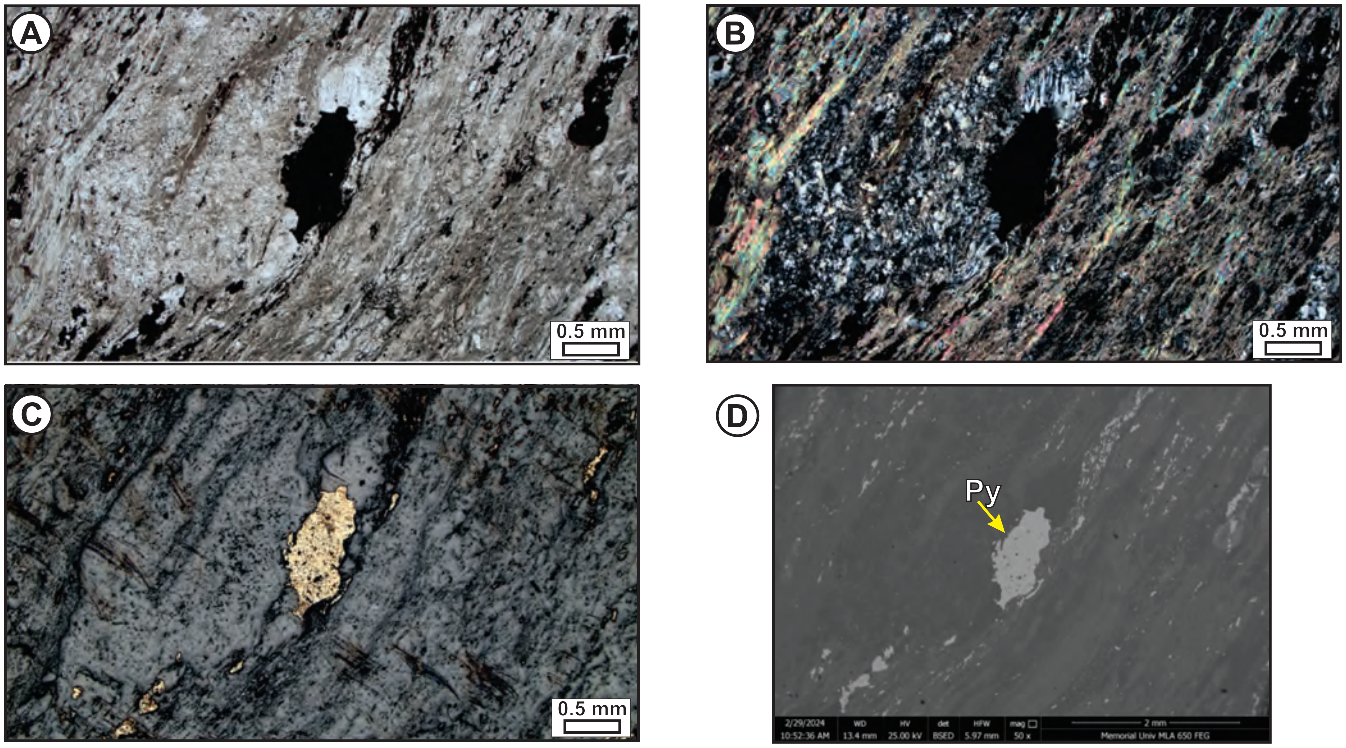

Plate 22. *A) Plane-polarized light photomicrograph of sample shown in Plate 21B, illustrating the strongly foliated white mica altered felsic volcaniclastic unit. Much of the pyrite is very fine-grained, however, minor coarse-grained pyrite is locally developed; B) Cross-polar photomicrograph of (A) highlighting the pervasive white mica alteration of the felsic volcaniclastic unit; C) Reflected light image of (B) showing predominantly pyrite (Py) within the white mica altered matrix of the fragmental unit; D) SEM image of the coarser grained pyrite, which is also host to fine-grained inclusions of galena and arsenopyrite.*

caniclastic unit hosting rare cm-scale sulphide clasts (Figure 14). The entire hole is predominated by Fe–Mg chlorite and lesser muscovite alteration, aside from one interval of phengite-dominated alteration associated with anomalous gold–silver enrichment between 60–90 m (Figure 14). Like other examples of distal transported ore (*e.g.*, Sandfill prospect), there is no evidence for the development of shorter wavelength white mica alteration in association with the occurrence of the mineralized clasts. The zone of phengite alteration (60–90 m) potentially represents an example of structurally controlled mineralization that is different from the regional phengite signature associated with unaltered sequences (*e.g.*, Sandy Lake Formation). This prospect represents the only example identified in the region whereby longer wavelength (>2210 nm) white-mica minerals related to hydrothermal alteration are associated with precious-metal mineralization.

WOODMAN'S BROOK

The Woodman's Brook prospect is located approximately 3 km east of the Middle Branch East prospect and is defined over a 1.5-km strike length in a north–south orientation and up to 600 m wide in an east–west direction (Figure 10). This area represents a zone of pyritic alteration developed within intermediate volcanic rocks of the hanging-wall sequence to the Airport Thrust Fault. Here, both mafic and intermediate volcanic rocks of the MMBG contain disseminated, stringer and vein-hosted styles of mineralization. The intermediate volcanic rocks are affected by variable white-mica alteration and silicification (Winter, 2000).

Previous Work

Early reconnaissance drilling, geological mapping, geochemical, and geophysical (IP) surveys were conducted in the area of East Branch River/Woodman's Brook in the early 1960s by the Buchans Mining Company and ASARCO (Swanson, 1962, 1963, 1964). This early work was followed-up in the mid-1980s by Abitibi-Price and BP with additional geophysical surveys and geological mapping (Thurlow, 1984; Barbour, 1985; Barbour *et al.*, 1990). The first drilling in the 1960s intersected anomalous zinc–lead–silver mineralization (*e.g.*, DDH BJ-046; Thurlow *et al.*, 1987). During the mid-1990s, the area was explored by Noranda, largely through compilation work (Arseneau *et al.*, 1995a), and by Newfoundland Mining and Exploration Ltd., through prospecting, mapping and an IP survey, the latter of which

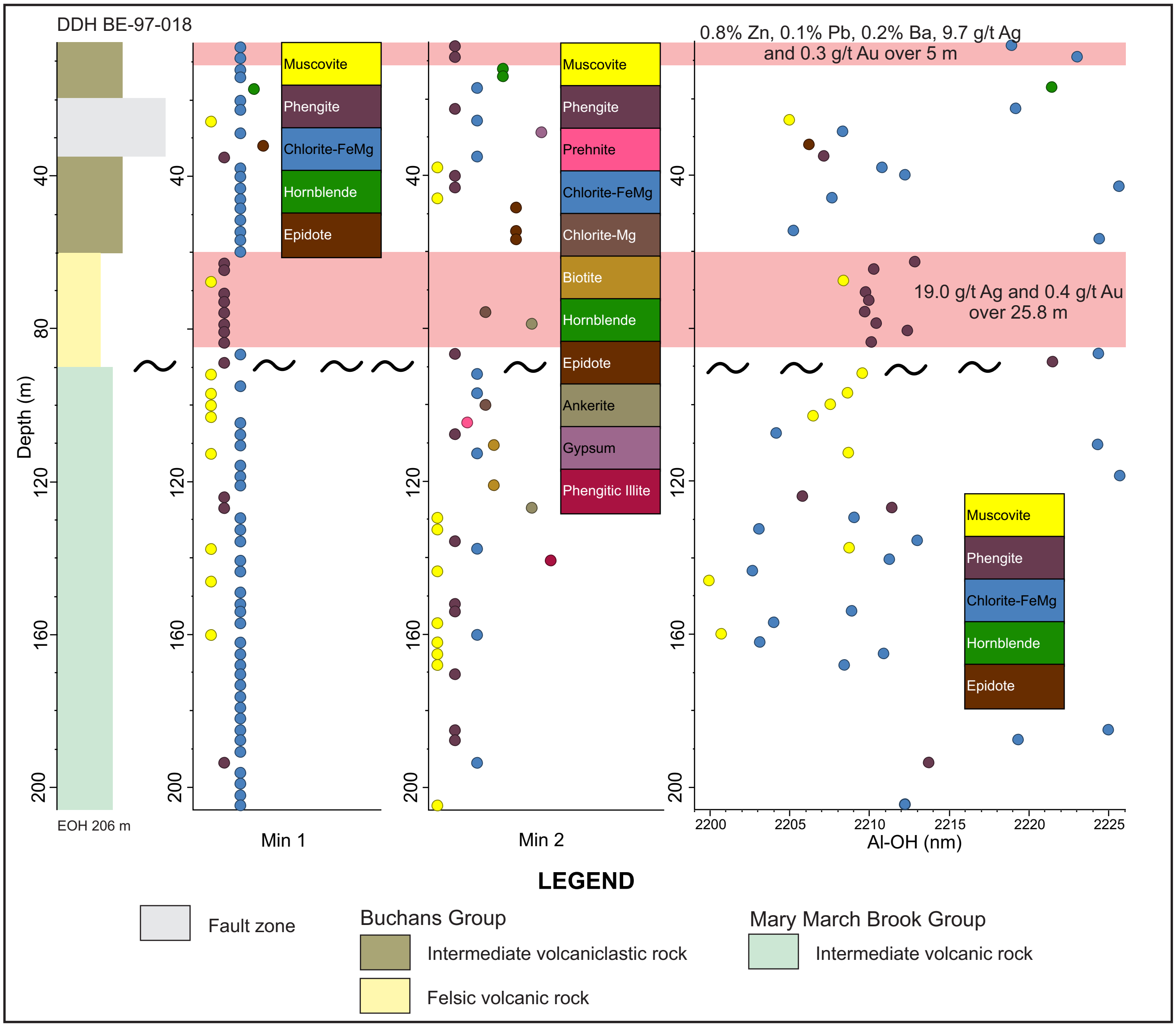

Figure 14. *Strip log for DDH BE-97-018, outlining the distribution of the spectral data, mineral 1 (Min 1) and mineral 2 (Min 2), along with the related Al-OH absorption wavelength feature and location of select mineralization within the Middle Branch East prospect. Assay values from Saunders* et al. *(1998, 2000d).*

identified a strong chargeability anomaly coincident with the zinc–lead–silver mineralization intersected in historical drilling (Tuach and Saunders, 1994; Saunders and Scott, 1995). Follow-up drilling identified several zones of pyritic alteration in association with base-metal enrichment (Saunders *et al.*, 1996). In the early 2000s, Buchans River Limited conducted additional geophysical and geochemical surveys over the area (Saunders *et al.*, 2000a; Pettit, 2000). In the mid-2010s, core from the area was re-logged by Altius Minerals (Seymour *et al.*, 2015), and a compilation of existing surficial geochemistry was completed by Canstar Resources (Patey, 2019).

Local Geology

The host rocks to the alteration at the Woodman's Brook prospect consist of quartz ± feldspar-phyric to aphanitic intermediate volcanic rocks of the MMBG. These volcanic rocks are conformably overlain by a thin sequence of siltstone, shale, and conglomerate, less than one metre thick, which marks the transitioning up section into sub-alkalic mafic volcanic rocks (Winter, 2000).

Mineralization

Mafic volcanic rocks in the area are reported to contain disseminated stringer and vein-hosted pyrite accompanied by minor sphalerite and chalcopyrite (Winter, 2000). This style of mineralization is associated with intersections of up to 0.6% Cu over 0.8 m and 0.6% Zn over 3 m (Saunders *et al.*, 1996). The mafic volcanic rocks are characterized by Fe–Mg chlorite–muscovite alteration in association with this mineralization. The intermediate volcanic rocks host disseminated and vein-hosted zinc–lead mineralization, which is locally developed over 50 m in drillcore (Plates 23 and 24). This style of mineralization locally assays up to 1.9% Zn, 2.6% Pb and 0.1% Cu over 0.5 m (Saunders *et al.*, 1996) and is associated with muscovite alteration based on spectral data. In addition to the base-metal mineralization, anomalous gold (<300 ppb)

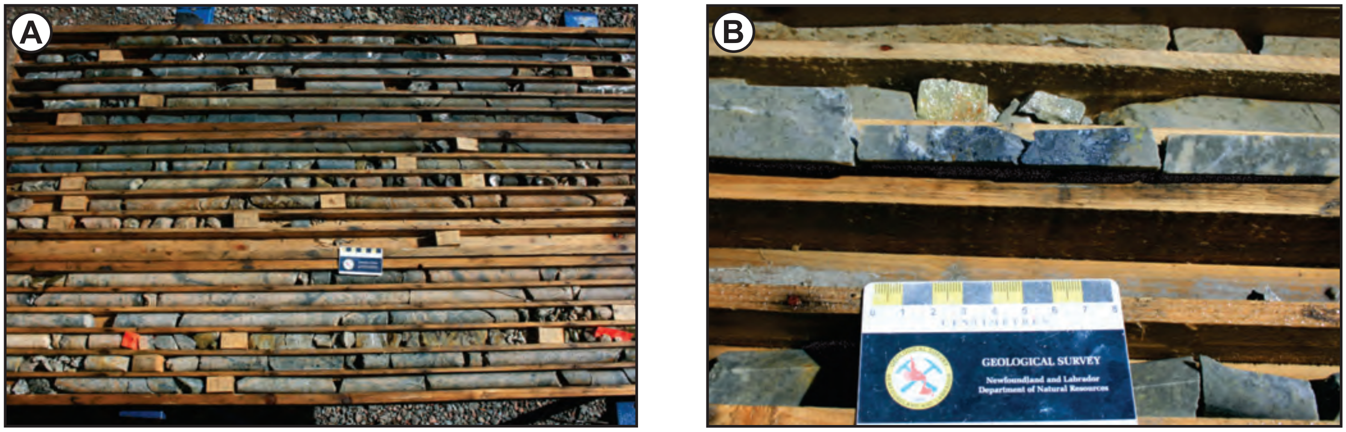

Plate 23. *A) Gradational transition from Fe–Mg-chlorite into a zone of muscovite-dominated white mica alteration hosted within intermediate volcanic rocks; Woodman's Brook prospect, DDH BJ-046, 30–50 m depth; B) Narrow sphalerite-rich vein crosscutting muscovite–pyrite-altered intermediate volcanic rocks; Woodman's Brook prospect, DDH BJ-046, 91.5 m depth. The mineralized vein assayed >1.0% Zn, 0.8% Pb, 0.1% Cu, 27.6 g/t Ag and 0.2 g/t Au over 0.1 m (Thurlow* et al.*, 1987).*

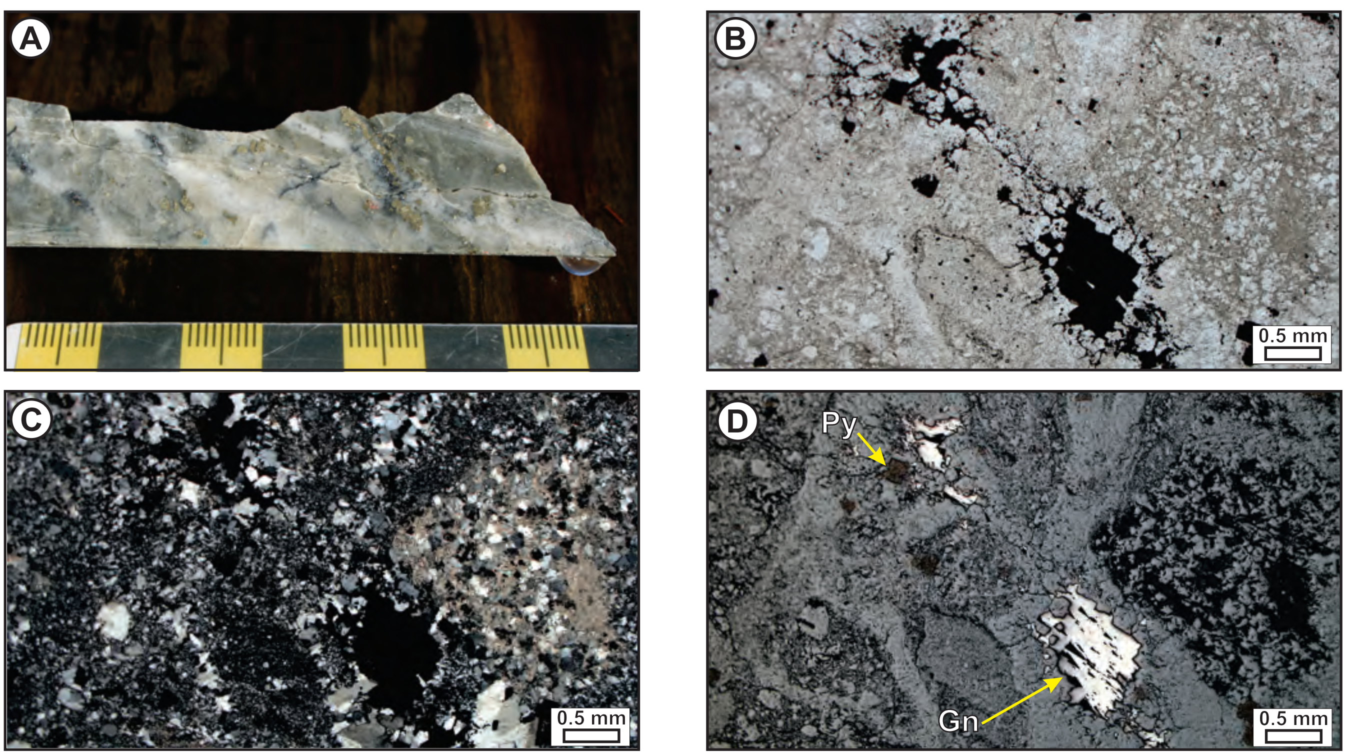

Plate 24. *A) Quartz–muscovite altered intermediate volcanic rock crosscut by sulphide-bearing stockwork-style veining; DDH BE-95-003, 113 m depth; B) Plane-polarized light photomicrograph of sample shown in (A) outlining the distribution of the sulphide mineralization associated with quartz veining; C) Cross-polar photomicrograph of (B) highlighting the pervasive white mica alteration of the intermediate volcanic host rock; D) Reflected light image of (C) outlining abundant galena (Gn) and lesser pyrite (Py) within the vein-hosted sulphides.*

is also reported from the area, most notably from drillhole BJ-046 (Figure 10).

Alteration

The Woodman's Brook prospect is associated with the development of "sericite" alteration accompanied by base-metal enrichment (Winter, 2000). A single drillhole was evaluated using SWIR to classify the white mica minerals developed in association with this mineralization. Spectral data indicates that the intermediate volcanic rocks, which are the main host to the mineralization, are dominated by muscovite–muscovitic illite and Fe–Mg-chlorite, where muscovite is the dominant signature immediately adjacent to mineralization (Figure 15). The Al-OH values within the variably altered intermediate volcanic rocks are relatively consistent throughout the sequence, ranging from 2200–2195 nm and displaying a minor shift to shorter wavelengths towards the bottom of the unit. Below the intermediate volcanic rocks, there is a gradational transition into mafic-dominated volcanic rocks characterized by Fe-chlorite–muscovite spectral signatures. This unit overlies volcaniclastic rocks and related sedimentary breccia that visually looks unaltered, but contains variable muscovite–muscovitic illite, phengite, and Fe–Mg-chlorite based on spectral data, along with a range of Al-OH values (Figure 15). Finally, the drillhole ends in mafic to intermediate volcanic rock displaying a predominate Fe–Mg chlorite spectral signature.

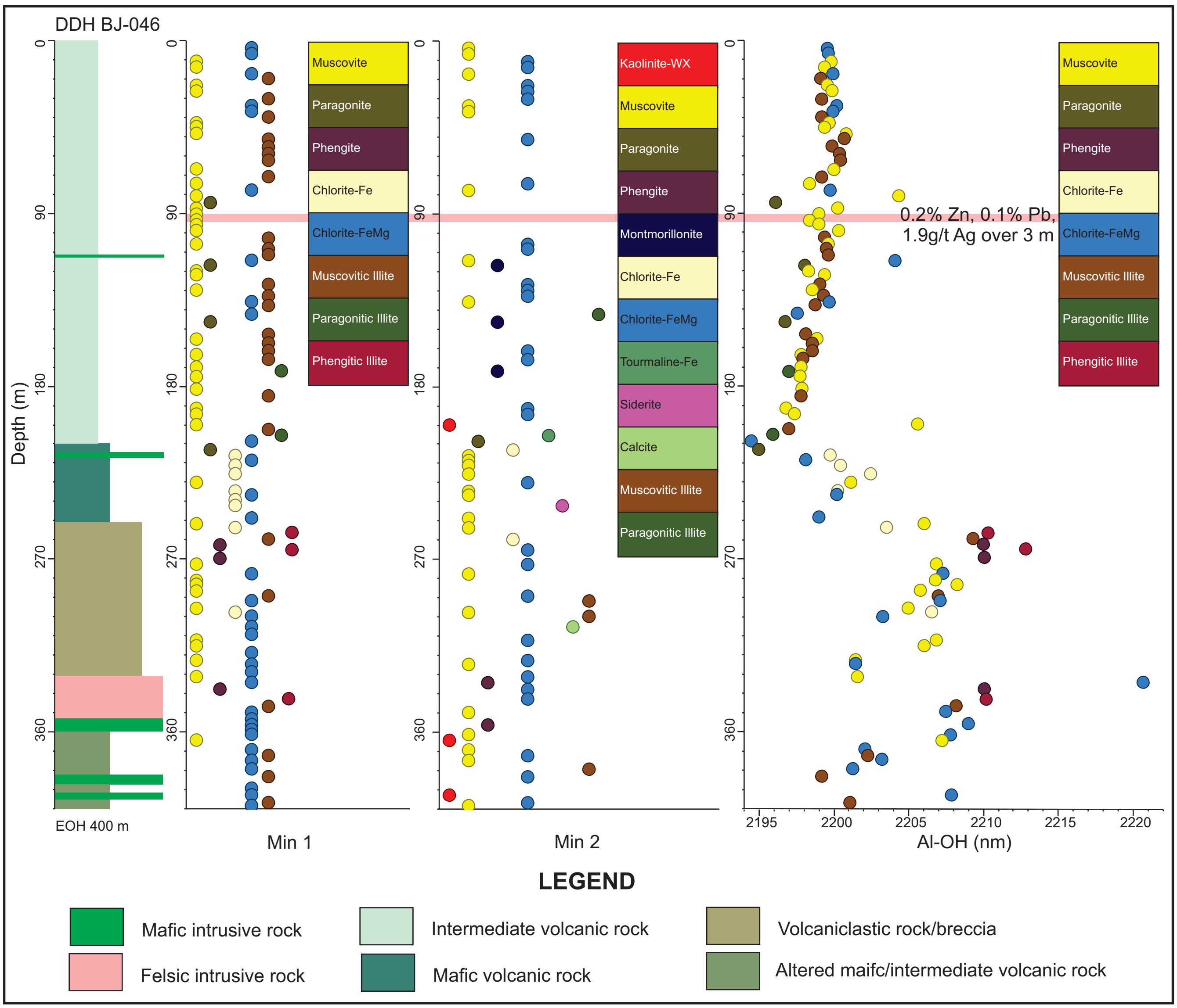

Figure 15. *Strip log for DDH BJ-046, outlining the distribution of the spectral data, mineral 1 (Min 1) and mineral 2 (Min 2), along with the related Al-OH absorption wavelength feature and location of select mineralization within the Woodman's Brook prospect. Assay values from Saunders* et al. *(1996).*

TOWER

The Tower prospect is located approximately 1.5 km to the southeast of the Woodman's Brook prospect (Figure 16). This region represents the eastern extension of the Powerline–Airport fault system, termed the Airport Fault, which emplaces rocks of the MMBG over the Red Indian Lake Group (Thurlow *et al.*, 1992; Zagorevski *et al.*, 2016; Figure 16). The area contains a recently recognized zone of advanced argillic alteration that displays a close spatial association with this regional fault structure (Sparkes, 2022), but the altered rocks are relatively undeformed. This area represents the only other occurrence of advanced argillic alteration identified outside of the Mary March prospect (*see* below). The affinity of the rocks hosting this hydrothermal alteration remains uncertain, but limited geochemical sampling demonstrates that it is hosted within both felsic and intermediate volcanic rocks. This alteration zone has been traced intermittently in both outcrop and drillcore over a 3-km strike length.

Previous Work

Abitibi-Price was the first to conduct reconnaissance drilling in this area in the early 1940s and again in the late 1970s. Then in the mid- to late 1980s BP-Selco conducted additional follow-up work, which identified anomalous base-metal enrichment in the area (Thurlow, 1984; Thurlow *et al.*, 1987; Barbour *et al.*, 1990, 1991; Desnoyers *et al.*, 1992). Noranda evaluated the Tower prospect during the 1990s and refined the distribution of the "sericitic" alteration and overlying soil anomalies containing base-metal enrichment, defining an anomalous zone over an approximate strike length of 1.2 km (Squires, 1994a; Banville, 1998a, b). During the late 1990s and the early 2000s, Buchans River Limited furthered

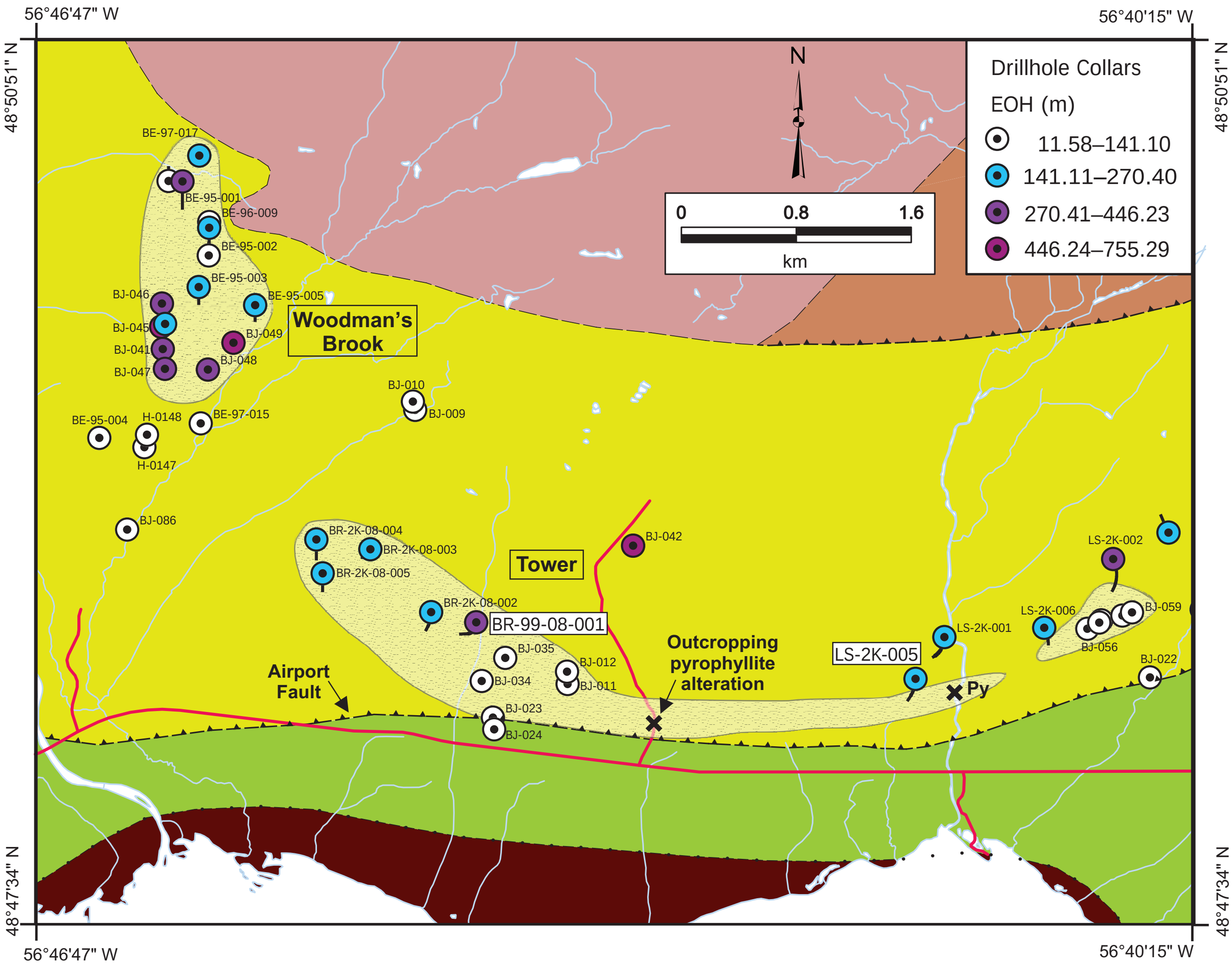

Figure 16. *Location map showing the distribution of diamond-drill holes and geology within the area of the Tower prospect. Refer to Figure 1 for legend.*

investigations in the area through various geophysical surveys and diamond drilling (Saunders *et al.*, 1999, 2000b, c; Wallis, 2001). Results from this work identified a prominent IP anomaly associated with the approximate outline of the alteration zone, in addition to intersecting elevated zinc and barium in drillcore, returning up to 2.1% Zn and 2.2% Ba over 1 m in separate samples (Saunders *et al.*, 2000c). Most recently a portion of the area was covered by soil sampling carried out by Buchans Resources Limited (Moore and Butler, 2019).

Local Geology

The rocks intersected in drillcore at the Tower prospect primarily consists of aphanitic to quartz and feldspar phyric intermediate volcanic rocks, locally interbedded with rare 5–10 m felsic flows. Limited observations from drillcore suggest the intermediate volcanic rocks overlie mafic volcanic rocks to the south. Industry mapping of the area has defined the location of the Airport Fault, with interbedded and well-sorted felsic pyroclastic, bedded tuffs, chert, siltstone and arkose forming the footwall rocks to this structure, and locally silicified and altered interbedded mafic to felsic volcanic rocks within the hanging wall (Thurlow, 1984). The recently identified zone of advanced argillic alteration occurs structurally above the footwall sequence and below the intermediate to mafic dominated hanging-wall sequence. However, due to the lack of outcrop and the limited drilling in the area of the alteration, the exact relationship between the alteration and the hanging-wall sequence remains uncertain; relationships from the eastern portion of the zone suggest a conformable transition from the alteration into the overlying hanging-wall rocks (*see* below).

Mineralization

The anomalous zinc, lead and copper intersected in drillcore primarily consists of disseminated and lesser vein-hosted mineralization (Plate 25). This mineralization is primarily hosted within the intermediate volcanic rocks and related synvolcanic intrusive units. The highest grade mineralization is reported from drillhole BR-2K-08-002, which returned assay values of up to 2.1% Zn over 1 m (Figure 16; Saunders *et al.*, 2000c). Anomalous zinc mineralization has been traced up to 3 km to the east, where drillhole LS-2K-001 intersected 0.1% Zn over 12 m (Figure 16; Saunders *et al.*, 2000c).

Alteration

The use of SWIR spectrometry on outcrops and drillcore at the Tower prospect has identified the development of argillic to advanced argillic alteration, consisting of paragonite–paragonitic illite ± montmorillonite ± pyrophyllite, within felsic and intermediate volcanic rocks. This style of alteration has been identified in drillholes BJ-023 and LS-2K-005 (Figure 16), and when combined with outcrop occurrences of similar alteration, highlights the 3-km strike length

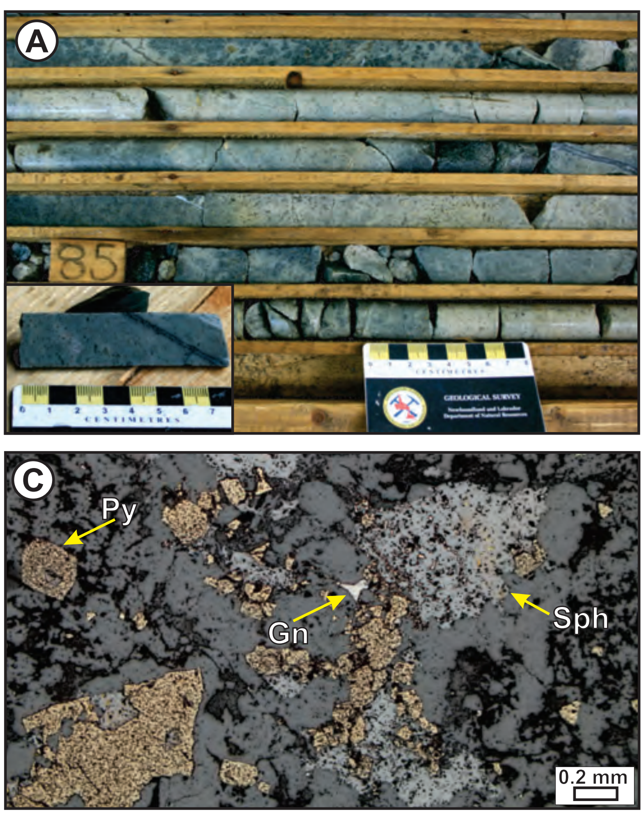

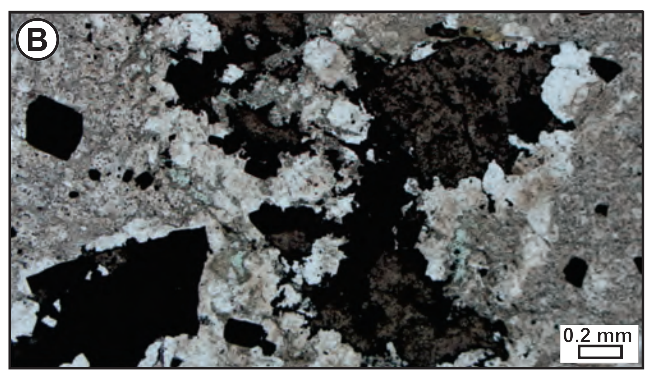

Plate 25. *A) Pervasively altered intermediate volcanic rock consisting of Fe–Mg-chlorite–muscovitic illite. The alteration is associated with disseminated pyrite throughout and is locally crosscut by sulphide-bearing quartz veins; Tower prospect, DDH BJ-035, 18–30 m depth. Sample shown in the inset (GS-22-51) assayed 0.7% Zn, 0.01% Pb, 0.02% Cu, 0.4 g/t Ag and 2300 ppb Hg over 0.9 m; B) Plane-polarized light photomicrograph of sample shown in the inset in (A) illustrating the quartz vein hosting sulphide mineralization within the sample; C) Reflected light image of (B) showing the distribution of pyrite (Py), sphalerite (Sph) hosting finely disseminated chalcopyrite, and galena (Gn).*

of the hydrothermal alteration, which remains open both to the east and west. Rocks, marginal to this zone, consist of variably developed muscovite–muscovitic-illite–Fe–Mg-chlorite alteration.

Drillhole LS-2K-005 intersected the eastern known extent of the advanced argillic alteration and provides the best relationships with regards to the hanging wall and footwall rocks relative to the hydrothermal alteration zone. The hanging-wall rocks above the alteration zone consist of aphanitic to weakly feldspar-phyric intermediate volcanic rocks characterized by a Fe–Mg-chlorite spectral signature, which transitions to Fe-chlorite within 30 m of the argillic to advanced argillic alteration zone (Figure 17). These volcanic rocks overlie a polymict lithic breccia, which is host to the development of paragonite–paragonitic-illite ± montmorillonite ± pyrophyllite, whereby the central core of the zone is defined by the rare occurrence of pyrophyllite around 185-m depth (Plate 26). This alteration zone is up to 70-m thick in drillcore but is barren with respect to base- and precious-metal values. The argillic to advanced argillic alteration is enveloped by, and gradational into, Fe-chlorite alteration up to 30-m thick (Plate 27; Figure 17). The polymict lithic breccia unit conformably overlies mafic volcanic rocks, having an Fe-chlorite-dominated spectral signature without associated white mica minerals, and locally displaying a well-developed hyaloclastite texture.

In the northwestern portion of the prospect, SWIR data collected from drillhole BR-99-08-001 illustrates the predom-

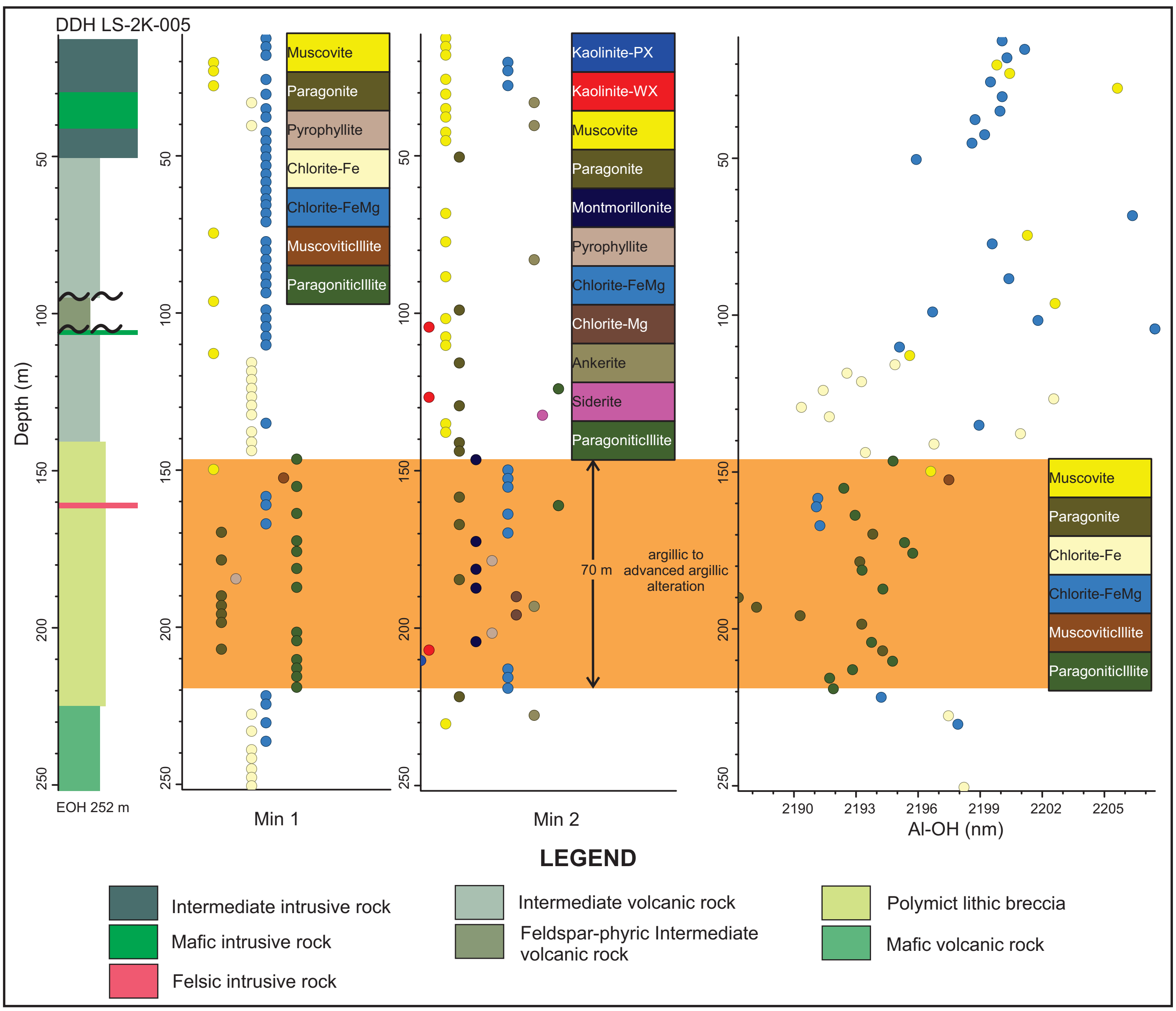

Figure 17. *Strip log for DDH LS-2K-005, outlining the distribution of the spectral data, mineral 1 (Min 1) and mineral 2 (Min 2), along with the related Al-OH absorption wavelength feature within the eastern portion of the Tower prospect.*

inance of phengite within the host intermediate volcanic rocks, which, here, is interpreted as the background regional signature. This unit is host to local base-metal enrichment, returning up to 0.12% Zn over 66.5 m (Saunders *et al.*, 2000b). This base-metal enrichment occurs immediately above a transition in the white mica signature of the host volcanic sequence and correlates with the upper contact of a polymict lithic breccia unit (Figure 18; Plate 28). Below this unit, the stratigraphy consists of intermediate volcanic rocks interbedded with rhyolite flows up to 10-m thick and rare quartz- and feldspar-phyric felsic intrusive rocks. The Al-OH values decrease to the bottom of the drillhole from the base of the aphyric intermediate volcanic unit, transitioning from ~2215 nm at 180 m depth to 2199 nm at 298 m depth.

LITTLE SANDY

The Little Sandy prospect is located approximately 4.5 km to the east of the Tower prospect and is hosted within

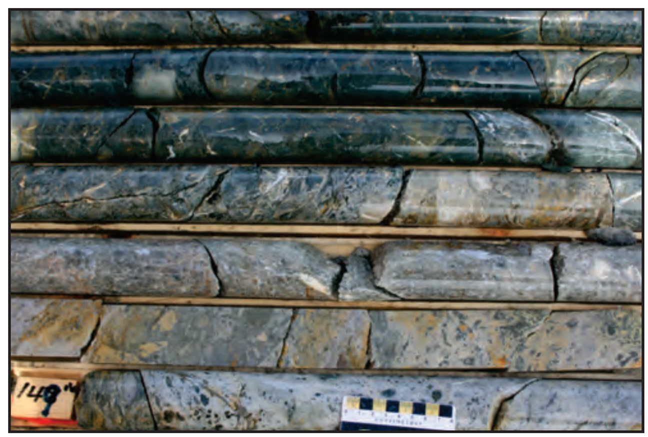

Plate 27. *Photograph of the upper gradational contact of the Tower alteration zone, transitioning from Fe-chlorite (top) to paragonitic illite ± montmorillonite (bottom) altered polymict lithic breccia; DDH LS-2K-005, 146 m depth.*

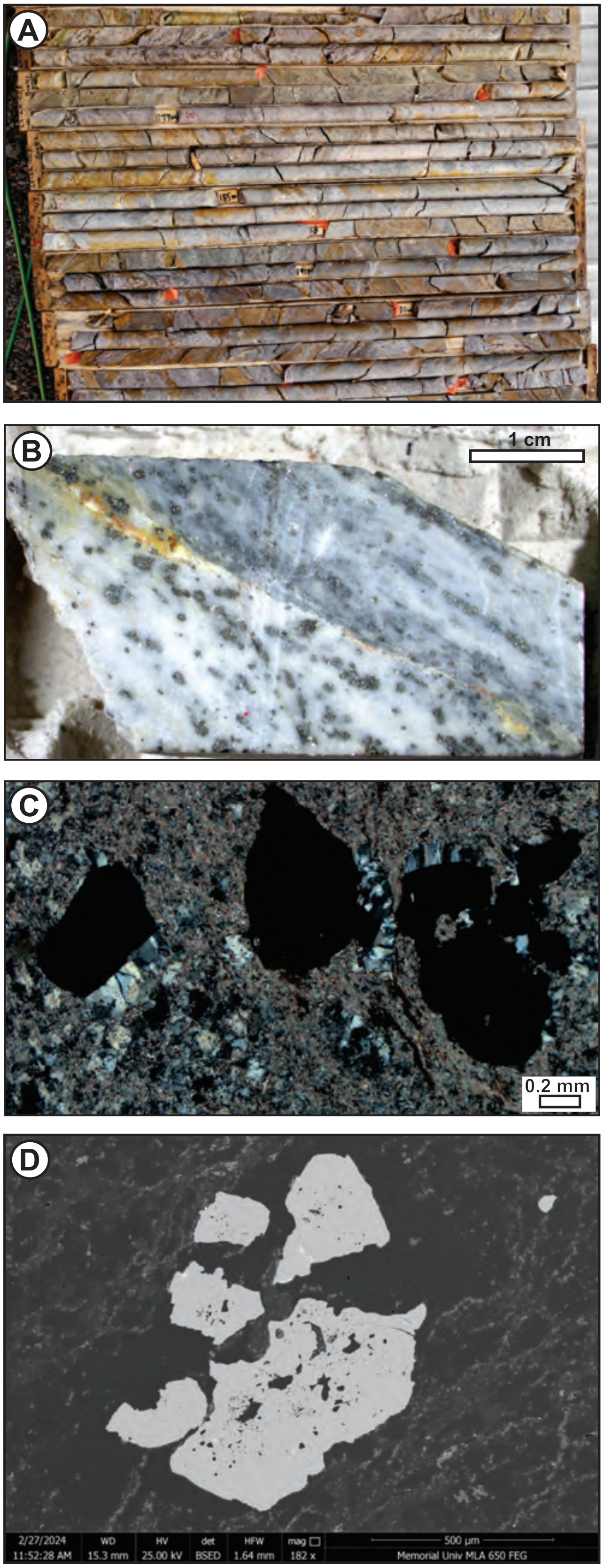

Plate 26. *A) Central core of the argillic to advanced argillic alteration zone hosting rare pyrophyllite spectral signatures in association with the bleached alteration near the center of the photograph; DDH LS-2K-005, 185 m depth; note that one row of drillcore is approximately 1.5 m in length. B) Paragonite-dominated white mica alteration hosting abundant disseminated pyrite throughout; DDH LS-2K-005, 184.5 m depth; C) Cross-polar photomicrograph highlighting the pervasive white mica alteration of the groundmass, which is host to secondary quartz–pyrite. Note the local inclusion of the altered groundmass within the pyrite; D) SEM image illustrating the characteristic "spongey" appearance of the pyrite within the central core of the alteration zone.*

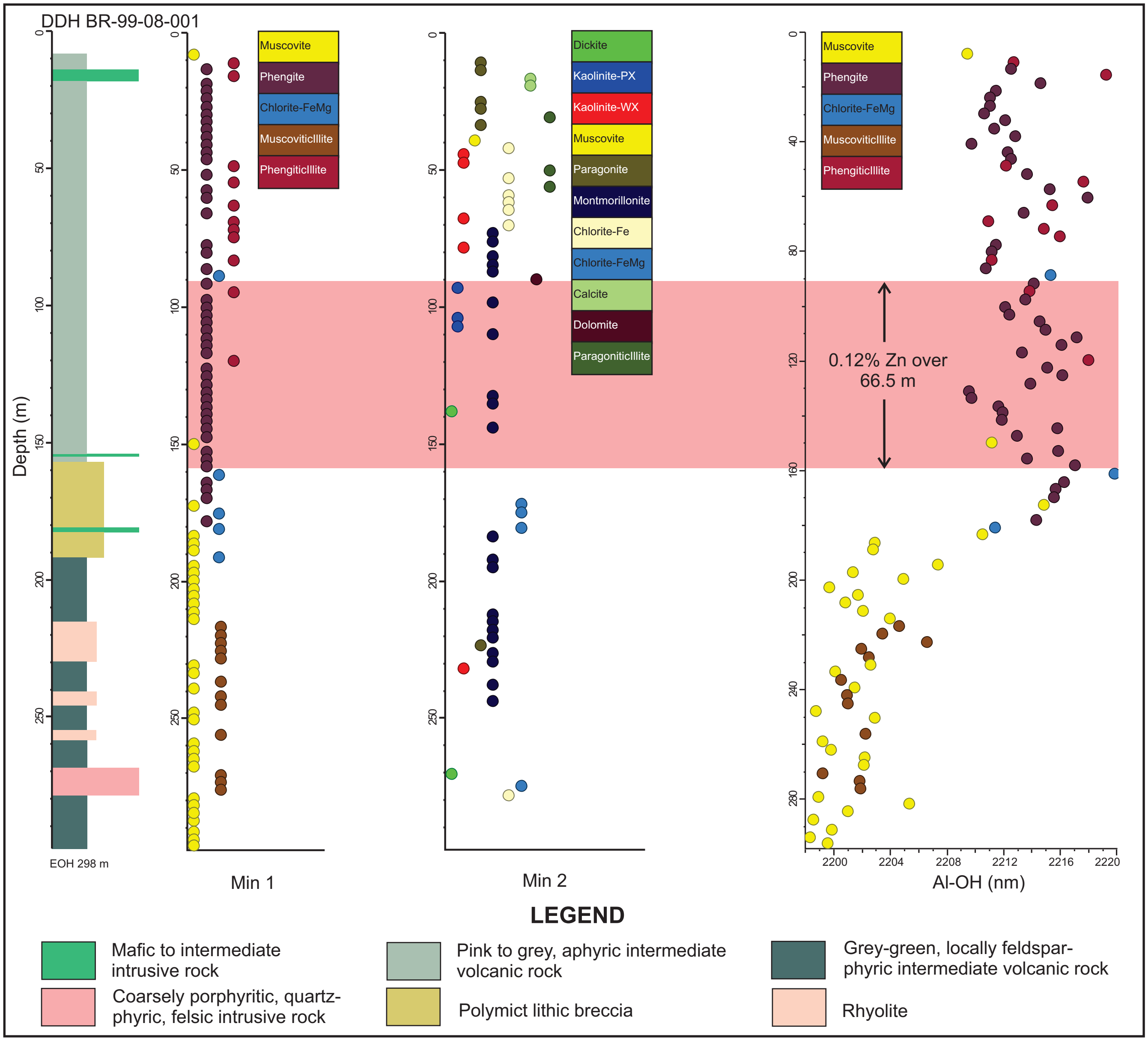

Figure 18. *Strip log for DDH BR-99-08-001, outlining the distribution of the spectral data, mineral 1 (Min 1) and mineral 2 (Min 2), along with the related Al-OH absorption wavelength feature within the northwestern portion of the Tower prospect. Assay values from Saunders* et al. *(2000b).*

Plate 28. *Transitional zone from phengite-dominated (top) into muscovite-dominated white mica spectral signatures developed near the sharp contact between a polymict lithic breccia and overlying weakly feldspar-phyric intermediate volcanic rock; DDH BR-99-08-001, 144–180 m depth. Note that one row of drillcore is approximately 1.5 m in length.*

mafic to intermediate volcanic rocks (Figure 1). These rocks are variably chloritized and silicified proximal to the development of copper-dominated stockwork-style mineralization. This area has been explored since the early 1940s; however, the first publicly available documented work does not occur until the early 1970s. The Little Sandy prospect is defined by 27 drillholes distributed over 800-m of strike length and contains a non-43-101 compliant resource estimate of 160 000 tonnes at 1.9% Cu (historical ASARCO documents). The drilling conducted to date at the prospect has outlined several zones of "sericite"–pyrite alteration, which are associated with a prominent IP geophysical anomaly extending for upwards to 4.5 km along strike (Saunders *et al.*, 2000c); however, only the immediate area of the Little Sandy prospect was evaluated as part of this study.

Previous Work

The prospect was first discovered in outcrop by ASARCO and was subsequently drilled in the early 1940s, and again in the 1950s. During the late 1970s, Price Company Limited and ASARCO conducted additional exploration in the area, which included drilling twenty-four holes (Barbour, 1978; Pearce and Thurlow, 1979). Abitibi-Price continued exploration during the early- to mid-1980s, which was followed by investigations by BP-Selco in the late 1980s. Noranda conducted geophysical and geochemical surveys, and limited diamond drilling in the area surrounding the Little Sandy prospect in the early- to mid-1990s (Graves and Squires, 1992; Squires, 1994a; Arseneau *et al.*, 1995b). During the same time, Newfoundland Mining and Exploration and GT Exploration also conducted work in the area, which largely consisted of compilation work and geochemical surveys (Saunders, 1997a, b). Buchans River Limited (now Buchans Minerals Corp.) has explored the area from the early 2000s until present, conducting various geophysical and geochemical surveys in addition to diamond drilling (Saunders *et al.*, 2000b, c; Saunders, 2001; Harris and Woods, 2001b; Wallis, 2001; Wallis and Barrett, 2001; Moore *et al.*, 2008, 2013a), with the most recent work summarized in Moore and Butler (2019).

Local Geology

The geology of the Little Sandy area consists of interbedded and interfingering mafic, intermediate, and felsic volcanic rocks (Thurlow and Swanson, 1981). The mineralization in the area is largely confined to the mafic volcanic rocks; felsic volcanic breccias are present but are not mineralized (Winter, 2000). The development of a separate alteration zone to the west of the main prospect, which structurally overlies relatively unaltered mafic volcanic rocks, implies the area is more structurally complex than illustrated on geology maps of the area (Figure 19; *see* below). These northeast–southwest trending structures potentially correlate with two sub-parallel airborne EM anomalies that are evident in a recent airborne survey (*e.g.*, Seymour, 2017).

Mineralization

The mineralization developed at the prospect consists of stockwork-style veining, consisting of quartz–pyrite–chalcopyrite, hosted in chloritized and silicified mafic volcanic rocks, locally forming a stratiform zone. This mineralization has been interpreted as being both epigenetic, and VMS-related by Barbour (1978) and Winter (2000), respectively. In contrast to other prospects in the region, the mineralization at the Little Sandy prospect is primarily copper dominated, with only minor values of accompanying lead and zinc. Early work reported elevated gold values in association with the copper mineralization (Barbour, 1978), however subsequent work has not replicated these results. Anomalous gold (<250 ppb) is locally noted distal from the main alteration zone in association with pyritic alteration hosted in felsic volcanic rocks (*e.g.*, 234 ppb over 1.5 m; DDH LS-2K-007; Saunders *et al.*, 2000c). The best assay results are reported from drillhole LS-07-017, which returned 8.4% Cu over 0.5 m (Plate 29) and occurs within a broader interval assaying 2.1% Cu over 9.3 m (Moore and Butler, 2008).

Alteration

Limited spectral data was collected from the immediate area of the Little Sandy prospect, but several relationships can be observed from this data. Drillhole BJ-013 is located in the central core of the prospect (Figure 19). This drillhole

Plate 29. *Photograph of massive chalcopyrite-dominated veins hosted within greyish, silicified, mafic to intermediate volcanic rocks, locally displaying relic breccia textures; DDH LS-07-017, ~88 m depth. The interval below the scale card assayed 8.4% Cu, 0.01% Zn, 0.01% Pb and 9.9 g/t Ag over 0.5 m (Moore and Butler, 2008) and is characterized by Fe-chlorite–paragonite alteration.*

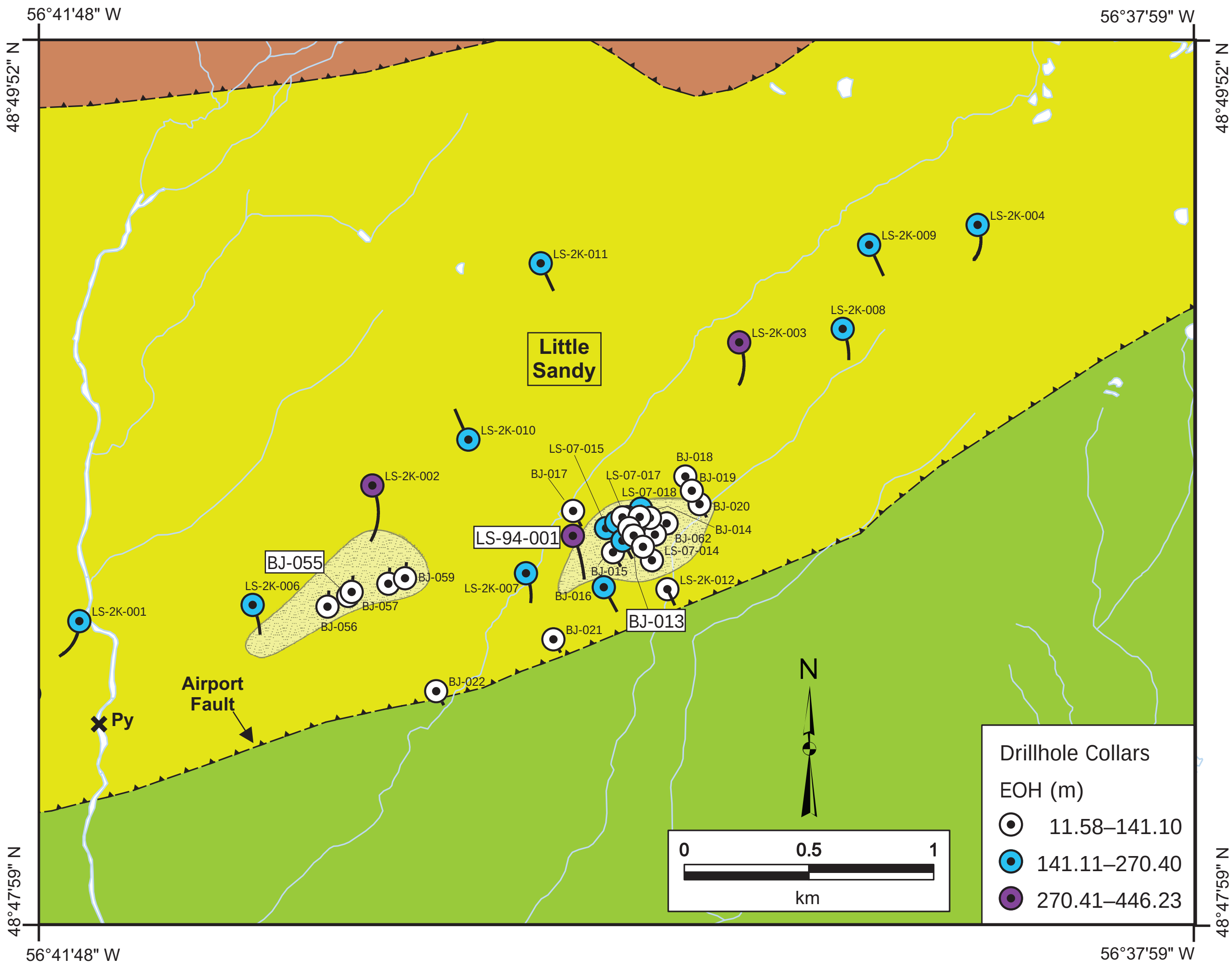

Figure 19. *Location map showing the distribution of diamond-drill holes and geology within the area of the Little Sandy prospect. Refer to Figure 1 for legend.*

collars into a felsic-dominated monolithic breccia unit and then transitions into underlying, locally mineralized, mafic volcanic rocks (Plate 30). The upper monolithic breccia is characterized as a mixture of Fe–Mg- and Fe-chlorite along with lesser muscovite and rare carbonate spectral signatures. The lower portion of this unit, along with the underlying mineralized mafic volcanic rocks display a shift to Fe-chlorite dominated spectral signatures in association with the development of paragonite white mica alteration (Figure 20). This mineralized zone is associated with the shortest wavelength white-mica alteration observed in the drillhole and represents a similar style of alteration to that noted in association with mineralization in drillhole LS-07-017 (Plate 29).

Drillhole LS-94-001 is located 200 m to the west of BJ-013 and is devoid of any significant mineralization. This drillhole collars into a mixed sequence of felsic and mafic volcanic rocks before transitioning into a mafic-dominated sequence toward to the bottom of the drillhole. These rocks are characterized by Fe–Mg-chlorite and lesser Fe-chlorite and muscovite spectral signatures (Figure 21). Aside from the weak to moderate disseminated pyrite hosted within the mafic volcanic rocks toward the bottom of the drillhole, this sequence is largely unaltered.

A series of drillholes, located 800 m west of drillhole LS-94-001 (DDH BJ-055-59; Figure 19), outline an alteration zone consisting of Fe-chlorite–paragonitic illite–paragonite–montmorillonite (Plate 31). This alteration is hosted within a polymict lithic breccia unit like that observed at the Tower prospect and may represent the along strike extension of this alteration zone (Figure 22). The white mica dominated alteration is confined to the felsic to intermediate rocks, which structurally overlie relatively unaltered mafic volcanic rocks

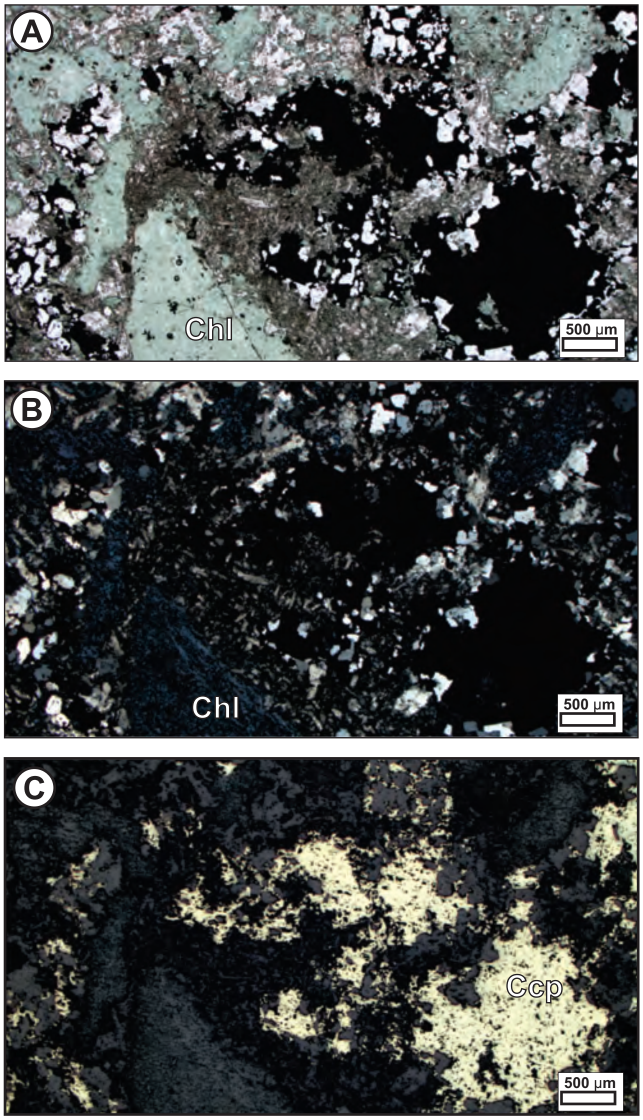

Plate 30. *A) Plane-polarized light photomicrograph of chalcopyrite-dominated mineralization hosted within an Fe–Mg chlorite (Chl)–quartz altered mafic volcanic rock; DDH BJ-038, 51.5 m depth; B) Cross-polar photomicrograph of (A) highlighting the pervasive chlorite alteration locally associated with a distinctive blue birefringence; C) Reflected light image of (B) outlining the distribution of chalcopyrite (Ccp) within the sample, which displays irregular margins and is intergrown with quartz.*

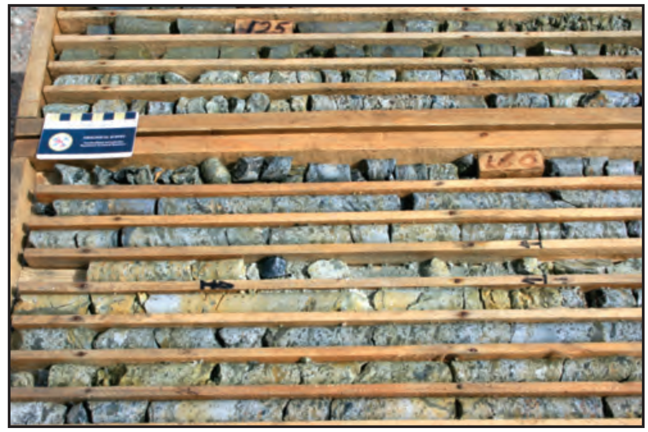

Plate 31. *Paragonitic illite–Fe-chlorite dominated alteration developed within a polymict lithic breccia unit. An assay from the centre of the photograph produced 0.2% Zn and 0.1% Cu and 2.6 g/t Ag over 0.4 m (Thurlow* et al.*, 1987); however, much of the alteration zone remains unsampled; DDH BJ-055, ~50 m depth.*

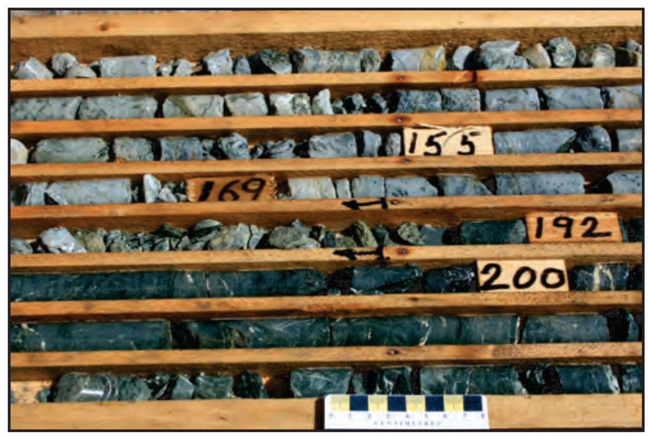

Plate 32. *Sharp structural contact separating altered polymict lithic breccia from underlying relatively unalerted mafic volcanic rocks displaying a Fe–Mg-chlorite dominated spectral signature; DDH BJ-056 ~60 m depth.*

(Plate 32). The latter is characterized by Fe–Mg–chlorite-dominated spectral signatures. This zone of white mica alteration is magnetite destructive, with the magnetic susceptibility of the alteration zone contrasting that of the surrounding intermediate to mafic volcanic rocks, which are weakly to moderately magnetic. Limited assay data from this alteration zone include assays of up to 0.2% Zn and 0.1% Cu and 2.6 g/t Ag over 0.4 m (Thurlow *et al.*, 1987). In addition, core re-logging by Altius Minerals of a drillhole to the immediate north of this zone (DDH LS-2K-002; Figure 19) noted local massive sulphide hosted within a felsic pyroclastic breccia unit that returned assays of 0.6% Zn, 0.3% Cu and 5.6g/t Ag over 0.5 m (Seymour *et al.*, 2015).

SEAL POND

The Seal Pond prospect is located some 10 km northeast of the Little Sandy prospect, along the projected strike of the MMBG (Figure 1). Mineralization in the area has a strike length of approximately 1.8 km and is defined by 14 drillholes (Figure 23). Here, felsic volcanic rocks are locally host

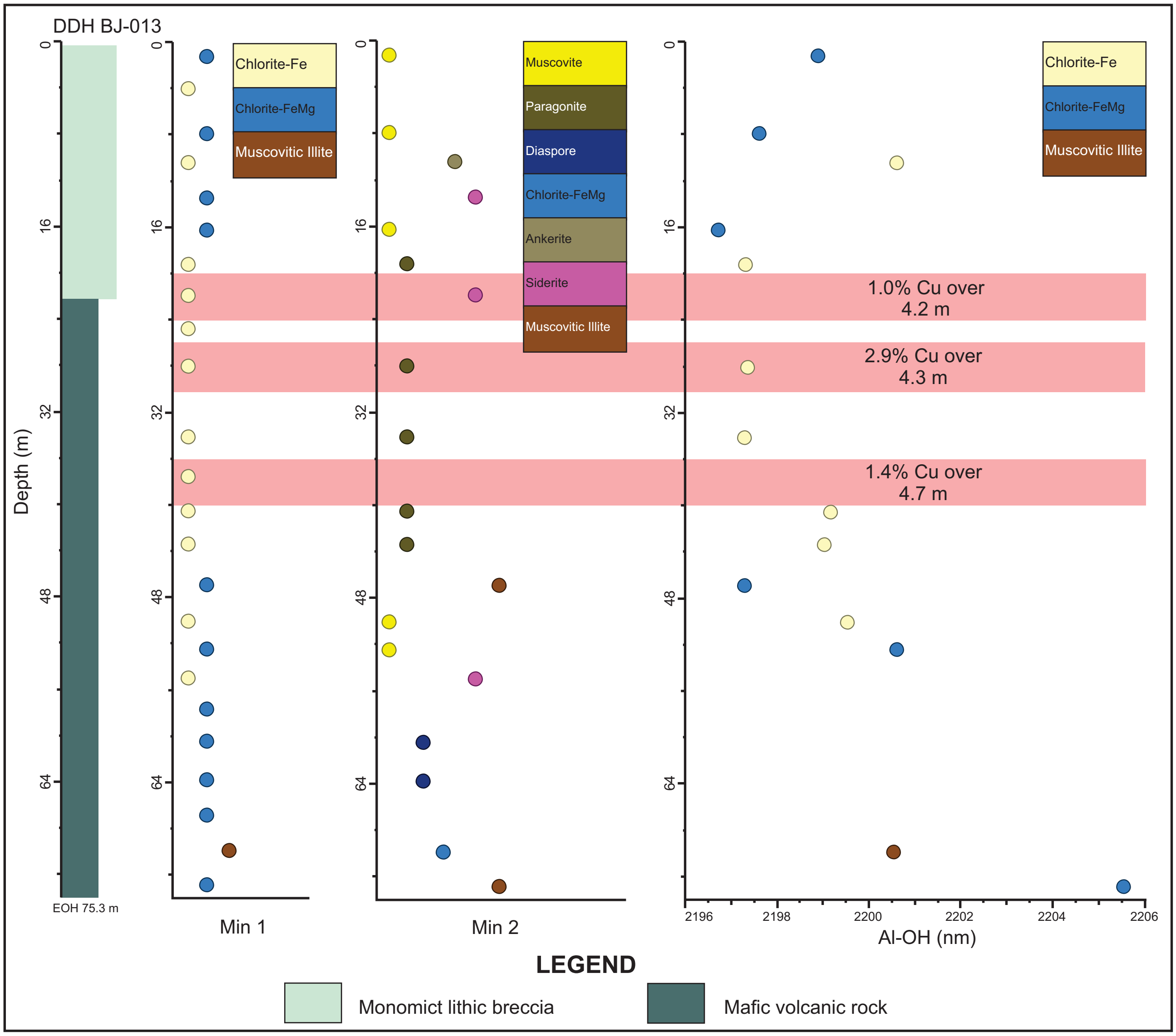

Figure 20. *Strip log for DDH BJ-013, outlining the distribution of the spectral data, mineral 1 (Min 1) and mineral 2 (Min 2), along with the related Al-OH absorption wavelength feature, Little Sandy prospect. Assay values from Pearce and Thurlow (1979).*

to the development of VMS-style mineralization in association with "sericite" alteration (Squires, 1996).

Previous Work

A detailed account of the mineral exploration conducted can be found in Sparkes (2022). Mineralization was first identified in the area by Noranda in the early 1990s through basal-till sampling, which targeted an airborne geophysical anomaly (Squires, 1994b). Additional exploration work was conducted during the mid-1990s in the form of soil sampling, geophysical surveying, and diamond drilling (Squires and McDonald, 1995; McDonald, 1995). Results from this drilling locally intersected zones of sericitic alteration accompanied by sulphide mineralization, which returned values of up to 3.3% Zn and 0.5% Cu over 0.1 m (Squires, 1996). Noranda continued work in the area up to the late 1990s (Noranda Mining and Exploration Inc., 1998), which was then followed by Vinland Resources in the 2000s (Chislett, 2004, 2005, 2007; Chislett and Graves, 2004; Chislett *et al.*, 2005; Chislett and Wilton, 2006). As part of regional compilation work by Altius Minerals in the mid-2010s, drillcore from the area was re-logged, noting narrow intersections of previously unsampled base-metal mineralization. The best intersections reported from this re-sampling included 13.45% Zn, 0.4% Cu and 2 g/t Ag over 0.2 m and 4.68% Cu, 0.4% Zn and 6.8g/t Ag over 0.25 m (Seymour *et al.*, 2015). Most recent work in the area consisted of trenching that targeted

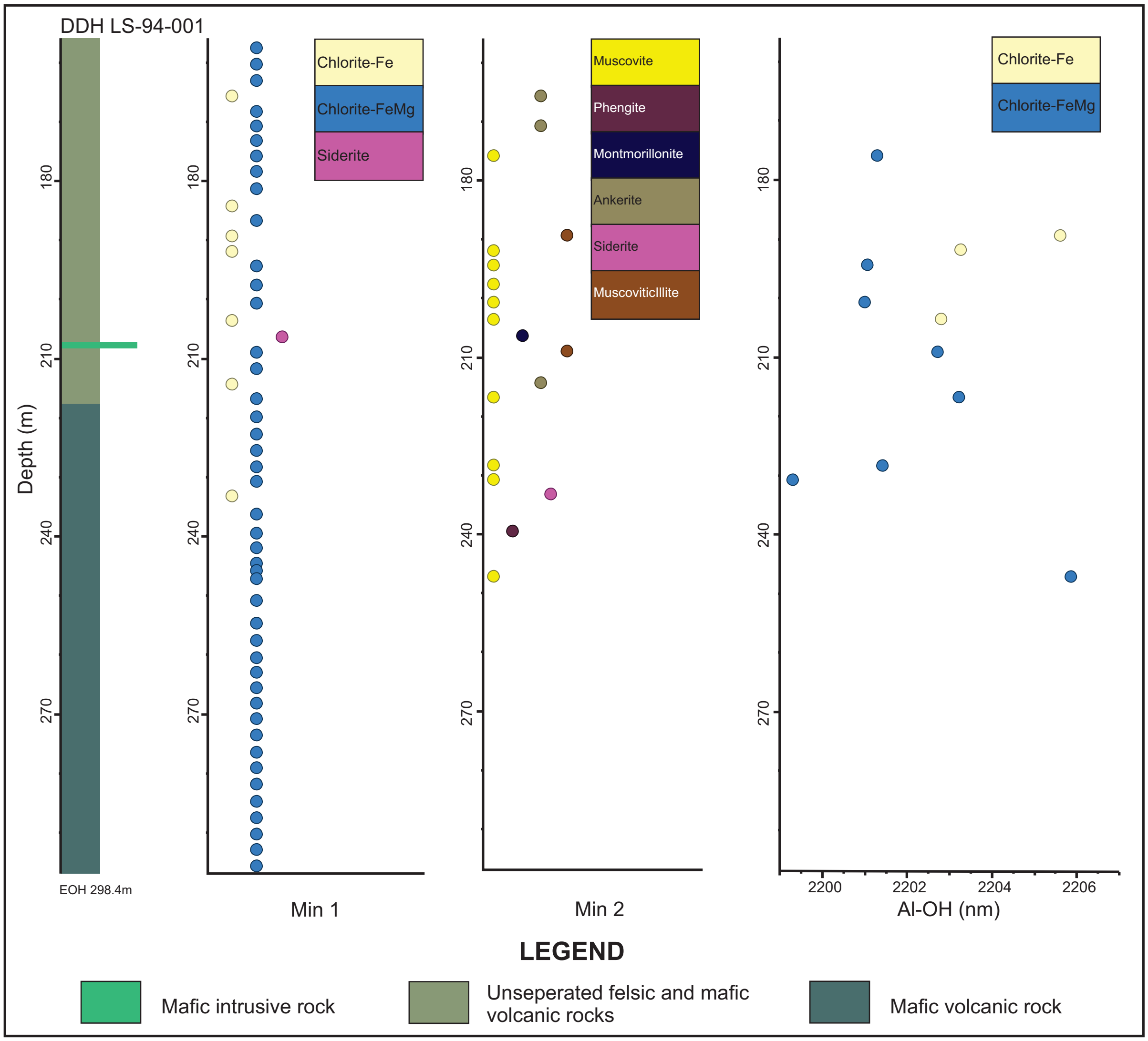

Figure 21. *Partial strip log for DDH LS-94-001, outlining the distribution of the spectral data, mineral 1 (Min 1) and mineral 2 (Min 2), along with the related Al-OH absorption wavelength feature, Little Sandy prospect.*

historical soil anomalies and exposed several zones of altered and mineralized felsic volcanic rocks, which locally assayed up to 1.4% Zn and 0.2% Cu (Patey, 2020).

Local Geology

The main occurrence consists of variably deformed mafic volcanic rocks with intermixed intermediate to felsic volcanic rocks, which are intruded by both felsic, quartz–feldspar porphyry, and mafic dykes. The presence of "sericite" alteration is spatially associated with the development of localized VMS-style mineralization, which occurs as semi-massive bands, fine-grained disseminations, and stockwork-style veins (Squires, 1996; Plate 33). In areas of lower strain, locally well-preserved, primary fragmental volcanic textures are visible in drillcore (Plate 34). The area of the Seal Pond alteration zone corresponds with a northeast–southwest trending magnetic low on regional airborne surveys, with the majority of drillholes that intersect base-metal mineralization located along the north-northwestern extent of this magnetic low. One drillhole (SP-04-003; Figure 23), located within the central portion of this magnetic low, intersected "footwall-style" VMS alteration up to 26 m in core length, consisting of "sericite"–silica alteration along with altered and highly fractured rhyolite that assayed up to 0.4% Zn and 0.2% Cu over 2.2 m (Chislett, 2004; Seymour *et al.*, 2015).

Mineralization

Zinc–copper mineralization is dominant within the prospect, with no significant development of lead or barite (Seymour, 2017). Narrow intersections of high-grade massive sulphide mineralization have been reported in association with "sericitic" alteration zones. Assay highlights from the area

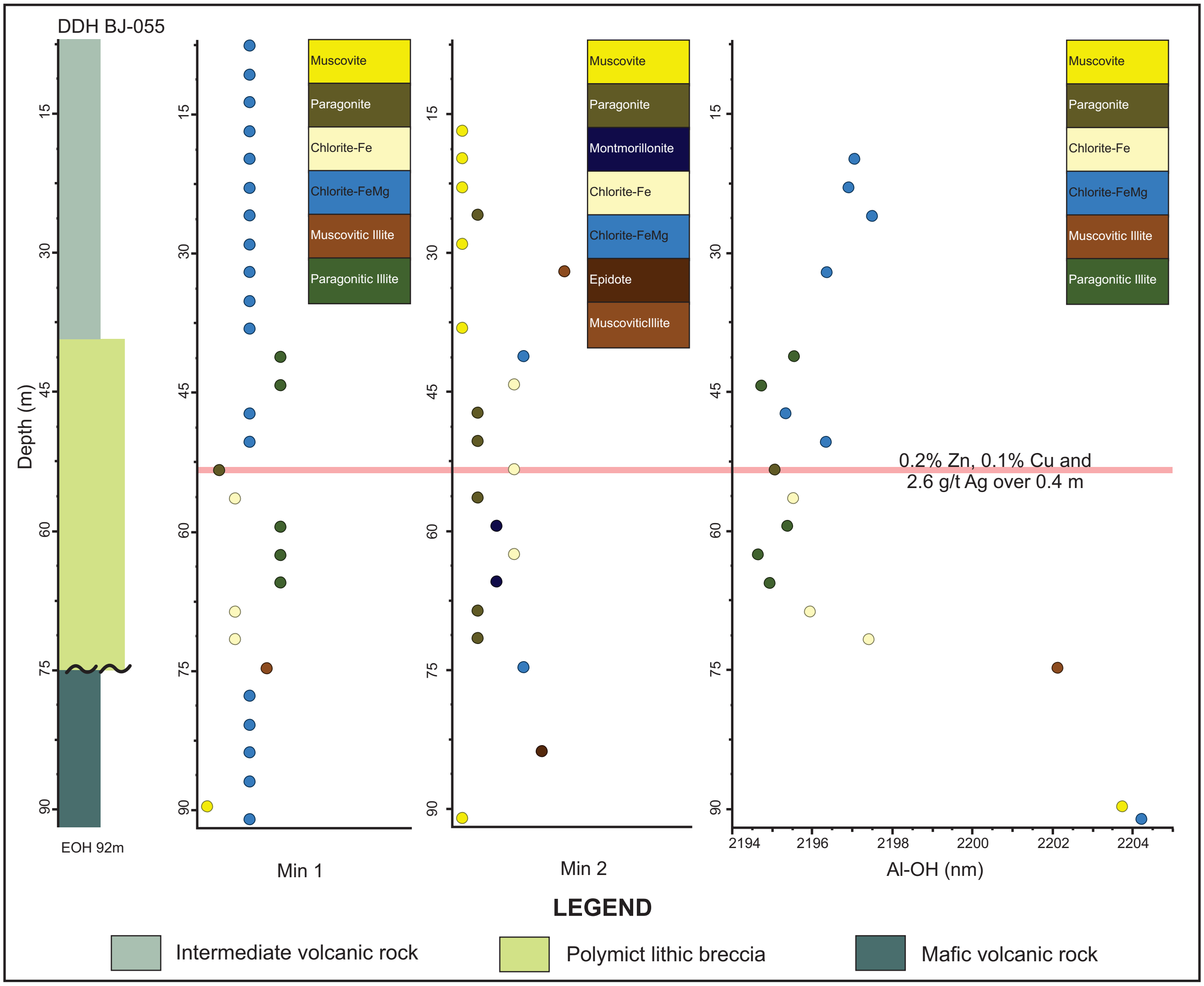

Figure 22. *Partial strip log for DDH BJ-055, outlining the distribution of the spectral data, mineral 1 (Min 1) and mineral 2 (Min 2), along with the related Al-OH absorption wavelength feature, Little Sandy prospect. Note the pronounced termination of the white mica alteration in relation to the fault structure around 75 m depth. Assay values from Thurlow et al. (1987).*

include up to 3.45% Zn, 0.4% Cu and 2 g/t Ag over 0.2 m (DDH SP-05-005, 271 m depth), from a 10-cm wide band of semi-massive sulphide consisting of sphalerite–chalcopyrite–pyrite within the matrix of a felsic fragmental volcanic rock (Seymour *et al.*, 2015). The best copper intersection assayed 4.7% Cu, 0.4% Zn and 6.8 g/t Ag over 0.25 m (DDH SP-06-016, 133 m depth) and is from a semi-massive pyrite band hosting disseminated chalcopyrite (Seymour *et al.*, 2015). Anomalous gold is also reported from the same hole, locally assaying 0.3 g/t Au over 1.9 m at ~164 m depth (Seymour *et al.*, 2015).

Alteration

Limited spectral data was collected from the Seal Pond area, primarily targeting the alteration zone intersected in drillhole SP-95-001, along with analysis of several representative samples from other drillholes in the area. Drillhole SP-95-001 predominantly consists of variably altered intermediate volcanic rocks intruded by felsic and intermediate dykes (Figure 24). The upper portion (10–80 m) of this drillhole consists of an Fe–Mg chlorite dominated spectral signature along with lesser phengite, and is inferred to be relatively unaltered, even though this interval is locally reported to contain vein-hosted mineralization (Squires, 1996). Below 80 m depth, locally significant intervals of muscovite–pyrite alteration are developed, which is accompanied by a notable shift in the Al-OH values from ~2217 to 2200 nm (Plate 35). Limited sampling of this zone has been carried out, the alteration is locally host to anomalous copper and zinc values of up to 0.8% Cu and 0.3% Zn over 0.3 m, along with anom-

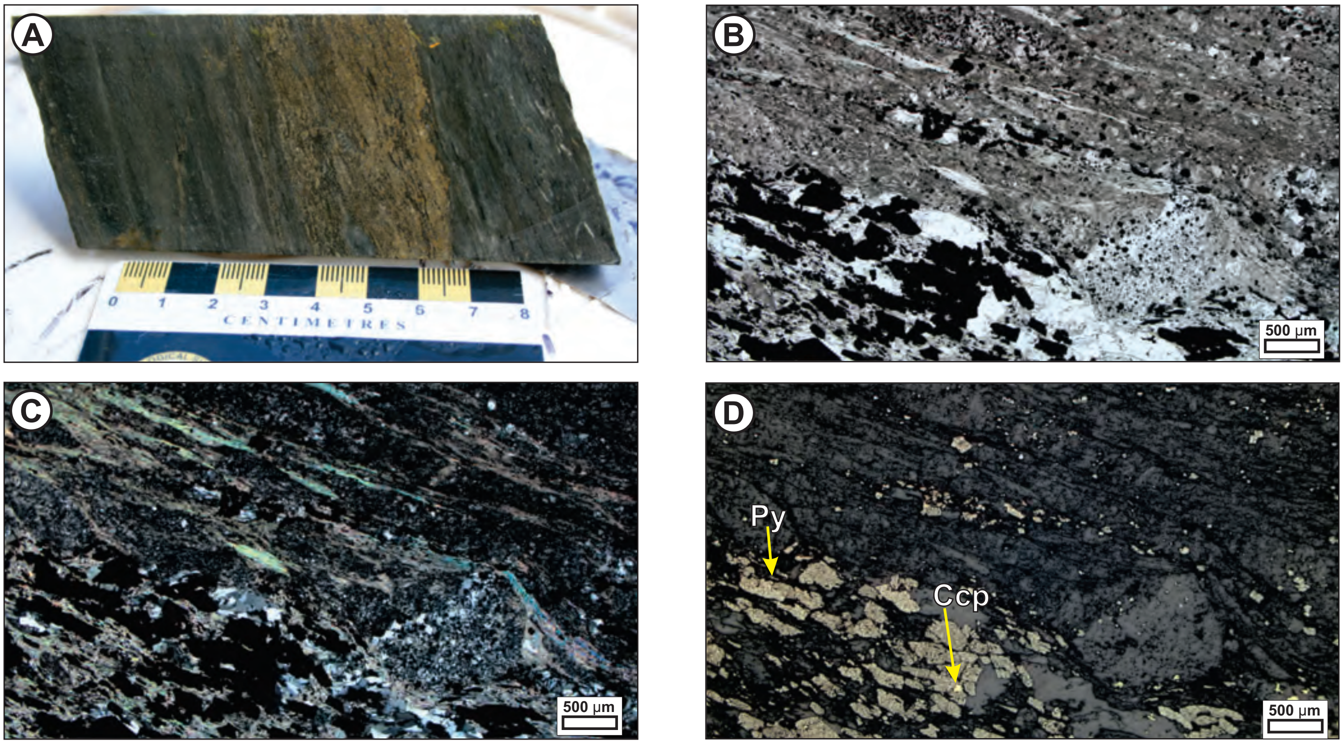

Plate 33. *A) Band of semi-massive sulphide containing predominantly pyrite along with lesser sphalerite and chalcopyrite, hosted within a strongly foliated fragmental volcanic rock with Fe–Mg chlorite–paragonite alteration; DDH SP-05-006, 232.5 m depth; B) Plane-polarized light photomicrograph of the sample shown in (A) highlighting the fragmental nature of the host rock, which is moderately foliated. Sulphides occur as fine-grained disseminations throughout the host rock in addition to the semi-massive sulphide band; C) Cross-polar photomicrograph of (B) highlighting the abundant white mica alteration developed parallel to the foliation; D) Reflected light image of (C) showing the distribution of predominantly pyrite (Py) along with lesser chalcopyrite (Ccp) within the sample.*

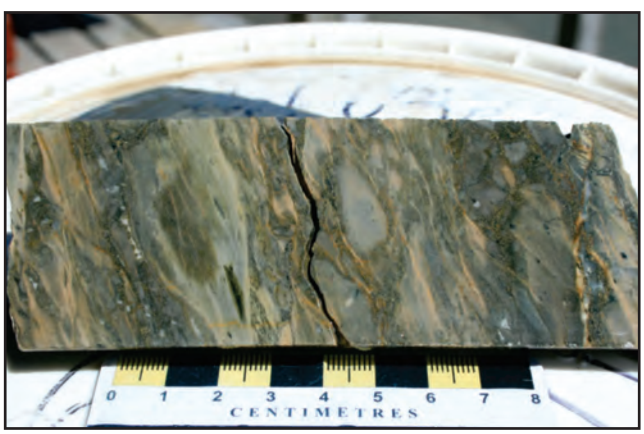

Plate 34. *Fragmental volcanic unit hosting muscovite alteration in association with disseminated pyrite; DDH SP-06-016, 191.5 m depth.*

Plate 35. *Upper gradational contact of the muscovite–pyrite alteration zone transitioning from Fe–Mg chlorite dominated intermediate volcanic rocks at the top of the photograph; DDH SP-95-001, 89–105 m depth.*

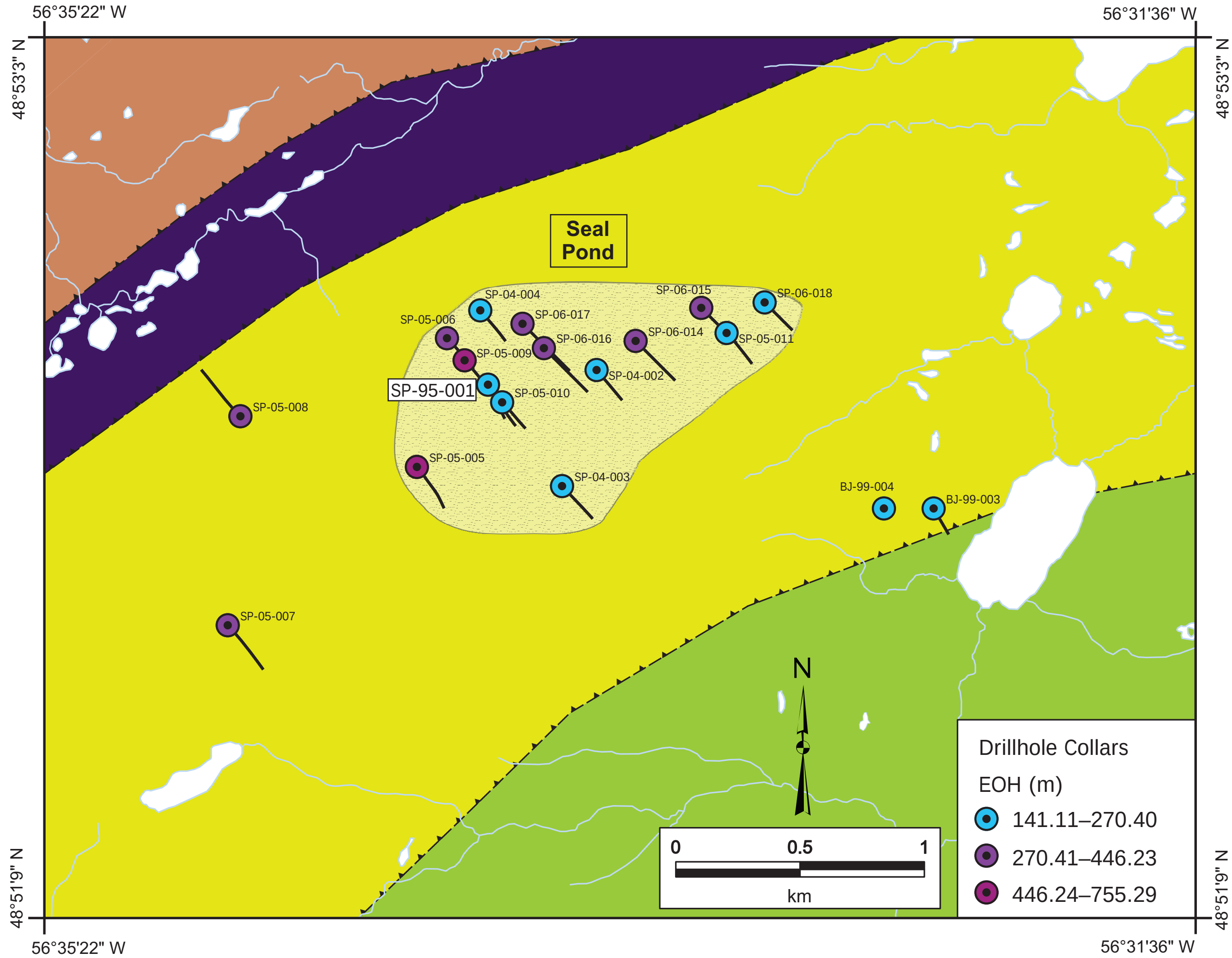

Figure 23. *Location map showing the distribution of diamond-drill holes and geology within the area of the Seal Pond prospect. Refer to Figure 1 for legend.*

alous gold values of up to 240 ppb over 1 m (Squires, 1996). The alteration is variably developed and continues to a downhole depth of approximately 160 m, where the alteration gradually diminishes and Fe–Mg chlorite again becomes predominant within the host intermediate volcanic rocks.

BEAVER POND

Six kilometres to the east of the Seal Pond prospect is the Beaver Pond prospect (Figure 1). This prospect represents the most northeastern zone of "sericite" alteration intersected in drillcore within the MMBG. Here, a moderate to strong zone of hydrothermal alteration is developed within felsic volcanic rocks of the MMBG. Samples from these felsic volcanic rocks to the north and west of the prospect are noted to display localized hydrothermal alteration with associated anomalous values of silver, arsenic, and mercury (Squires, 1994c).

Previous Work

This area was initially identified through reconnaissance basal-till sampling (Thurlow and Anderson, 1984) and was further investigated with an IP survey conducted by BP-Selco during the late 1980s (McKenzie and Hoffman, 1986). The area of the prospect was also highlighted by a soil survey that identified a significant zinc anomaly (Poole *et al.*, 1987). The Beaver Pond prospect was also investigated by Noranda (Squires *et al.*, 1992; Graves and Squires, 1992; Squires and Marenghi, 1993) and Tech (Pickett and Scott, 1992) during the 1990s. Celtic Minerals conducted work in the 1990s and 2000s, which included an IP survey that confirmed the existence of the historical anomaly (Greene and Thurlow, 1997; Stuckless *et al.*, 2009). Recent mapping in the area by Canstar Resources has identified a new zone of alteration to the north of the main prospect, consisting of "sericite" alteration and silicification within felsic volcanic rocks containing anom-

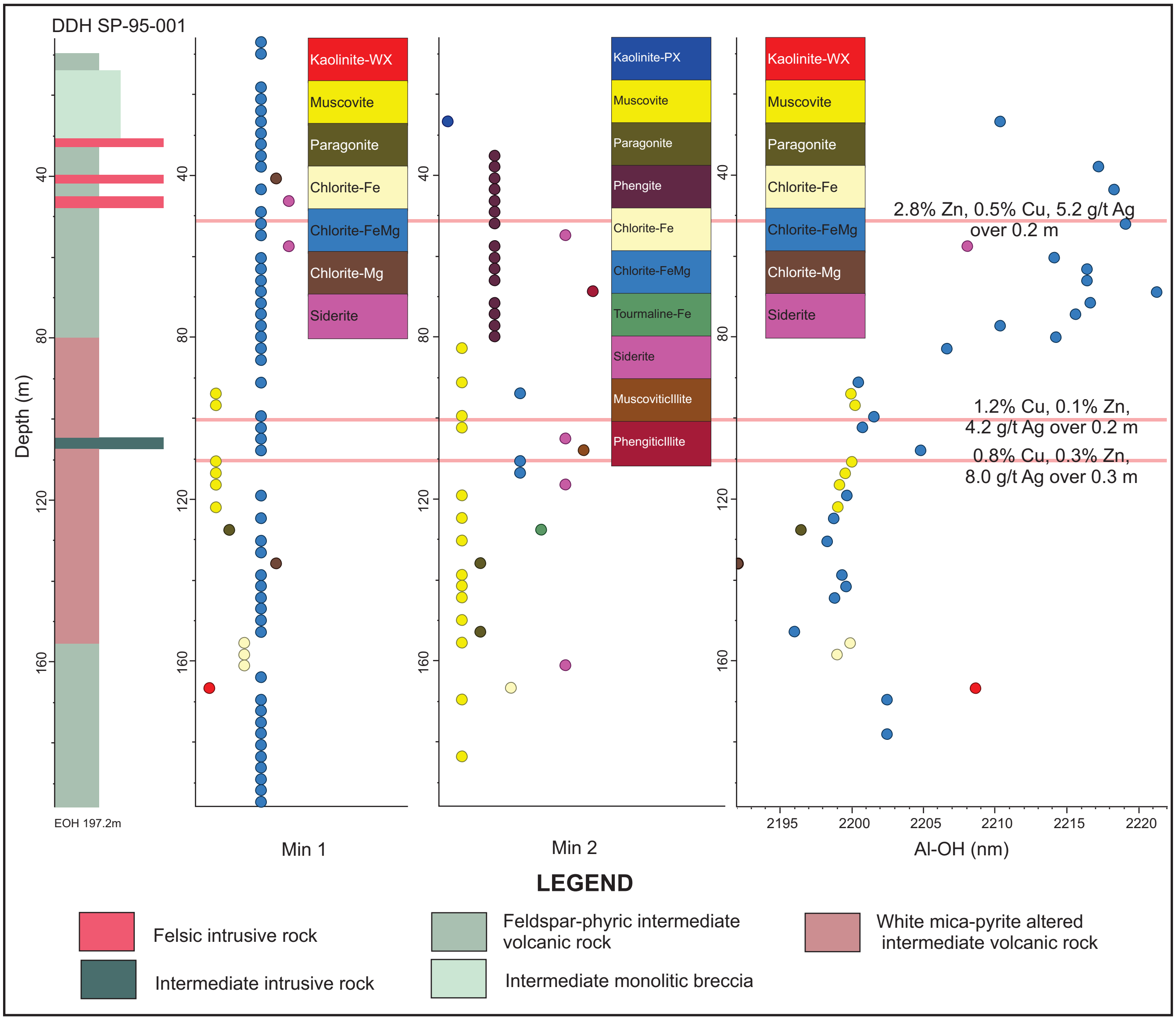

Figure 24. *Strip log for DDH SP-95-001, outlining the distribution of the spectral data, mineral 1 (Min 1) and mineral 2 (Min 2), along with the related Al-OH absorption wavelength feature, Seal Pond prospect. Assay values from Squires (1996).*

alous gold and silver (Patey, 2020). Two drillholes have tested the Beaver Pond prospect, which intersected variably silicified and sericitized felsic volcanic rocks locally hosting stringer sulphide mineralization containing anomalous base- and precious-metal enrichment. Similar styles of alteration were also intersected in a drillhole approximately 2.5 km to the northeast (BJ-082; Figure 25; McKenzie and Hoffman, 1986), which occurs along a coincident regional magnetic low that extends northeast from the Beaver Pond area. This same magnetic anomaly is also coincident with an untested zinc and gold soil anomaly (Woods, 1988), which occurs approximately 1 km along strike to the northeast of the Beaver Pond prospect. Xmet Inc. investigated the area, along strike, to the southwest of the Beaver Pond alteration zone and drill tested a geophysical conductor coincident with an area of anomalous soil geochemistry, some 3 km southwest of the Beaver Pond prospect, but no significant alteration was intersected (Yeomans, 2011).

Local Geology

The area of the Beaver Pond prospect consists of tholeiitic mafic and felsic volcanic rocks of the MMBG (Zagorevski and Rogers, 2009; Zagorevski *et al.*, 2015, 2016). Mafic volcanic rocks primarily consist of pillow basalt and are generally unaltered to weakly altered. The felsic volcanic rocks consist of crypto domes and related pyroclastic rocks, locally containing variable white mica alteration and

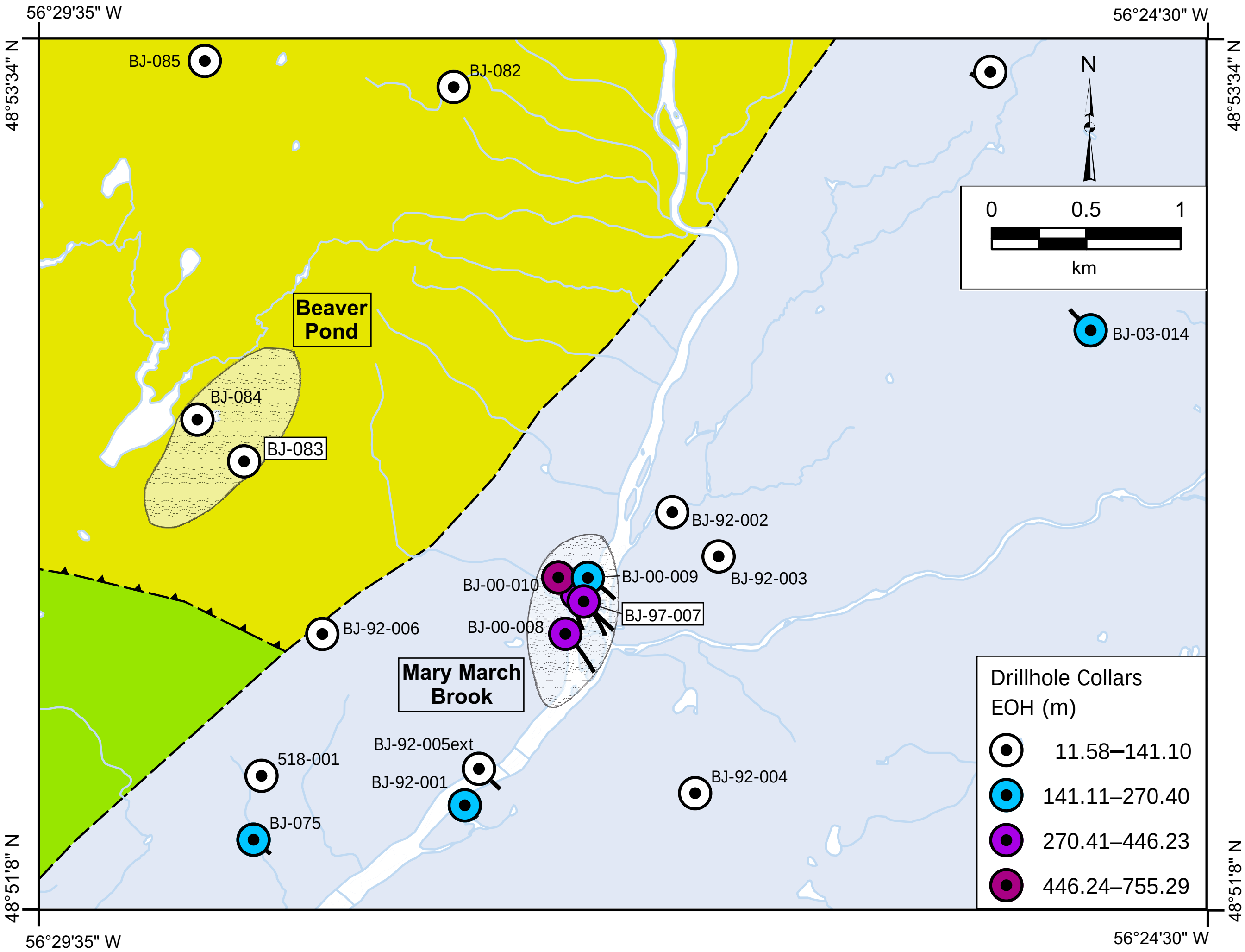

Figure 25. *Location map showing the distribution of diamond-drill holes and geology within the area of the Beaver Pond and Mary March Brook prospects. Refer to Figure 1 for legend.*

fine-grained disseminated pyrite and lead–zinc sulphides, in addition to anomalous values of silver, arsenic and mercury (Squires, 1994c). The alteration developed within the felsic volcanic rocks is noted to be most intense around the immediate area of Beaver Pond (Squires and Marenghi, 1993).

Mineralization

Only two drillholes have tested the immediate area of the Beaver Pond prospect, which intersected variably silicified and sericitized felsic volcanic rocks locally hosting stringer sulphide mineralization containing anomalous base metals and gold. The best results from this zone returned 0.6% Cu, >1.0% Pb, >1.0% Zn, 98 g/t Ag and 0.72 g/t Au over 0.03 m (DDH BJ-083; Thurlow *et al.*, 1987). This alteration zone consists of an aerially extensive variably developed white mica dominated alteration, hosting anomalous values of zinc, lead, copper, silver and gold along with anomalous indicator elements such as arsenic and mercury.

Alteration

Limited spectral data was collected from the Beaver Pond area, with only one drillhole being examined (DDH BJ-083; Figure 25). This drillhole is dominated by Fe–Mg chlorite along with variably developed silicification and associated white mica alteration. The drillhole collars within a variably altered polymict lithic breccia unit characterized by muscovite and Fe–Mg chlorite dominated spectral signatures, with the more visually altered sections of the drillhole being dominated by muscovite. This spectral signature continues downhole to a depth of 93 m where there is a notable shift in the Al-OH values from ~2202 to ~2193 nm, associated with the development of Fe–Mg chlorite–paragonite-

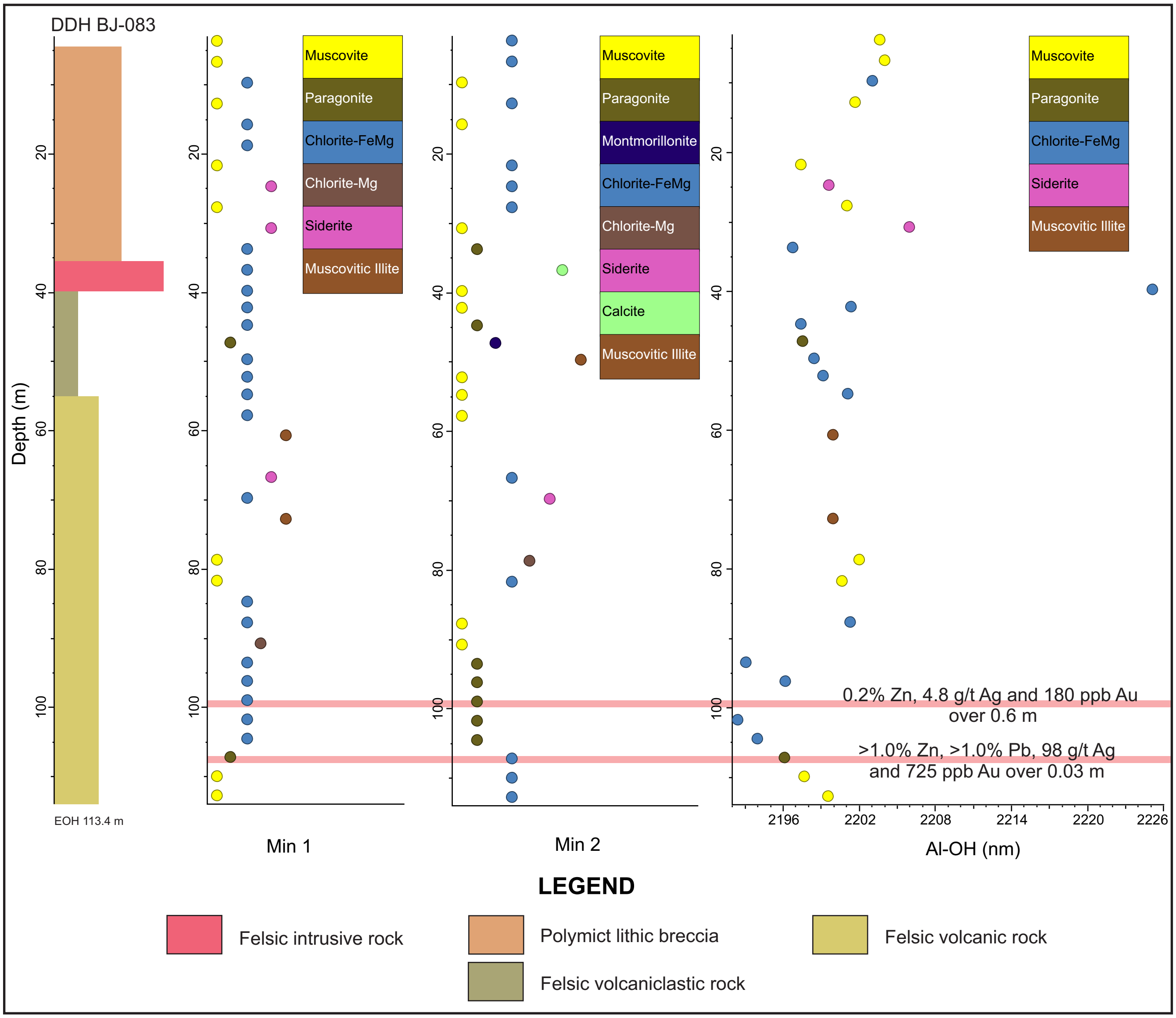

Figure 26. *Strip log for DDH BJ-083, outlining the distribution of the spectral data, mineral 1 (Min 1) and mineral 2 (Min 2), along with the related Al-OH absorption wavelength feature, Beaver Pond prospect. Assay values from Thurlow* et al. *(1987).*

dominated alteration (Figure 26). This zone of alteration, extending from ~93–109 m is accompanied by localized base- and precious-metal enrichment, predominantly hosted within crosscutting pyrite-rich veins (Plate 36). Below 109 m the Al-OH values associated with the muscovite dominated alteration trend towards longer spectral wavelengths, however, the core is visually altered to the end of the drillhole.

MARY MARCH BROOK

The Mary March Brook prospect is located approximately 2 km southeast of the Beaver Pond prospect (Figure 25). This prospect has been the focus of intermittent exploration since the early 1980s, however outcrop in the area is limited, so much of the geological information is gained from diamond-drill holes. This prospect has been tested by nine drillholes, distributed over a strike length of approximately 1.5 km (Figure 25). Drilling has locally intersected zones of "sericite" alteration up to 65 m wide (DDH BJ-97-007; Graves, 2000). However, only limited assaying of these alteration intersections has been conducted, with the best value reported being 0.07% Cu over 0.4 m (Pickett and Scott, 1992). Rock units within the Mary March Brook area have been correlated both with the Red Indian Lake Group (Zagorevski *et al.*, 2016), as well as the Gullbridge structural tract (O'Brien, 2009; Sparkes *et al.*, 2021) and is therefore labelled as BRAB undivided in Figure 1.

Plate 36. *Silicified felsic volcanic rock, locally crosscut by cm-scale sulphide veining. Sample from the bottom of the photograph returned 0.6% Cu, >1.0% Pb, >1.0% Zn, 98 g/t Ag and 0.72 g/t Au over 0.03 m (Thurlow* et al.*, 1987); DDH BJ-083, 107 m depth.*

Plate 37. *Muscovitic illite–pyrite alteration hosted within an intermediate volcanic rock; DDH BJ-97-007, 200 m depth.*

Previous Work

Work in this area has primarily focused on following up on the discovery of mineralized boulders within Mary March Brook, which assayed up to 14.4% Zn, 9.3% Pb and 0.17% Cu (Pickett and Scott, 1992). Early exploration work in this area during the 1980s and 1990s included much of the same work that covered the Beaver Pond prospect (*e.g.*, Barbour, 1983, 1984; Poole, 1986; Poole *et al.*, 1987; Squires *et al.*, 1992). The Mary March Brook prospect was first drilled in the early 1990s (Pickett and Scott, 1992), and subsequent drilling was conducted in the late 1990s and early 2000s (Chislett, 1997; Graves, 2000, 2001).

Local Geology

The geology of the area comprises red and green mafic volcanic rocks, intermediate and felsic volcanic and related volcaniclastic rocks, and lesser sedimentary rocks (Pickett and Scott, 1992). Several mafic and felsic intrusions are noted in the area, along with rare occurrences of red sandstone and conglomerate, inferred to be Carboniferous, which are noted in drillholes farther to the northeast.

Mineralization

No significant *in situ* mineralization has been identified in the area of the Mary March Brook prospect. However, weak to moderately developed white mica alteration hosted within felsic to intermediate volcanic rocks has been locally intersected in drillcore (Plate 37). Aside from locally significant pyrite, this alteration is barren with respect to base and precious metals.

Alteration

Several drillholes were examined from the Mary March Brook area, but only weak to moderate white mica alteration was identified with the use of SWIR. Muscovitic illite is the dominant white mica alteration, which is primarily developed within felsic to intermediate volcanic rocks. Within DDH BJ-97-007, the upper 120 m of the drillhole contain several intrusive units hosted within mafic volcanic rocks, which are characterized by Fe–Mg-chlorite, and lesser Mg-chlorite (Figure 27). These rocks are interlayered or structurally interleaved with felsic volcanic rocks displaying a phengitic illite to muscovitic illite spectral signature between 120–140 m depth. At around 175 m depth, a similar unit is characterized by more predominant muscovitic illite alteration, which continues up to 240 m. Below this the drillhole intersects massive, fine-grained aphanitic rhyolite, which appears relatively unaltered, and displays a range of spectral signatures, from muscovite to phengite (Figure 27).

CONNELL

Approximately 5.5 km to the east-northeast of the Little Sandy prospect is the Connell prospect, which is hosted within rocks assigned to the Red Indian Lake Group of Zagorevski *et al.* (2006; Figure 1). This prospect is poorly exposed and is defined by seven drillholes and limited surface trenching that outline a zone extending approximately 200-m along strike (Figure 28). This prospect contains exhalative-style mineralization hosted within volcaniclastic rocks and is associated with weak to moderate silicification and "sericite" ± carbonate alteration, locally accompanied by finely disseminated pyrite and rare chalcopyrite or galena (Squires, 1994d). Limited drilling in the area has tested the original geophysical anomaly; however, soil sampling along strike to the southwest has identified an area of anomalous zinc that has yet to be fully investigated (*e.g.*, Squires *et al.*, 1992).

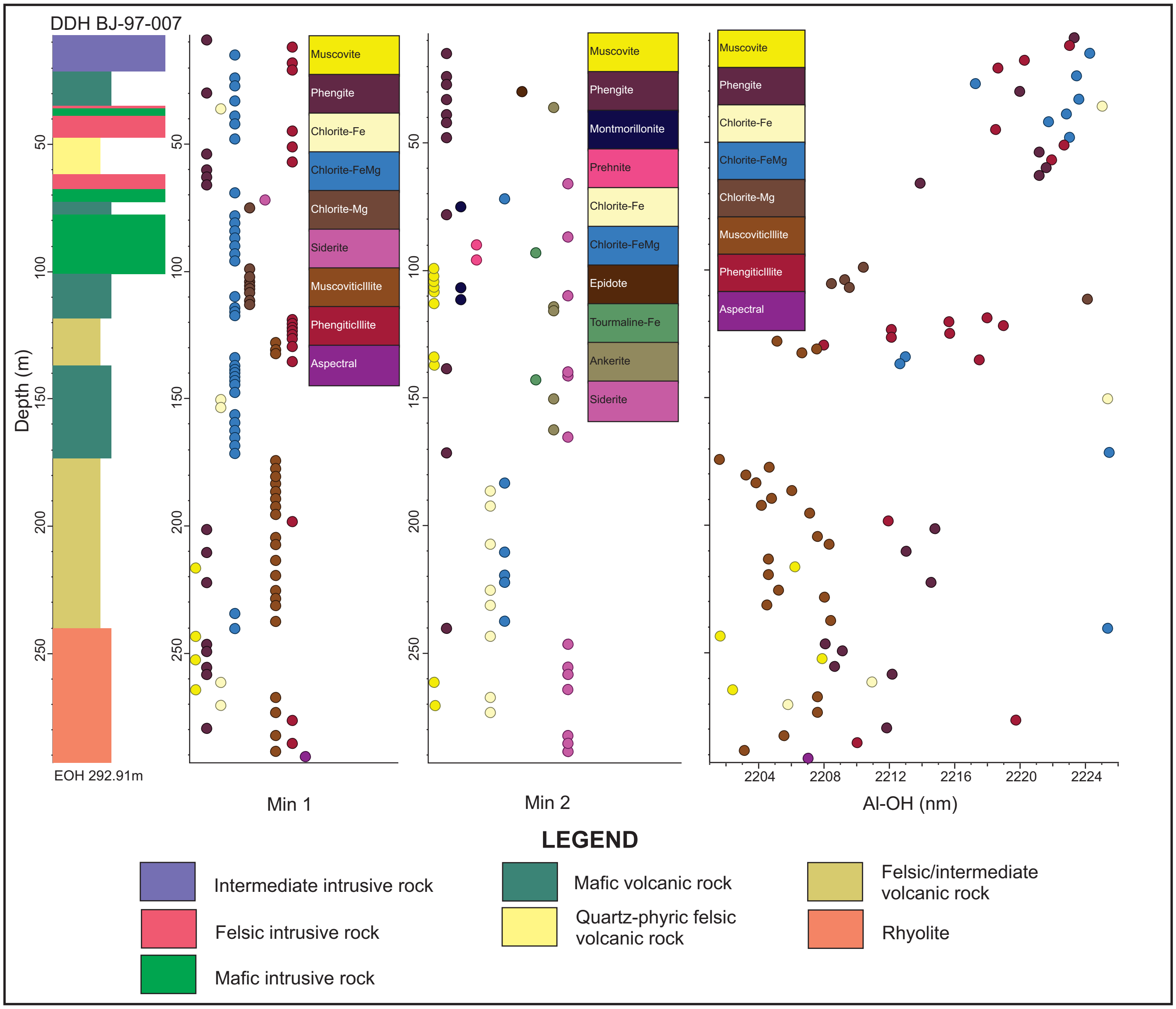

Figure 27. *Strip log for DDH BJ-97-007, outlining the distribution of the spectral data, mineral 1 (Min 1) and mineral 2 (Min 2), along with the related Al-OH absorption wavelength feature, Mary March Brook prospect.*

Previous Work

This prospect was discovered in the late 1920s by Hans Lundberg during a pioneering regional geophysical survey (equipotential). Trenching of the geophysical anomaly led to the discovery of an ore lens which, at the time, returned 1.0 m of 31.30% Zn, 6.20% Pb, 0.20% Cu, 9.60 opt Ag and 0.09 opt Au (source – old Memo in Asarco files; Squires, 1994d). The earliest reported work on the Connell prospect is from the late 1960s (Laughlin, 1967), with no further work reported until the 1990s, when Noranda initiated exploration in the area. Noranda conducted compilation work along with mapping, soil and basal-till sampling, and geophysical surveys along with limited drilling (Graves and Squires, 1992; Sheppard, 1997; Squires, 1994d; Banville *et al.*, 1998a, b). The only other available report that covers the area is an airborne geophysical survey conducted by Xstrata and Canstar in the early 2010s (Wolfson, 2012).

Local Geology

Mineralization within the Connell prospect occurs within a steeply northwest dipping volcaniclastic sequence, consisting of chert, siltstone, and crystal-lithic tuffs (Graves and Squires, 1992). The volcanic rocks are predominantly felsic to intermediate in composition and are locally quartz- and feldspar-phyric (Plate 38A). These rocks form the footwall sequence to the Airport Fault and are associated with a distinct magnetic low on airborne surveys.

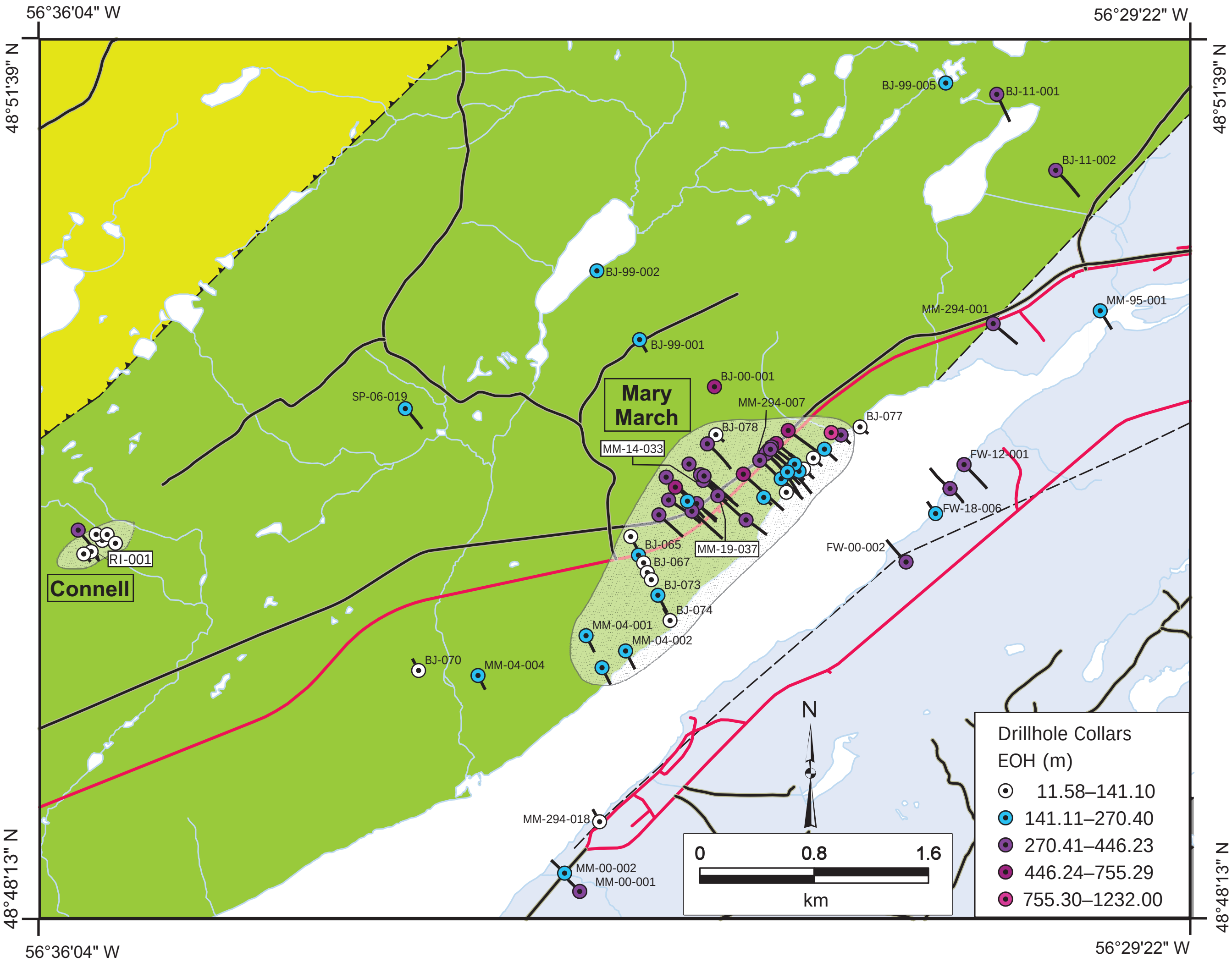

Figure 28. *Location map showing the distribution of diamond-drill holes and geology within the area of the Connell and Mary March prospects. Refer to Figure 1 for legend.*

Plate 38. *A) Feldspar-phyric felsic volcanic rock occurring within the footwall of the main mineralized chert horizon. This sample consists of phengite-dominated white mica alteration and contains 0.1% Zn, 0.1% Cu and 0.09% Pb over 1 m (DDH RI-001, 85 m depth). B) Pale-grey, cm-scale, chert bed (top row in photograph) hosting disseminated chalcopyrite–pyrite overlying iron–chlorite–muscovitic illite altered felsic to intermediate volcanic rocks (DDH RI-001, 30 m depth).*

Mineralization

Historical drilling, which undercut the main area of mineralization exposed by trenching, is reported to have intersected 0.6 m of 25.4% Zn, 11.9% Pb, 0.3% Cu, 4.6 opt Ag and 0.1 opt Au (source – old Memo in Asarco files; Squires, 1994d). The main mineralized horizon consists of fine-grained laminated sphalerite and galena interbedded within massive, laminated chert and is interpreted to represent a distal, stratiform, style of mineralization (Graves and Squires, 1992).

Alteration

Much of the core observed from the prospect was largely unaltered, with the predominant spectral signatures consisting of phengite and phengitic illite along with Fe-chlorite. However, minor muscovitic illite is developed in DDH RI-001 both above and below the locally developed mineralized chert horizon (Plate 38B; Figure 29). The upper portion of the volcaniclastic dominated sequence, immediately below the chert horizon is characterized by shorter wavelength Al-OH values relative to those observed in the rest of the drillhole and is associated with muscovitic illite–muscovite alteration (Figure 29). Farther downhole the values return to longer spectral wavelengths (~2222 nm) within similar volcaniclastic rocks. The spatial association of the shorter wavelength white mica alteration with the development of rare exhalative-style mineralization suggests the overall shift in the Al-OH values is related to the development of mineralization, as noted elsewhere in the region. However, as noted above, weakly mineralized feldspar-phyric tuff occurs towards the bottom of the drillhole in association with phengite alteration (Plate 38A), so the noted shift to shorter wave-

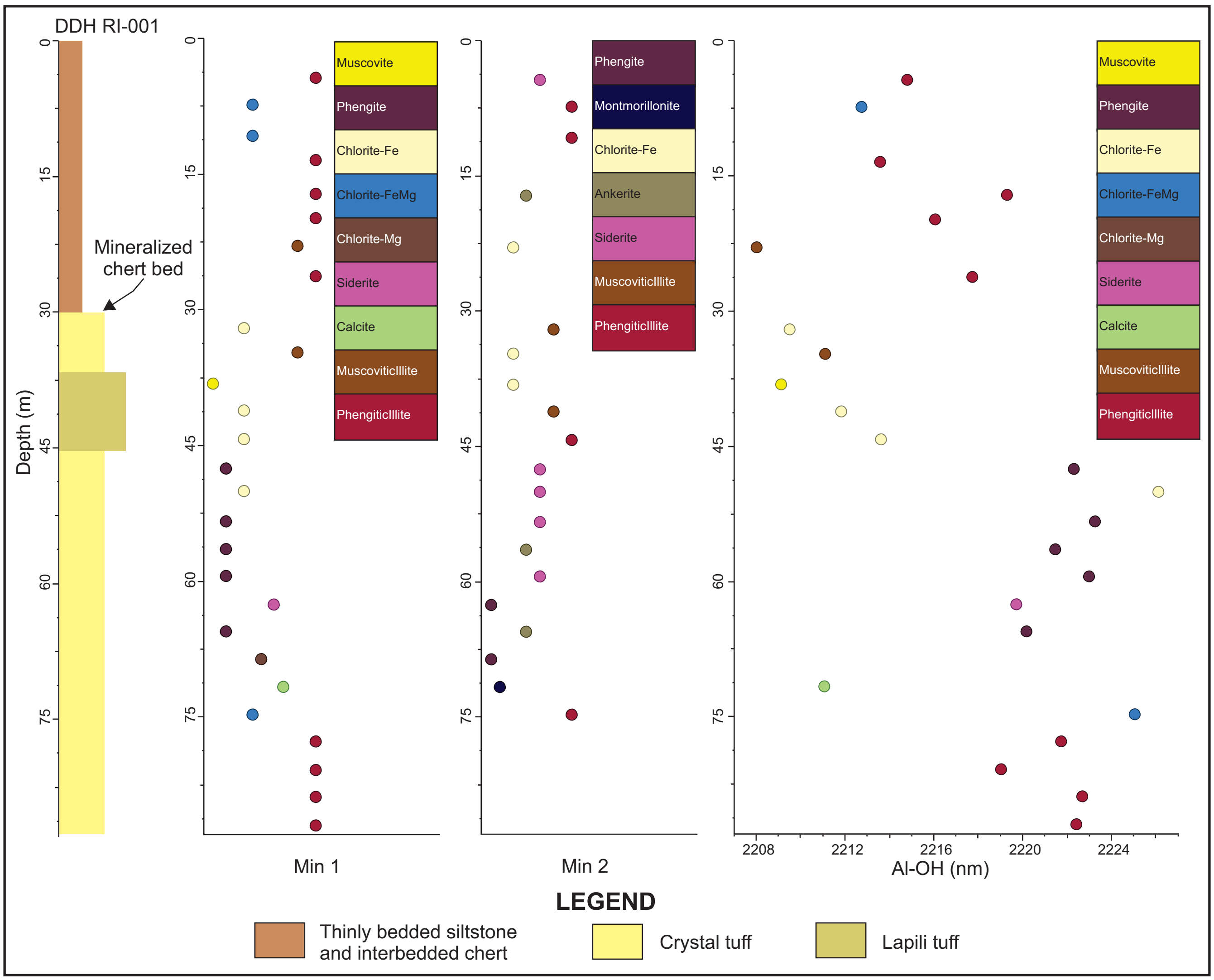

Figure 29. *Strip log for DDH RI-001, outlining the distribution of the spectral data, mineral 1 (Min 1) and mineral 2 (Min 2), along with the related Al-OH absorption wavelength feature, Connell prospect.*

length white mica minerals is not everywhere developed in association with mineralization.

MARY MARCH

The Mary March prospect is located approximately 4.5 km to the east of the Connell prospect and is also hosted within rocks of the Red Indian Lake Group (Figure 28). Outside of the main Buchans area, the Mary March alteration zone has received the most intensive mineral exploration, which first began in the early 1980s. To date, a total of fifty drillholes exist within the general area of the prospect, which represents one of the most significant zones of hydrothermal alteration developed within the study area (*see* below). This drilling has defined two ore-horizons, namely the Nancy April prospect in the west, and the Mary March prospect in the east. Aluminous alteration in the form of pyrophyllite and alunite has been identified throughout the area (Sparkes 2022; Sparkes and Hinchey, 2023), which locally displays a spatial association with VMS-related mineralization. Early geochemical samples from the alteration locally returned values of up to 41% Al_2O_3 (Thurlow, 1999), indicating the aluminous nature of the hydrothermal alteration in this area. Although early interpretations assumed the alteration represented a later overprinting event superimposed on the VMS mineralization, recent investigations using SWIR demonstrate the alteration to be more widespread and synchronous with the VMS-related mineralization (Sparkes and Hinchey, 2023).

Previous Work

This section provides a summary of the exploration and related highlights within the area of the Mary March prospect; a more detailed review can be found in Oosterman (2015). Abitibi-Price first conducted prospecting around the Mary March prospect in the late 1970s, which resulted in the discovery of numerous boulders of altered and weakly pyritic volcanic rocks (Barbour and Thurlow, 1981). The area was investigated using various geophysical surveys along with the first drilling, which targeted a weak IP anomaly (Thurlow *et al.*, 1982). BP-Selco subsequently explored the area from the mid-1980s to the early 1990s, conducting an airborne geophysical survey, along with various ground geophysical and geochemical surveys and diamond drilling (Thurlow *et al.*, 1987; Woods, 1988; Barbour *et al.*, 1988, 1989, 1991; Woods *et al.*, 1988; Desnoyers *et al.*, 1992). One of the most notable outcomes from this work was the delineation of a large base-metal soil anomaly around the Mary March prospect (Woods *et al.*, 1988). As part of this exploration program, trenching was carried out which uncovered the first presence of advanced argillic alteration (alunite) associated with anomalous gold, mercury, cadmium, molybdenum and zinc (Barbour *et al.*, 1989).

In the late 1990s, Phelps Dodge Corporation began exploration in the region, which resulted in the discovery of two zones of massive sulphide mineralization, namely the Mary March and Nancy April prospects, which returned drill-hole intersections of up to 10.1% Zn, 1.68% Pb, 0.64% Cu, 122.1 g/t Ag and 4.2 g/t Au over 9.63 m (Jagodits and Thurlow, 2000). The property was taken over by Candor Venture Corporation in the mid-2000s, who conducted drilling along strike to the southwest in addition to conducting a geophysical survey over Red Indian Lake (Waldie, 2004a, b; Woods and Northcott, 2005). From this work, a narrow zone of semi-massive sulphide mineralization was intersected in drillcore, returning assays of up to 0.3% Zn, 0.04% Cu, 0.06% Pb, 8.2 g/t Ag and 274 ppb Au over 1.0 m, which represents the southwestern most drilling along the alteration zone (DDH MM-04-002; Figure 28; Waldie, 2004b).

Canstar Resources Inc., which was formed from an amalgamation between Candor and Nustar Resources, has held the mineral claims over the prospect since 2005. The company has conducted several geophysical surveys and diamond drilling programs (Wolfson, 2012; Greene and Wolfson, 2013; Oosterman, 2015). Most recent work on the prospect includes trenching in 2019 that identified a zone of transported ore clasts, locally assaying up to 5.7% Cu, 0.3% Zn, 29.4 g/t Ag and 1.2 g/t Au, along strike to the northeast of the main prospect (Patey, 2020).

Local Geology

The Mary March prospect is hosted within a sequence of mafic, intermediate and felsic volcanic rocks of the Red Indian Lake Group, consisting of flows and related volcaniclastic deposits. The volcanic sequence is primarily dominated by locally pillowed mafic volcanic rocks and mafic to intermediate hyaloclastite breccia, and lesser, locally flow-banded, rhyolite and related hyaloclastite. The emplacement of rhyolite cryptodomes, display a spatial association with the formation of advanced argillic alteration and localized VMS mineralization, which has been traced along strike for up to 2 km. This advanced argillic alteration and related massive sulphide mineralization is largely hosted in volcaniclastic rocks consisting of lapilli tuff, tuff breccia and interbedded volcaniclastic sandstone and siltstone marginal to the rhyolite. The aerial distribution of the advanced argillic and marginal argillic alteration surrounding the Mary March area is spatially associated with a pronounced aeromagnetic low, which has a strike length of up to 3 km. This area forms one of the most significant zones of hydrothermal alteration within the region and given the development of rhyolite flows and related advanced argillic alteration is indicative of a vent proximal environment.

Two significant fault structures, namely the Mary March and the Nancy April thrust faults form northeast trending and steeply northwest dipping structures, which locally result in the structural duplication of the mineralized horizon and related advanced argillic alteration (Sparkes and Hinchey, 2023). A distinct, locally flow-banded, rhyolite is restricted to the footwall zone of the Mary March thrust fault. The advanced argillic alteration displays a spatial association with the contact zone between this unit and overlying intermediate to felsic volcaniclastic rocks and its development is inferred to be related to the emplacement of the rhyolite unit.

Mineralization

Massive sulphide mineralization generally occurs in structurally complex zones proximal to thrust faults in the area, along with stringer and local disseminated sulphide mineralization developed within both mafic and felsic volcanic rocks in the structural footwall of both the Nancy April and Mary March thrust faults. The most significant massive sulphide intersection comes from the area of the immediate footwall zone to the Mary March thrust fault, which returned 10.1% Zn, 1.7% Pb, 0.6% Cu, 122.1 g/t Ag and 4.2 g/t Au over 9.6 m (DDH MM-294-007; Figure 28; Jagodits and Thurlow, 2000). Here, high-grade massive sulphide is interbedded with mineralized lithic material and more massive pyrite but is highly disrupted due to faulting and the intrusion of post-mineral mafic and felsic dykes, which also intrude along the fault structures. In contrast, the massive sulphide mineralization identified in the hanging wall of the Nancy April thrust fault largely consists of massive pyrite, which is locally associated with anomalous Au (up to 330 ppb), Ag (up to 14 g/t) Se (up to 92 ppm) and Te (up to 30 ppm; Oosterman, 2015). The structural panel between the two thrust faults is host to well-developed stringer- and disseminated mineralization hosted within mafic to intermediate volcanic rocks, locally returning intersections of up to 1.0% Zn, 0.2% Pb and 2.9 g/t Ag over 93.7 m (DDH MM-14-033; Figure 28; Oosterman, 2015).

Alteration

The SWIR data collected from the Mary March area indicates the presence of pyrophyllite, kaolinite and alunite in several drillholes, outlining two separate zones of advanced argillic alteration, a western zone associated with the Nancy April prospect, and an eastern zone associated with the Mary March prospect (Sparkes, 2022; Sparkes and Hinchey, 2023). Both zones are associated with the development of argillic to advanced argillic alteration within the immediate footwall rocks to VMS-related mineralization.

Within the eastern alteration trend, SWIR investigations of the Mary March prospect highlight several dominant alteration assemblages related to the development of argillic and advanced argillic alteration. The footwall rocks to the Mary March thrust fault are characterized by phengitic white mica alteration distal from the main zone of advanced argillic alteration. Here, the phengite altered intermediate to felsic lapilli tuff and tuff breccia quickly transitions through muscovitic illite and then into paragonite–paragonitic illite–pyrophyllite advanced argillic alteration over a span of approximately 20 m (Figure 30; Plate 39). The development of this advanced argillic alteration is centred on the contact between the underlying flow-banded rhyolite and overlying volcaniclastic sediments. Below the advanced argillic alteration, the white mica alteration transitions back into muscovitic illite and then to phengite, and the Al-OH values return to longer spectral wavelengths (~2220 nm). Unfortunately, due to inaccessibility, the drillholes examined as part of this study were located to the southwest of the VMS mineralization developed at the Mary March prospect and the advanced argillic alteration was not observed in direct association with any VMS-style mineralization. However, based on industry reports and sections (*e.g.,* Jagodits and Thurlow, 2000), a similar stratigraphic setting within the footwall zone, approximately 500 m along strike to the northeast, is host to the development of VMS mineralization associated with the Mary March prospect; no SWIR investigations have been conducted in this area of the prospect.

Situated structurally above the footwall intermediate to felsic volcanic rocks, and the Mary March thrust fault, is a mafic to intermediate dominated volcanic sequence (structural hanging wall; stratigraphic footwall; *see* below) which is characterized by Fe–Mg chlorite and lesser phengite and phengitic illite alteration. These rocks are separated from the underlying sequence by the Mary March thrust fault (Figure 30). The structural hanging-wall rocks are host to stringer- and local disseminated VMS mineralization, associated with Fe–Mg chlorite alteration. These rocks represent the country rock into which the structural footwall rhyolite is emplaced, based on regional outcrop relationships. Upper portions of this structural panel contain moderate to strong phengite to phengitic illite white mica alteration, proximal to the Nancy April thrust fault. This phengitic alteration also displays a spatial association with the intrusion of intermediate dykes within the mafic volcanic rocks. These intermediate dykes are of similar composition to the intermediate hyaloclastite volcanic rocks within the same sequence and are therefore inferred to be comagmatic.

The advanced argillic alteration occurring within the structural hanging wall of the Nancy April thrust fault is inferred to represent the structural repetition of Mary March ore horizon. Within the hanging wall of the Nancy April thrust fault, intermediate to felsic tuff breccia, locally containing felsic fragments displaying well-developed perlitic fracturing, is host to pyrophyllite-dominated advanced argillic alteration

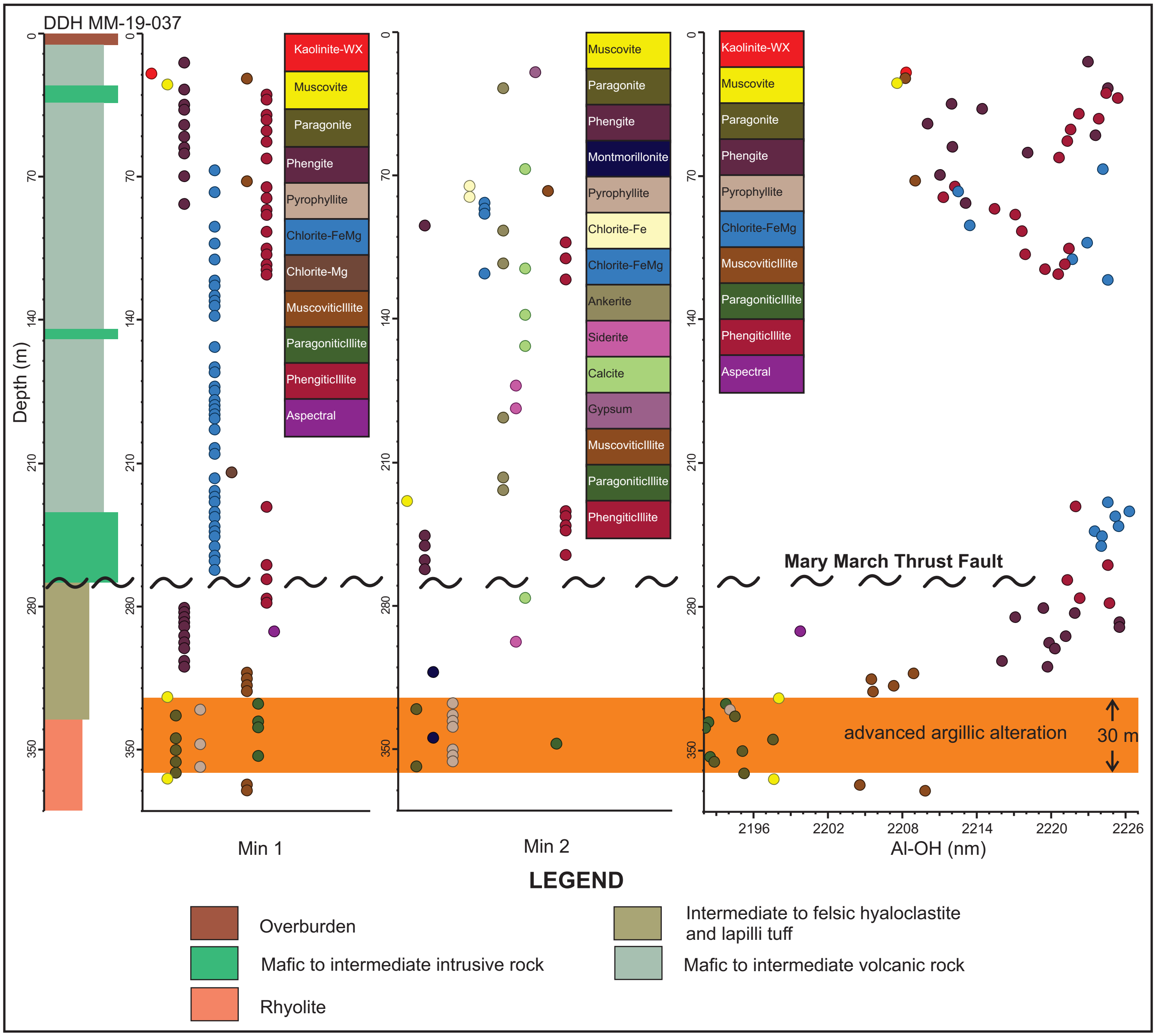

Figure 30. *Strip log for DDH MM-19-037, outlining the distribution of the spectral data, mineral 1 (Min 1) and mineral 2 (Min 2), along with the related Al-OH absorption wavelength feature, Mary March prospect.*

up to 30 m thick (Figure 31; Plate 40). Here copper–gold VMS-related mineralization occurs at the transition from the advanced argillic into marginal argillic alteration. This mineralization is also associated with anomalous silver, arsenic, bismuth, mercury, molybdenum, antimony, selenium, and tellurium. Locally developed massive pyrite, presumed to be exhalative, is located 150 m along-strike to the southwest in a similar stratigraphic setting. Here, the massive pyrite alteration is underlain by paragonite–paragonitic illite–montmorillonite argillic alteration hosted in intermediate to felsic lapilli tuff, which is truncated at depth by the Nancy April thrust fault. Immediately below the thrust fault are mafic to intermediate volcanic rocks hosting Fe–Mg chlorite and phengitic alteration along with local stringer- and disseminated VMS mineralization. These rocks represent the same sequence occurring within the hanging wall of the Mary March thrust fault (Figure 30).

The SWIR investigations of the footwall rocks to the Mary March thrust fault indicate an overall transition from pyrophyllite dominated advanced argillic alteration in the northeast to pyrophyllite–kaolinite–alunite dominated associations in the southwest. However, no such variation has been identified within the hanging-wall zone of the Nancy April thrust fault, where the advanced argillic alteration is only noted to contain pyrophyllite. In the southwestern por-

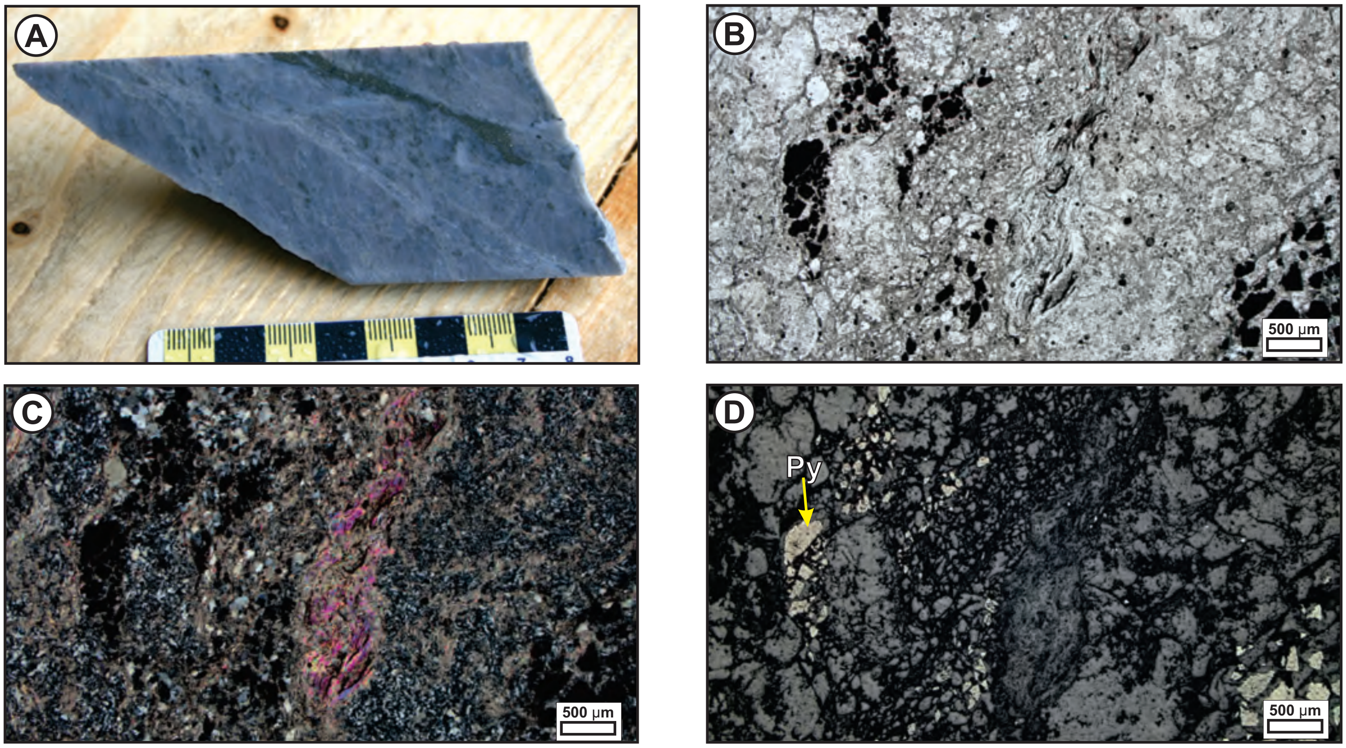

Plate 39. *A) Pyrophyllite–paragonite altered felsic volcanic rock crosscut by a later pyrite-filled fracture; DDH MM-19-037, 351 m depth; B) Plane-polarized light photomicrograph of the sample shown in (A), which is dominated by quartz–pyrophyllite–paragonite alteration along with lesser, patchy sulphides; C) Cross-polar photomicrograph of (B) highlighting the pyrophyllite alteration in the centre of the frame; D) Reflected light image of (C) highlighting the abundance of pyrite (Py) within the advanced argillic alteration.*

Plate 40. *Gradational transition from an Fe–Mg chlorite altered intermediate volcanic rock and related hyaloclastite to muscovite and then paragonite white mica alteration. Photograph is taken just above the mineralized zone shown in Figure 31; DDH MM-19-033, 64 m depth.*

tion of the Mary March prospect, the alteration within the footwall of the Mary March thrust fault displays a zonation from muscovite–paragonite–pyrophyllite, transitioning up section into kaolinite–alunite and then into relatively unaltered phengitic intermediate volcanic rocks (DDH BJ-074; Sparkes, 2022). Here, the footwall advanced argillic alteration is up to 65 m thick (core length); this alteration is located some 800 m to the southwest of drillhole MM-19-037 (Figure 30). The alteration within the hanging wall of the Nancy April thrust fault in the southwestern portion of the prospect is predominated by paragonite but still contains rare pyrophyllite (*e.g.*, DDH BJ-065; Sparkes, 2022), indicating a transition to less acidic hydrothermal conditions to the southwest within this structural panel.

GEOCHEMISTRY

This section provides a summary of the geochemical results for samples obtained largely from drillcore. The following discussion of the geochemical results has been grouped into three broad sections based primarily on the geographical location of the related prospects and secondly on the lithological group hosting the prospect. Sampling primarily focused on areas of hydrothermal alteration and discrimination dia-

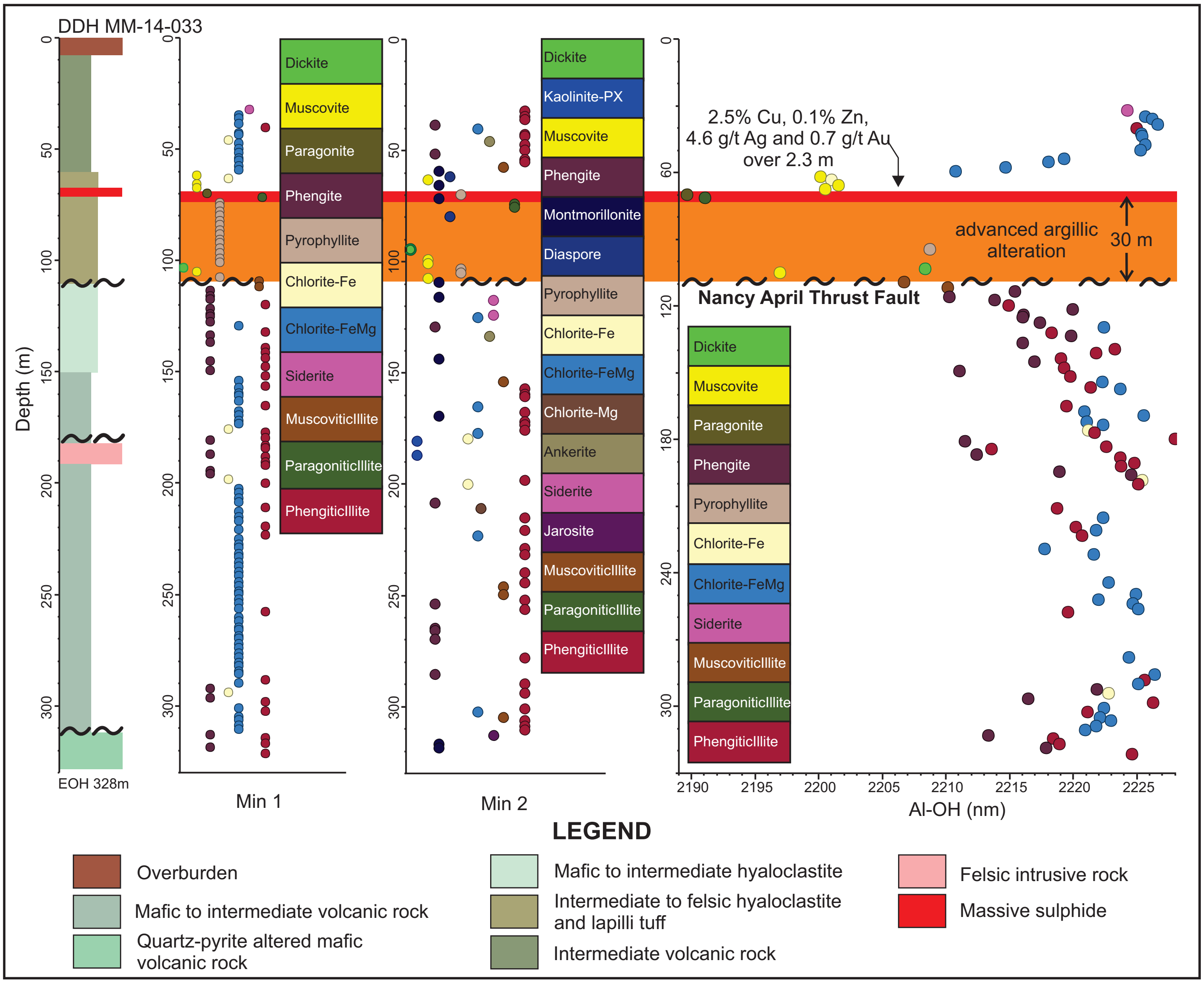

Figure 31. *Strip log for DDH MM-14-033, outlining the distribution of the spectral data, mineral 1 (Min 1) and mineral 2 (Min 2), along with the related Al-OH absorption wavelength feature, Nancy April prospect. Assay values from Oosterman (2015).*

grams are used to illustrate the abundance of various rock compositions for individual prospects, in comparison to those of the immediate Buchans area. To compare the rock units examined in this study with those of the Buchans area, the immobile element plots utilizing the ratios of Zr/Y *vs.* Th/Yb and Zr/Al_2O_3 vs. Al_2O_3/TiO_2, with fields defined by Allen *et al.* (2024) for units within the Buchans area, were used for comparison purposes. Discrimination diagrams are also utilized to compare various alteration indices and element ratios with the results of the SWIR data from the various zones of hydrothermal alteration, providing supporting data for both datasets, which highlights certain prospects that contain both anomalous alteration mineralogy and geochemistry. In the following diagrams, the samples are colour coded by either the dominant alteration phase based on SWIR analysis, or by rock type depending on the topic of discussion.

BUCHANS AREA AND PROSPECTS TO THE IMMEDIATE EAST OF THE AIRPORT THRUST FAULT

Buchans Area

The geochemical data from the area of the Buchans deposits (Lucky Strike and Rothermere), are compared with the Airport, Sandfill/Middle Branch, Middle Branch East and Powerhouse prospects (Figure 32). From these diagrams it is evident that samples plotting within the rhyolite/dacite field are most abundant at the Buchans, Sandfill/Middle Branch and Powerhouse prospects. Those samples from the Buchans area plotting outside the main cluster within the rhyolite/dacite field with Nb/Y ratios greater than 0.2 represent dated samples, with the muscovite sample representing a rhyolite

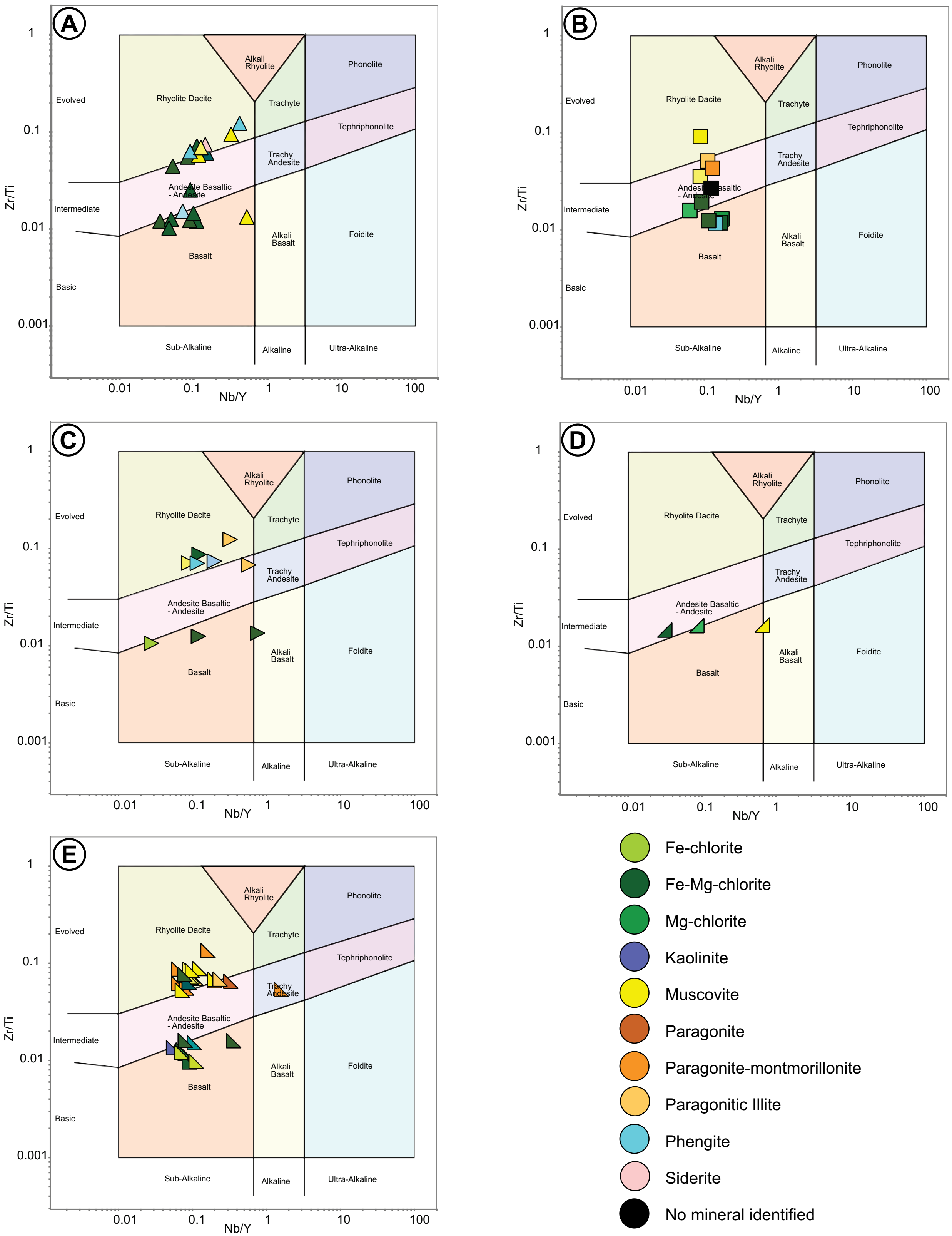

Figure 32. *Nb/Y* vs. *Zr/Ti discrimination diagram (Pearce, 1996). Samples are colour coded to the predominant alteration phase as determined by SWIR analysis. A) Buchans area; B) Airport prospect; C) Sandfill/Middle Branch prospect; D) Middle Branch East prospect; E) Powerhouse prospect.*

dyke intruding along the Old Buchans fault and the phengite sample representing a tuff from the Lundberg Hill Formation (Sparkes and Hamilton, 2024; Figure 32A). The mafic volcanic rocks are dominated by chlorite alteration, however one sample, displaced to the right of the main group, contains muscovite alteration and represents a mineralized, hydrothermally altered, sample from the footwall zone of the Lucky Strike deposit with an anomalously high Nb content. Most of the samples from the Buchans area plot within the transitional 1 field of Allen *et al.* (2024; Figure 33A). The two samples plotting in the calc-alkaline 1 field represent the geochronology samples, with the tuff sample plotting in the lower left and the late-stage rhyolite dyke in the upper right. The single sample plotting within the calc-alkaline 2 field is from a quartz porphyry unit. Samples plotting within the rhyolite/dacite field in Figure 32A predominantly overlap the field of rhyolite 4 of Allen *et al.* (2024), while most of the basalt samples overlap with the field of basalt 3 (Figure 34A). The two felsic samples with Al_2O_3/TiO_2 ratios greater than 100 represent the two geochronology samples noted above.

Chlorite alteration is associated with some of the mineralized samples from the area of the Lucky Strike deposit (Winter, 2000). However, as noted here, the footwall zone of the deposit is also associated with a zone of white mica dominated alteration. A comparison plot of the Hashimoto index versus the advanced argillic alteration index, shown in Figure 35, highlights three samples within the database displaying strong muscovite alteration, along with one sample containing chlorite–paragonite alteration, all plotting near the muscovite node (Figure 35A). Two of the three muscovite-bearing samples contain the characteristically bright-green "sericite" alteration of the footwall rocks to the Lucky Strike deposit. These samples are representative of the white mica dominated footwall alteration zone, with samples assaying up to 3.5% Zn, 2.0% Pb and 0.7% Cu over 0.9 m. The abundance of chlorite alteration developed in the area is also highlighted in the Hashimoto *vs.* chlorite–carbonate–pyrite index diagram, which illustrates that the majority of samples from the Buchans area plot within the alteration field near the chlorite–pyrite node (Figure 36A). Altered rocks from the Buchans area also show significant sodium depletion within the footwall rocks to massive sulphide mineralization, as shown in Figure 37A. This sodium depletion is associated with mercury and barium enrichment, a feature that is highlighted by the Duck Pond alteration index, which is a discrimination diagram of Ba/Sr *vs.* Hg/Na_2O (Figure 38A). Based on this diagram, the samples plotting in Duck Pond field are representative of the most prospective altered samples, and include the mineralized samples noted above, along with most of the muscovite altered footwall rocks. The muscovite-bearing sample plotting in the lower left portion of the diagram is representative of the post-alteration rhyolite dyke.

Airport

The felsic to intermediate volcanic rocks of the Airport prospect are dominated by white mica alteration (muscovite and paragonite), while the more mafic to intermediate volcanic rocks are chlorite dominated (Figure 32B). The samples affected by white mica alteration and plotting within the andesite/basaltic andesite field represent hydrothermally altered volcanic rocks, while the sample containing muscovite-dominated alteration and plotting within the rhyolite/dacite field represents a less altered quartz–feldspar-phyric protolith. The remainder of the samples displaying chlorite-dominated alteration and plotting within both the andesite/ basaltic andesite and basalt fields are representative of intermediate to mafic volcanic rocks and associated hyaloclastite. Samples plotting in the andesite/basaltic andesite and basalt fields primarily plot within the transitional 1 field of Allen *et al.* (2024; Figure 33B), and this includes the two least altered samples of these compositions. The single felsic sample plots within the tholeiitic field, while the remaining samples in that field consist of altered and mineralized material containing variable pyritic alteration. The single sample plotting within the transitional 2 field is also representative of a strongly altered paragonite-bearing sample. In Figure 34B the felsic volcanic sample overlaps the field of rhyolite 1 of Allen *et al.* (2024), while the intermediate samples broadly overlap with the dacite and andesite–dacite fields, with those samples having a Al_2O_3/TiO_2 ratio greater than 40 representing hydrothermally altered material based on SWIR analysis. The mafic volcanic samples overlap the fields of basalt 2, 3, and 5 of Allen *et al.* (2024), with the cluster of three samples plotting in the basalt 3 field are the least altered based on visual examination of the samples (Figure 34B).

The two samples with the highest advanced argillic alteration index from the prospect represent the most intensely altered based on SWIR, consisting of paragonite and paragonitic illite alteration (Figure 35B). Chlorite alteration is more abundant, but is only locally intense, as indicated by the two samples displaying both elevated alteration (AI) and chlorite–carbonate–pyrite (CCPI) indices (Figures 35B and 36B). Sodium depletion is significantly less than that detected in the Buchans area, with the most significant depletion associated with chlorite, paragonite and paragonitic illite alteration (Figure 37B). The same two samples displaying an alteration index greater than 85 also plot within the Duck Pond field in Figure 38B.

Sandfill

Samples collected from the Sandfill/Middle Branch prospect predominantly plot within the rhyolite/dacite field in Figure 32C, with the samples containing a Nb/Y ratio greater than 0.3 representing a felsic intrusive unit. The mafic

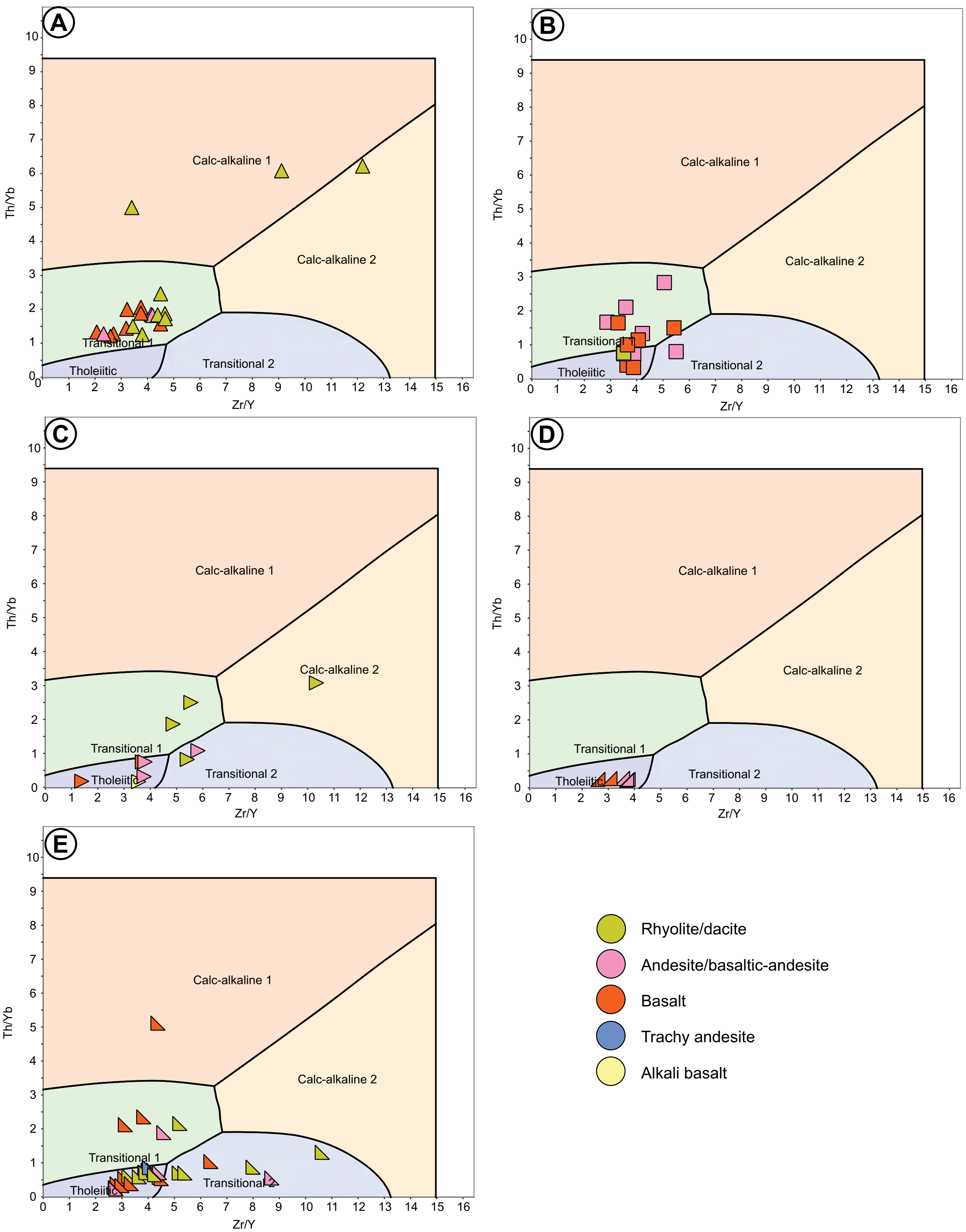

Figure 33. *Zr/Y* vs. *Th/Yb discrimination diagram for the Buchans area (Allen* et al., *2024). Samples are colour coded to rock type, as determined from Figure 32. A) Buchans area; B) Airport prospect; C) Sandfill/Middle Branch prospect; D) Middle Branch East prospect; E) Powerhouse prospect.*

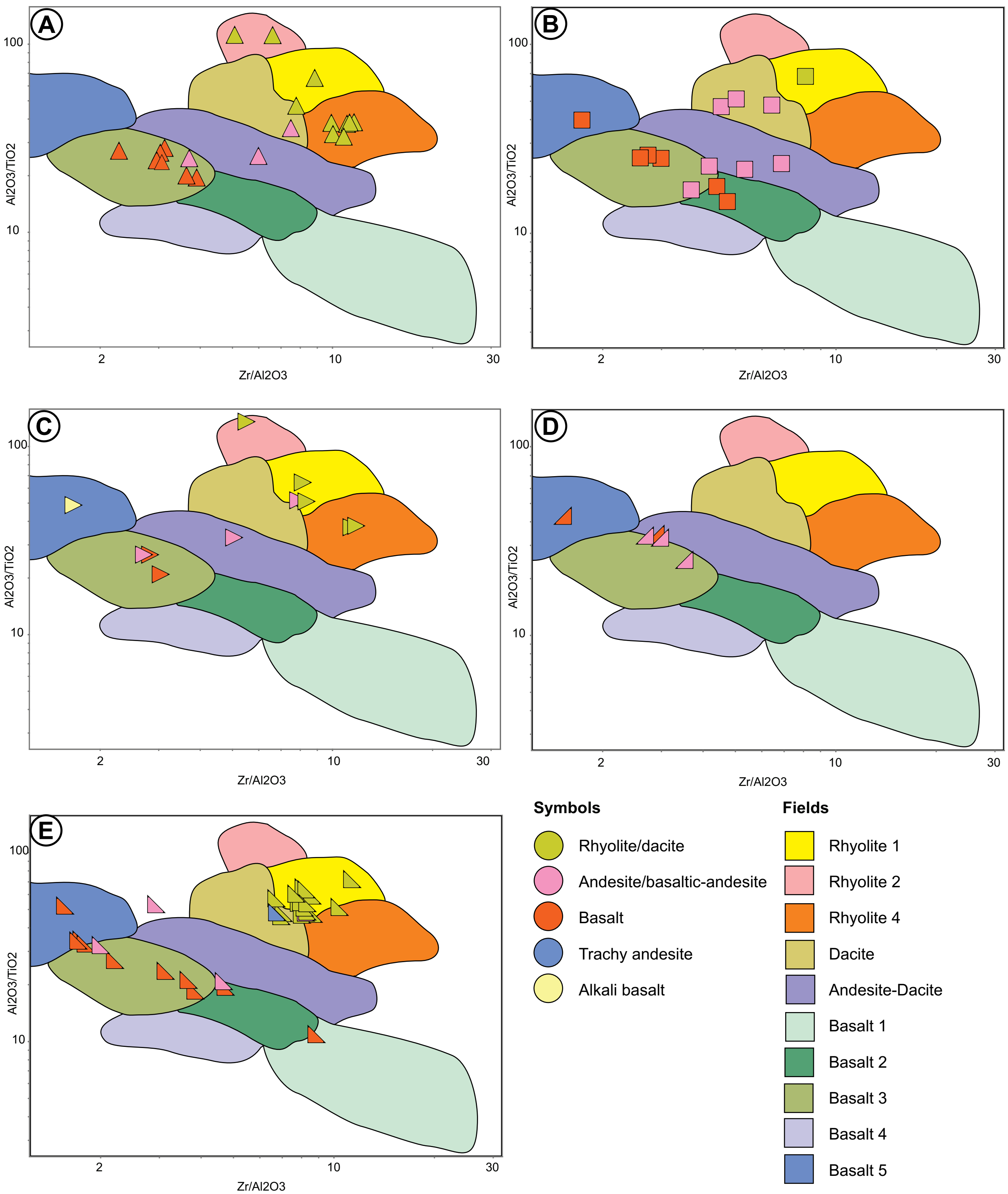

Figure 34. *Zr/*Al_2O_3 vs. Al_2O_3*/*TiO_2 *discrimination diagram outlining the fields from Allen* et al. *(2024) displaying samples from the Buchans area. Samples are colour coded to rock type, as determined from Figure 32. A) Buchans area; B) Airport prospect; C) Sandfill/Middle Branch prospect; D) Middle Branch East prospect; E) Powerhouse prospect.*

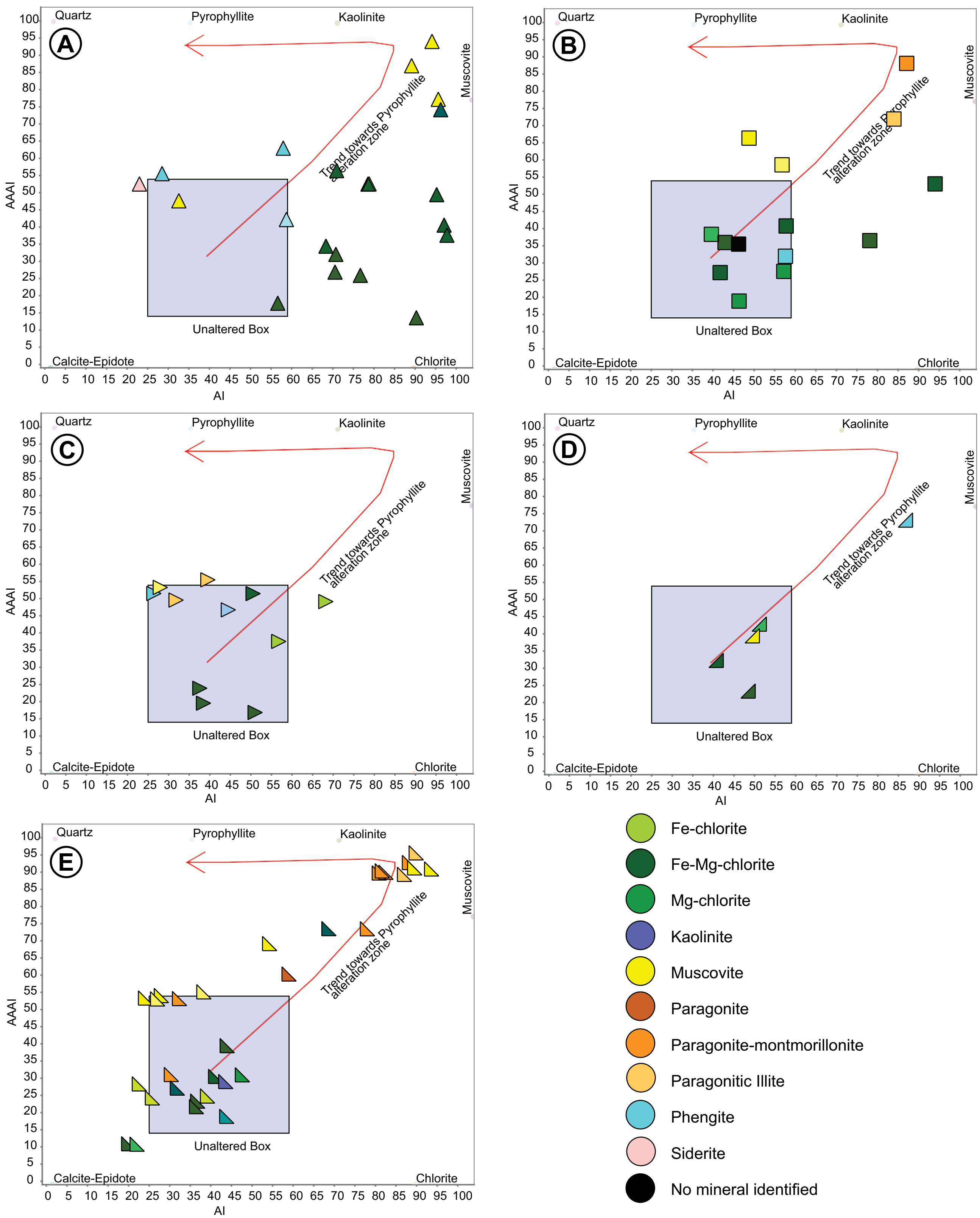

Figure 35. *Alteration box plot of the alteration index (AI) vs. advanced argillic alteration index (AAAI; Williams and Davidson, 2004) for the Buchans area. Samples are colour coded to the predominant alteration phase as determined by SWIR analysis. A) Buchans area; B) Airport prospect; C) Sandfill/Middle Branch prospect; D) Middle Branch East prospect; E) Powerhouse prospect.*

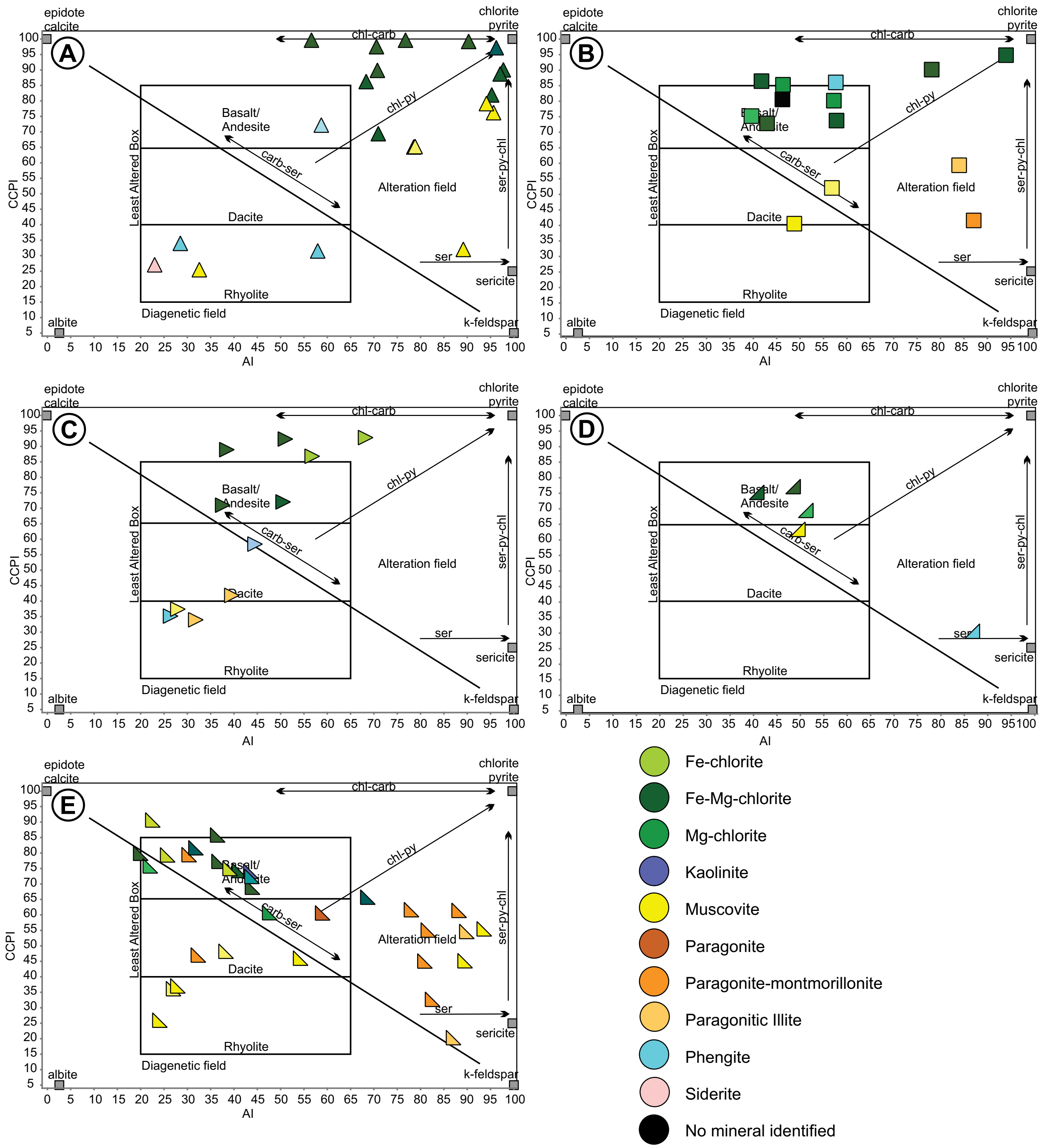

Figure 36. *Alteration box plot of the alteration index (AI) vs. the chlorite–carbonate–pyrite index (CCPI; Large* et al.*, 2001) for the Buchans area. Samples are colour coded to the predominant alteration phase as determined by SWIR analysis. A) Buchans area; B) Airport prospect; C) Sandfill/Middle Branch prospect; D) Middle Branch East prospect; E) Powerhouse prospect.*

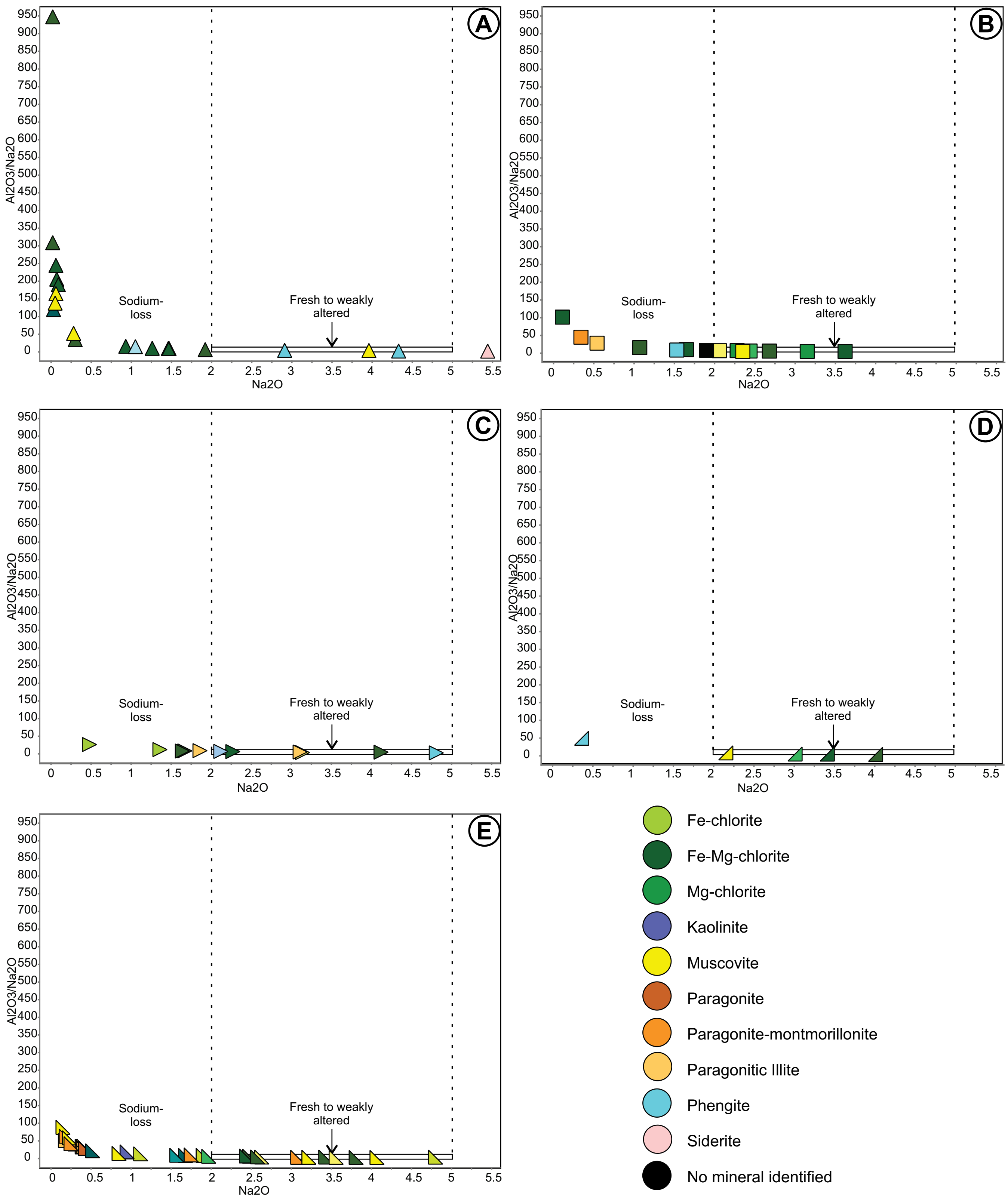

Figure 37. *Spitz–Darling index (Spitz and Darling, 1978) of the Na_2O* vs. *Al_2O_3/Na_2O discrimination diagram (modified from Ruks* et al.*, 2006) for the Buchans area. Samples are colour coded to the predominant alteration phase as determined by SWIR analysis. A) Buchans area; B) Airport prospect; C) Sandfill/Middle Branch prospect; D) Middle Branch East prospect; E) Powerhouse prospect.*

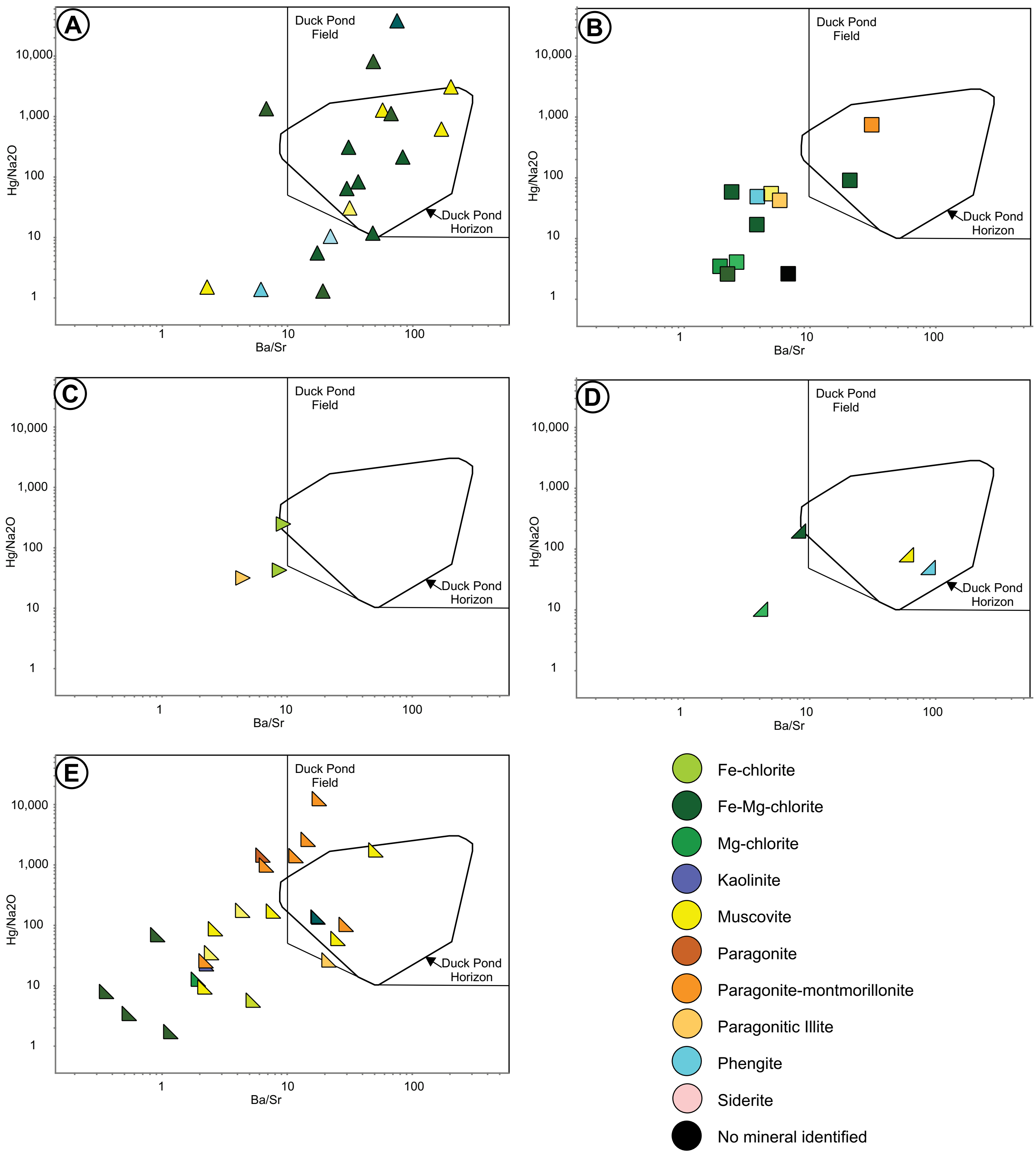

Figure 38. *Duck Pond alteration index discrimination diagram (Collins, 1989) for the Buchans area. Samples are colour coded to the predominant alteration phase as determined by SWIR analysis. A) Buchans area; B) Airport prospect; C) Sandfill/Middle Branch prospect; D) Middle Branch East prospect; E) Powerhouse prospect.*

volcanic rocks display a range in Nb/Y values and represent least altered, chlorite-dominated, rocks of the hanging-wall sequence to the Airport Thrust Fault (Figure 32C). Samples from the area plot within a variety of fields on the magmatic affinity diagram of Allen *et al.* (2024). The two felsic volcanic units plotting within the transitional 1 field are representative of felsic volcanic rocks of the Buchans River Formation located within the footwall of the Airport Thrust Fault (Figure 33C). In contrast, the samples plotting within the tholeiitic field contain intermediate to mafic volcanic rocks of the hanging-wall sequence. The single sample within the calc-alkaline 2 field is from a felsic intrusive unit, while the two samples plotting within the transitional 2 field represent felsic to intermediate volcanic rocks of the hanging-wall sequence. Samples of the felsic volcanic rocks form two clusters on the Zr/Al_2O_3 vs. Al_2O_3/TiO_2 discrimination diagram, with those samples having a Zr/Al_2O_3 ratio greater than 10 corresponding with rhyolite 4 of Allen *et al.* (2024), and the other cluster corresponding with rhyolite 1 (Figure 34C). A cluster of three intermediate to mafic samples on the same diagram, overlap with the field of basalt 3 of Allen *et al.* (2024; Figure 34C).

As noted in the section on alteration, no significant white mica alteration was identified within the area of the Sandfill/Middle Branch prospect, supported by Figures 35C and 36C. Likewise, only minimal sodium depletion and no barium or mercury enrichment was identified in the samples from the area (Figures 37C and 38C).

Middle Branch East

Like the Sandfill/ Middle Branch prospect, samples of intermediate to mafic rocks from the Middle Branch East prospect display similar Zr/Ti ratios but display a range in Nb/Y values, with the sample having the highest Nb/Y value displaying the most intense hydrothermal alteration (Figure 32D). All the samples plot within the tholeiitic field, overlap the fields of basalt 3 and basalt 5 of Allen *et al.* (2024; Figures 33D and 34D), and display similar ratios to the intermediate to mafic rocks of the Sandfill/Middle Branch prospect shown in Figure 34C.

Relationships observed at this prospect are similar to those at the Sandfill/Middle Branch prospect. Limited sampling of the area has not identified any significant alteration aside from a single sample of phengitic alteration (Figures 35D and 36D), which is associated with anomalous gold mineralization. Samples hosting mineralized clasts, mentioned above, are characterized by chlorite alteration, but plot within the unaltered field of Figure 35D. No significant sodium depletion is evident in the area, aside from the sample of phengitic alteration (Figure 37D), but rare mercury and barium enrichment is noted within a sample hosting the mineralized ore clasts in addition to the phengite altered sample hosting anomalous gold (Figure 38D).

Powerhouse

Outside of the main Buchans area, the Powerhouse prospect contains the greatest abundance of felsic volcanic rocks plotting in the rhyolite/dacite field (Figure 32E). The second most abundant rock type within this area consists of basalt from the hanging-wall sequence of the Airport Thrust Fault. The single outlier within the mafic field consists of a magnetic mafic dyke. The outliner plotting within the trachy andesite field contains paragonite alteration and anomalously high Nb. Most of the felsic and mafic volcanic rocks plot within the tholeiitic field of Allen *et al.* (2024; Figure 33E). Samples plotting above, in the transitional 1 field, consist of mafic volcanic rocks, fragmental mafic and intermediate volcanic rocks and a felsic dyke. The single sample within the calc-alkaline 1 field represents a mafic volcanic rock from the lower portion of the hanging-wall sequence. Samples plotting in the transitional 2 field largely consist of paragonite altered felsic volcanic rocks. On the Zr/Al_2O_3 *vs.* Al_2O_3/TiO_2 discrimination diagram from Allen *et al.* (2024), the felsic volcanic rocks largely overlap the field of rhyolite 1, while the mafic volcanic rocks overlap the fields of basalt 2, basalt 3, and basalt 5 (Figure 34E).

The white mica alteration developed at this prospect represents some of the most intensely altered rocks observed along the Airport Thrust Fault, with a cluster of samples largely consisting of paragonite-dominated alteration, plotting between the muscovite and kaolinite nodes in Figure 35E. This cluster includes a mineralized sample containing 1.4% Zn over 0.7 m. The same samples plot within the alteration field, near the sericite node, in Figure 36E. Samples classified as muscovite and paragonite and plotting in the upper left of the unaltered box field of Figure 35E are representative of a prominent quartz-phyric intrusive unit that is relatively unaltered. The white mica altered samples display moderate sodium depletion, which is also locally accompanied by mercury enrichment (Figures 37E and 38E).

MARY MARCH BROOK GROUP PROSPECTS

Woodman's Brook

Samples from the Woodman's Brook prospect plot almost entirely within the andesite/basaltic andesite field, aside from one sample plotting within the rhyolite/dacite field and another which plots within the basalt field (Figure 39A). The single sample plotting within the rhyolite/dacite field consists of a felsic volcaniclastic tuff, while the sample plotting within the basalt field is from a mafic dyke. The remainder of the samples form a tight cluster displaying both chlorite

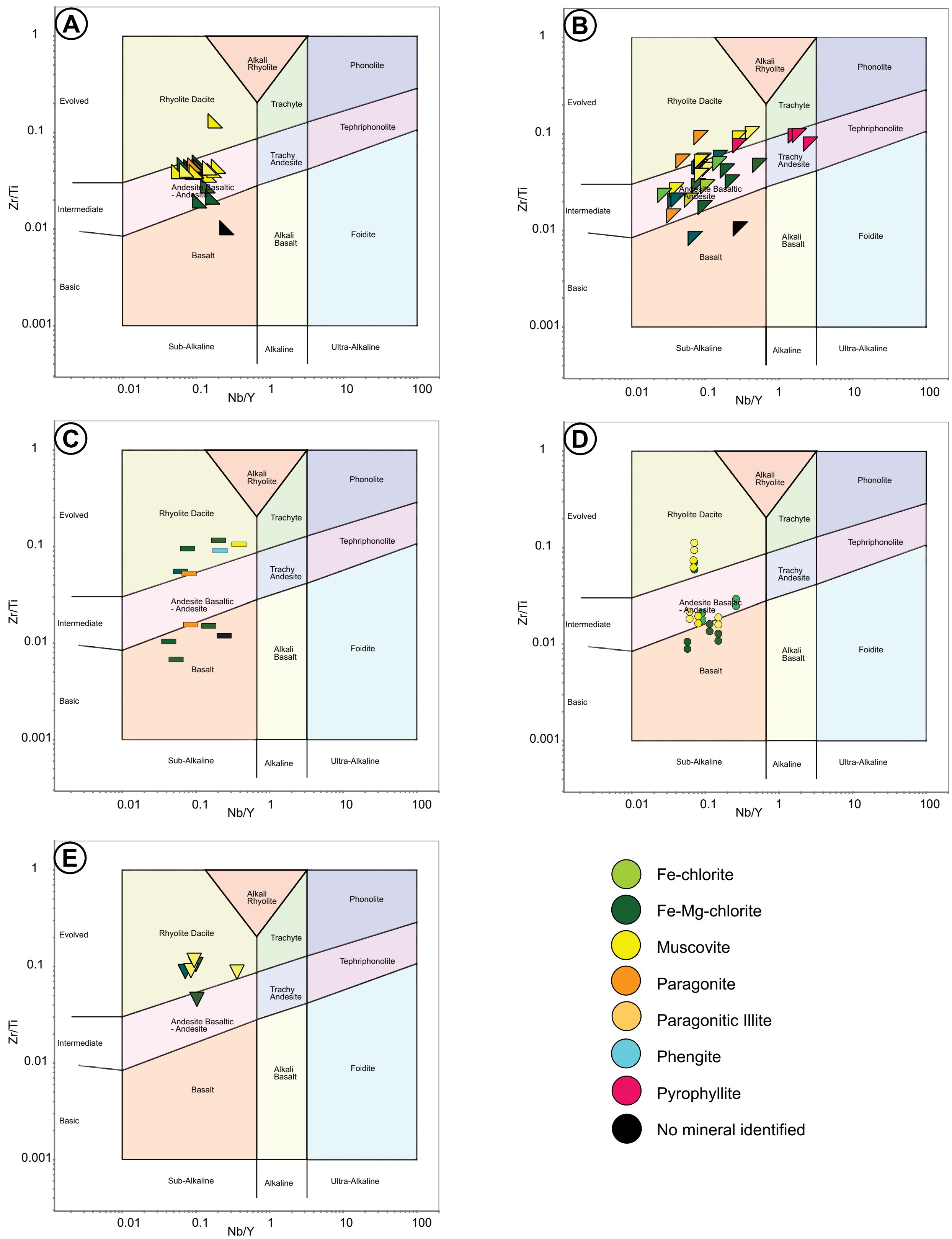

Figure 39. *Nb/Y* vs. *Zr/Ti discrimination diagram (Pearce, 1996) for the Mary March Brook group prospects. Samples are colour coded to the predominant alteration phase as determined by SWIR analysis. A) Woodman's Brook prospect; B) Tower prospect; C) Little Sandy prospect; D) Seal Pond prospect; E) Beaver Pond prospect.*

and muscovite-dominated alteration. The intermediate volcanic rocks mostly plot within the tholeiitic field of Allen *et al.* (2024), whilst the sample from the mafic dyke falls within the transitional 2 field (Figure 40A). On the Zr/Al_2O_3 *vs.* Al_2O_3/TiO_2 discrimination diagram, most of the intermediate samples plot within the dacite field of Allen *et al.* (2024; Figure 41A).

Both chlorite and muscovite alteration dominate samples from the prospect, with muscovite altered samples displaying higher advanced argillic alteration index (AAAI) values relative to the chlorite altered samples (Figure 42A). Two groups of samples are evident in Figure 43A, with those plotting to the lower right being dominated by muscovite alteration and trending towards sericite and locally hosting anomalous zinc. The samples plotting in the upper right are dominated by chlorite alteration but also include a small subset with muscovite-dominated alteration and contain anomalous copper. Altered samples display weakly developed sodium depletion, which is most prominent in the muscovite-altered samples (Figure 44A). The samples displaying sodium depletion are also locally accompanied by anomalous mercury enrichment and plot within the Duck Pond field in Figure 45A.

Tower

Samples from the Tower prospect predominantly plot within the andesite/basaltic andesite and rhyolite/dacite fields on the Nb/Y *vs.* Zr/Ti discrimination diagram (Figure 39B), with most plotting within the andesite/basaltic andesite field. Samples plotting within the rhyolite/dacite field contain paragonite, muscovite and pyrophyllite alteration, with several samples containing advanced argillic alteration displaying a shift to the right, into the trachy andesite field (Figure 39B). The intermediate samples contain white mica and chlorite dominated alteration, similar to the intermediate volcanic rocks of the Woodman's Brook area. The two samples plotting within the basalt field consist of a mafic dyke, which plots to the right, while the other sample is from a mafic volcanic unit located in the extreme eastern portion of the property and maybe analogous to mafic volcanic rocks from the Little Sandy area (*see* below). Similar to the Woodman's Brook area, most samples plot within the tholeiitic field of Allen *et al.* (2024), while the sample from the mafic dyke falls within the transitional 2 field (Figure 40B). The intermediate sample plotting within the transitional 1 field is representative of a relatively fresh volcanic rock to the extreme north of the prospect, while the felsic sample plotting within the upper right of the field is pyrophyllite altered. The other intermediate sample plotting within the calc-alkalic 2 field represents a post-mineralization dyke, which crosscuts the hydrothermal alteration in the area (Sparkes and Hamilton, 2024). The two felsic samples plotting within the calc-alkalic 1 and calc-alkalic 2 fields represent dykes crosscutting the volcanic sequence. The remaining samples containing pyrophyllite dominated advanced argillic alteration display significant yttrium and ytterbium depletion, and do not fall within the fields, as their Zr/Y and Th/Yb ratios plot outside of the defined fields. The intermediate volcanic rocks broadly overlap those from the Woodman's Brook prospect, plotting primarily in the dacite field of Allen *et al.* (2024), whilst the main cluster of felsic volcanic rocks plot within the rhyolite 1 field (Figure 41B). The trachy andesite samples plotting in the rhyolite 1 field represent pyrophyllite altered felsic volcanic rocks. The cluster of intermediate volcanic rocks to the lower right of the main group, plotting within the andesite–dacite field, represent rocks from the extreme eastern portion of the alteration zone, while the mafic dyke sample plots in basalt 1 field to the bottom right of Figure 41B. The single sample of mafic volcanic rock overlaps with basalt 3 of Allen *et al.* (2024).

Samples of the advanced argillic alteration from the prospect plot near the pyrophyllite node in Figure 42B, while several other samples plotting along the trend line towards the pyrophyllite node are also associated with the zone of advanced argillic alteration. Most of the white mica-bearing samples, plotting to the upper left of the unaltered box field, are related to the white mica alteration zone intersected in drillcore located to the northwest of the main zone of advanced argillic alteration (DDH BR-99-08-001 and BR-2K-08-005; Figure 16). The AI *vs.* CCPI discrimination diagram is less applicable to zones of advanced argillic alteration, with the majority of the pyrophyllite samples plotting within the least altered field (Figure 43B). The most intensely altered samples display moderate sodium depletion (Figure 44B), which is also accompanied by local mercury and barium enrichment (Figure 45B).

Little Sandy

Two main rock types predominate at the Little Sandy prospect, which consist of mafic and felsic volcanic rocks containing variable chlorite and lesser white mica alteration (Figure 39C). These rocks predominantly plot within the tholeiitic field of Allen *et al.* (2024) (Figure 40C). The single mafic sample plotting within the transitional 2 field represents a mafic dyke, and the felsic sample plotting within the calc-alkaline 2 field represents a quartz–feldspar porphyry dyke (Figure 40C). The remaining two felsic samples plotting outside of the tholeiitic field consist of volcaniclastic rocks and may contain a mixed signature. Samples plotting in the rhyolite/dacite field form a cluster on the Zr/Al_2O_3 *vs.* Al_2O_3/TiO_2 discrimination diagram overlapping the rhyolite 1, 4 and dacite fields, with the three samples forming a tight cluster representing the volcaniclastic samples and a rhyolite dyke (Figure 41C). The two felsic volcanic samples that plot to the lower left were collected proximal to mineralization and over-

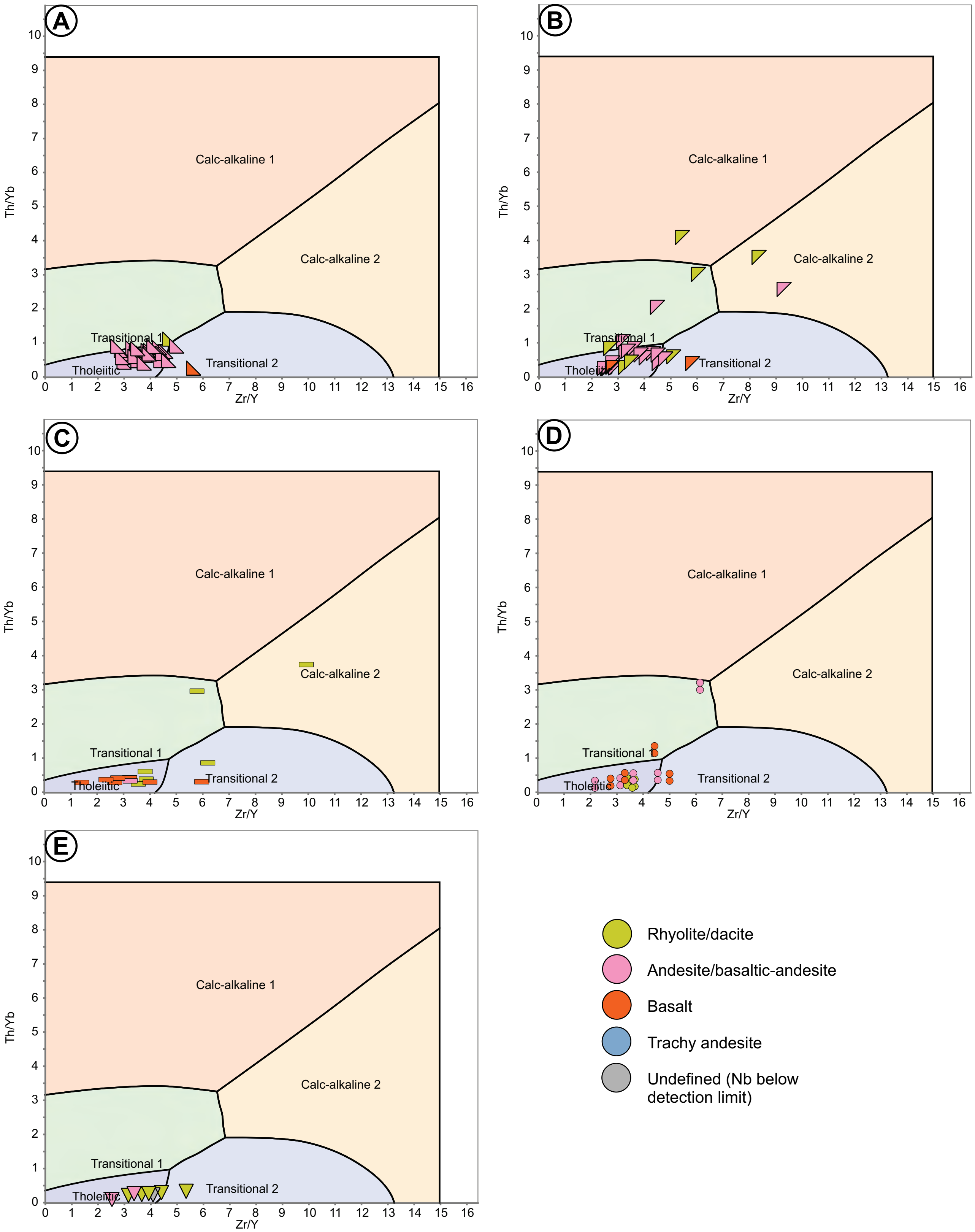

Figure 40. *Zr/Y* vs. *Th/Yb discrimination diagram (Allen* et al.*, 2024) for the Mary March Brook group prospects. Samples are colour coded to rock type, as determined from Figure 39. A) Woodman's Brook prospect; B) Tower prospect; C) Little Sandy prospect; D) Seal Pond prospect; E) Beaver Pond prospect.*

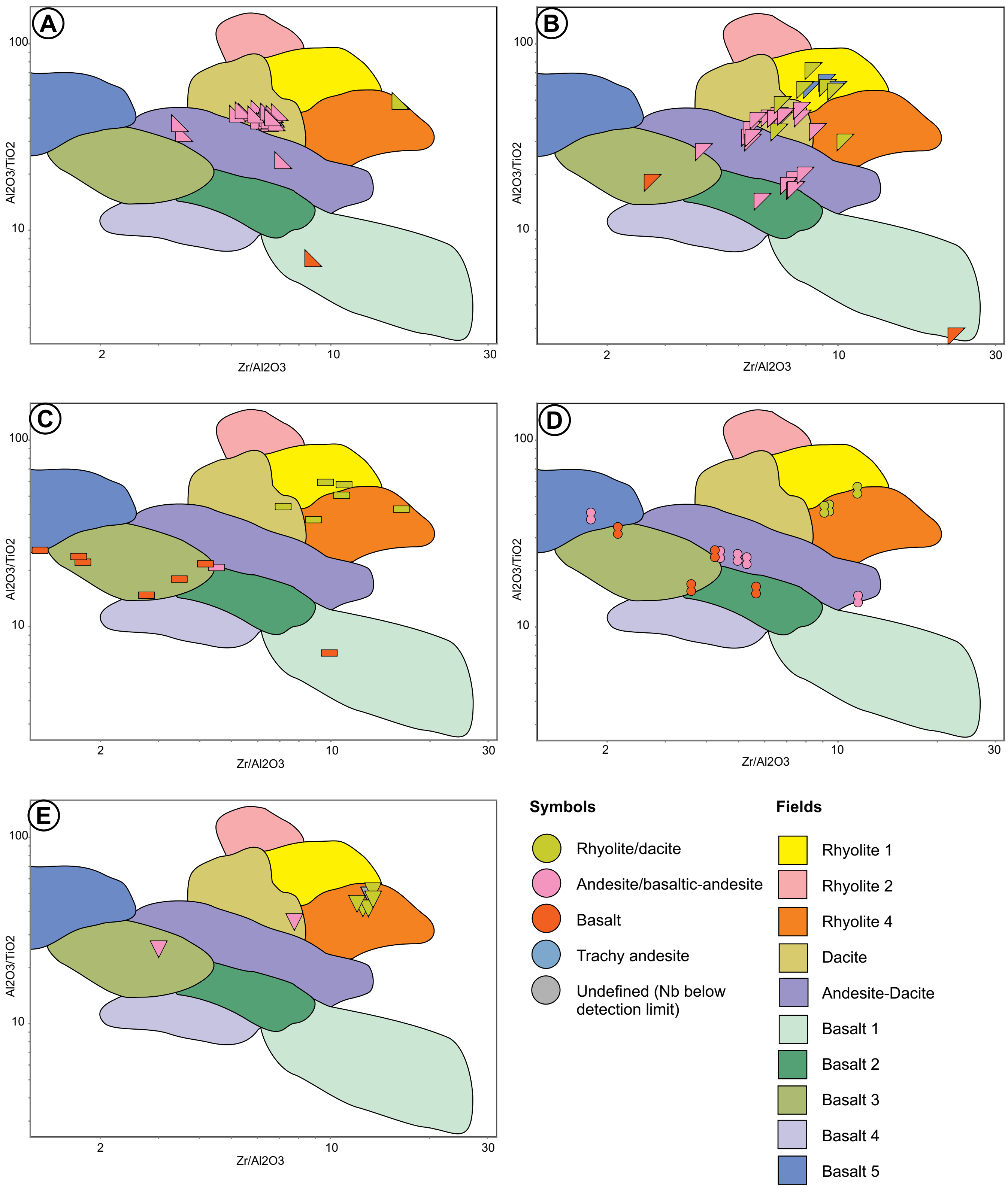

Figure 41. *Zr/Al_2O_3* vs. *Al_2O_3/TiO_2 discrimination diagram outlining the fields from Allen* et al. *(2024) displaying samples from the Mary March Brook group prospects. Samples are colour coded to rock type, as determined from Figure 39. A) Woodman's Brook prospect; B) Tower prospect; C) Little Sandy prospect; D) Seal Pond prospect; E) Beaver Pond prospect.*

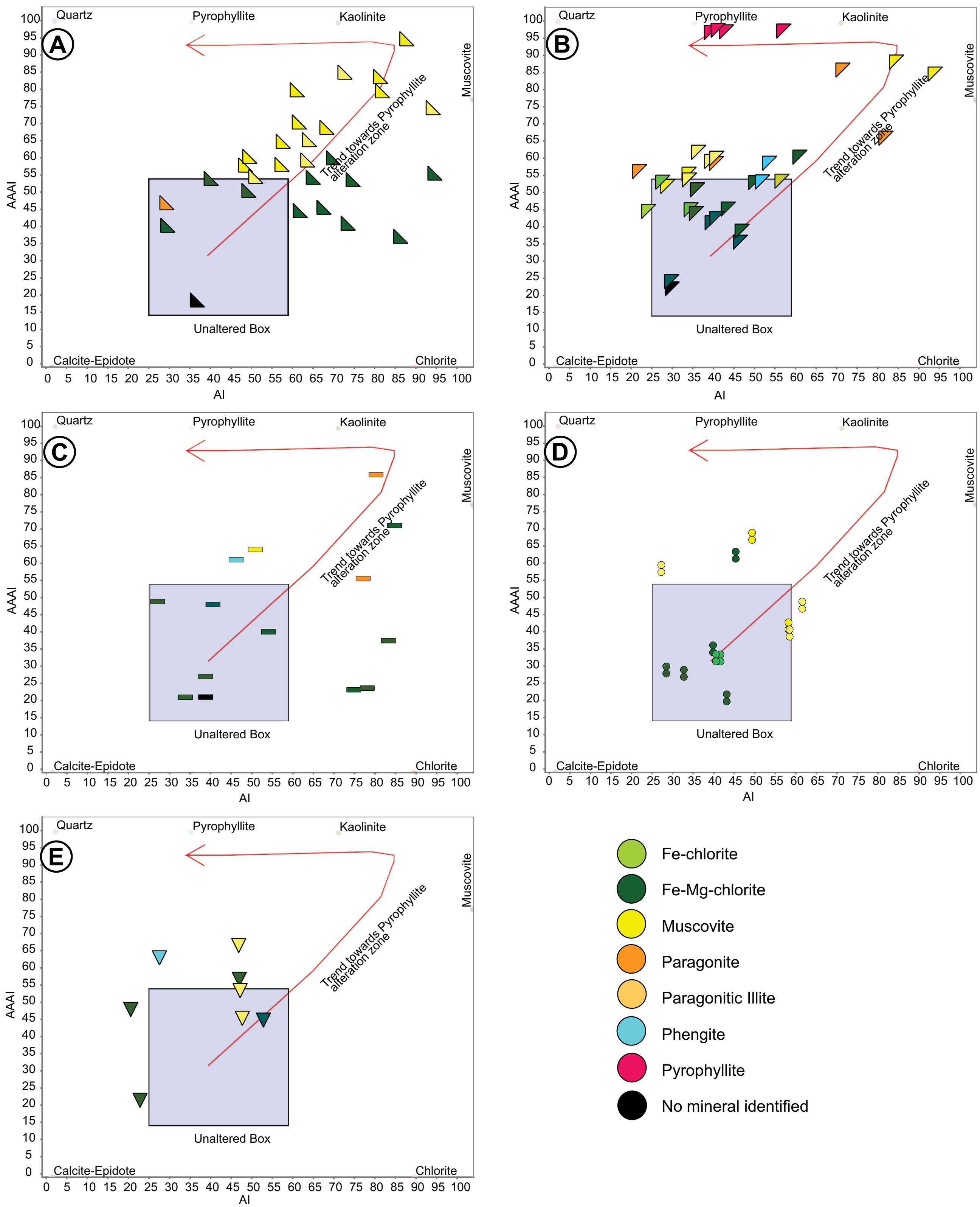

Figure 42. *Alteration box plot of the alteration index (AI)* vs. *advanced argillic alteration index (AAAI; Williams and Davidson, 2004) for the Mary March Brook group prospects. Samples are colour coded to the predominant alteration phase as determined by SWIR analysis. A) Woodman's Brook prospect; B) Tower prospect; C) Little Sandy prospect; D) Seal Pond prospect; E) Beaver Pond prospect.*

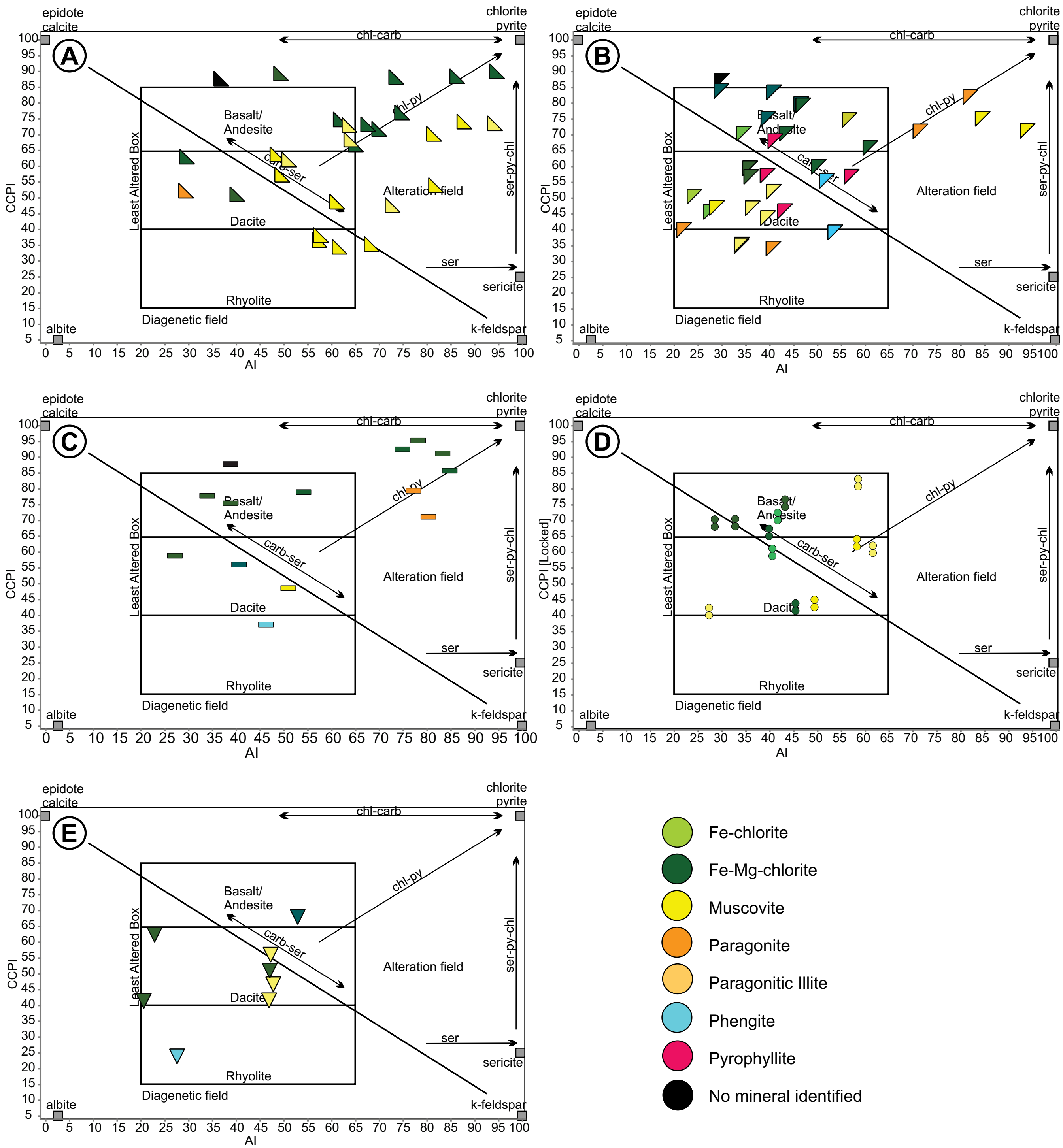

Figure 43. *Alteration box plot of the alteration index (AI)* vs. *the chlorite–carbonate–pyrite index (CCPI; Large* et al.*, 2001) for the Mary March Brook group prospects. Samples are colour coded to the predominant alteration phase as determined by SWIR analysis. A) Woodman's Brook prospect; B) Tower prospect; C) Little Sandy prospect; D) Seal Pond prospect; E) Beaver Pond prospect.*

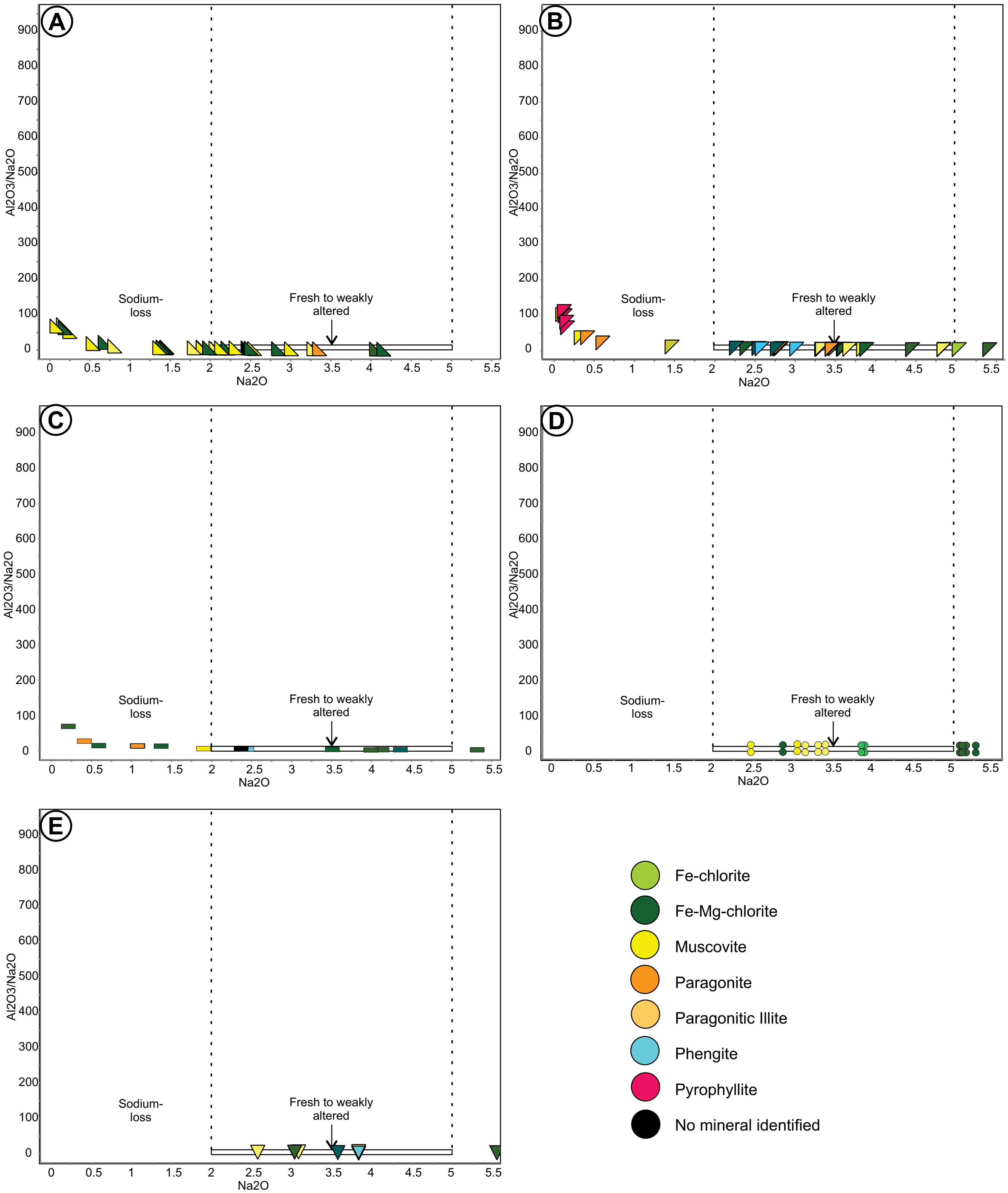

Figure 44. *Spitz–Darling index (Spitz and Darling, 1978) of the Na_2O vs. Al_2O_3/Na_2O discrimination diagram (modified from Ruks* et al.*, 2006) for the Mary March Brook group prospects. Samples are colour coded to the predominant alteration phase as determined by SWIR analysis. A) Woodman's Brook prospect; B) Tower prospect; C) Little Sandy prospect; D) Seal Pond prospect; E) Beaver Pond prospect.*

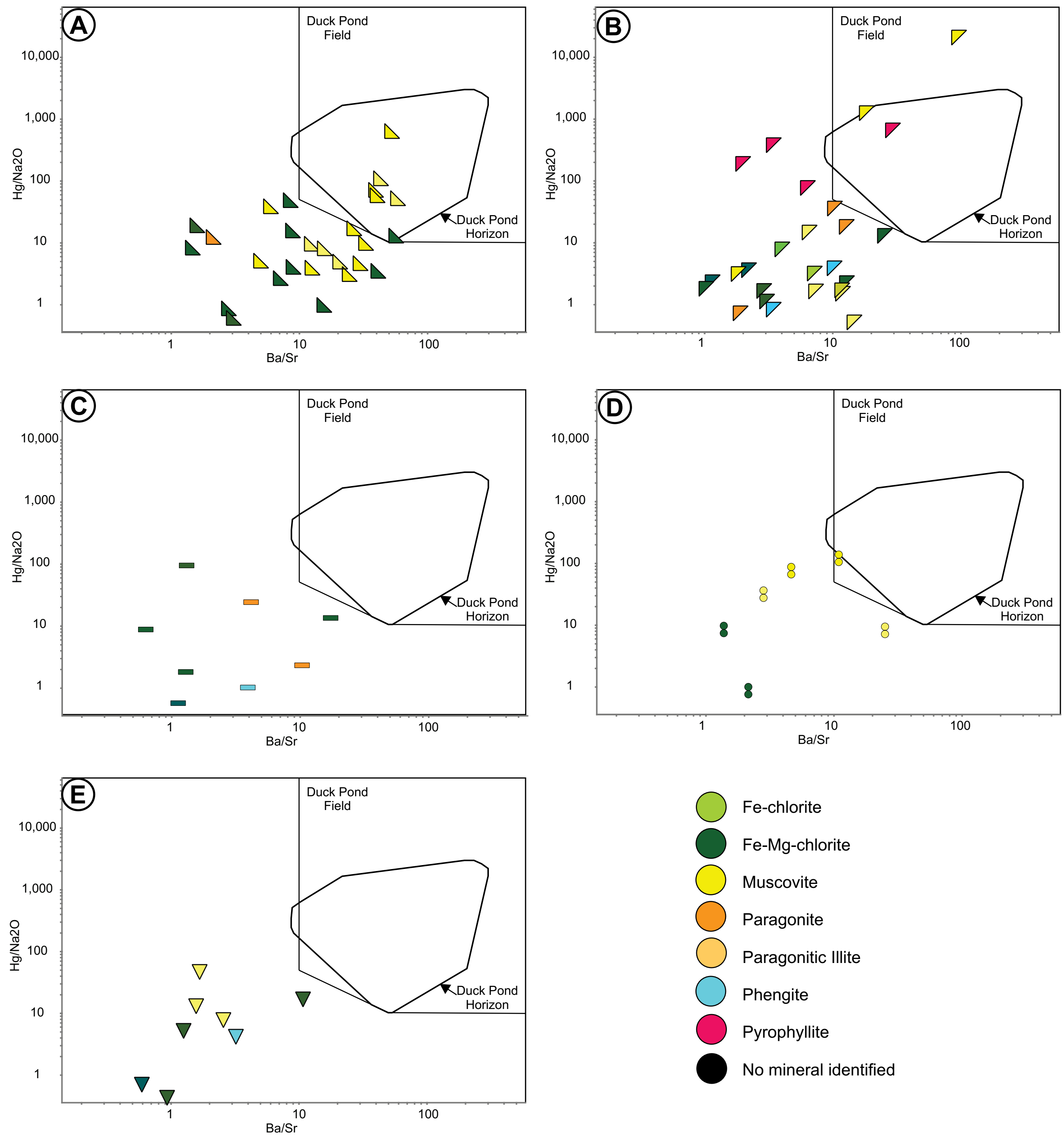

Figure 45. *Duck Pond alteration index discrimination diagram (Collins, 1989) for the Mary March Brook group prospects. Samples are colour coded to the predominant alteration phase as determined by SWIR analysis. A) Woodman's Brook prospect; B) Tower prospect; C) Little Sandy prospect; D) Seal Pond prospect; E) Beaver Pond prospect.*

lap the dacite and rhyolite 4 fields of Allen *et al.* (2024); Figure 41C). The single sample, plotting to the right of the cluster, also represents a sample from a volcaniclastic unit. Samples plotting within the mafic to intermediate fields in Figure 39C form two distinct groups in Figure 41C, while the single sample plotting in the basalt 1 field represents a mafic dyke. The remaining samples broadly overlap basalt 3 of Allen *et al.* (2024), with the three samples plotting to the far left consisting of pyritic and chlorite altered mafic volcanic rocks.

Samples plotting close to the pyrophyllite trend line in Figure 42C are representative of altered rocks from the immediate area of the Little Sandy prospect, as well as the alteration zone noted to the immediate northwest. The same samples along with three chlorite–pyrite altered samples form a cluster near the chlorite–pyrite node in Figure 43C, representing the most altered samples from the area. These samples locally display weakly developed sodium depletion, but this alteration is not accompanied by any significant mercury or barium enrichment (Figures 44C and 45C).

Seal Pond

Rock units within the area of the Seal Pond prospect are dominated by mafic volcanic rocks, along with lesser felsic volcanic rocks as shown in Figure 39D. These rocks are affected by white mica and lesser chlorite alteration. Similar to the Little Sandy prospect, these rocks primarily plot within the tholeiitic field of Allen *et al.* (2024), while the two samples plotting to the right within the transitional 2 field represent weak to moderately altered samples containing muscovite (Figure 40D). The two samples plotting in the transitional 1 field represent samples of mafic and intermediate dykes. Samples form three main groups on the Zr/Al_2O_3 *vs.* Al_2O_3/TiO_2 discrimination diagram, with the felsic samples plotting in a similar position as those from the Little Sandy prospect, falling within the rhyolite 4 field (Figure 41 D). Mafic and intermediate rocks overlap the fields of basalt 2, 3 and andesite-dacite of Allen *et al.* (2024). Samples with Zr/Al_2O_3 ratios between three and six represent the main volcanic sequence hosting the mineralization. The two samples with lower Zr/Al_2O_3 represent a tuffaceous rock (basalt 5 field) and a mafic intrusive rock (basalt 3 field). The single intermediate sample with a Zr/Al_2O_3 ratio greater than 10 consists of an intermediate intrusive unit.

No significant hydrothermal alteration was identified in the area of the Seal Pond prospect, aside from some moderate muscovite alteration. In Figure 42D, altered mafic to intermediate samples plot to the right of the unaltered box field, while the altered felsic volcanic samples plot above this field. Similarly, the altered mafic to intermediate volcanic samples are only associated with weak to moderate CCPI ratios (Figure 43D). No sodium depletion is associated with the altered samples from the area, but minor mercury and barium enrichment is noted (Figures 44D and 45D).

Beaver Pond

The bulk of the samples from the Beaver Pond area plot within the rhyolite/dacite field as illustrated in Figure 39E, with the single sample plotting to the right containing anomalously high Nb. Most samples plot within the tholeiitic field of Allen *et al.* (2024), except for one sample that plots within the transitional 2 field; the latter is from an altered felsic volcanic rock (Figure 40E). The felsic volcanic samples form a tight cluster on the Zr/Al_2O_3 *vs.* Al_2O_3/TiO_2 discrimination diagram, plotting within the rhyolite 4 field of Allen *et al.* (2024; Figure 41E). The two intermediate samples represent volcanic rocks distal to the main occurrence. No significant hydrothermal alteration was sampled, as indicated by the Ishikawa alteration versus the advanced argillic alteration indices shown in Figure 42E. In addition, no significant chlorite alteration was identified as indicated by the Ishikawa alteration vs. CCPI discrimination diagram (Figure 43E). Finally, no sodium depletion, or mercury or barium enrichment is associated with samples collected from the prospect (Figures 44E and 45E).

RED INDIAN LAKE GROUP PROSPECTS

Mary March Brook

Units within the area of the Mary March Brook prospect include felsic, intermediate and mafic compositions with the intermediate rocks displaying the most intense white mica alteration (Figure 46A). The felsic volcanic sample plotting within the calc-alkaline 2 field of Figure 47A represents a dated sample from the eastern end of the southern BRAB (Sparkes and Hamilton, 2024). The other two felsic samples represent material from altered and fragmental volcanic units and are not representative of a homogeneous volcanic protolith. Intermediate volcanic rocks also display a wide distribution, with those samples plotting within the calc-alkaline 2 field representing intrusive rocks, and a fragmental volcanic unit. The single intermediate sample plotting within the calc-alkaline 1 field is from an intermediate fragmental unit, while those samples plotting within the transitional 1 field are representative of relatively unaltered, locally flow-banded, volcanic rocks. The single intermediate sample plotting in the tholeiitic field is from an altered fragmental unit and is not representative of a homogeneous volcanic protolith (Figure 47A). Mafic volcanic rocks from the area are distributed into two groups, with those samples plotting within the transitional 1 field representing possible mafic intrusive rocks. Those mafic samples plotting within the tholeiitic field are representative of relatively unaltered mafic volcanic rocks of

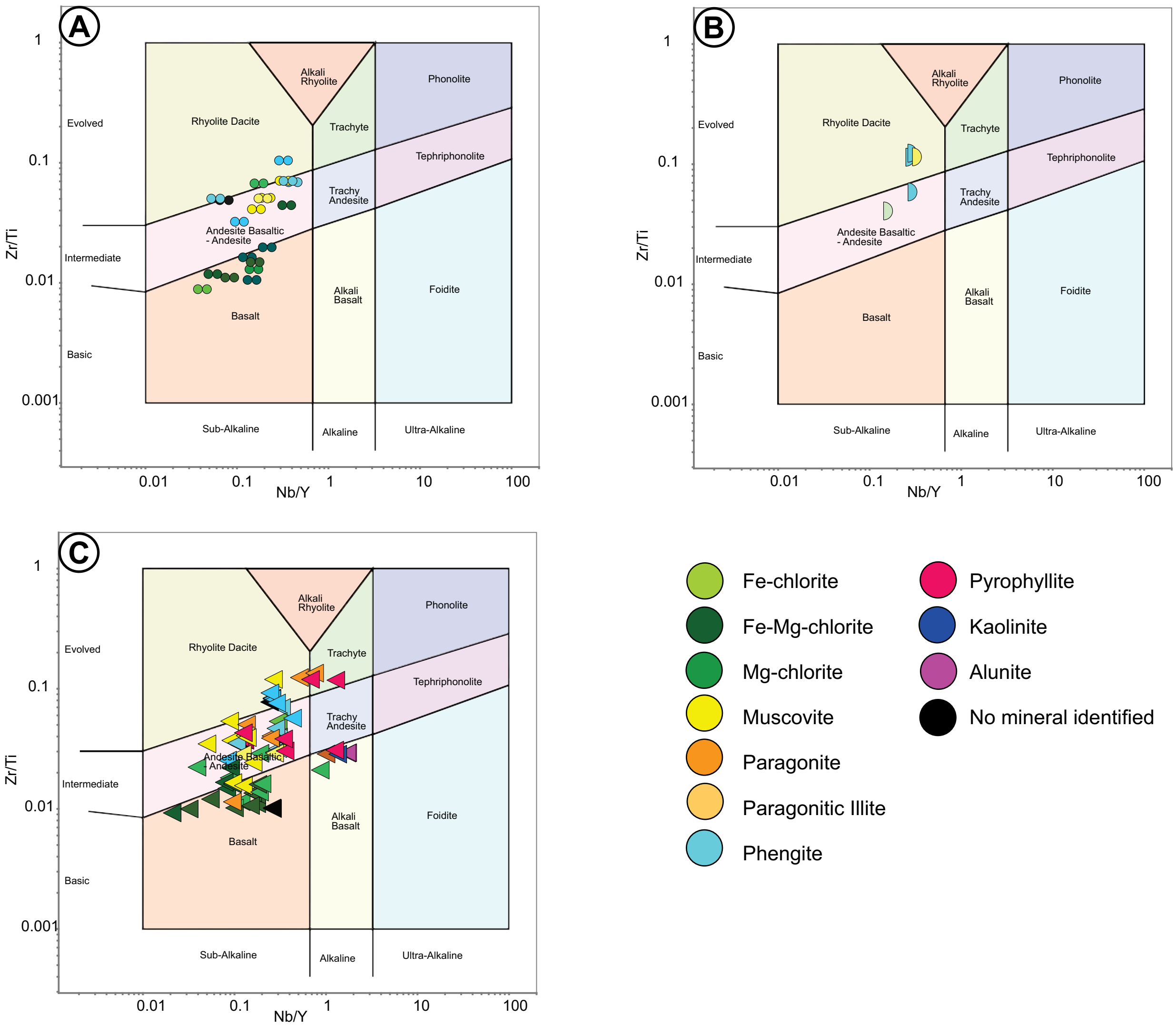

Figure 46. *Nb/Y* vs. *Zr/Ti discrimination diagram (Pearce, 1996) for the Red Indian Lake Group prospects. Samples are colour coded to the predominant alteration phase as determined by SWIR analysis. A) Mary March Brook prospect; B) Connell prospect; C) Mary March prospect.*

the area (Figure 47A). The relatively unaltered intermediate rocks that plot within the transitional 1 field of Figure 47A, form a cluster to the right in Figure 48A, plotting within the rhyolite 4 field of Allen *et al.* (2024). This cluster also includes the intermediate intrusive units and the dated felsic sample from the area. The mafic volcanic rocks plotting within the tholeiitic field of Figure 47A display a range of values on the Zr/Al_2O_3 *vs.* Al_2O_3/TiO_2 discrimination diagram, but mainly overly the basalt 2 and 3 fields (Figure 48A).

Only weak to moderate white mica alteration is identified within the Mary March Brook area, with the single sample of phengite alteration plotting along the pyrophyllite trend line, representing an altered fragmental volcanic (Figure 49A). The mafic volcanic rocks display elevated values of the CCPI as shown in Figure 50A but have only minor associated sodium depletion (Figure 51A). Likewise, no elevated values of mercury or barium were detected (Figure 52A).

Connell

The samples from the Connell area largely consisted of tuffaceous rocks and interlayered chert. The samples of volcanic rock range from intermediate to felsic on the Nb/Y *vs.* Zr/Ti discrimination diagram shown in Figure 46B, with the samples largely dominated by a phengitic white mica signature. Both the felsic and intermediate rocks plot within the transitional 1 field in Figure 47B, with three of the felsic samples forming a tight cluster on the Zr/Al_2O_3 *vs.* Al_2O_3/TiO_2 discrimination diagram (Figure 48B). These samples represent tuffaceous rocks and are most representative of the volcanic rocks in the area.

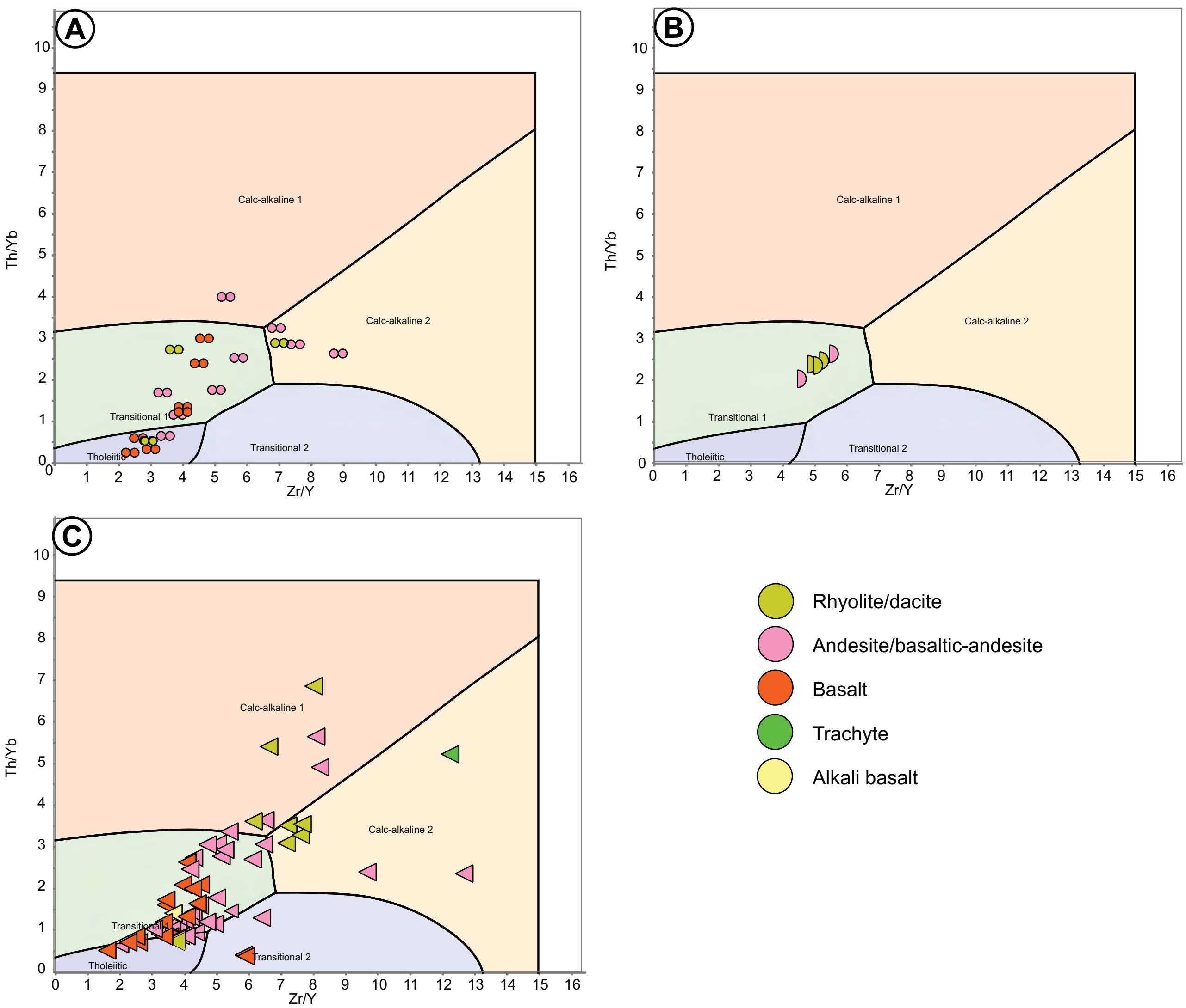

Figure 47. *Zr/Y* vs. *Th/Yb discrimination diagram (Allen* et al.*, 2024) for the Red Indian Lake Group prospects. Samples are colour coded to rock type, as determined from Figure 46. A) Mary March Brook prospect; B) Connell prospect; C) Mary March prospect.*

The single sample displaying an elevated AAAI value in Figure 49B consists of altered tuff shown in Plate 38A, while a muscovite dominated sample displays an elevated AI value. The same muscovite altered sample plots within the "alteration field" of Figure 50B. These same two samples with anomalous AAAI and AI values display minor sodium depletion (Figure 51B). Only the muscovite-bearing sample, interpreted as the most altered sample from the area, was analyzed for mercury, and this sample plots outside of the Duck Pond field of Figure 52B.

Mary March

The Mary March prospect displays a range of rock compositions, including mafic, intermediate and felsic volcanic rocks, along with intense hydrothermal alteration which causes samples to plot within the trachyte and alkali basalt fields (Figure 46C). Most mafic and intermediate rocks from the area largely plot within the transitional 1 field in Figure 47C and include several samples containing advanced argillic alteration. However, the bulk of the advanced argillic alteration display variable Th/Yb and Zr/Y ratios and primarily plot within the calc-alkaline 1 and calc-alkaline 2 fields. The mafic samples plotting in the transitional 2 field represent samples of mafic dykes, which postdate the alteration (Figure 47C). The cluster of felsic samples plotting within the rhyolite 1 field are related to the advanced argillic alteration developed at the prospect (Figure 48C). The felsic volcanic rocks plotting below and to the right within the rhyolite 4 field are representative of the footwall rhyolite related to the development

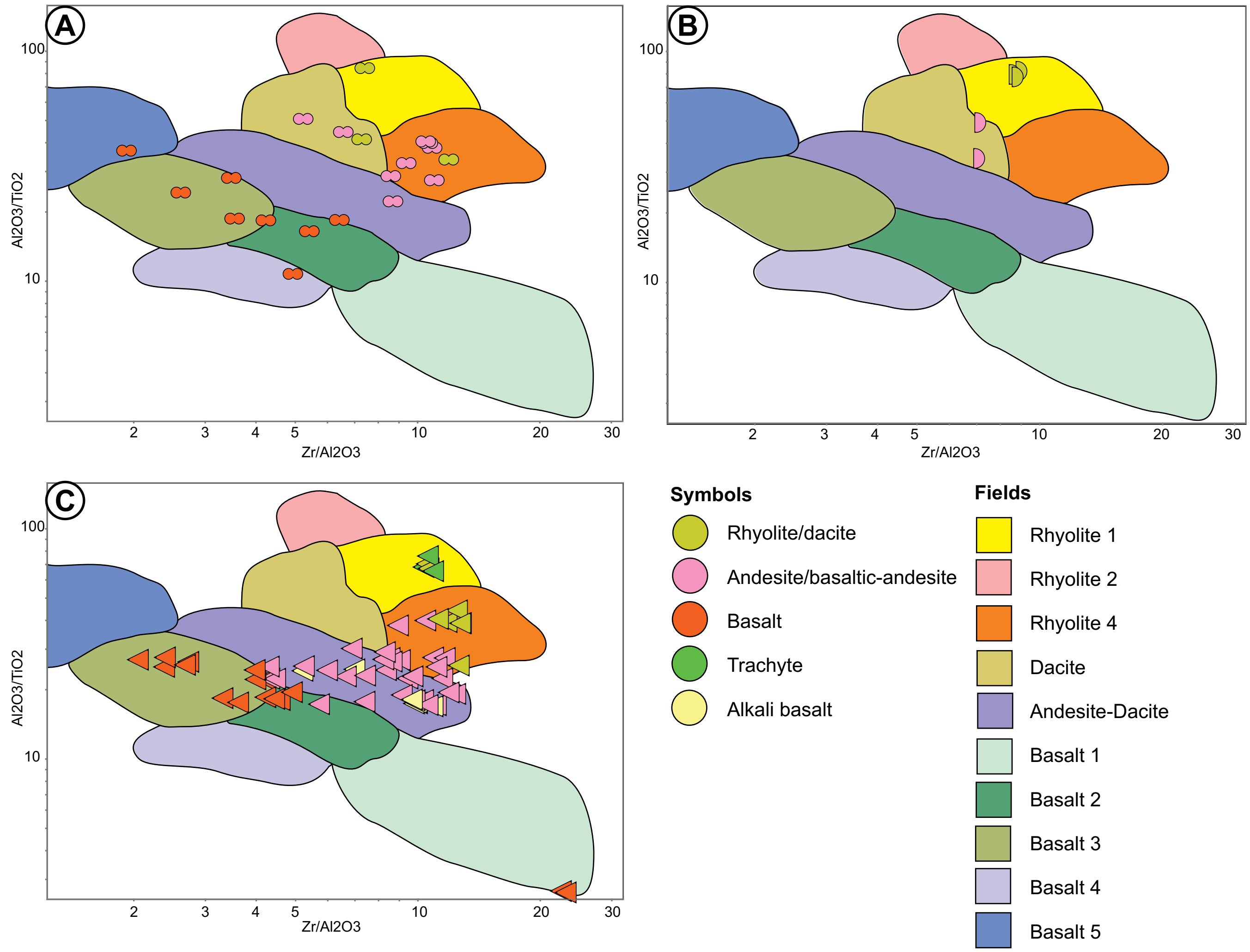

Figure 48. *Zr/Al_2O_3* vs. *Al_2O_3/TiO_2 discrimination diagram outlining the fields from Allen* et al. *(2024) displaying samples from the Red Indian Lake Group prospects. Samples are colour coded to rock type, as determined from Figure 46. A) Mary March Brook prospect; B) Connell prospect; C) Mary March prospect.*

of the VMS mineralization at the prospect. The intermediate volcanic rocks display a significant range in Zr/Al_2O_3 ratios, with both altered and relatively unaltered samples plotting within the same areas. The mafic volcanic rocks form two discrete clusters, representing two separable volcanic units (Figure 48C). The cluster with Zr/Al_2O_3 ratios less than three, also have Th/Yb less than one and are more tholeiitic in composition. The mafic volcanic rocks with Zr/Al_2O_3 ratios greater than three plot within the central portion of the transitional 1 field shown in Figure 47C. The two mafic samples plotting in the lower right portion of Figure 48C represent mafic dykes.

The advanced argillic alteration samples are well defined in Figure 49C, which highlights the range of muscovite–paragonite through to pyrophyllite–kaolinite–alunite advanced argillic alteration. However, it should be highlighted that one sample dominated by alunite alteration plots within the unaltered box field in Figure 49C, as this sample only contains 12.9 weight percent SiO_2 but also contains 36.7 percent Al_2O_3, which is not factored into the advanced argillic alteration index and highlights the importance of using SWIR in support of geochemistry. The bulk of the advanced argillic alteration is barren of base- and precious-metal mineralization, while stockwork-style mineralization hosted within the mafic volcanic rocks is associated with strong chlorite alteration, with mineralized samples plotting in the upper right of Figure 50C. The mineralized chlorite altered sample, along with the white mica and advanced argillic alteration, display significant sodium depletion, along with phengite altered rhyolite samples that are footwall to the alteration zone (Figure 51C). The sodium depletion is also associated with mercury and barium enrichment, with numerous samples plotting within the Duck Pond field in Figure 52C, but these samples

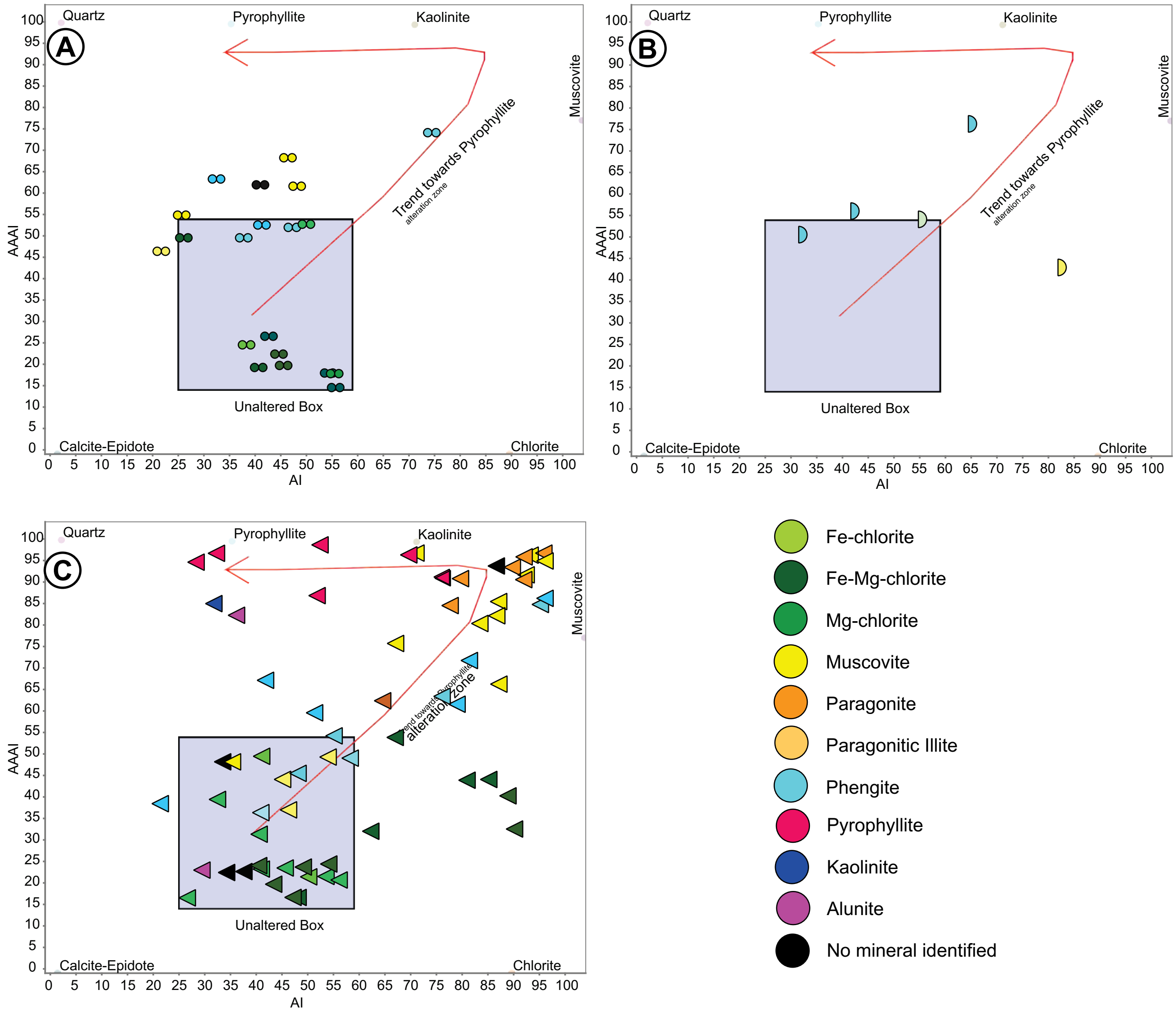

Figure 49. *Alteration box plot of the alteration index (AI)* vs. *advanced argillic alteration index (AAAI; Williams and Davidson, 2004) for the Red Indian Lake Group prospects. Samples are colour coded to the predominant alteration phase as determined by SWIR analysis. A) Mary March Brook prospect; B) Connell prospect; C) Mary March prospect.*

are largely dominated by muscovite–paragonite alteration along with samples of the phengite-bearing footwall rhyolite. The majority of the advanced argillic alteration display lower Ba/Sr ratios as this style of alteration is accompanied by strontium enrichment, and therefore plot to the left outside of the Duck Pond field, but still display elevated Hg/Na_2O ratios (Figure 52C.)

SULPHUR ISOTOPES

To further investigate the origin of the hydrothermal fluids related to the development of the two zones of advanced argillic alteration in the southern BRAB, six samples were analyzed for sulphur isotopic compositions by Secondary Ion Mass-Spectrometry (SIMS). Two samples from each of the advanced argillic alteration zones (Tower and Mary March), along with two samples from the Lucky Strike deposit were selected for comparison (Plate 41; Table 2). Pyrite in each sample was targeted for analysis, with one to three spot analyses performed on three to four grains from each sample.

Mary March

The two samples from the Mary March area included one from the Mary March horizon and one from the Nancy April horizon. The sample from the Mary March horizon consisted

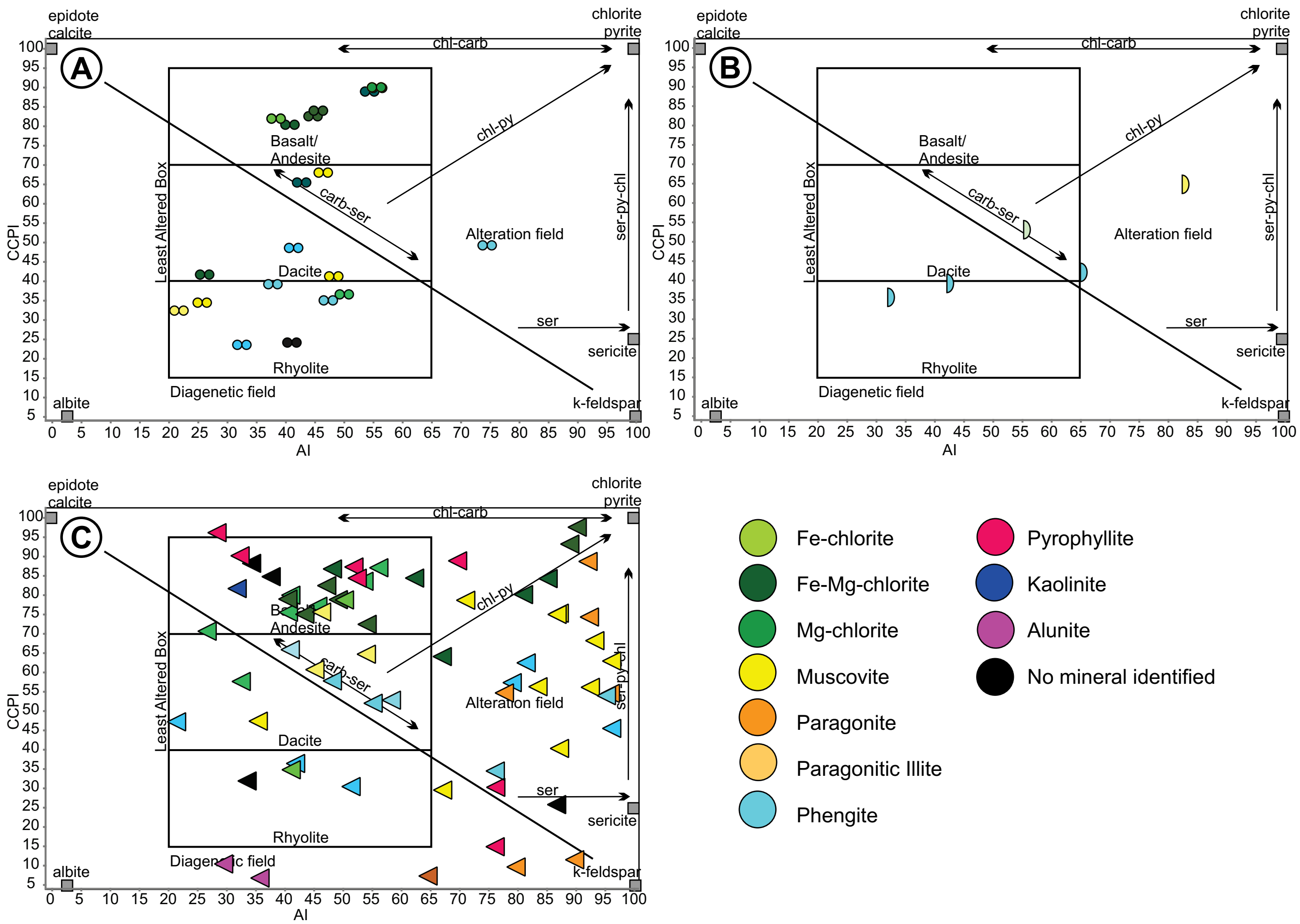

Figure 50. *Alteration box plot of the alteration index (AI)* vs. *the chlorite–carbonate–pyrite index (CCPI; Large* et al.*, 2001) for the Red Indian Lake Group prospects. Samples are colour coded to the predominant alteration phase as determined by SWIR analysis. A) Mary March Brook prospect; B) Connell prospect; C) Mary March prospect.*

of a pyrite-rich vein crosscutting pyrophyllite alteration developed near the contact of the footwall rhyolite (Plate 41A; Figure 30). In total nine $\delta^{34}S$ spot analyses from three different pyrite grains produced $\delta^{34}S$ values ranging from -1.0 to -11.1 per mil, with an average of -8.0 (Plate 42A; Figure 53). The sample from the Nancy April horizon was collected from a clast of massive pyrite that contained anomalous silver, selenium and tellurium occurring within paragonite-dominated footwall alteration (Plate 41B; Sparkes and Hinchey, 2023, plate 9). Eight analyses were obtained from this sample, from three separate pyrite grains. These analyses produced $\delta^{34}S$ values ranging from -0.6 to -3.9 per mil, with an average of -2.4 (Plate 42B; Figure 53).

Tower

The two samples collected from the Tower prospect include one from the western end of the advanced argillic alteration zone and one from the eastern end. The pyrophyllite alteration in the western end of the alteration zone is devoid of significant pyrite, so a sample was selected from marginal chlorite–muscovitic illite alteration hosted in a strongly altered intermediate volcanic rock from DDH BJ-012 (Plate 41C; Figure 16). Five analyses were obtained from two separate pyrite grains. These analyses produced $\delta^{34}S$ values ranging from 7.3 to 9.3 per mil, with an average of 8.3 (Plate 42C; Figure 53). A single analysis from a third pyrite grain produced a $\delta^{34}S$ value of -10.2, but this single analysis was not duplicated within the alteration zone (Table 2). The sample from the eastern portion of the alteration zone was collected from paragonite–pyrite alteration developed marginal to pyrophyllite identified in DDH LS-2K-005 (Plate 26; Plate 41D; Figure 16). This sample contains the hydrothermal “spongey” pyrite phases as noted above, from which nine analysis from three separate grains produced $\delta^{34}S$ values ranging from 0.8 to 4.7 per mil, with an average of 3.0 (Plate 42D; Figure 53).

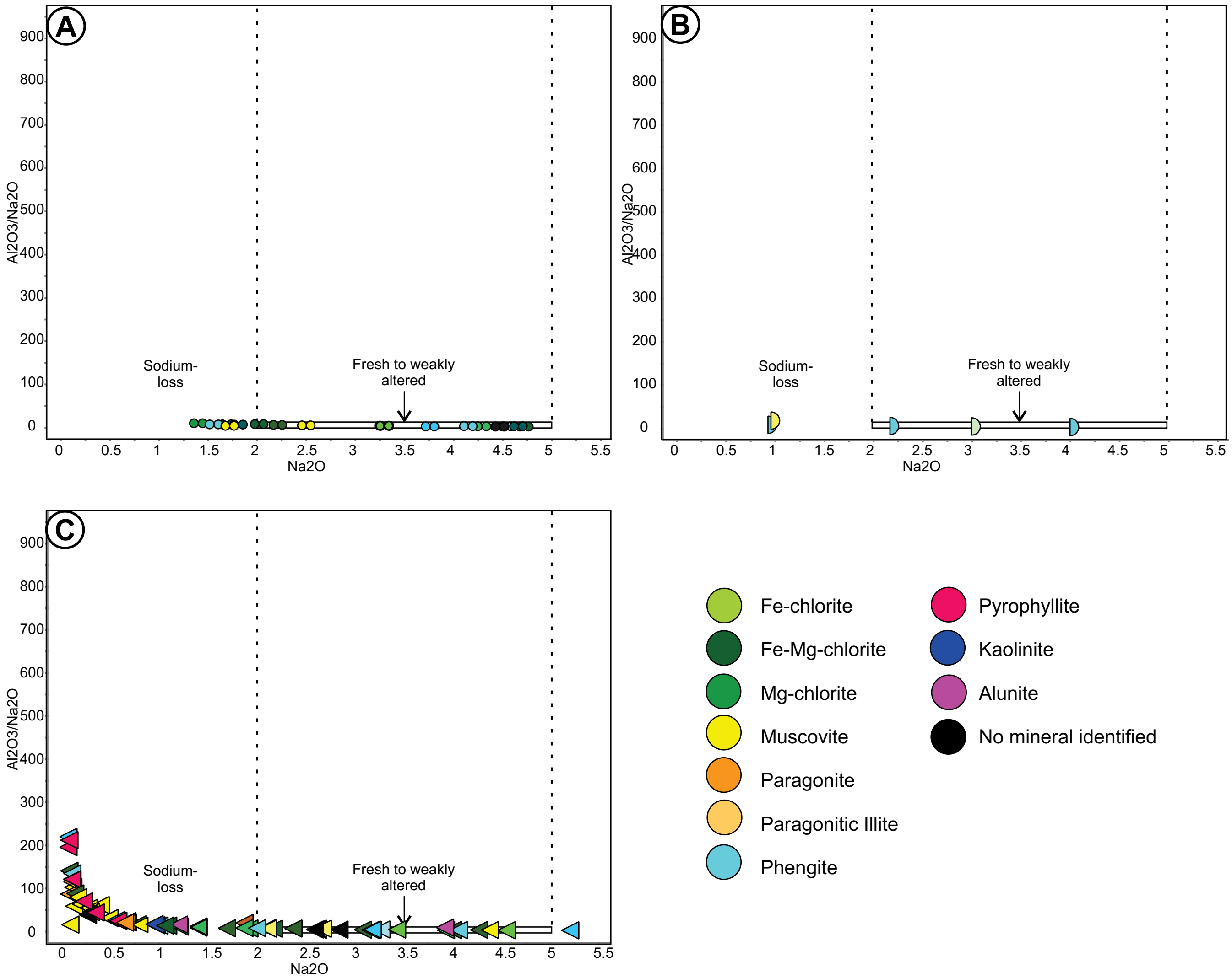

Figure 51. *Spitz–Darling index (Spitz and Darling, 1978) of the* Na_2O vs. Al_2O_3/Na_2O *discrimination diagram (modified from Ruks* et al.*, 2006) for the Red Indian Lake Group prospects. Samples are colour coded to the predominant alteration phase as determined by SWIR analysis. A) Mary March Brook prospect; B) Connell prospect; C) Mary March prospect.*

Lucky Strike

For comparison, two samples from the Lucky Strike deposit were analyzed to provide data from known VMS mineralization in the region. The two samples consisted of a quartz–sulphide stockwork vein hosted within a chloritized mafic volcanic rock, and a sample of disseminated pyrite–barite and base-metal sulphides, with both samples being representative of the footwall zone to *in situ* massive sulphide mineralization (Plate 41E, F). Nine spot analyses from three different pyrite grains from the sample of euhedral pyrite within stockwork veining produced $\delta^{34}S$ values ranging from 6.6 to 12.6 per mil, with an average of 8.3 (Plate 42E; Figure 53). Analysis from the second sample produced two separate populations, with three analyses from one pyrite grain producing $\delta^{34}S$ values from 5.4 to 6.0 per mil, with an average of 5.7, while four analyses from two different pyrite grains produced values from 19.3 to 22.9 per mil, with an average of 21.0. The latter two grains are observed to be intergrown with barite (Plate 42F).

DISCUSSION

The collection of systematic downhole SWIR spectral data from areas previously reported to contain significant "sericite" alteration in drillcore, provides an effective means of subdividing these prospects based on their white mica and/or aluminous alteration signatures. Five subdivisions are proposed for the prospects evaluated based on the SWIR data, these are: 1) advanced argillic (Tower, Mary March), 2) argillic (Powerhouse), 3) phyllic – muscovite-dominated (Buchans area (Lucky Strike/Rothermere), Airport,

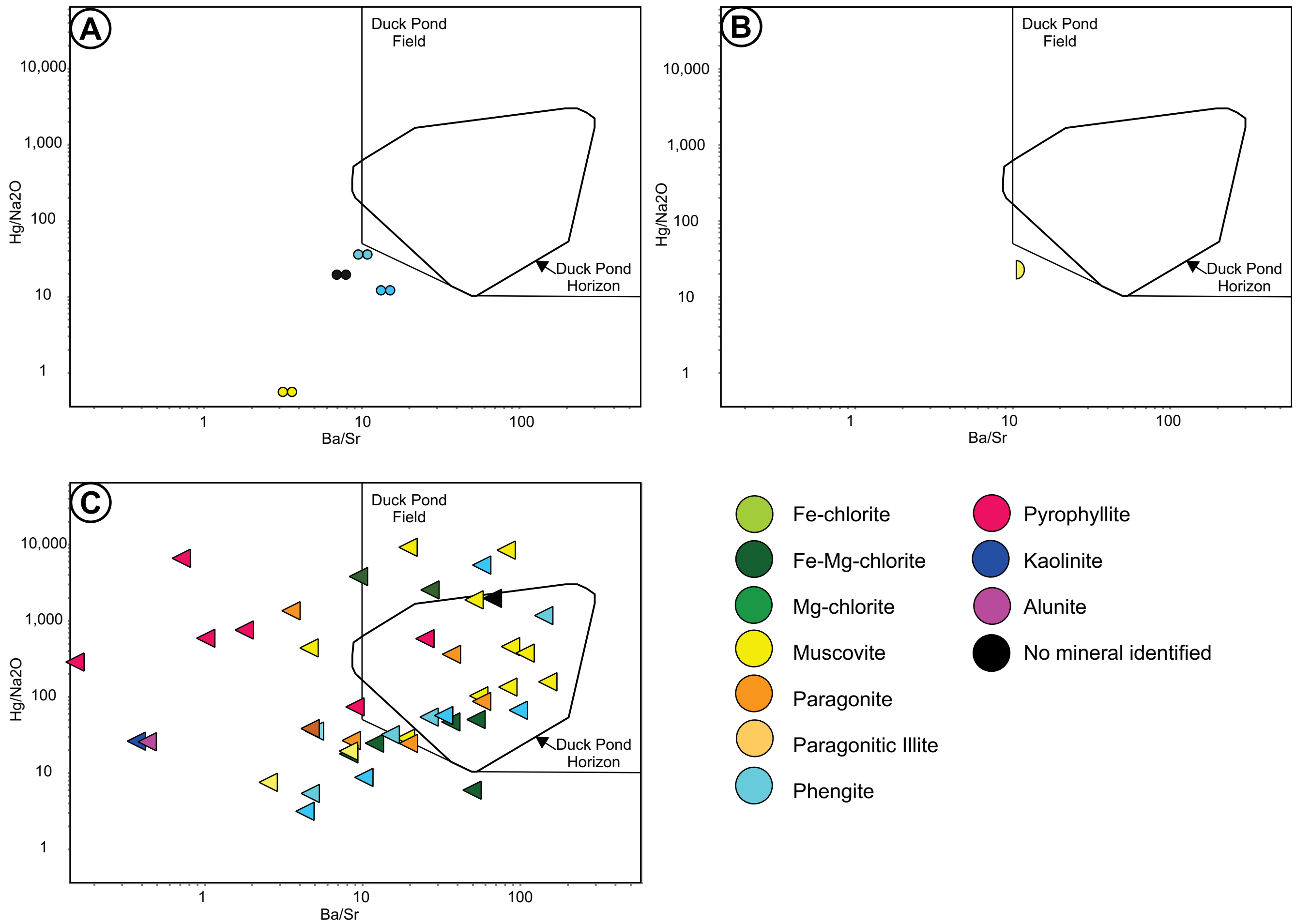

Figure 52. *Duck Pond alteration index discrimination diagram (Collins, 1989) for the Red Indian Lake Group prospects. Samples are colour coded to the predominant alteration phase as determined by SWIR analysis. A) Mary March Brook prospect; B) Connell prospect; C) Mary March prospect.*

Woodman's Brook, Seal Pond, Beaver Pond), 4) phyllic – chlorite-dominated (Little Sandy), 5) sub-propylitic (Sandfill/Middle Branch, Middle Branch East, Mary March Brook, Connell). These subdivisions highlight areas of more intense hydrothermal alteration and provide valuable data for mineral exploration by enabling the recognition of structural panels intersected in drillcore that contain prospective alteration and associated geochemical characteristics and thus represent potential follow-up targets.

The association of zinc dominated mineralization with white mica alteration in the region (Figure 54) is subdivided into samples dominated by white mica alteration and those dominated by chlorite alteration. Figure 54A illustrates that most samples dominated by white mica alteration are zinc dominated. The higher grade (>1000 ppm Zn) samples are associated with white mica minerals displaying Al-OH wavelength values less than 2205 nm and are thus classified as either muscovite or paragonite (Figure 54B). In Figure 54C, D, which show chlorite-dominated samples containing lesser white mica alteration based on the spectral data, there is a similar, yet less defined, relationship. Such relationships highlight zones of advanced argillic, argillic and phyllic alteration as potential follow-up targets for mineral exploration, given the spatial association of such zones with VMS-related mineralization in the region.

Zinc-dominated mineralization is also highlighted by the enrichment of barium and mercury relative to strontium and sodium, as is illustrated in Figure 55. This enrichment is commonly developed within paragonite and muscovite-dominated white mica alteration. The rare occurrence of phengite-altered samples plotting within the Duck Pond field are representative of the footwall felsic volcanic rocks to the VMS mineralization developed at the Mary March prospect. However, it is also noteworthy that several samples plotting within the Duck Pond field are not mineralized but still display prospective alteration with associated geochemical enrichment. These

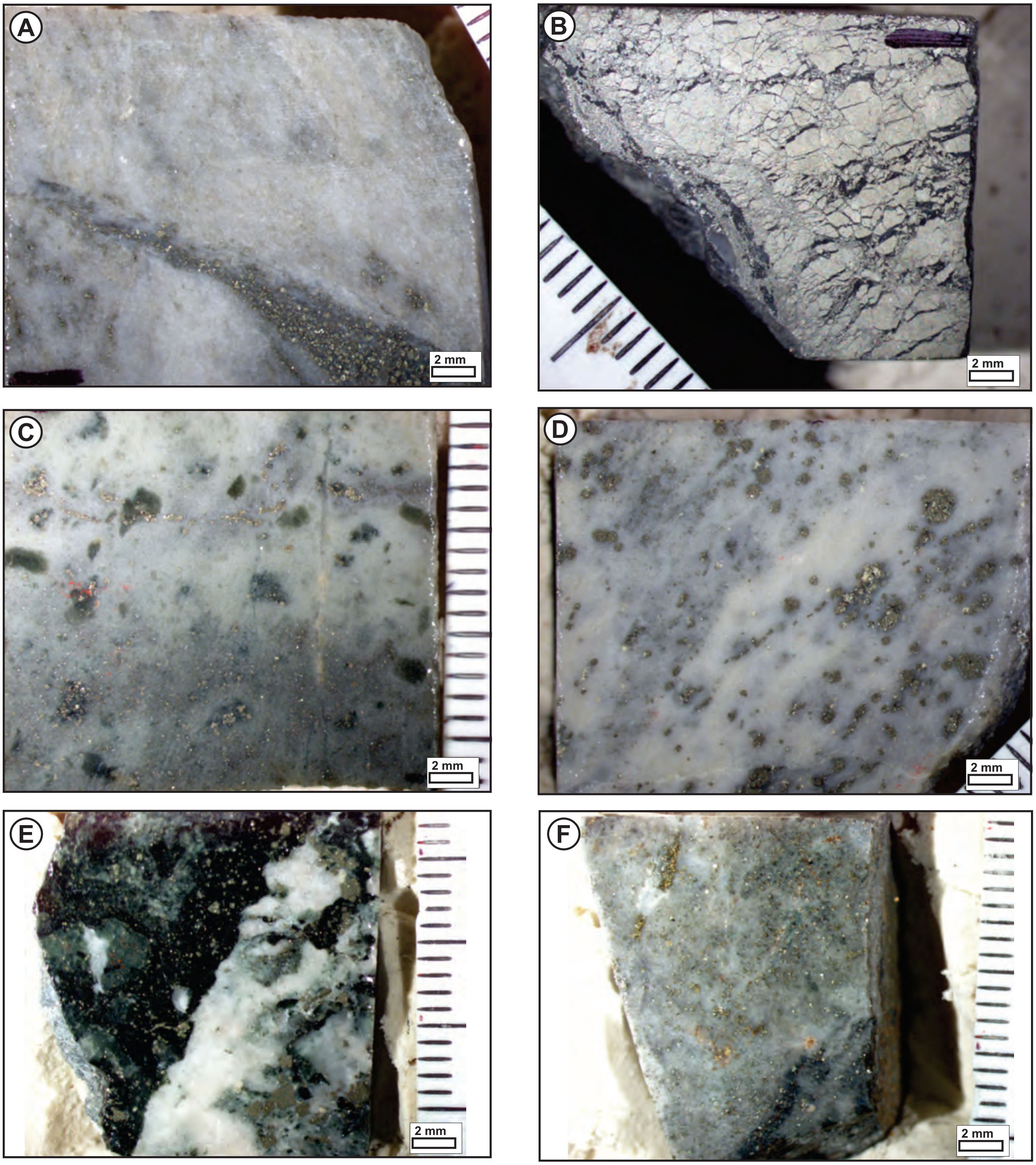

Plate 41. *Samples submitted for sulphur isotope analysis. A) Pyrophyllite alteration crosscut by pyrite-rich vein; GS-22-039, Mary March horizon, Mary March prospect; B) Massive pyrite clast contained in paragonite-dominated footwall alteration; GS-22-056, Nancy April prospect; C) Chlorite–muscovitic illite alteration hosting disseminated pyrite; GS-22-047, western end of the Tower prospect; D) Paragonite-dominated alteration hosting disseminated pyrite; GS-22-112, eastern end of the Tower prospect; E) Stockwork mineralization below the Lucky Strike deposit; GS-22-169; F) Disseminated pyrite with barite below the Lucky Strike deposit; GS-22-170. For sample location data refer to Table 2.*

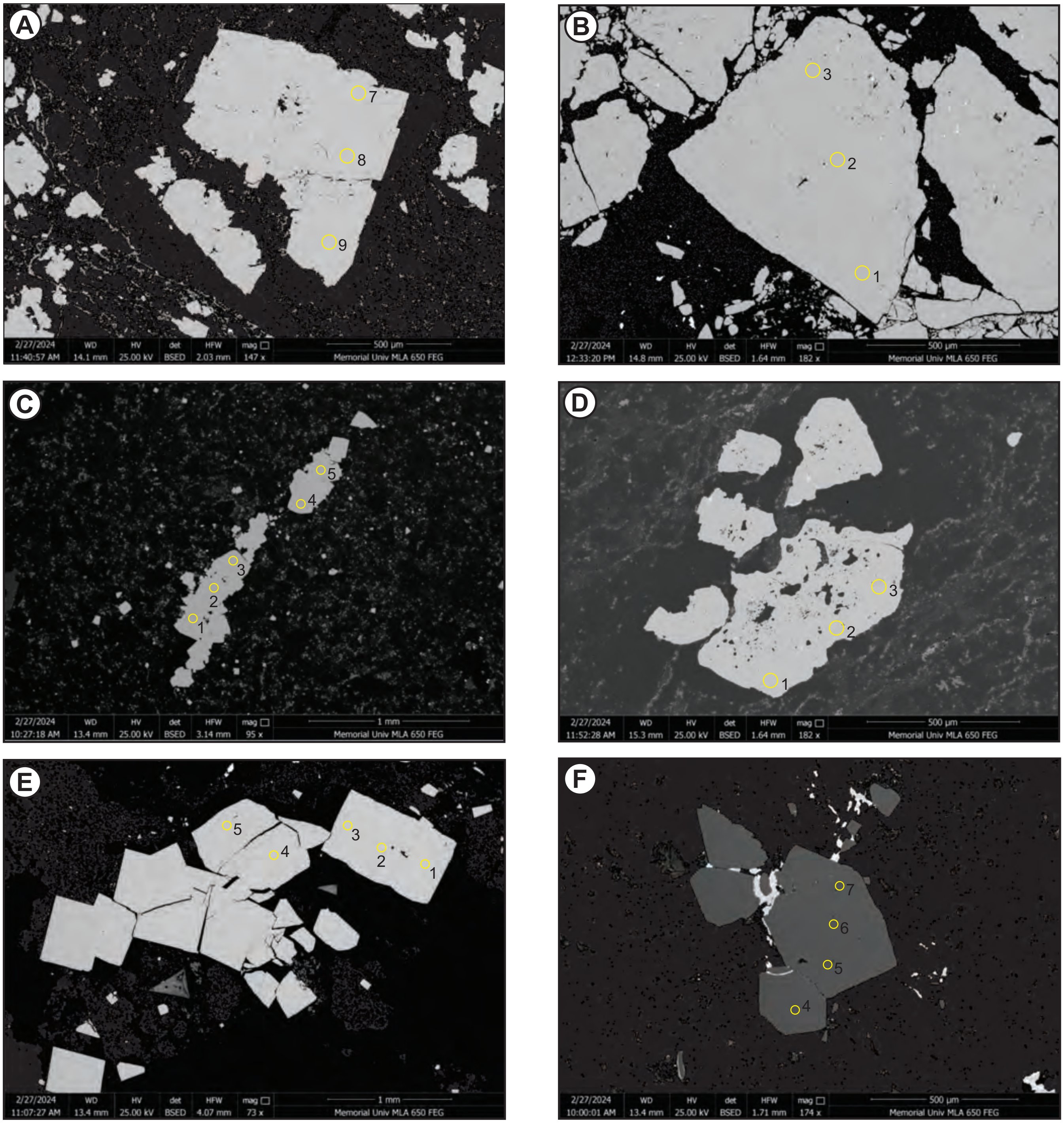

Plate 42. *SEM images of samples submitted for sulphur isotope analysis. A) Image of pyrite grain three, from which points 7–9 were collected for sample GS-22-039, Mary March prospect; B) Image of pyrite grain one, from which points 1–3 were collected for sample GS-22-056, Mary March prospect; C) Image of pyrite grains one (lower left) and two (upper right), from which points 1–5 were collected for sample GS-22-047, Tower prospect; D) Image of pyrite grain one, from which points 1–3 were collected for sample GS-22-112, Tower prospect; E) Image of pyrite grains one and two, from which points 1–5 were collected for sample GS-22-169, Lucky Strike deposit; F) Image of pyrite grains two and three, from which points 4–7 were collected for sample GS-22-170, Lucky Strike deposit. Refer to Table 2 for additional information.*

Table 2. Sample information and results for the six samples investigated for sulphur isotope analysis

Sample ID	DDH	Depth (m)	Mineral	Grain	Point	34S/32S (per mil)	Sample ID	DDH	Depth (m)	Mineral	Grain	Point	34S/32S (per mil)
Mary March Prospect (Mary March horizon)							*Tower Prospect*						
GS-22-039	MM-19-037	350.6	Pyrite	1	1	-11.1	GS-22-112	LS-2K-005	184.6	Pyrite	1	1	2.3
			Pyrite	1	2	-11.0				Pyrite	1	2	3.7
			Pyrite	1	3	-7.1				Pyrite	1	3	1.5
			Pyrite	2	4	-10.1				Pyrite	2	4	4.6
			Pyrite	2	5	-1.0				Pyrite	2	5	3.6
			Pyrite	2	6	-8.5				Pyrite	3	7	0.8
			Pyrite	3	7	-7.4				Pyrite	3	8	4.7
			Pyrite	3	8	-7.6				Pyrite	3	9	3.1
			Pyrite	3	9	-8.3							
							Lucky Strike Deposit						
Mary March Prospect (Nancy April horizon)							GS-22-169	H-0246	29.9	Pyrite	1	1	7.2
GS-22-056	MM-14-035	72.5	Pyrite	1	1	-0.9				Pyrite	1	2	8.3
			Pyrite	1	2	-0.8				Pyrite	1	3	7.4
			Pyrite	1	3	-0.6				Pyrite	2	4	7.5
			Pyrite	2	4	-3.0				Pyrite	2	5	7.4
			Pyrite	2	5	-3.7				Pyrite	3	6	12.6
			Pyrite	2	6	-3.9				Pyrite	3	7	9.5
			Pyrite	3	7	-3.0				Pyrite	3	8	8.0
			Pyrite	3	8	-3.7				Pyrite	3	9	6.6
Tower Prospect							*Lucky Strike Deposit*						
GS-22-047	BJ-012	18.0	Pyrite	1	1	8.0	GS-22-170	H-2889	24.7	Pyrite	1	1	5.8
			Pyrite	1	2	8.5				Pyrite	1	2	6.0
			Pyrite	1	3	9.3				Pyrite	1	3	5.4
			Pyrite	2	4	7.3				Pyrite	2	4	21.6
			Pyrite	2	5	8.4				Pyrite	3	5	22.9
			Pyrite	3	6	-10.2				Pyrite	3	6	20.0
										Pyrite	3	7	19.3
										Chalcopyrite	4	8	6.3
										Chalcopyrite	4	9	4.4

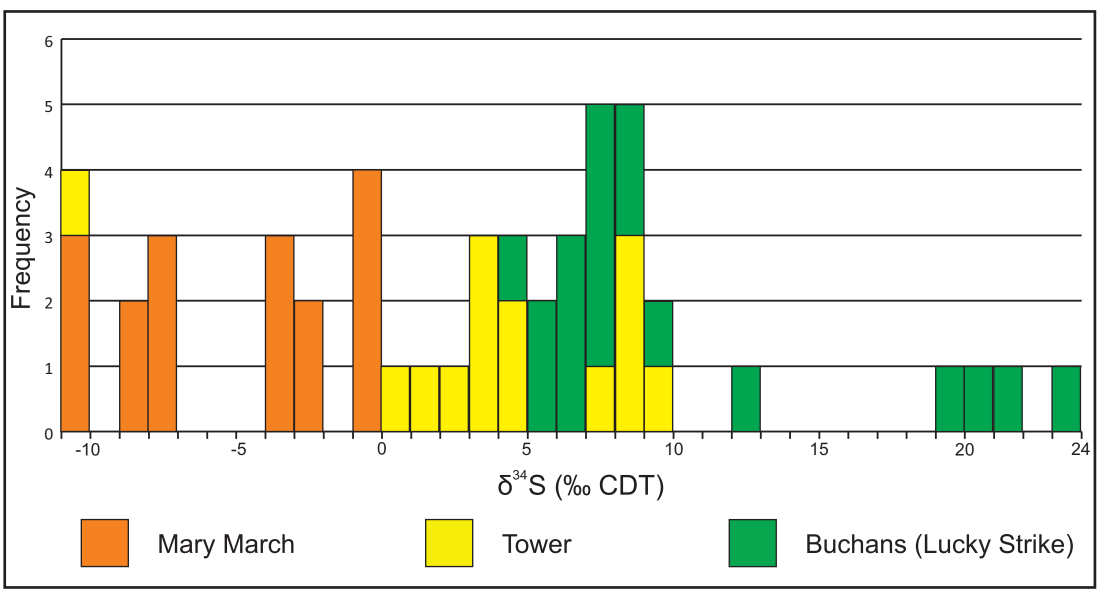

Figure 53. *Histogram summarizing the $\delta^{34}S$ values obtained from pyrite analysis from three areas within the southern Buchans–Roberts Arm Belt.*

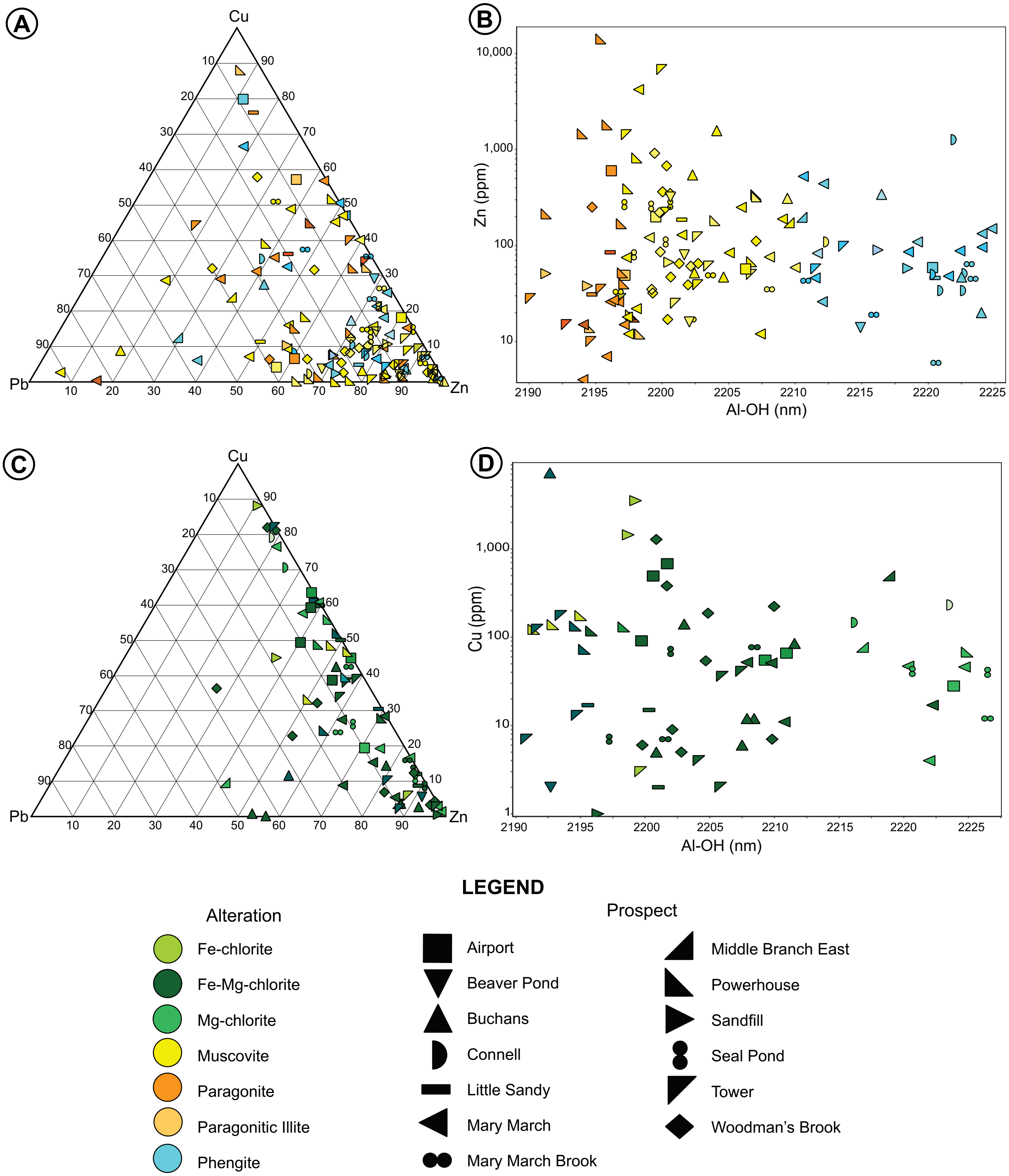

Figure 54. *A) Ternary plot outlining the Pb–Cu–Zn content of samples dominated by white mica alteration sampled for geochemical analysis; B) Discrimination diagram of the Al-OH wavelength feature* vs. *zinc concentration; C) Ternary plot outlining the Pb–Cu–Zn content of samples dominated by chlorite alteration sampled for geochemical analysis; D) Discrimination diagram of the Al-OH wavelength feature* vs. *copper concentration.*

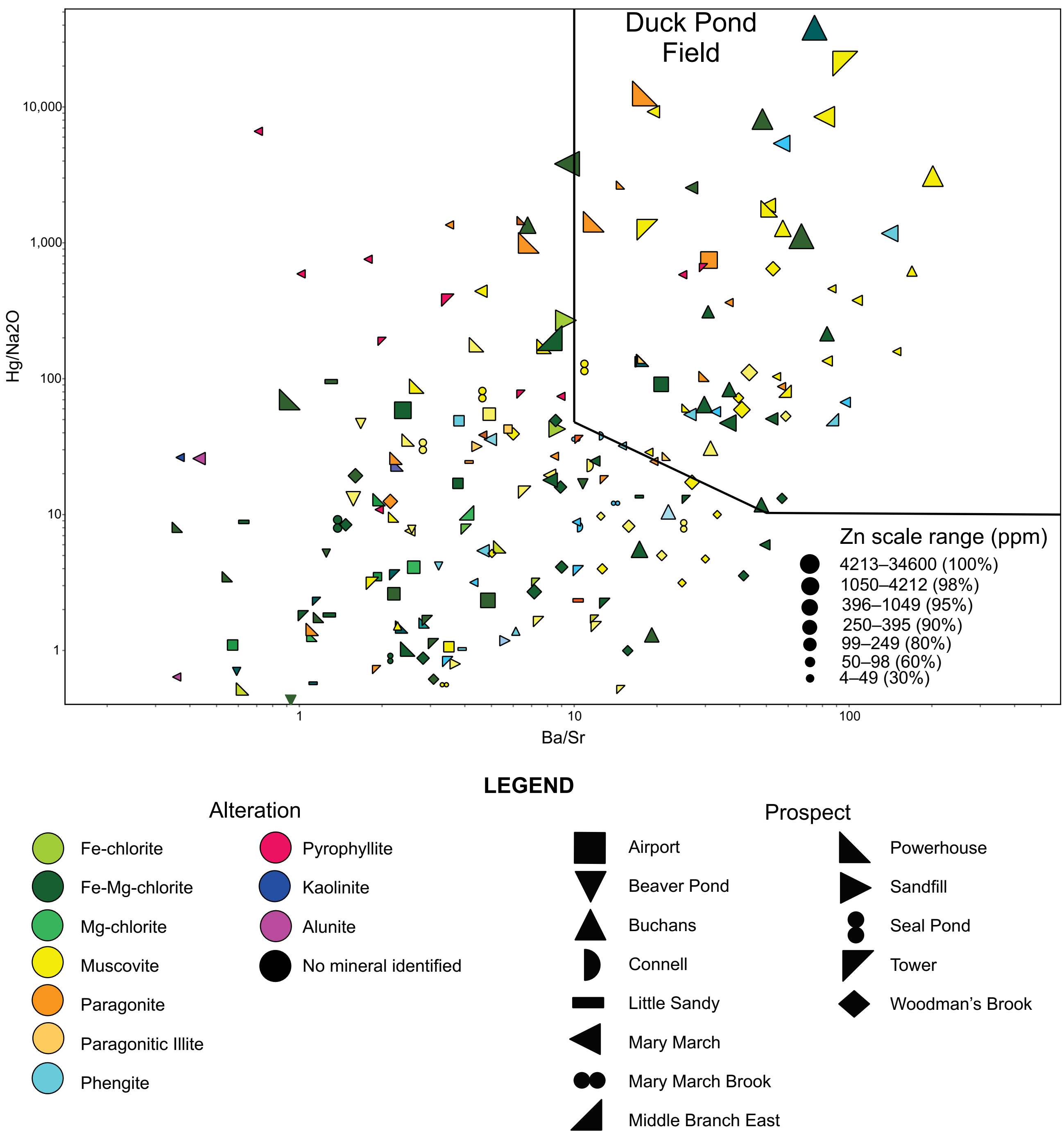

Figure 55. *Duck Pond alteration index discrimination diagram (Collins, 1989) for all samples, colour coded to the predominant alteration phase as determined by SWIR analysis and sized based on zinc content.*

data highlight prospects such as the Powerhouse and Tower, where the alteration and geochemical signatures of potential VMS mineralization are present, but no mineralization has yet been identified.

BUCHANS AREA (LUCKY STRIKE/ ROTHERMERE DEPOSITS)

In the vicinity of the main Buchans deposits, SWIR data highlight the alteration signature associated with the development of VMS at the ore horizon. Within the footwall zone of the Lucky Strike deposit, rocks are dominated by muscovitic illite and lesser montmorillonite and Fe–Mg-chlorite alteration. The development of this alteration is best illustrated by the Al-OH spectral wavelength feature, with intact sequences displaying a systematic shift toward shorter spectral wavelengths with decreasing distance from mineralization. Within areas of *in situ* massive sulphide, significant alteration is observed within the immediately underlying footwall rocks, locally extending for up to 70 m beneath the base of the mineralization. Distal from the mineralized zone, similar rocks to those immediately adjacent to the mineralization are characterized by phengite and phengitic illite white mica signatures and longer (~2220 nm) Al-OH spectral wavelength features.

Similar features are observed in association with the proximal transported ore of the nearby Rothermere deposit (Figure 56). However, with this style of mineralization, the rock unit hosting the ore clasts overlie relatively unaltered rocks, but still displaying lower Al-OH spectral wavelength features proximal to mineralization, and thus the overall footprint of the related alteration is restricted to the mineralized debris flows and the immediate adjacent rocks. Such a relationship with the hanging-wall rocks would imply that the deposition of the ore horizon and the immediately overlying rocks is contemporaneous.

The two main rock compositions forming the footwall to mineralization in the Buchans area are rhyolite (rhyolite 4) and basalt (basalt 3; Allen and Schofield, 2023). These rock units represent the two main lithologies sampled for geochemical analysis (Figure 34), with samples displaying variable chlorite–white mica alteration. These altered samples display anomalous alteration indices, such as the AAAI (Williams and Davidson, 2004), Ishikawa alteration index (AI; Ishikawa *et al.*, 1976), chlorite-carbonate-pyrite index (CCPI; Large *et al.*, 2001) and the Duck Pond index (Collins, 1989; Figures 35A, 36A and 38A). These various indices highlight both white mica and chlorite altered samples as being geochemically anomalous, supporting the SWIR results.

The $\delta^{34}S$ sulphur isotope values obtained from two separate samples ranged from 5 to 8 per mil (Figure 53). These values correspond to similar values reported by Kowalik *et al.* (1981) from analyses of seventeen separate samples of pyrite from both the Lucky Strike massive sulphide ore and the underlying stockwork zone that ranged from 6.4 to 8.7 per mil. This range in values are typical of those reported for other examples of VMS mineralization in the region (*e.g.*, Brueckner *et al.*, 2015). However, even though the presence of features such as locally bladed barite within the footwall zone of the Lucky Strike deposit, which may imply that VMS mineralization potentially formed within a transitional VMS to epithermal environment (*e.g.*, van Hees, 2011), no supporting sulphur isotope values for a potential magmatic contribution to the hydrothermal fluids related to mineralization have yet been identified. Despite this, the associated precious-metal (Au–Ag) enrichment, along with other epithermal suite elements such as Bi (up to 837 ppm), Mo (up to 655 ppm), Sb (up to 1043 ppm) and Te (up to 31 ppm; Zagorevski and Rogers, 2011), are supportive of a magmatic contribution to the overall hydrothermal system.

AIRPORT

Limited spectral work was conducted at this prospect, however the recognition of hydrothermal alteration like that observed proximal to the main Buchans deposits illustrate that the area is prospective for the development of VMS mineralization. A more thorough evaluation of the drillcore from the area, with the aid of SWIR, may provide a better picture with regards to the development and distribution of the hydrothermal alteration, and could potentially provide vectors towards areas of more intense hydrothermal fluid flow. The most prospective alteration was detected in DDH H-0258 from the Airport South prospect (Figure 6), but this drillhole was only investigated through select hand samples and thus represents a priority target for additional follow-up work. The geochemistry for these samples also supports their anomalous characteristics, displaying elevated AAAI and AI indices, in addition to one of the two samples plotting within the prospective Duck Pond field (Figures 35B, 36B and 38B). The other sample plotting with the Duck Pond field represents a sample collected proximal to a small semi-massive band of pyrite within the host mafic volcanic rocks and displays the most pronounced sodium depletion observed in the area (DDH H-2845, 270 m depth; Figure 6).

Detailed analysis of the host rocks and their relationship to the development of the alteration is outside the scope of this study. However, preliminary analysis highlights geochemical similarities of the intermediate volcanic rocks occurring within the hanging wall of the Airport Thrust Fault with those of the Woodman's Brook prospect. It remains unclear as to whether the host rocks are indeed related to the regional Lundberg Hill Formation as suggested by Allen and Schofield (2023), but if that interpretation is correct, the

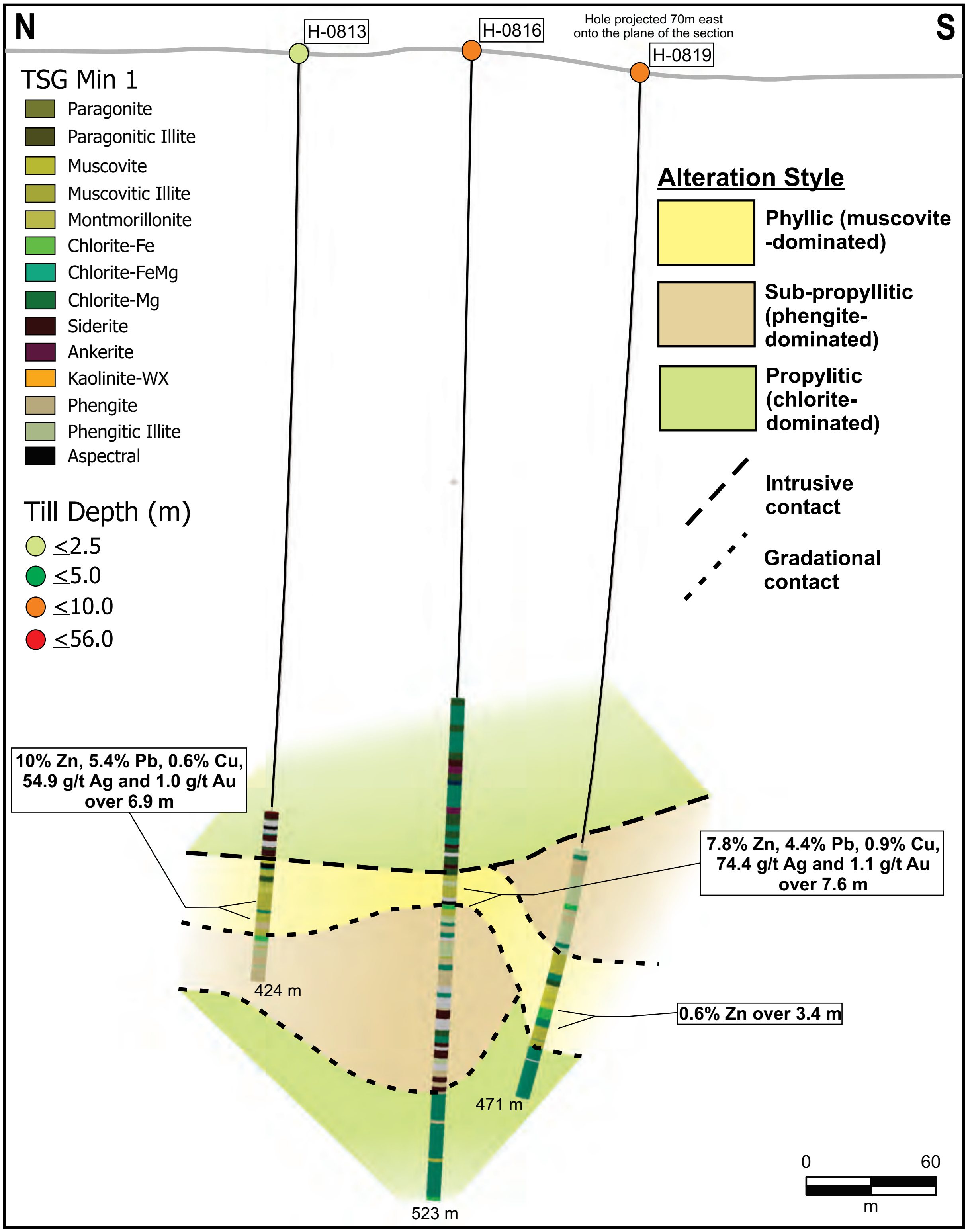

Figure 56. *Schematic north–south section of the Rothermere deposit illustrating the distribution of muscovite-dominated white mica alteration in association with the mineralized horizon hosting transported ore. Felsic to intermediate rocks immediately underlying and marginal to the ore horizon display background phengite and phengitic illite-dominated white mica alteration, while mafic volcanic and intrusive rocks display chlorite-dominated spectral signatures. Assay data compiled from historical ASARCO drill logs.* See *Plate 1 for the location of the drillholes shown in the cross-section.*

observed alteration and related mineralization could represent footwall-related alteration features potentially related to the nearby *in situ* Oriental or Lucky Strike deposits. If the current structural interpretation for this prospect is correct, then it represents one of the rare examples of alteration and related mineralization developed within the hanging wall of the Airport Thrust Fault, thus highlighting the potential of the hanging-wall rocks for hosting additional mineralization.

Weakly developed zones of white mica alteration are also observed within the structural hanging-wall sequence where it displays a spatial association with the development of stockwork-style mineralization, like that observed at the Airport prospect. Likewise, the occurrence of mineralization farther to the east at the Woodman's Brook prospect further highlights the potential for VMS mineralization within the hanging-wall rocks of the Airport Thrust Fault.

SANDFILL/MIDDLE BRANCH

The main host to mineralization in the area of the Sandfill and Middle Branch prospects is the Buchans River Formation, occurring as mineralized clasts and representing transported ore. However, in contrast to the vent proximal environment of the Rothermere deposit, the rocks hosting mineralization in this area are characterized by a phengitic white mica signature, which is inferred to support its deposition distal from the hydrothermal vent (Figure 57). The presence of weakly developed phyllic alteration within the felsic volcanic rocks of the Buchans River Formation in drillhole H-1910, represents a SWIR anomaly. This alteration is visually not as intense as that observed elsewhere in the region, but given the limited examination of the area, other drillholes nearby should be investigated with SWIR spectrometry to better define the extent of this anomalous alteration; this alteration was not sampled for geochemical analysis as part of this study.

POWERHOUSE

The Powerhouse prospect represents the eastern extent of volcanic rocks correlated with the Buchans River Formation. In this area, thick intervals of altered felsic volcanic rocks, analogous to those observed farther to the west at the Clementine deposit, have been intersected in drillcore (*cf.* Calhoun and Hutchinson, 1981; Figures 58 and 59). The felsic volcanic rocks of the Powerhouse prospect locally display thick intervals of paragonitic illite–montmorillonite alteration, which has been demonstration elsewhere in the region to represent a footwall signature to VMS mineralization (Sparkes and Hinchey, 2023). This argillic alteration is associated with mercury enrichment, which is also noted in association with other potential examples of hybrid bimodal–felsic VMS systems in the area (*e.g.*, Tower, Mary March prospects). The local development of anomalous zinc enrichment over significant widths (*e.g.*, 0.1 % over 17.4 m, DDH

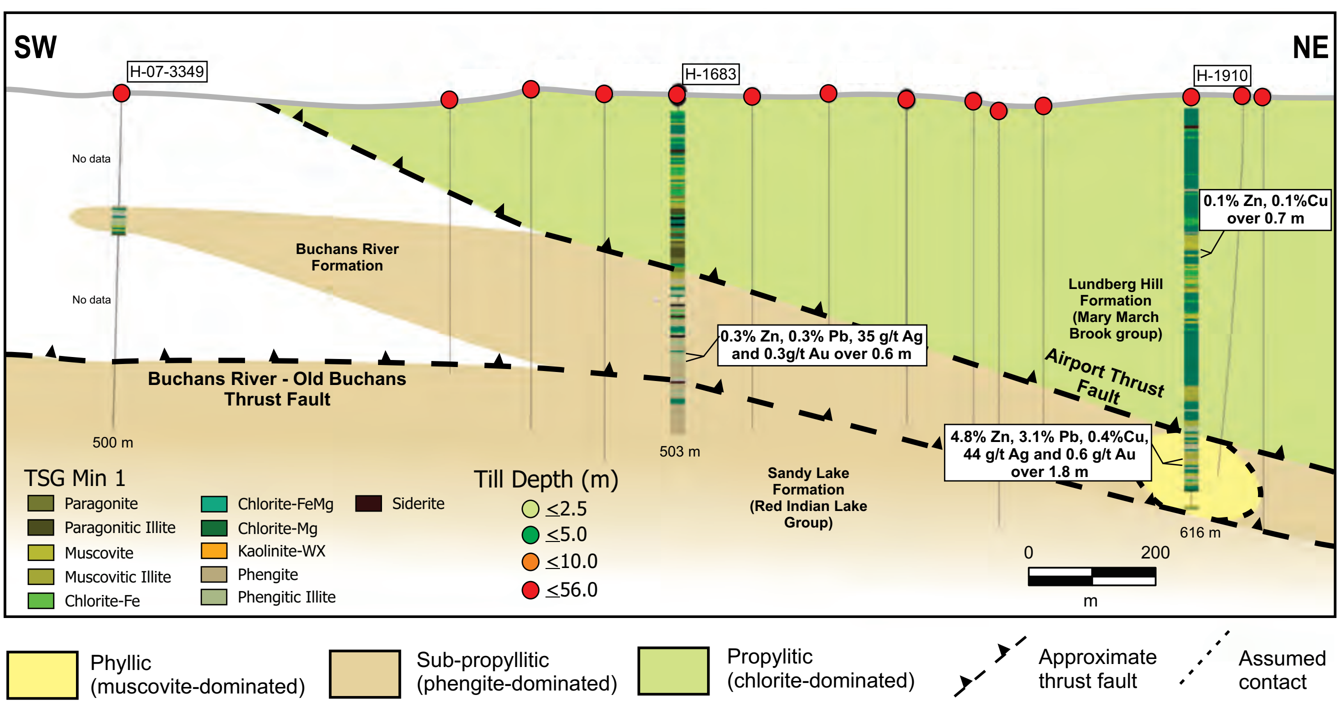

Figure 57. *Schematic northeast–southwest section of the Sandfill/Middle Branch prospects illustrating the distribution of phengite-dominated white mica alteration in association with the mineralized clast-bearing footwall rocks structurally underlying the Airport Thrust Fault.* See *Figure 6 for the location of the drillholes shown in the cross-section. Assay data compiled from Harris* et al. *(1997), historical ASARCO drill logs, and this study.*

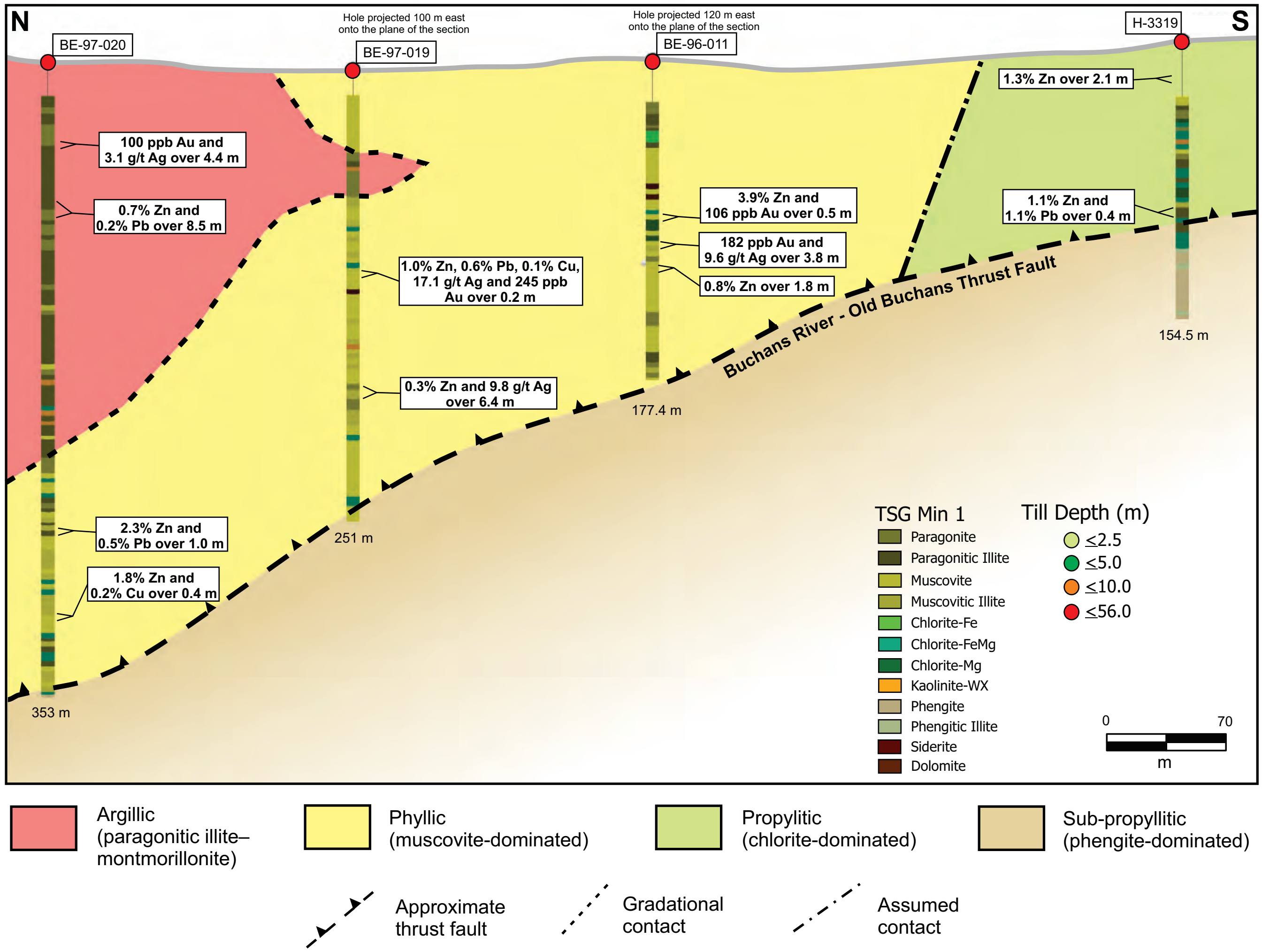

Figure 58. *Schematic north–south section of the Powerhouse prospects illustrating the distribution of phyllic and argillic alteration in association with mineralized drillhole intersections.* See *Figure 10 for the location of the drillholes shown in the cross-section. Assay data compiled from Thurlow and Barbour (1986) and Saunders* et al. *(1996, 1998, 2000d).*

BE-99-04-001; Saunders *et al.*, 1996) is also supportive of a footwall environment to VMS mineralization.

The current limits of drilling within the Powerhouse prospect have delineated a significant alteration zone, locally hosting stringer and disseminated sulphide mineralization that remains open both down dip to the north-northeast and along strike to the southeast. This zone of hydrothermal alteration is locally masked by rocks of the structurally overlying Lundberg Hill Formation (Figure 59). No drilling has been conducted to the northeast of BE-97-020 (Figure 10), which intersects some of the thickest (up to 350 m), intensely altered, felsic volcanic rocks of the Buchans River Formation that were observed during this study. Therefore, prospective, stratigraphically higher levels of this area remain untested. In addition, much of the drilling conducted to the east of BE-97-020 remained in mafic to intermediate volcanic rocks correlated with the hanging-wall sequence of Airport Thrust Fault and thus failed to fully test the eastern extent of the Powerhouse alteration zone. Recent investigations of this eastern area have highlighted anomalous soil samples producing results of up to 0.1% Zn, 0.3% Pb and 0.04% Cu (Moore and Butler, 2019).

The felsic volcanic rocks from this area overlap the field of rhyolite 1 of Allen *et al.* (2024 and references therein), but elsewhere in the Buchans area this unit largely postdates hydrothermal alteration, aside from the area around the Clementine prospect farther west. These altered felsic volcanic rocks display many of the geochemical characteristics observed in the Buchans area, including anomalous AAAI, AI and Duck Pond indices along with localized sodium depletion (Figures 35E, 36E and 38E). Similar hydrothermal alteration displaying anomalous geochemistry re-occurs some

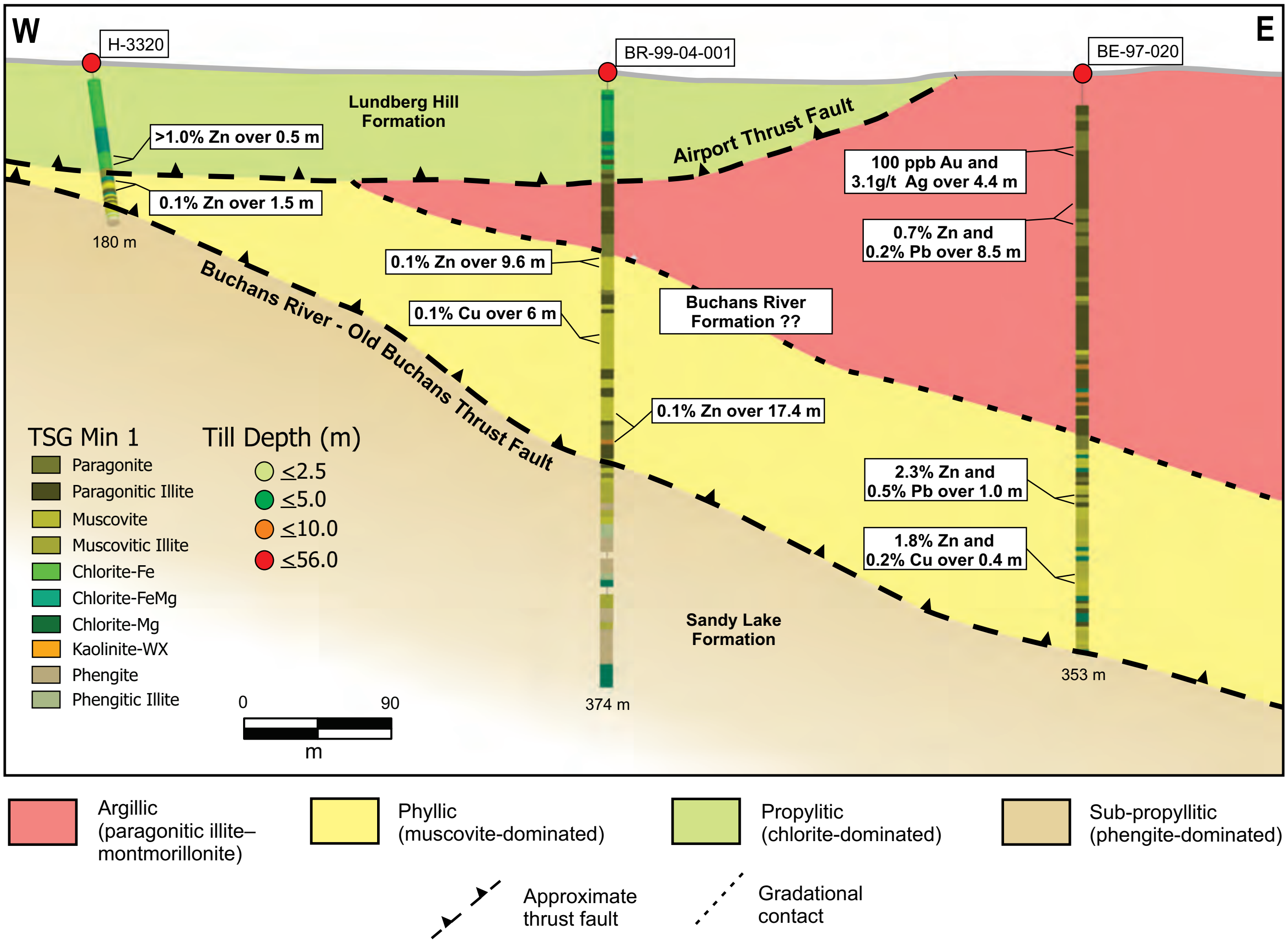

Figure 59. *Schematic east–west section of the Powerhouse prospects illustrating the distribution of phyllic and argillic alteration in association with mineralized drillhole intersections.* See *Figure 10 for the location of the drillholes shown in the cross-section. Assay data compiled from Thurlow and Barbour (1986), Harris* et al. *(1999), and Saunders* et al. *(1998, 2000d).*

seven kilometres to the east in the area of the Tower prospect, with few diamond drillholes occurring within this intervening area, representing another prospective region for additional follow-up.

MIDDLE BRANCH EAST

The Middle Branch East prospect represents a unique area, as it is the only known occurrence of rocks inferred to be correlative with the Buchans River Formation within the hanging wall of the Airport Thrust Fault. These rocks host mineralized clasts, resembling similar examples of transported ore within the region, and represent a prospective area for further mineral exploration as the distribution of the host unit is poorly defined. Similar to the Sandfill prospect, this transported ore is not associated with any significant hydrothermal alteration.

In addition to the base-metal enrichment, the inferred structural zone separating the rocks of the Buchans River Formation from the underlying rocks tentatively correlative with the Lundberg Hill formation, is associated with anomalous gold enrichment and phengitic white mica alteration (Figure 14). This rare example of presumed structurally controlled mineralization is unique to the Middle Branch East prospect and requires further SWIR analyses to establish the full extent of this zone within other drillholes in the area. The two samples plotting within the Duck Pond field in Figure 38D, are representative of this alteration zone, although the related mineralization and alteration are not inferred to be related to the development of VMS-style mineralization.

WOODMAN'S BROOK

The area of the Woodman's Brook prospect represents the most northeastern occurrence of white mica alteration associated with base-metal enrichment. The prospect is hosted within the mafic to intermediate volcanic rocks of the hanging-wall sequence to the Airport Thrust Fault. Elsewhere to the west, these rocks have been correlated with the Lundberg Hill Formation (Allen *et al.*, 2024 and references therein). Below the altered intermediate volcanic rocks hosting the variably developed white mica alteration (Figure 15), there is a marked decrease in base-metal enrichment upon transitioning into the underlying, chlorite-dominated, mafic volcanic and related volcaniclastic rocks. These rocks are characterized by an overall shift to longer wavelength Al-OH values (from ~2198 to ~2207 nm), associated with the muscovite alteration, relative to the overlying intermediate volcanic sequence. This drillhole (BJ-046, Figure 15) is not interpreted to have reached the Airport Thrust Fault, but the fault was intersected in a drillhole 1 km to the west (DDH BJ-044; Figure 10), at a depth of 454 m.

The intermediate rocks of the Woodman's Brook prospect display geochemical similarities to the rocks occurring above the Airport Thrust Fault at the Airport prospect. These rocks display anomalous AAAI, AI and CCPI alteration indices, with several of the muscovite altered samples plotting within the Duck Pond field (Figures 42A, 43A and 45A).

TOWER

The Tower prospect represents the only other alteration zone, in addition to the Mary March prospect, known to contain advanced argillic alteration assemblages. SWIR data highlights an alteration trend that can be traced intermittently over a 6-km strike length. This trend is associated with numerous surficial geochemical anomalies, which historically have been attributed to the transportation of ore along the now abandoned railway (*cf.* Squires, 1994a). However, based on the SWIR results, an area of hydrothermal alteration is now defined, in-part, parallel with the railway. This alteration zone corresponds with an airborne time domain electromagnetic anomaly (*cf.* Seymour, 2017), which continues to the west, beyond the current limits of diamond drilling towards the area of the Powerhouse prospect. A schematic cross section of the area highlights the spatial association of the argillic to advanced argillic hydrothermal alteration with the regional trace of the Airport Fault (Figure 60). The combination of the alteration signatures indicative of footwall alteration to possible VMS-style mineralization, as observed elsewhere in the region (*cf.* Sparkes and Hinchey, 2023), in addition to the spatial correlation of this alteration zone with surficial geochemical and airborne geophysical anomalies, highlights the underexplored potential of this area.

Altered felsic volcanic rocks hosting the development of the advanced argillic alteration correlate with rhyolite 1 of Allen *et al.* (2024 and references therein) and display geochemical similarities to the altered felsic volcanic rocks of the Powerhouse prospect. The intermediate volcanic rocks from the area display geochemical similarities to those from the Woodman's Brook prospect, although the exact relationship between the felsic and intermediate volcanic rocks was not observed. Felsic dykes, of similar composition, are observed crosscutting the intermediate volcanic rocks. Samples of the advanced argillic alteration display the highest AAAI values, which is accompanied by locally significant sodium-depletion. Most of the samples of advanced argillic alteration plot outside of the Duck Pond field in Figure 45B, however two muscovite-bearing samples, one from the central and one from the eastern portion of the alteration zone plot within the prospective field. The advanced argillic alteration is otherwise devoid of base- or precious-metal enrichment, but it's development points to a potential vent proximal environment that is prospective for hybrid bimodal–felsic style VMS mineralization like that developed at the Mary March prospect. A felsic dyke crosscutting the eastern portion of the advanced argillic alteration zone provides a minimum age limit of 467.51 ± 0.44 Ma, indicating the alteration could be coeval with the *ca.* 470 Ma Buchans Group farther to the west (Sparkes and Hamilton, 2024).

The $\delta^{34}S$ sulphur isotope values obtained from this area display two distinct populations. Those from the western portion of the alteration zone, ranging from 7.3 to 9.3 per mil, are like those reported from the main Buchans area. However, those from the eastern portion of the zone, which display an intimate association with the development of advanced argillic alteration have values ranging from 0.8 to 4.7 per mil, with an average of 3.0, in association with the "spongey" pyrite phase. These values are distinctly lower than those obtained from the western portion of the alteration zone and overlap the range of igneous sulphur (-5 to 5 per mil) outlined by Hoefs (2009). These values, combined with the development of advanced argillic alteration, are supportive of a magmatic contribution to the hydrothermal fluids associated with the development of the Tower alteration zone.

LITTLE SANDY

Mineralization developed within the area of the Little Sandy prospect is unique, as it represents an example of mafic-hosted, copper-dominated, mineralization that is associated with Fe-chlorite alteration. This area is associated with an extensive IP geophysical anomaly, which has received minimal drill testing outside of the immediate area of the Little Sandy prospect. The IP anomaly remains open to the northeast and is coincident with basal-till zinc anomalies. One drillhole has tested this anomaly and locally intersected 1.0% Zn, 0.3% Cu and 1.0 g/t Ag over 0.5 m (Saunders, 2000b; Seymour *et al.*, 2015).

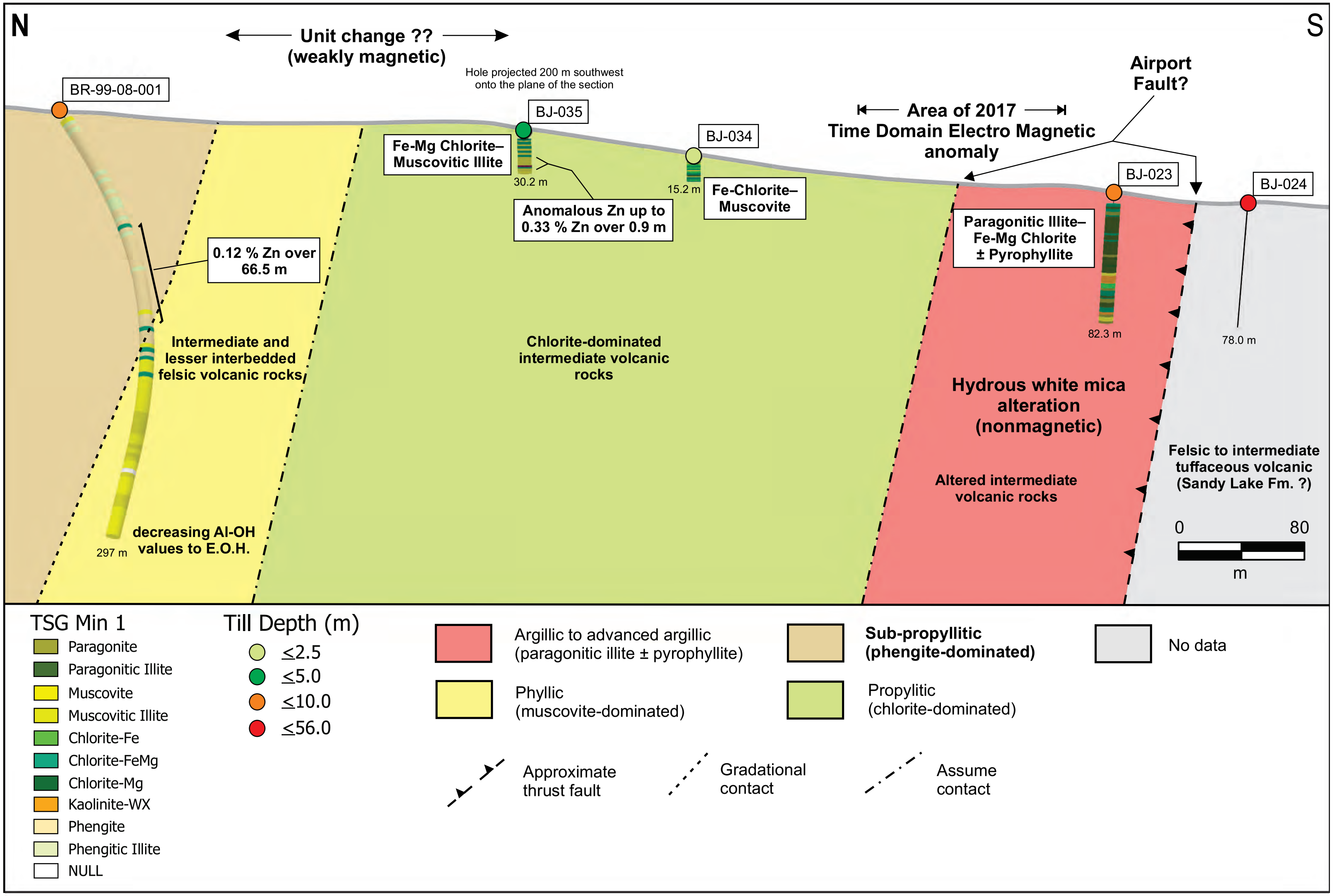

Figure 60. *Schematic north–south section of the Tower prospects illustrating the distribution of phyllic and argillic alteration in association with mineralized drillhole intersections.* See *Figure 16 for the location of the drillholes shown in the cross-section. Assay data compiled from Thurlow* et al. *(1987) and Saunders* et al. *(2000b).*

Early (*ca.* 1970s) drilling intersected a significant zone of white mica dominated alteration approximately 1 km to the west of the Little Sandy prospect. This alteration is visually similar to that observed in drillcore from the eastern end of the Tower prospect, as well as in outcrop in the area of the Little Sandy River and may represent the along-strike extension of this alteration zone. This trend corresponds with an airborne time-domain electromagnetic anomaly, which could be highlighting the clay alteration developed in the area. Limited observations from drillcore suggest that localized thrusting is developed within the area, highlighted by the structural juxtaposition of altered intermediate volcanic rocks and relatively unaltered mafic volcanic rocks. The zones of white mica-dominated alteration are magnetite destructive, and the magnetic susceptibility of the alteration contrasts that of the surrounding intermediate to mafic volcanic rocks. A detailed magnetic survey of the area could potentially better define these zones of alteration and aid in the recognition of thrust structures, allowing for more targeted exploration of prospective thrust panels in the area.

Spectral analysis is less applicable in this area, given the predominance of chlorite alteration in association with the development of the stockwork-style mineralization. Geochemistry from the area highlights similarities with the Tower prospect, displaying similar felsic volcanic rocks overlapping the rhyolite 1 field and mafic volcanic samples overlapping the basalt 3 field in Figure 41C. Chlorite altered samples are associated with high AI and CCPI values, but only weak to moderate sodium depletion, and none of the samples from the area plot within the Duck Pond field (Figure 45C).

SEAL POND

The Seal Pond prospect occurs within an area of poor outcrop exposure and thus the delineation of the alteration zone is largely based on diamond drilling, of which only limited sampling was conducted. The volcanic rocks hosting the alteration are geochemically similar to those of the Little Sandy prospect, however the alteration observed at the Seal Pond prospect is more white mica dominated. This white mica alteration displays similar relationships to that observed in association with the development of VMS-style mineralization elsewhere in the region, such as the systematic shift of the Al-OH spectral feature to lower spectral wavelengths proximal to mineralized zones. Only one drillhole was examined in its entirety with SWIR analyses from the Seal Pond prospect, however the local mention of pyrophyllite-style alteration in industry drill logs highlight potential holes for additional follow-up (*e.g.*, DDH SP-06-016; *cf.* Chislett and Wilton, 2006). Geochemically, the area is dominated by mafic to intermediate volcanic rocks with variable white mica- and chlorite-dominated alteration. However, limited sampling of the local area did not identify any geochemically anomalous alteration indices, aside from one sample that falls within the Duck Pond field in Figure 45D. Anomalous samples plotting within the Duck Pond field have been reported from more detailed sampling of DDH SP-95-001 by Squires (1996), and a review of core from the area located previously unsampled sulphide mineralization (*e.g.*, Seymour *et al.*, 2015). Additional insights could be gained through more systematic geochemical sampling of drillholes across the known distribution of the alteration zone.

BEAVER POND

The Beaver Pond prospect locally hosts anomalous base- and precious-metal mineralization and represents a zone of hydrothermal alteration developed along trend from the Mary March prospect. However, based on current geological maps of the area, these two prospects are hosted by two distinct geological units, namely the Mary March Brook and Red Indian Lake groups (Figure 1). Limited geochemical sampling of the felsic volcanic rocks from these two areas highlights potential similarities, as both overlap the fields of rhyolite 4 in Figures 41E and 48C, respectively. In addition, the development of anomalous gold–silver mineralization in association with the hydrothermal alteration is unique to only a few areas in the region. However, further work is required to test such potential correlations between these two prospects. Within the intervening area between these two prospects there exists zinc–lead–copper soil anomalies that have yet to be fully investigated (*e.g.*, Woods, 1988). This anomalous zone represents the most significant anomaly between the Mary March and Beaver Pond prospects and is coincident with a magnetic low in airborne surveys, potentially highlighting a zone of hydrothermal alteration.

The single drillhole that was evaluated from the prospect is moderately to strongly altered throughout, with localized Fe–Mg chlorite–paragonite alteration associated with mineralization, along with locally developed narrow (<1 m) intervals of hydrothermal brecciation. This drillhole (DDH BJ-083) collars directly into alteration, which extends to the end of the drillhole, highlighting an extensive zone of hydrothermal alteration that has yet to be fully defined, and has only been sampled intermittently. The limited sampling conducted as part of this study failed to identify any samples displaying anomalous alteration indices, but weakly anomalous values of gold, silver and mercury were detected in muscovite altered samples.

MARY MARCH BROOK

Despite the overall lack of noteworthy hydrothermal alteration, the local presence of unsourced mineralized boulders at surface highlights the potential of this area. The occurrence of anomalous base-metal values in soil samples to the southwest suggests that the intervening area between the Beaver Pond and Mary March Brook prospects in the north and the Mary March prospect in the south remains a prospective target for future mineral exploration, containing several untested geochemical and geophysical anomalies (*e.g.*, Woods, 1988; Rice *et al.*, 2000). The geochemical sampling conducted as part of this study failed to identify any samples displaying anomalous alteration indices.

CONNELL

The alteration developed at this prospect is indicative of a distal signature relative to that expected to be developed proximal to a hydrothermal vent. However, the presence of exhalative-style VMS mineralization highlights the overall prospectivity of the host stratigraphy. Samples from the area that display anomalous alteration indices such as the AAAI and CCPI come from samples of chert and are not representative of hydrothermally altered material. However, one sample from an interbedded felsic volcanic rock displaying phengite white mica alteration did contain anomalous values of zinc, lead and copper.

The presence of an untested zinc in soil anomaly along strike to the southwest (*e.g.*, Connell West, Squires *et al.*, 1992) that remains open and contains values that are equal to, or greater than, the concentrations identified over the main Connel prospect highlight the underexplored nature of this area. This anomaly corresponds with a localized EM anomaly, and because drilling in the area is limited to the main Connell prospect, the potential of the host stratigraphy along strike of known mineralization has yet to be fully evaluated.

MARY MARCH

The Mary March prospect represents the largest zone of advanced argillic alteration that was examined during this study, spanning more than two kilometres along strike through multiple drillhole intersections. This alteration zone was discussed by Sparkes and Hinchey (2023), where it was proposed to represent an example of a hybrid bimodal–felsic style VMS system (Galley *et al.*, 2007), similar to that proposed for examples of VMS mineralization in the Tulks Volcanic Belt by Hinchey (2011).

The SWIR analysis of drillcore, as well as surface outcrops, has identified alunite, pyrophyllite, dickite and kaolinite, which are diagnostic of advanced argillic alteration (Gifkins *et al.*, 2005). This zone of advanced argillic alteration transitions along strike and up-section from pyrophyllite, through paragonite and muscovite and then to phengite dominated alteration. The advanced argillic alteration, which is primarily developed along the Mary March ore horizon, is structurally repeated along the Nancy April thrust fault, and forms the Nancy April ore horizon (Figure 61). Alunite alteration appears to be confined to the southwestern portion of the Mary March horizon. These alteration zones are associated with distinct magnetic low anomalies in airborne surveys, with the southeasternmost anomaly, associated with the Mary March horizon, extending to the southwest beyond the current limits of diamond drilling.

Both alteration horizons are locally associated with the development of VMS-style mineralization, with the Mary March horizon returning the highest-grade intersection discovered in the southern BRAB outside of the main Buchans area. This VMS mineralization is locally accompanied by appreciable gold enrichment, assaying 12.2 g/t Au and 660 g/t Ag in association with 16.8% Zn, 3.5% Pb and 0.2% Cu over 0.9 m (Thurlow, 2001). Rare sulphide intersections within the Nancy April horizon have returned assays of up to 2.5% Cu, 0.1% Zn, 8.6 g/t Ag and 0.7 g/t Au over 2.3 m (Oosterman, 2015), within a mineralized zone that also contains elevated As (up to 1.1%), Bi (up to 48 ppm), Hg (6 ppm), Mo (up to 13 ppm), Sb (up to 95 ppm), Se (up to 216 ppm) and Te (up to 146 ppm).

The volcanic succession hosting the mineralization is primarily composed of locally pillowed mafic volcanic rocks and mafic to intermediate hyaloclastite breccia, with flow-banded rhyolite present within the footwall zone of the Mary March horizon. The emplacement of this rhyolite unit appears to be associated with the development of the advanced argillic alteration concentrated along its margin. The footwall rhyolite displays geochemical similarities to rhyolite 4 of Allen *et al.* (2024 and references therein), which is also the signature associated with the footwall to the main mineralization within the Buchans area. Samples of the hydrothermal alteration display anomalous alteration indices such as the AAAI, AI and CCPI (Figures 49C and 50C). In addition, samples from the area display the most significant sodium depletion noted outside of the main Buchans area, and numerous samples plot within the prospective Duck Pond field (Figures 51C and 52C).

The $\delta^{34}S$ sulphur isotope values obtained from the area form two populations. The sample from the pyrophyllite alteration zone developed within the margin of the footwall rhyolite give $\delta^{34}S$ values ranging from -1.0 to -11.1 per mil, with an average of -8.0 per mil. In contrast, the sample from the Nancy April horizon, obtained from what is inferred to be exhalative-style massive sulphide mineralization, produced $\delta^{34}S$ values ranging from -0.6 to -3.9 per mil, with an average of -2.4 per mil. The values from the Nancy April horizon are somewhat similar to those of the Tower prospect, while the sample from the altered footwall rhyolite are extremely negative, well below the lower range of igneous sulphur (-5 to 5 per mil) outlined by Hoefs (2009). The association of these

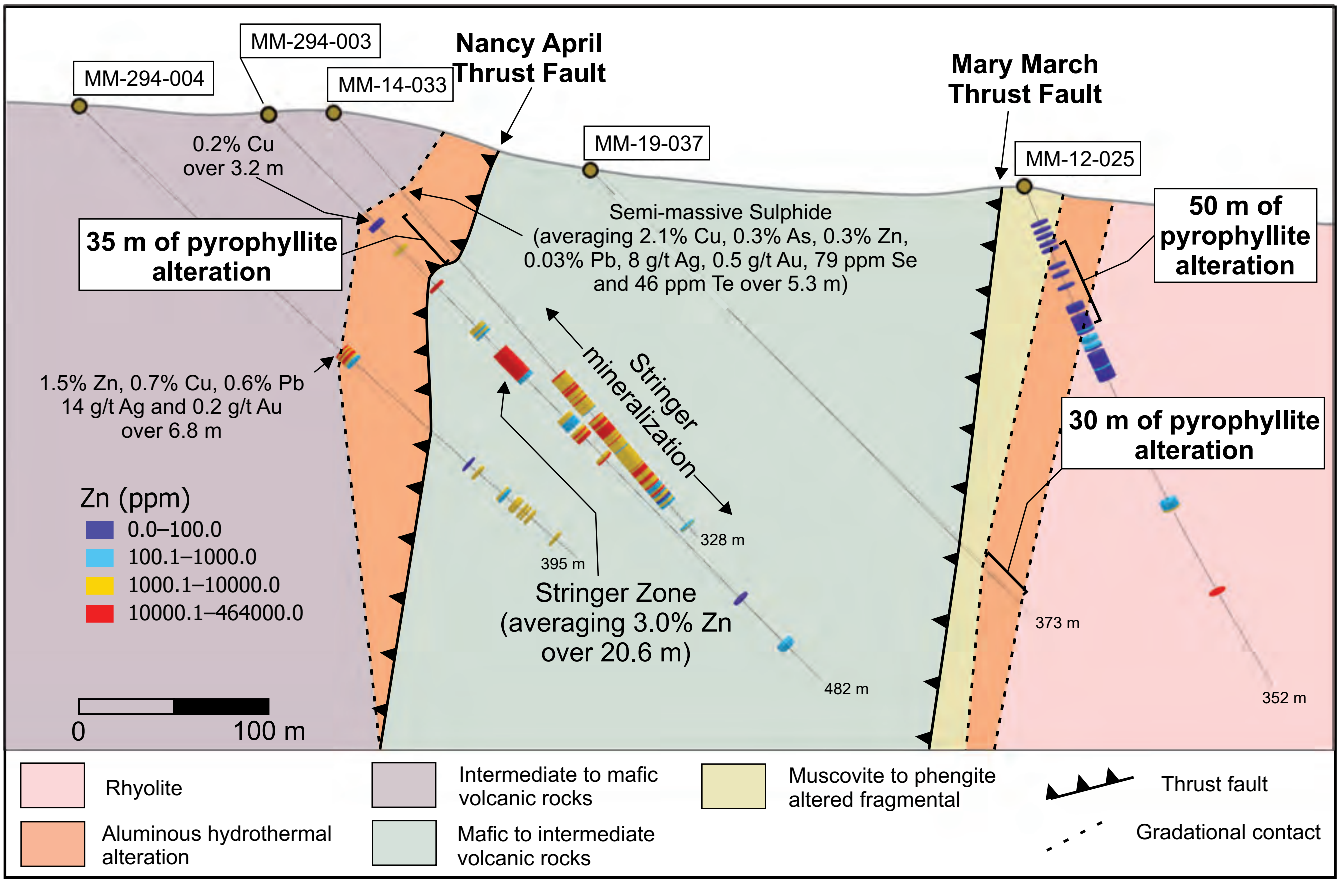

Figure 61. *Schematic northwest–southeast section of the Mary March prospects illustrating the distribution of advanced argillic alteration in association with mineralized drillhole intersections.* See *Figure 28 for the location of the drillholes shown in the cross-section. Assay data from Jagodits and Thurlow (2000), Green and Wolfson (2013) and Oosterman (2015).*

lower values with the development of advanced argillic alteration implies a potential magmatic component to the hydrothermal fluids associated with the alteration zone, like that noted at the Tower prospect. In addition, the enrichment in the epithermal suite of elements (As, Bi, Hg, Mo, Sb, Se and Te) is also supportive of a magmatic contribution to the hydrothermal fluid associated with the development of VMS-style mineralization.

CONCLUSION

The application of SWIR spectrometry in further subdividing zones of “sericite” alteration within the southern portion of the BRAB allows for the identification of more prospective areas of hydrothermal alteration and enables the comparison of the various alteration zones associated with the development of VMS-style mineralization in the region. These data, when combined with geochemical sampling constrained by the SWIR results, provide a database that permits the characterization and ranking of these hydrothermal alteration zones.

The collection of SWIR data has led to the recognition of potential hybrid bimodal–felsic styles of VMS mineralization which represents a new deposit model for the region (*e.g.*, Sparkes and Hinchey, 2023). The development of advanced argillic alteration in association with VMS mineralization is somewhat unique. Based on current mapping of the southern BRAB, this style of alteration occurs within both the Mary March Brook (Tower prospect), and the Red Indian Lake (Mary March prospect) groups. However, as noted above, the Tower prospect shares several commonalities with the Powerhouse prospect and may represent the eastern extension of rocks associated with the Buchans River Formation. Geochemical sampling of units hosting the argillic to advanced argillic alteration supports a potential correlation. Altered felsic volcanic rocks from both the Powerhouse and Tower prospect plot within the tholeiitic and rhyolite 1 fields (Figures 32E, 33E, 34E, 39B, 40B and 41B), while the felsic volcanic rocks that are footwall to VMS mineralization at both the Buchans deposits and the Mary March prospect are both transitional to calc-alkaline and plot within rhyolite 4 field (Figures 32A, 33A, 34A, 46C, 47C and 48C). Rocks of the Buchans River Formation represent the main host to the development of VMS mineralization and related hydrothermal alteration within the Buchans camp. Similar styles of alteration and VMS mineralization at the Tower and Mary March prospects highlight several commonalities with the Buchans camp and suggest potential correlations. However, such an inference requires further detailed stratigraphic studies, supported by geochemical and geochronological analyses, to test for potential stratigraphic correlations between these areas.

The successful application of SWIR spectrometry in evaluating alteration zones of the southern BRAB highlights the usefulness of this technique in providing real-time data that aids in vectoring towards prospective horizons within the volcanic stratigraphy. This study represents an initial first pass and was broad in scope. Future work should be directed toward more detailed investigations of areas displaying anomalous alteration and geochemical signatures indicative of prospective mineralizing environments. In addition, the application of SWIR guided geochemical sampling to future drilling in the region would greatly benefit exploration efforts in recognizing drillholes that represent potentially "near-misses". The application of new techniques, such as SWIR, provides new avenues for evaluating areas with significant legacy data like the southern BRAB, which will hopefully lead to new discoveries in the region.

ACKNOWLEDGMENTS

During the course of this project, I have had the pleasure of working with several field assistants. I would like to thank Richard Smith, Emily Scott and Hailey Hunt-Alward for providing enthusiastic support and hard work both in the field and in the office. Cooperation from company personnel, Bob Patey (Canstar Resources Inc.), and Paul Moore, David Butler and Derrick Keats (Buchans Minerals; now Canterra Minerals Corp.) greatly benefited the authors understanding of the Mary March and Buchans areas. William Oldford is gratefully acknowledged for assistance in the Buchans core library. John Hinchey reviewed an early version of the manuscript, and his recommendations improved the content of this report.

REFERENCES

Allen, R. and Schofield, M.
2023: Volcanic facies, lithogeochemistry and vectors to ore at Buchans massive sulphide camp, Newfoundland. Stage 1 Final Report. Unpublished internal company report prepared for Buchans Minerals Resources.

Allen, R.L., Schofield, M. and Sparkes, G.W.
2024: Volcanic-facies mapping and related hydrothermal alteration studies of the Buchans Camp, southern Buchans–Roberts Arm Belt, central Newfoundland. *In* Current Research. Government of Newfoundland and Labrador, Department of Industry, Energy and Technology, Geological Survey, Report 24-1, pages 1-30.

Arseneau, V., Banville, R., Collins, C., Huard, A., Kendle, F., Lee, D., Perry, I. and Squires, G.
1995a: Assessment report on review and compilation for 1994 submission for the East Branch Project for fee simple grant volume 1 folio 61 in the Buchans Railbed and Buchans Highway areas, central Newfoundland. Newfoundland and Labrador Geological Survey, Assessment File 12A/15/0740, 18 pages.

1995b: Assessment report on diamond drilling exploration for 1994 submission for the Little Sandy Project for fee simple grant volume 1 folio 62 in the Red Indian Lake area, central Newfoundland. Newfoundland and Labrador Geological Survey, Assessment File 12A/15/0743, 45 pages.

AusSpec International Ltd.
2008: Spectral analysis guides for mineral exploration (GMEX): Practical applications handbook, 3rd edition.

Banville, R., Huard, A., Hussey, A., Sheppard, D., Woods, G., Ascough, G. and Betrand, M.
1998a: Assessment report on geological, geochemical, geophysical, trenching and diamond drilling exploration for 1996 submission for the Anglo-Newfoundland Development Company Limited Charter, fee simple grants volume 1 folio 61 and volume 2 folio 29, and Reid Lots 227-229, 231-232, 234-235 and 247 in the Victoria Lake-Red Indian Lake area, central Newfoundland, 15 reports. Newfoundland and Labrador Geological Survey, Assessment File 12A/0853, 1686 pages.

Banville, R., Huard, A., Sheppard, D., Woods, G., Drolet, B. and Bertrand, M.J.
1998b: Assessment report on geological, geochemical, geophysical and diamond drilling exploration for 1997 submission for the Anglo-Newfoundland Development Limited Charter, Reid Lots 227, 229, 234 and 247 and fee simple grants volume 1 folio 61 and volume 2 folio 29 in the Victoria Lake-Red Indian Lake areas, central Newfoundland, 10 reports. Newfoundland and Labrador Geological Survey, Assessment File 12A/1015, 786 pages.

Barbour, D.M.
1978: Report on compilation and re-examination of diamond drill core from the Little Sandy Brook area, central Newfoundland. Newfoundland and Labrador Geological Survey, Assessment File 12A/15/1394, 20 pages.

1983: Second year assessment report on geological, geophysical and geochemical surveys for licence 2329 on claim blocks 2227-2228 and 2548-2551 in the Buchans Junction area, Newfoundland. Newfoundland and Labrador Geological Survey, Assessment File 12A/0359, 57 pages.

1984: Third year assessment report on geological, geochemical and geophysical exploration for licence 2329 on claim blocks 2227-2228 and 2548-2551 and claims 14116-14121 and 14123-14147 in the Buchans Junction and Mary March River areas, Newfoundland. Newfoundland and Labrador Geological Survey, Assessment File 12A/0398, 39 pages.

1985: Assessment report on geophysical exploration and relogging of drill core for 1985 submission for crown lease 1 on lot A, crown lease 3 on lot E and crown lease 5 on lot J in the Buchans Junction area, Newfoundland. Newfoundland and Labrador Geological Survey, Assessment File 12A/0448, 14 pages.

Barbour, D.M., Desnoyers, D.W., Dunphy, B.A., Graves, R.M., Kieley, J.W., King, B.M., McKenzie, C.B., Poole, J.C. and Thurlow, J.G.
1991: Assessment report on geological, geochemical, geophysical, trenching and diamond drilling exploration for 1990 submission for the Anglo Newfoundland Development Company Limited Charter, crown lease lots A-B, E-F and P-R, fee simple grants volume 1 folios 43, 61-62 and 110, volume 2 folios 23 and 25, special volume 2 folio 307 and Reid Lots 227-228, 231-233 and 247 in the Buchans, Great Burnt Lake, Valentine Lake, Victoria Lake, Tulks River and Lloyds River areas, central Newfoundland, 6 reports. Newfoundland and Labrador Geological Survey, Assessment File 12A/0609, 2134 pages.

Barbour, D.M., Desnoyers, D.W., Graves, R.M., Kieley, J.W., King, B.M., McKenzie, C.B., Poole, J.C., Thurlow, J.G., Balch, S. and MacNeil, J.
1990: Assessment report on geological, geochemical, geophysical, trenching and diamond drilling exploration for the Victoria Lake project for 1989 submission for the Anglo-Newfoundland Development Company Limited charter, Reid lots 227-228, 231-233 and 247, fee simple grants volume 1, folios 43, 61 and 110 and volume 2 folios 23 and 29 and for crown lease lots A, B, E, J and N to R in the Buchans, Red Indian Lake, Valentine Lake, Jacks Pond and Daniels Pond areas, central Newfoundland, 5 reports. Newfoundland and Labrador Geological Survey, Assessment File NFLD/1970, 1260 pages.

Barbour, D.M., Desnoyers, D.W., Gubins, A., McKenzie, C.B., Thurlow, J.G., Woods, G., Wright, J.A. and Polzer, B.
1988: Assessment report on geological, geochemical, geophysical, trenching and diamond drilling exploration for 1987 submission for the Anglo Newfoundland Development Company Limited charter, crown lease lots A-B, E-F, J and N-R, fee simple grants volume 1 folios 43, 61-62 and 110, volume 2 folios 23, 25 and 29 special volume 2 folio 307 and Reid lots 227-229, 231-235 and 247 in the Buchans, Great Burnt Lake, Valentine Lake, Mary March, Victoria River and Sandy Lake areas, Newfoundland, 3 reports. Newfoundland and Labrador Geological Survey, Assessment File 12A/0504, 3376 pages.

Barbour, D.M., Desnoyers, D.W., McKenzie, C.B., Thurlow, J.G., Delaney, P., Churchill, R., Vatcher, S.V., Balch, S., Sinclair, I.G.L., Legault, J.M. and Konings, M.
1989: Assessment report on geological, geochemical, geophysical, trenching and diamond drilling exploration for 1988 submission for the Mary March and Victoria Lake projects on the Anglo Newfoundland Development Company Limited charter, Reid lots 228-229, 231-233 and 247, fee simple grants volume 1 folios 43, 61-62 and 110, volume 2 folios 23, 25 and 29, special volume 2 folio 307 and crown lease lots A, E-F and J in the Buchans, Red Indian Lake, Victoria Lake, Pats Pond and Jacks Pond areas, Newfoundland, 14 reports. Newfoundland and Labrador Geological Survey, Assessment File NFLD/1788, 1280 pages.

Barbour, D. and Thurlow, J.G.
1981: Exploration report for 1980 in the Anglo Newfoundland Development charter and associated Reid lots 228-233 and 247, Newfoundland. Newfoundland and Labrador Geological Survey, Assessment File NFLD/1242, 441 pages.

Brueckner, S.M., Piercey, S.J. Layne, G.D., Piercey, G. and Sylvester, P.J.
2015: Variations of sulphur isotope signatures in sulphides from the metamorphosed Ming Cu(–Au) volcanogenic massive sulphide deposit, Newfoundland Appalachians, Canada. Mineralium Deposita, Volume 50, pages 619-640.

Calhoun, T.A. and Hutchinson, R.W.
1981: Determination of flow direction and source of fragmental sulphides, Clementine deposit, Buchans, Newfoundland. *In* The Buchans Orebodies: Fifty Years of Mining and Exploration. *Edited by* E.A. Swanson, D.F. Strong and J.G. Thurlow. Geological Association of Canada, Special Paper 22, pages 187-204.

Chislett, A.
1997: Sixth year assessment report on diamond drilling and trenching exploration for licence 4325 on claim blocks 7245, 7515 and claims 15717-15718 in the Buchans Junction area, central Newfoundland. Newfoundland and Labrador Geological Survey, Assessment File 12A/16/0774, 20 pages.

2004: Assessment report on IP and gravity geophysical surveys conducted on 8th year claims 7418M, 7th year claims 7502M, 6th year claims 7503M, 2nd year claims 9283M, 2nd year claims 9402M, 1st year claims 9756M and 1st year claims 10285M at Buchans Junction, central Newfoundland Seal Pond and Lapland Pond Grids Buchans Junction Property. Newfoundland and Labrador Geological Survey, Assessment File 12A/1141, 157 pages.

2005: Tenth year assessment report on diamond drilling exploration for licence 7418M on claims in the Seal Pond area, near Buchans Junction, central Newfoundland. Newfoundland and Labrador Geological Survey, Assessment File 12A/1217, 26 pages.

2007: First year, third year and eleventh year supplementary report on geophysical and diamond drilling exploration for licences 7418M, 8756M and 12481M on claims in the Buchans Junction area, central Newfoundland, 2 reports. Newfoundland and Labrador Geological Survey, Assessment File 12A/1330, 44 pages.

Chislett, A., Delaney, P. and Burton, G.B.
2005: Third year and eighth year supplementary assessment report on diamond drilling exploration for licences 7502M, 9283M and 9402M on claims in the Buchans Junction area, central Newfoundland, 2 reports. Newfoundland and Labrador Geological Survey, Assessment File 12A/15/1174, 80 pages.

Chislett, A. and Graves, R.M.
2004: First and fourth year assessment report on geophysical and diamond drilling exploration for licences 7502M and 9618M-9619M on claims in the Buchans Junction area, central Newfoundland, 3 reports. Newfoundland and Labrador Geological Survey, Assessment File 12A/1140, 138 pages.

Chislett, A. and Wilton, D.
2006: Ninth year supplementary report on diamond drilling exploration for licence 11548M on claims in the Buchans Junction area, central Newfoundland. Newfoundland and Labrador Geological Survey, Assessment File 12A/15/1286, 37 pages.

Collins, C.J.
1989: Report on geochemical exploration in the Duck Pond-Tally Pond area, central Newfoundland. Noranda Exploration Company Limited, Newfoundland and Labrador Geological Survey, Assessment File 12A/1033, 87 pages.

Desnoyers, D.W., Kieley, J.W. and McKenzie, C.B.
1992: Assessment report on geological, geochemical, geophysical, trenching and diamond drilling exploration for 1991 submission on Reid Lots 227-229 and 231-232, Anglo-Newfoundland Development Company Limited Charter, crown lease 1 on Lot A, crown lease 2 on Lot B and crown lease 4 on Lot F, fee simple grants volume 1 folios 61 and 62 and volume 2 folio 29 in the Red Indian Lake and Buchans areas, Newfoundland, 5 reports. Newfoundland and Labrador Geological Survey, Assessment File 12A/0633, 1907 pages.

Entwistle, L.P. and Barnes, M.P.
1971: Report on the exploration possibilities at the Buchans Unit, Newfoundland. Newfoundland and Labrador Geological Survey, Assessment File 12A/15/0129, 34 pages.

Finch, C., Roldan, R., Walsh, L., Kelly, J. and Amor, S.
2018: Analytical methods for chemical analysis of geological materials. Government of Newfoundland and Labrador, Department of Natural Resources, Geological Survey, Open File NFLD/3316, 67 pages.

Galley, W.D., Hannington, M.D. and Jonasson, I.R.
2007: Volcanogenic massive sulphide deposits. *In* Mineral Deposits of Canada: A Synthesis of Major Deposit-types, District Metallogeny, the Evolution of Geological Provinces, and Exploration Methods. *Edited by* W.D. Goodfellow. Mineral Deposits Division, Geological Association of Canada, Special Publication 5, pages 141-161.

Gifkins, C., Herrmann, W. and Large, R.
2005: Altered volcanic rocks: a guide to description and interpretation. Centre for Ore Deposits Research, University of Tasmania, Australia, 275 pages.

Graves, R.M.
2000: Ninth year supplementary assessment report on geophysical and diamond drilling exploration for licence 4861 on claim blocks 6645-6647, 7515 and 8464 and claims 15717-15718 in the Buchans Junction area, central Newfoundland, 2 reports. Newfoundland and Labrador Geological Survey, Assessment File 12A/16/1187, 86 pages.

2001: Second, third and tenth year assessment report on prospecting and geophysical and diamond drilling exploration for licences 6193M, 7000M-7002M, 7503M and 8127M on claims in the Buchans Junction area, central Newfoundland, 2 reports. Newfoundland and Labrador Geological Survey, Assessment File 12A/1004, 145 pages.

Graves, G. and Squires, G.
1992: Assessment report on prospecting, compilation, geophysical and geochemical exploration for 1992 submission on Reid Lots 229 and 231-232 and fee simple grants volume 1 folios 43 and 62, volume 2 folios 23 and 29 and special volume 2 folio 307 in the Long Lake, Beatons Pond, Mary March River, Wileys Lake, Buchans Junction and Red Indian Lake areas, Newfoundland, 2 reports. Newfoundland and Labrador Geological Survey, Assessment File 12A/0666, 96 pages.

Greene, B.J. and Thurlow, J.G.
1997: First year assessment report on geological and geochemical exploration for licences 4575m and 4778m on claims in the Buchans Junction area, central Newfoundland, 2 reports. Newfoundland and Labrador Geological Survey, Assessment File 12A/0807, 101 pages.

Greene, B. and Wolfson, I.
2013: First year supplementary assessment report on diamond drilling exploration for licence 20398M on claims in the Buchans Junction area, central Newfoundland. Newfoundland and Labrador Geological Survey, Assessment File 12A/15/1651, 116 pages.

Halley, S.W., Dilles, J.H. and Tosdal, R M.
2015: Footprints: hydrothermal alteration and geochemical dispersion around porphyry copper deposits. SEG Newsletter, Issue Number 100, pages 11-17.

Harrington, M., Cullen, M., O'Connor, S., McKeen, T., Roy, D., Moore, P. and Butler, D.
2019: NI 43-101 technical report and mineral resource estimate on the Lundberg deposit, Buchans area, Newfoundland and Labrador, Canada, 176 pages.

Harris, J., Saunders, P. and Reed, L.E.
1999: First year, third year supplementary, fourth year supplementary and seventh year supplementary assessment report on diamond drilling exploration and relogging of diamond drill core for licence 4272 on claim blocks 7916-7917 and 7919-7921 and claims 16512-16514, licence 4294 on claim block 7896, licence 4805 on claim 16398, licence 4806 on claims 16397, 16399-16401, 16424-16426 and 17686-17688, licence 4823 on claims 16431-16432 and licences 4974M and 6973M on claims in the Buchans area, central Newfoundland. Newfoundland and Labrador Geological Survey, Assessment File 12A/15/0946, 1999, 304 pages.

Harris, J. and Woods, D.V.
2001a: Eighth year and eighth year supplementary assessment report on geophysical and diamond drilling exploration for licence 4317 on claim block 7984 and licence 4875 on claim blocks 6663 and 7793-7794 in the Buchans area, central Newfoundland, 2 reports. Newfoundland and Labrador Geological Survey, Assessment File 12A/15/0976, 76 pages.

2001b: Assessment report on geophysical and diamond drilling exploration for 2000 submission for fee simple grant volume 1 folio 62 and for fourth, sixth and eighth year assessment for licence 4603 on claim 16496, licence 4859 on claim blocks 7916-7917 and claim 16513, and licence 5649M on claims in the Buchans area, central Newfoundland, 2 reports. Newfoundland and Labrador Geological Survey, Assessment File 12A/15/0996, 101 pages.

Henley, R.W. and Thornley, P.
1981: Low grade metamorphism and the geothermal environment of massive sulphide formation, Buchans, Newfoundland. *In* The Buchans Orebodies: Fifty Years of Mining and Exploration. *Edited by* E.A. Swanson, D.F. Strong and J.G. Thurlow. Geological Association of Canada. Special Paper 22, pages 205-228.

Hinchey, J.
2011: The Tulks Volcanic Belt, Victoria Lake Supergroup, central Newfoundland – geology, tectonic setting and volcanogenic massive sulphide mineralization. Government of Newfoundland and Labrador, Department of Natural Resources, Geological Survey, Report 2011-02, 185 pages.

Hoefs, J.
2009: Stable Isotope Geochemistry, 6th edition. Springer, Berlin, Heidelberg.

Ishikawa, Y., Sawaguchi, T., Ywaya, S. and Horiuchi, M.
1976: Delineation of prospecting targets for Kuroko deposits based on modes of volcanism of underlying dacite and alteration haloes. Mining Geology, Volume 26, pages 105-117.

Jagodits, F.L. and Thurlow, J.G.
2000: Assessment report on geological, geochemical, geophysical and diamond drilling exploration for 1999 submission for the Anglo-Newfoundland Development

Company Limited Charter, fee simple grant Volume 2 Folio 29 and Reid Lot 247, and for first and ninth year assessment for licence 4117 on claim block 8058 and licences 6967M-6970M on claims in the Buchans Junction area, central Newfoundland, 2 reports. Newfoundland and Labrador Geological Survey, Assessment File 12A/1026, 342 pages.

Kirkham, R.V
1987: Buchans geology, Newfoundland. Geological Survey of Canada, Paper 86-24, 288 pages.

Kowalik, J., Rye, R.O. and Sawkins, F.J.
1981: Stable-isotope study of the Buchans, Newfoundland, polymetallic sulphide deposit. *In* The Buchans Orebodies: Fifty Years of Mining and Exploration. *Edited by* E.A. Swanson, D.F. Strong and J.G. Thurlow. Geological Association of Canada, Special Paper 22, pages 229-254.

Large, R.R., Gemmell, J.B., Paulick, H. and Huston, D.L.
2001: The alteration box plot: A simple approach to understanding the relationships between alteration mineralogy and lithogeochemistry associated with VHMS deposits. Economic Geology, Volume 96, pages 957-971.

Laughlin, W.N.
1967: Geologists report of the Red Indian Lake Syndicate properties in the Buchans Junction area, Newfoundland. Newfoundland and Labrador Geological Survey, Assessment File 12A/10/0036, 73 pages.

McDonald, S.
1995: Assessment report on prospecting, geophysical and geochemical exploration for 1994 submission for the Anglo Newfoundland Development Company Limited Charter, fee simple grant volume 1 folio 43 and Reid Lot 247 and third year assessment report for licence 4175 on claim blocks in the Seal Pond, Millertown and Mary March Provincial Park areas, central Newfoundland, 2 reports. Newfoundland and Labrador Geological Survey, Assessment File 12A/15/0732, 55 pages.

McKenzie, C.B. and Hoffman, S.
1986: Fifth year assessment report on geochemical, geophysical and diamond drilling exploration for the Victoria Lake project for licence 2329 on claim blocks 2227 and 2548-2549 and claims 14116-14121, 14123-14126 and 14140-14157 in the Buchans Junction area, central Newfoundland, 2 reports. Newfoundland and Labrador Geological Survey, Assessment File 12A/0425, 113 pages.

Moore, P. and Butler, D.
2019: Assessment report on compilation, resource estimation, and geophysical and diamond drilling exploration for 2019 submission for fee simple grants volume 1 folios 61-62, and for first, second, fifth, sixth, twelfth, thirteenth and fourteenth year assessment for licences 10524M. 10525M, 11431M, 11432M, 11796M, 13320M, 13423M, 13539M, 20606M, 21328M, 22209M, 22211M, 22213M, 22224M, 22682M, 25434M and 26626M on claims in the Red Indian Lake Area, Buchans, central Newfoundland. Newfoundland and Labrador Geological Survey, Assessment File 12A/1880, 1547 pages.

Moore, P., Butler, D., Cullen, M., Hilchey, A., Myers, K.L., LeDrew, B. and Barrett, T.J.
2013b: Assessment report on resource estimation, engineering studies, and geochemical and diamond drilling exploration for 2012 and 2013 submission for mining leases 222 and 223 and for first and eighth year assessment for licences 11431M, 11433M and 20606M on claims in the Buchans area, central Newfoundland, 5 reports. Newfoundland and Labrador Geological Survey, Assessment File 12A/15/1710, 1854 pages.

Moore, P., Butler, D., Hearst, R., Mokubung, K., Moraga, C., O'Brien, P. J. and McLaren, S.
2008: Assessment report on compilation and geochemical, geophysical and diamond drilling exploration for 2007 submission for fee simple grants volume 1 folios 61-62, and for first, second, twelfth and fifteenth year assessment for licences 5668M, 8295M, 10452M-10453M, 10524M-10526M, 10546M-10548M, 10551M, 11431M-11433M, 11793M-11799M, 11801M, 11808M, 13320M, 13423M and 13539M on claims in the Buchans Area, central Newfoundland, 5 reports. Newfoundland and Labrador Geological Survey, Assessment File 12A/15/1484, 847 pages.

Moore, P., Butler, D.J. and Lambert, G.
2013a: Assessment report on geophysical exploration for 2012 submission for fee simple grant volume 1 folio 62, and for sixteenth year assessment for licence 19080M on claims in the Little Sandy area, near Buchans, central Newfoundland. Newfoundland and Labrador Geological Survey, Assessment File 12A/15/1656, 106 pages.

Moore, P., Butler, D., Webster, P.C., Barr, P.J.F., Hearst, R., Lambert, G. and O'Brien, P.J.
2009: Assessment report on compilation, resource estimation, and geophysical and diamond drilling exploration for 2008 submission for fee simple grants volume 1 folios 61-62, and for second, third, fourth, thirteenth

and sixteenth year assessment for licences 5668M, 8295M, 10452M-10453M, 10524M-10526M, 10546M-10548M, 10551M, 11431M-11433M, 11793M-11799M, 11801M, 11808M, 13320M, 13423M and 13539M on claims in the Buchans area, central Newfoundland, 5 reports. Newfoundland and Labrador Geological Survey, Assessment File 12A/15/1368, 1377 pages.

Noranda Mining and Exploration Incorporated
1998: Report on compilation, exploration history and mineral potential for properties available for option in the Red Indian Lake - Victoria Lake - Tally Pond area, central Newfoundland. Newfoundland and Labrador Geological Survey, Assessment File 12A/1231, 224 pages.

O'Brien, B.H.
2009: Geology of the Little Joe Glodes Pond–Catamaran Brook region with emphasis on the Robert's Arm volcanic belt (parts of NTS 12H/1 and 12A/16), west-central Newfoundland. Map 2009-28. Government of Newfoundland and Labrador, Department of Natural Resources, Geological Survey, Open File NFLD/3053.

Oosterman, D.
2015: Third year assessment report on geophysical and diamond drilling exploration for licence 20398M on claims in the Buchans Junction area, central Newfoundland. Newfoundland and Labrador Geological Survey, Assessment File 12A/15/1693, 231 pages.

Patey, B.
2019: Fourth year assessment report on prospecting and compilation for licence 23592M on claims in the Buchans to Buchans Junction, Mary March area, central Newfoundland. Newfoundland and Labrador Geological Survey, Assessment File 12A/15/1878, 46 pages.

2020: First, third, fourth and eight year assessment report on compilation and prospecting on licences and fee simple lots in the Buchans area, central Newfoundland. Newfoundland and Labrador Geological Survey, Assessment File 12A/1905, 36 pages.

Pearce, J.A.
1996: A user's guide to basalt discrimination diagrams. *In* Trace Element Geochemistry of Volcanic Rocks: Applications for Massive Sulphide Exploration. *Edited by* D.A. Wyman. Geological Association of Canada, Short Course Notes, Volume 12, pages 79-113.

Pearce, D. and Thurlow, J.G.
1979: Exploration report for 1978 on the fee simple grant on the Little Sandy prospect, Newfoundland. Newfoundland and Labrador Geological Survey, Assessment File 12A/15/0258, 32 pages.

Pettit, W.
2000: Third year supplementary, fifth year supplementary, sixth year, sixth year supplementary, and seventh year supplementary assessment report on re-interpretation of geophysical data for licence 4293 on claim block 7898, licence 4294 on claim block 7896, licence 4470 on claim block 4919, licence 4497 on claim 16090, licence 4547 on claim 16171, licence 4603 on claim 16946, licence 4744 on claims 16406-16407, licence 4805 on claim 16398, licence 4806 on claims 16397, 16399-16401, 16424-16426 and 17686-17688, licence 4823 on claims 16431-16432, and licence 5649M on claims in the Buchans area, central Newfoundland. Newfoundland and Labrador Geological Survey, Assessment File 12A/15/0965, 11 pages.

Pickett, J.W. and Scott, W.J.
1992: First year assessment report on geological, geochemical, geophysical and diamond drilling exploration for licence 4114 on claim blocks 7245 and 7515 and licence 4209 on claim blocks 15717-15718 in the Mary March River, Joe Glodes Brook and Buchans Junction areas, central Newfoundland, 3 reports. Newfoundland and Labrador Geological Survey, Assessment File 12A/16/0640, 203 pages.

Pontual, S., Merry, N. and Gamson, P.
1997: G-Mex volume 1: Spectral interpretation field manual; Arrowtown, New Zealand. Ausspec International Pty. Ltd., 86 pages.

Poole, J.C.
1986: First year assessment report on prospecting and geochemical exploration for licence 2681 on claim block 4068 in the Buchans Junction area, central Newfoundland. Newfoundland and Labrador Geological Survey, Assessment File 12A/0426, 31 pages.

Poole, J.C., Thurlow, J.G. and Hoffman, S.
1987: First year assessment report on geological and geochemical exploration for license 2705 on claim blocks 4069-4070 in the Buchans Junction area, central Newfoundland. Newfoundland and Labrador Geological Survey, Assessment File 12A/16/0460, 27 pages.

Ruks, T.W., Piercey, S.J., Ryan, J.J., Villeneuve, M.E. and Creaser, R.A.
2006: Mid- to Late Paleozoic K-feldspar augen granitoids of the Yukon-Tanana Terrane, Yukon, Canada: Implications for crustal growth and tectonic evolution of

the Northern Cordillera. Geological Society of America Bulletin, Volume 118, pages 1212-1231.

Saunders, P.
1997a: Second and third year assessment report on prospecting and geochemical exploration for licence 4548 on claim 16507, licence 4793 on claims 1642016421 and licences 4724m and 4973m on claims in the Red Indian Lake area, central Newfoundland. Newfoundland and Labrador Geological Survey, Assessment File 12A/15/0788, 28 pages.

1997b: First year assessment report on geological and geochemical exploration and relogging of diamond drill core for licence 4548 on claim 16507, licence 4793 on claims 1642016421, licence 4794 on claims 1641716419, licence 4795 on claim 16422 and licences 4601m and 4973m on claims in the Little Sandy Lake area, near Buchans, central Newfoundland. Newfoundland and Labrador Geological Survey, Assessment File 12A/15/0878, 107 pages.

2001: Assessment report on geochemical exploration for 2000 submission for fee simple grant volume 1 folio 62 and for second year, second year supplementary, third year, fourth year, fifth year, eighth year, and eighth year supplementary assessment for licence 4319 on claim blocks 6663-6664 and 7793-7794, licence 4858 on claim blocks 7919-7921 and claims 16512 and 16514, licence 4859 on claim blocks 7916-7917 and claim 16513 and licences 4973M, 5576M, 5668M, 6285M, 6712M, 6715M, 7225M and 7376M on claims in the Buchans area, central Newfoundland, 2 reports. Newfoundland and Labrador Geological Survey, Assessment File 12A/0983, 106 pages.

Saunders, P. and Scott, W.J.
1995: First and second year assessment report on geological, geochemical and geophysical exploration for licence 4293 on claim block 7898, licence 4294 on claim block 7896, licence 4295 on claim block 7855, licence 4470 on claim block 4919, licence 4497 on claim block 16090, licence 4547 on claim block 16171 and licence 4603 on claim block 16496 in the Buchans River, Middle Branch River, East Branch River and Woodmans Brook areas, central Newfoundland, 2 reports. Newfoundland and Labrador Geological Survey, Assessment File 12A/15/0728, 48 pages.

1996: First, second and third year assessment report on geophysical exploration for licence 4806 on claims 16397, 16399-16401, 16424-16426 and 17686-17688, licence 4317 on claim block 7984 and licence 4319 on claim blocks 7792-7794 and claim 16441 in the Buchans area, central Newfoundland, 2 reports. Newfoundland and Labrador Geological Survey, Assessment File 12A/15/0756, 32 pages.

Saunders, P., Harris, J., Reed, L.E. and Woods, D.V.
2000a: First year supplementary, third year supplementary, fifth year supplementary, seventh year supplementary and eighth year assessment report on geophysical and diamond drilling exploration for licence 4273 on claim block 7915, licence 4293 on claim block 7898, licence 4294 on claim block 7896, licence 4317 on claim block 7984, licence 4806 on claims 16397, 16399-16401, 16424-16426 and 17686-17688, licence 4823 on claims 16431-16432, and licences 5649M and 7420M on claims in the Buchans area, central Newfoundland, 3 reports. Newfoundland and Labrador Geological Survey, Assessment File 12A/15/0968, 190 pages.

Saunders, P., Harris, J. and Scott, S.A.
2000b: Assessment report on geophysical and diamond drilling exploration for 1999 submission for fee simple grants volume 1 folios 61-62 and for first year, first year supplementary, second year supplementary, third year, fourth year supplementary and fifth year supplementary assessment for licence 4548 on claim 16507, licence 4793 on claims 16420-16421 and licences 4973M, 5769M, 6192M, 6303M-6305M, 6474M and 7319M on claims in the Little Sandy Lake area, near Buchans, central Newfoundland, 2 reports. Newfoundland and Labrador Geological Survey, Assessment File 12A/15/0942, 86 pages.

Saunders, P., Harris, J., Wilton, D.H.C. and Winter, L.S.
2000d: Assessment report on geochemical exploration for 2000 submission for fee simple grants volume 1 folios 61-62 and for first year and first year supplementary to seventh year supplementary assessment for licence 4273 on claim block 7915, licence 4293 on claim block 7898, licence 4294 on claim block 7896, licence 4317 on claim block 7984, licence 4319 on claim blocks 6663-6664 and 7793-7794, licence 4547 on claim 16171, licence 4548 on claim 16507, licence 4603 on claim 16946, licence 4744 on claim 16406-16407, licence 4793 on claims 16420-16421, licence 4805 on claim 16398, licence 4806 on claims 16397, 16399-16401, 16424-16426 and 17686-17688, licence 4823 on claims 16431-16432, licence 4858 on claim blocks 7919-7921 and claims 16512 and 16514, licence 4859 on claim blocks 7916-7917 and claims 16513 and licences 4973M, 5649M, 5668M, 6003M, 6712M, 7319M and 7420M on claims in the Buchans area, central Newfoundland, 2 reports. Newfoundland and Labrador Geological Survey, Assessment File 12A/15/0951, 197 pages.

Saunders, P., Harris, J., Winter, L., Wilton, D.H.C., Spurvey, P. and Scott, W.J.
1998: First, third, fourth and fifth year assessment report on geochemical, geophysical and diamond drilling exploration for licence 4273 on claim block 7915, licence 4293 on claim block 7898, licence 4294 on claim block 7896, licence 4295 on claim block 7855, licence 4470 on claim block 4919, licence 4497 on claim 16090, licence 4547 on claim 16171, licence 4603 on claim 16496, licence 4744 on claim 16406, licence 4805 on claim 16398 and licences 5574m, 5649m-5651m and 6003m on claims in the Buchans area, central Newfoundland, 6 reports. Newfoundland and Labrador Geological Survey, Assessment File 12A/15/0854, 399 pages.

Saunders, P., Harris, J. and Woods, D. V.
2000c: Assessment report on geophysical and diamond drilling exploration for 2000 submission for fee simple grants volume 1 folios 61-62 and the Anglo-Newfoundland Development Company Limited Charter and for second year and second year supplementary to sixth year supplementary assessment for licence 4548 on claim 16507, licence 4793 on claims 16420-16421 and licences 5651M, 6192M, 6303M-6307M, 6429M and 7219M-7223M on claims in the Little Sandy Lake area, near Buchans, central Newfoundland, 3 reports. Newfoundland and Labrador Geological Survey, Assessment File 12A/15/0991, 244 pages.

Saunders, P., Reed, L.E. and Woods, D.V.
1999: Assessment report on prospecting and geophysical exploration for 1999 submission for the Anglo-Newfoundland Development Company Limited Charter and fee simple grant volume 1 folio 61 and for first year supplementary, second year, third year supplementary, fourth year supplementary, fifth year supplementary, seventh year, and seventh year supplementary assessment for licence 4272 on claim blocks 7916-7921, licence 4294 on claim block 7896, licence 4319 on claim blocks 7793-7794 and claim 16441, licence 4497 on claim 16090, licence 4793 on claims 16420-16421 and licences 6044M, 6277M and 6715M on claims in the Buchans area, central Newfoundland, 4 reports. Newfoundland and Labrador Geological Survey, Assessment File 12A/15/0941, 90 pages.

Saunders, P., Scott, W.J. and Laletsang, K.B.
1996: First, second and third year assessment report on geological, geochemical, geophysical and diamond drilling exploration for licence 4294 on claim block 7896, licence 4295 on claim block 7855, licence 4470 on claim block 4919, licence 4547 on claim 16171, licence 4603 on claim 16496 and licence 4744 on claims 16406-16407 in the Buchans Brook, Middle Branch, East Branch and Woodman's Brook areas, central Newfoundland, 2 reports. Newfoundland and Labrador Geological Survey, Assessment File 12A/15/0753, 169 pages.

Sawkins, F.J. and Kowalik, J.
1981: The source of ore metals at Buchans: magmatic versus leaching models. *In* The Buchans Orebodies: Fifty Years of Mining and Exploration. *Edited by* E.A. Swanson, D.F. Strong and J.G. Thurlow. Geological Association of Canada. Special Paper 22, pages 255-267.

Seymour, C.
2017: First, second and third year assessment report on compilation, modelling, re-logging of diamond drill core and geological and geochemical exploration for licences 22217M, 22222M, 23555M, 23588M, 23589M, 23590M, 23591M, 23592M, 24172M, 24921M, 24922M, 24998M and 25386M on claims in the Buchans to Buchans Junction area, central Newfoundland. Newfoundland and Labrador Geological Survey, Assessment File NFLD/3386, 264 pages.

Seymour, C., King, A. and King, J.
2015: First year assessment report on compilation, modelling, geophysical interpretation, re-logging of diamond drill core and geological and geochemical exploration for licences 22217M-22218M, 22221M-22222M, 22225M, 22227M-22228M, 22240M, 22247M, 22331M, 22471M, 22473M-22475M, 22487M, 22522M, 22820M-22821M, 23224M-23225M, 23227M and 23294M on claims in the Buchans to Buchans Junction area, central Newfoundland, 2 reports. Newfoundland and Labrador Geological Survey, Assessment File 12A/1730, 257 pages.

Sheppard, D.
1997: First year assessment report on prospecting, compilation and geochemical exploration for license 4673m on claims in the Mary Marchs Brook area, central Newfoundland. Newfoundland and Labrador Geological Survey, Assessment File 12A/16/0908, 38 pages.

Squires, G.
1994a: First year assessment report on geological, geochemical and geophysical exploration and relogging of drill core for licence 4302 on claim blocks 4962-4963, 4965-4966 and 8248 and for 1993 submission on fee simple grant volume 1 folios 61-62 in the East Branch Brook, Buchans Highway and Red Indian Lake areas, Newfoundland. Newfoundland and Labrador Geological Survey, Assessment File 12A/15/0716, 146 pages.

1994b: Assessment report on geological, geochemical and geophysical exploration for 1993 submission for the

Millertown Project on the Anglo Newfoundland Development Company Limited Charter and fee simple grant volume 1 folio 43 in the Mary March Provincial Park, Seal Pond and Red Indian Lake areas, central Newfoundland. Newfoundland and Labrador Geological Survey, Assessment File 12A/15/0709, 66 pages.

1994c: Second year assessment report on geochemical interpretations for licence 4254 on claim block 7807 in the Beaver Pond area, Newfoundland. Newfoundland and Labrador Geological Survey, Assessment File 12A/16/0691, 31 pages.

1994d: First and third year assessment report on geological, geochemical, geophysical and diamond drilling exploration for licence 4128 on claim block 7530 and licence 4284 on claim block 7817 and for 1993 submission on fee simple grant volume 2 folio 29 in the Red Indian Lake area, Newfoundland. Newfoundland and Labrador Geological Survey, Assessment File 12A/15/0720, 111 pages.

1996: Fourth year assessment report on geological, geochemical, geophysical and diamond drilling exploration for licence 4175 on claim block 8247 and for fee simple grant volume 1 folio 43 in the Seal Pond area, central Newfoundland. Newfoundland and Labrador Geological Survey, Assessment File 12A/15/0730, 72 pages.

Squires, G. and Marenghi, P.
1993: First and second year assessment report on geological, geochemical and geophysical exploration for licence 4156 on claim block 4897, licence 4157 on claim block 4898, licence 4158 on claim block , licence 4188 on claim block 7673 and licence 4254 on claim block 7807 in the Red Indian Lake and Seal Pond areas, Newfoundland. Newfoundland and Labrador Geological Survey, Assessment File 12A/0665, 62 pages.

Squires, G. and McDonald, S.
1995: Third year assessment report on prospecting, geochemical and geophysical exploration for licence 4175 on claim block 8247 and for 1994 submission for fee simple grant volume 1 folio 43 in the Seal Pond area, Newfoundland. Newfoundland and Labrador Geological Survey, Assessment File 12A/15/0694, 31 pages.

Squires, G., Smith, P.A. and Coulson, S.T.
1992: First year assessment report on geological, geochemical, geophysical and diamond drilling exploration for licence 4116 on claim blocks 3774, 7124 and 7191, licence 4117 on claim blocks 7490-7491, licence 4118 on claim blocks 7492-7493, licence 4123 on claim blocks 7524-7525, licence 4128 on claim block 7531, licence 4137 on claim block 12936, licence 4164 on claim block 7532, licence 4175 on claim blocks 7635-7639, 7644-7645 and 7647-7649, licence 4176 on claim blocks 7646 and 7650, licence 4186 on claim block 7672 and licence 4188 on claim block 7673 in the Buchans Junction, Joe Glodes Brook and Mary March Brook areas, central Newfoundland, 3 reports. Newfoundland and Labrador Geological Survey, Assessment File 12A/0636, 348 pages.

Sparkes, G.W.
2018: Preliminary investigations into the distribution of VMS-style mineralization within the central portion of the Buchans–Roberts Arm (volcanic) belt, central Newfoundland. *In* Current Research. Government of Newfoundland and Labrador, Department of Natural Resources, Geological Survey, Report 18-1, pages 167-184.

2019: Short wavelength infrared spectrometry of hydrothermal alteration zones associated with volcanogenic massive sulphide mineralization, Buchans–Roberts Arm Belt, central Newfoundland. *In* Current Research. Government of Newfoundland and Labrador, Department of Natural Resources, Geological Survey, Report 19-1, pages 97-121.

2020: The style and setting of select VMS occurrences, central Buchans–Robert's Arm Belt. *In* Current Research. Newfoundland. Government of Newfoundland and Labrador, Department of Natural Resources, Geological Survey, Report 20-1, pages 207-233.

2022: Short wavelength infrared spectrometry studies of sericitic alteration zones, southern Buchans–Roberts Arm Belt, Newfoundland. *In* Current Research. Government of Newfoundland and Labrador, Department of Industry, Energy and Technology, Geological Survey, Report 22-1, pages 85-118.

Sparkes, G.W. and Hamilton, M.A.
2024: New U–Pb age constraints on key units within the Buchans Camp, southern Buchans–Roberts Arm Belt, central Newfoundland. *In* Current Research. Government of Newfoundland and Labrador, Department of Industry, Energy and Technology, Geological Survey, Report 24-1, pages 79-96.

Sparkes, G.W., Hamilton, M.A. and Dunning, G.R.
2021: Age constraints on VMS mineralization, central Buchans–Roberts Arm Belt, Newfoundland. *In* Current Research. Government of Newfoundland and Labrador, Department of Industry, Energy and Technology, Geological Survey, Report 21-1, pages 49-64.

Sparkes, G.W. and Hinchey, J.G.
2023: White mica zonation patterns associated with hybrid bimodal-felsic VMS systems: examples from the Tulks Volcanic and Buchans–Roberts Arm belts, central Newfoundland. *In* Current Research. Government of Newfoundland and Labrador, Department of Industry, Energy and Technology, Geological Survey, Report 23-1, pages 99-125.

Spitz, G. and Darling, R.,
1978: Major and minor element lithogeochemical anomalies surrounding the Louvem copper deposit, Val d'Or, Quebec. Canadian Journal of Earth Sciences, Volume 15, pages 1161-1169.

Stuckless, E., Nielsen, P. and Dawson, D.J.W.
2009: Twelfth year assessment report on geophysical exploration for licence 7418M on claims in the Buchans Junction area, central Newfoundland, 2 reports. Newfoundland and Labrador Geological Survey, Assessment File 12A/1382, 41 pages.

Swanson, E.A.
1962: Diamond drilling data from Buchans Junction area, Newfoundland. Newfoundland and Labrador Geological Survey, Assessment File 12A/15/0100, 12 pages.

1963: Report on geochemical, geophysical and diamond drilling exploration for Anglo-Newfoundland Development Company Limited–American Smelting and Refining Company reduced reserved areas in the Buchans Junction, Diversion Lake and Grey River areas, Newfoundland. Newfoundland and Labrador Geological Survey, Assessment File NFLD/0329, 3 pages.

1964: Report on 1963 exploration in crown lands, Newfoundland. Newfoundland and Labrador Geological Survey, Assessment File NFLD/0328, 2 pages.

Swanson, E.A., Strong, D.F. and Thurlow, J.G., eds.
1981: The Buchans Orebodies: Fifty years of geology and mining: Geological Association of Canada, Special Paper 22, 350 pages.

Swinden, H.S.
1991: Geology and metallogeny of the Buchans–Robert's Arm Belt and related rocks. *In* Metallogenic Framework of Base and Precious Metal Deposits, Central and Western Newfoundland (Field Trip 1). *Edited by* H.S. Swinden, D.T.W. Evans and B.F. Kean. Geological Survey of Canada, Open File 2156, pages 81-83.

Swinden, H.S., Jenner, G.A. and Szybinski, Z.A.
1997: Magmatic and tectonic evolution of the Cambrian-Ordovician margin of Iapetus: geochemical and isotopic constraints from the Notre Dame Subzone, Newfoundland. *In* Nature of Magmatism in the Appalachian Orogen. *Edited by* A.K. Sinha, J.B. Whalen and J.P. Hogan. Geological Society of America, Memoir 191, pages 337-365.

Tallman, P.
1995: First year assessment report on diamond drilling exploration for the Buchans Project for licence 4273 on claim block 7915 in the Buchans River area, central Newfoundland. Newfoundland and Labrador Geological Survey, Assessment File 12A/15/0703, 26 pages.

Thurlow, J.G.
1981: Geology, ore deposits and applied rock geochemistry of the Buchans Group, Newfoundland. Unpublished Ph.D. Thesis. Memorial University of Newfoundland, St. John's, Newfoundland.

1984: Assessment report on geophysical exploration for 1983 submission on fee simple grant volume 1 folios 61-62 and volume 2 folio 23 and crown lease 1 on lot A, crown lease 2 on lot B, crown lease 3 on lot E and crown lease 4 on lot F in the Buchans area, Newfoundland. Newfoundland and Labrador Geological Survey, Assessment File 12A/15/0386, 34 pages.

1999: Assessment report on geological, geochemical and diamond drilling exploration for 1998 submission for the Anglo-Newfoundland Development Company Limited Charter, fee simple grant Volume 2 Folio 29 and Reid Lot 247, and for third and eighth year assessment for licence 4117 on claim block 8058 and licence 4763M on claims in the Buchans Junction area, central Newfoundland. Newfoundland and Labrador Geological Survey, Assessment File 12A/1025, 38 pages.

2001: Assessment report on diamond drilling exploration for 2000 submission for the Anglo-Newfoundland Development Company Limited Charter in the Buchans Junction area, central Newfoundland. Newfoundland and Labrador Geological Survey, Assessment File 12A/15/1166, 121 pages.

2010: Great Mining Camps of Canada 3. The History and Geology of the Buchans Mine, Newfoundland and Labrador. Geoscience Canada, Volume 37, pages 145-173.

Thurlow, J.G. and Anderson, D.
1984: Assessment report on geochemical, geophysical and diamond drilling exploration for 1983 submission for fee simple grant volume 1 folio 43 and volume 2 folio 29, Reid lots 228-229, 232 and 247 and Anglo Newfoundland Development Company Limited charter in the Buchans and Mary March River areas, Newfoundland, 2 reports.

Newfoundland and Labrador Geological Survey, Assessment File 12A/0385, 139 pages.

Thurlow, J.G. and Barbour, D.M.
1986: Assessment report on geochemical exploration for 1985 submission for the Victoria Lake project for Anglo Newfoundland Development Company charter, Reid lots 227-229, 231-233 and 247, crown lease lots A-B, E-F, J and N-R, fee simple grants volume 1 folios 43, 61-62 and 110, volume 2 folios 23, 25 and 29 and special volume 2 folio 307 in the Buchans area, Newfoundland. Newfoundland and Labrador Geological Survey, Assessment File 12A/0445, 108 pages.

Thurlow, J.G., Barbour, D.M., Desnoyers, D.W., Burton, G.B., MacNeil, J., Salib, P., Reed, L. and Balch, S.J.
1987: Assessment report on geological, geochemical, geophysical, trenching and diamond drilling exploration for 1986 submission for the Anglo Newfoundland Development Company Limited charter, Reid lots 227-229, 231-235 and 247, crown lease lots A-B, E and N-R and fee simple grants volume 1 folios 61-62 and 110 and volume 2 folios 23 and 29 in the Buchans, Great Burnt Lake, Valentine Lake, Mary March, Victoria Lake and Bobbys Pond areas, Newfoundland, 8 reports. Newfoundland and Labrador Geological Survey, Assessment File NFLD/1737, 2422 pages.

Thurlow, J.G., Barbour, D., Ford, G. and Head, T.
1982: Assessment report on geological, geochemical, geophysical and diamond drilling exploration for 1981 submission on Reid lots 227-234 and 247, Anglo Newfoundland Development Company Limited charter, crown lease 1 on lot A, crown lease 2 on lot B, crown lease 3 on lot E, crown lease 4 on lot F, crown lease 5 on lot J, crown lease 6 on lot K, crown lease 7 on lot L, crown lease 8 on lot M, crown lease 9 on lot N, crown lease 10 on lot O, crown lease 11 on lot P, crown lease 12 on lot Q and crown lease 13 on lot R, fee simple grants volume 1 folios 43, 61-62 and 110, volume 2 folios 23 and 25 and special volume 2 folios 307 and 311 in the Red Indian Lake and Buchans areas, Newfoundland. Newfoundland and Labrador Geological Survey, Assessment File NFLD/1320, 488 pages.

Thurlow, J.G., Spencer, C.P., Boerner, D.E., Reed, L.E. and Wright, J.A.
1992: Geological interpretation of a high resolution reflection seismic survey at the Buchans mine, Newfoundland. Canadian Journal of Earth Sciences, Volume 29, pages 2022-2037.

Thurlow, J.G. and Swanson, E.A.
1981: Geology and ore deposits of the Buchans area, central Newfoundland. *In* The Buchans Orebodies: Fifty Years of Mining and Exploration. *Edited by* E.A. Swanson, D.F. Strong and J.G. Thurlow. Geological Association of Canada, Special Paper 22, pages 113-142.

1987: Stratigraphy and structure of the Buchans Group. *In* Buchans Geology, Newfoundland. *Edited by* R.V. Kirkham. Geological Survey of Canada, Paper 86-24, pages 35-46.

Thurlow, J.G., Swanson, E.A. and Strong, D.F.
1975: Geology and lithogeochemistry of the Buchans polymetallic sulfide deposits, Newfoundland. Economic Geology, Volume 70, pages 130-144.

Tuach, J. and Saunders, P.
1994: First year assessment report on compilation, relogging of drill core and geochemical exploration for licence 4293 on claim block 7898, licence 4294 on claim block 7896, licence 4295 on claim block 7855, licence 4317 on claim block 7984 and licence 4319 on claim blocks 7792-7794 in the Buchans River area, central Newfoundland, 2 reports. Newfoundland and Labrador Geological Survey, Assessment File 12A/0680, 107 pages.

van Hees, G.W.
2011: Chemostratigraphy and alteration geochemistry of the Lundberg and Engine House volcanogenic massive sulfide mineralization, Buchans, central Newfoundland. Unpublished M.Sc. Thesis. University of Ottawa, Ottawa, Ontario.

Waldie, C.J.
2004a: Assessment report on prospecting, linecutting and geochemical exploration for 2004 submission for fee simple grant Volume 2 Folio 29, and for thirteenth year assessment for licence 10229M on claims in the Buchans Junction area, central Newfoundland. Newfoundland and Labrador Geological Survey, Assessment File 12A/1124, 42 pages.

2004b: Assessment report on diamond drilling exploration for 2004 submission for Reid Lot 247 in the Buchans Junction area, central Newfoundland. Newfoundland and Labrador Geological Survey, Assessment File 12A/15/1126, 47 pages.

Wallis, R.H.
2001: Assessment report on geological and geophysical interpretation for 2001 submission for fee simple grants volume 1 folios 61-62 and the Anglo-Newfoundland Development Company Limited Charter and for third year supplementary, fourth year supplementary, sixth year, sixth year supplementary and seventh year supplementary assessment for licence 4548 on claim 16507 and

licences 4973M, 5651M, 5769M, 6192M, 6474M, 7219M-7222M and 7758M on claims in the Little Sandy Lake area, near Buchans, central Newfoundland. Newfoundland and Labrador Geological Survey, Assessment File 12A/15/0990, 218 pages.

Wallis, R.H. and Barrett, T.J.
2001: Assessment report on geochemical interpretation for 2001 submission for fee simple grants volume 1 folios 61-62 and the Anglo-Newfoundland Development Company Limited Charter and for first year, second year, third year, fourth year, fourth year supplementary, fifth year, fifth year supplementary, sixth year, sixth year supplementary, seventh year, seventh year supplementary, eighth year, ninth year and ninth year supplementary assessment for licence 4273 on claim block 7915, licence 4293 on claim block 7898, licence 4294 on claim block 7896, licence 4295 on claim block 7855, licence 4317 on claim block 6665, licence 4470 on claim block 4919, licence 4497 on claim 16090, licence 4547 on claim 16171, licence 4548 on claim 16507, licence 4603 on claim 16946, licence 4744 on claim 16407, licence 4805 on claim 16398, licence 4823 on claims 16431-16432, licence 4858 on claim blocks 7919-7921 and claims 16512 and 16514, licence 4859 on claim blocks 7916-7917 and claim 16513, licence 4865 on claim 16399, licence 4867 on claims 16397, 16400-16401, 16424-16426 and 17688, licence 4868 on claim block 6648, licence 4869 on claim block 6649, licence 4875 on claim blocks 6663 and 7793-7794 and licences 4973M-4974M, 5649M-5652M, 5668M, 5769M, 6003M, 6192M, 6279M, 6285M, 6368M, 6429M, 6474M, 6712M, 6715M, 7219M-7222M, 7225M-7226M, 7376M, 7420M, 7758M, 7932M and 8025M on claims in the Buchans area, central Newfoundland, 2 reports. Newfoundland and Labrador Geological Survey, Assessment File 12A/0992, 242 pages.

Whalen, J., Zagorevski, A., McNicoll, V.J. and Rogers, N.
2013: Geochemistry, U–Pb geochronology, and genesis of granitoid clasts in transported volcanogenic massive sulfide ore deposits, Buchans, Newfoundland. Canadian Journal of Earth Sciences, Volume 50, pages 1116-1133.

Williams, N.C. and Davidon, G.J.
2004: Possible submarine advanced argillic alteration at the Basin Lake prospect, western Tasmania, Australia. Economic Geology, Volume 99, pages 987-1002.

Winter, L.S.
2000: Derivation of base-line geochemistry, petrography, and isotopic data from the host rocks to the Lucky Strike deposit and comparison with data from other alteration zones, Buchans Mining Camp, Newfoundland. Unpublished M.Sc. Thesis. Memorial University of Newfoundland, St. John's, Newfoundland.

Wolfson, I.
2012: Assessment report on geophysical exploration for 2012 submission for fee simple grant Volume 2 Folio 29 and Reid Lot 247, and for first and fourth year assessment for licences 6968M-6970M, 7962M, 19192M, 19430M and 20396M-20398M on claims in the Buchans Junction area, central Newfoundland, 3 reports. Newfoundland and Labrador Geological Survey, Assessment File 12A/1537, 156 pages.

Woods, G.
1988: First year assessment report on geochemical exploration for the Mary March project for licence 3335 on claim blocks 4997-4999 in the Buchans Junction and Beaver Pond areas, Newfoundland. Newfoundland and Labrador Geological Survey, Assessment File 12A/0512, 69 pages.

Woods, D.V. and Northcott, C.
2005: Assessment report on geophysical exploration for 2004 submission for Reid Lot 247 in the Millertown area, central Newfoundland. Newfoundland and Labrador Geological Survey, Assessment File 12A/15/1139, 223 pages.

Woods, G., Gubins, A. and Hoffman, S.
1988: Report on geochemical, geophysical and diamond drilling exploration for licence 2329 on claim blocks 2227-2228 and 2548-2551 and claims 14116-14121, 14123-14133 and 14135-14157, licence 2681 on claim block 4068 and licence 2705 on claim blocks 4069-4070 in the Buchans Junction-Mary Marchs Brook area, central Newfoundland. Newfoundland and Labrador Geological Survey, Assessment File 12A/1034, 65 pages.

Yeomans, W.C.
2011: Second year assessment report on diamond drilling exploration for licence 16037M on claims in the Buchans Junction area, central Newfoundland. Newfoundland and Labrador Geological Survey, Assessment File 12A/1573, 72 pages.

Zagorevski, A. and Rogers, N.
2008: Stratigraphy and structural geology of the Ordovician volcano-sedimentary rocks in the Mary March Brook area. *In* Current Research. Government of Newfoundland and Labrador, Department of Natural Resources, Geological Survey, Report 08-1, pages 101-113.

2009: Geochemical characteristics of the Ordovician volcano-sedimentary rocks in the Mary March Brook area. *In* Current Research. Government of Newfoundland and Labrador, Department of Natural Resources, Geological Survey, Report 09-1, pages 271-288.

2011: Geochemical data of the Buchans–Robert's Arm Belt and adjacent units in central Newfoundland and Notre Dame Bay regions. Geological Survey of Canada, Open File 6728, 13 pages.

Zagorevski, A., McNicoll, V., van Staal, C.R., Kerr, A. and Joyce, N.
2015: From large zones to small terranes to detailed reconstruction of an Early to Middle Ordovician arc-backarc system preserved along the Iapetus suture zone: A legacy of Hank Williams. Geoscience Canada, Volume 42, pages 125-150.

Zagorevski, A., McNicoll, V.J., Rogers, N. and van Hees, G.H.
2016: Middle Ordovician disorganized arc rifting in the peri-Laurentian Newfoundland Appalachians: Implications for evolution of intra-oceanic arc systems. Journal of the Geological Society, Volume 173, pages 76-93.

Zagorevski, A., Rogers, N., van Staal, C., McClenaghan, S. and Haslam, R.
2007: Tectonostratigraphic relationships in the Buchans area: a composite of Ordovician and Silurian terranes? *In* Current Research. Government of Newfoundland and Labrador, Department of Natural Resources, Geological Survey, Report 07-1, pages 103-116.

Zagorevski, A., Rogers, N., van Staal, C.R., McNicoll, V., Lissenberg, C.J. and Valverde-Vaquero, P.
2006: Lower to Middle Ordovician evolution of peri-Laurentian arc and backarc complexes in Iapetus; constraints from the Annieopsquotch accretionary tract, central Newfoundland. Geological Society of America Bulletin, Volume 118, pages 324-342.

APPENDICES

APPENDIX A: Sampling Framework
- A1 – Drillhole collar data
- A2 – Downhole survey data
- A3 – Sample locations and descriptions

APPENDIX B: New Analytical Data
- B1 – Whole-rock geochemistry
- B2 – Major-element and trace-element data for standards
- B3 – Major-element and trace-element data for duplicates
- B4 – Sulphur isotopes
- B5 – Spectral data
- B6 – Sample photographs

APPENDIX C: Historical Data
- C1 – Soil survey data
- C2 – Basal till data
- C3 – Drillhole assay data

APPENDIX D: Metadata
- D1 – Industry drill logs
- D2 – Assessment file index